Modulating mechanical cues and oxygen availability to regulate chondrogenesis within MSC laden hydrogels

Alan D. Irvine, B.A., B.A.I.

Supervisor

Prof. Daniel J. Kelly

External Examiner

Prof. Jan Herman-Kuiper

Internal Examiner

Prof. Rocco Lupoi

Monday 19th June 2017

A thesis project submitted to the University of Dublin in partial fulfillment of the requirements for the degree of Ph.D.

Declaration

I declare that this thesis has not been submitted as as an exercise for a degree at this or any other university and it is entirely my own work.

I agree to deposit this thesis in the University's open access institutional repository or allow the library to do so on my behalf, subject to Irish Copyright Legislation and Trinity College Library conditions of use and acknowledgement.

Alan Irvine

_____
Signature

_____
Date

Abstract

TISSUE engineering is a potential alternative to conventional surgical techniques for regenerating damaged tissues that lack the ability to spontaneously repair. MSCs are a promising cell source for tissue engineering strategies intended to treat a range of injuries and diseases. Within the synovial joint environment, a complex array of biochemical, environmental and biomechanical stimuli arise. If MSCs are to be successfully used *in vivo*, understanding the effects on their differentiation and function in response to these stimuli is vital. A central hypothesis of this thesis is that oxygen availability and mechanical stimulation can direct chondrogenic differentiation and hypertrophy of MSCs. This thesis examines the response of MSC-laden hydrogels to oxygen availability, substrate stiffness and dynamic compressive strain. The overall objective is to develop the precursor to an osteochondral graft by mechanically modulating chondrogenesis and hypertrophy of MSCs within a 3-dimensional hydrogel environment. To enable this, this thesis first systemically explored the response of MSCs undergoing chondrogenesis to altered levels of substrate stiffness, dynamic compression and oxygen availability. The application of dynamic compression after 21 days at different magnitudes in 20 % O_2 to dynamic compression to MSC-laden agarose hydrogels was found to alter calcification in a magnitude dependent manner. High magnitudes (20 % strain) tended to reduce the increases in calcification produced at moderate strains.

The thesis next explored the role of substrate stiffness in regulating chondrogenesis in altered oxygen environments. In MSC-laden, RGD-modified alginate hydrogels, it was found that soft hydrogels enhance early MSC chondrogenesis. Altering oxygen levels from from 20 % to 5 % altered the spatial distribution of cartilage-specific proteins producing a more homogenous tissue. In a subsequent study, dynamic compression applied after 5 days in 5 %

O$_2$ only affected MSC chondrogenesis and hypertrophy in stiff, less chondrogenic MSC-laden hydrogels. Here, moderate strains (10 %) enhanced MSC chondrogenesis and high strains (20 %) reduced MSC hypertrophy in stiff MSC-laden hydrogels in comparison to moderate strains (10 %).

The next stage of the thesis explored tailoring substrate stiffness, oxygen availability and local dynamic compressive strain magnitude in a gradient fashion, with the hypothesis that a precursor to an osteochondral-like tissue could be produced. Varying substrate stiffness throughout the depth in these alginate hydrogels and applying dynamic compression lead to spatial changes in MSC differentiation, but failed to produce an effective osteochondral precursor. The final stage of this thesis involved impregnating a MSC-laden alginate hydrogel into a 3-D printed polymeric scaffolds with a gradient profile. This created an environment that modulated local strain magnitude alone. Spatial differences in MSC chondrogenesis in gradient mesh constructs alone were observed. GAG production was enhanced in regions of low strain and hypertrophy was reduced in areas of high strain.

This thesis demonstrates that the MSC chondrogenesis and hypertrophy are mechano-regulated. It highlights the interdependence of oxygen availability, substrate stiffness and dynamic compression as well as the effect local variations in these stimuli can have on the development of engineered tissues. This work will aid in the understanding of MSC mechanobiology, optimum tissue engineering considerations for both cartilage and osteochondral tissue engineering and 3-D bioprinted scaffold design.

Acknowledgements

MY sincerest gratitude goes to Prof. Daniel Kelly for his guidance over the past four years. It has been privileged to work with someone who trusts your time as your own, yet also has great expectations and aspirations for each individual's research. Thank you for providing me with this opportunity to undertake such a challenging experience.

Many thanks to Prof. Conor Buckley, whose support and mentorship from the onset has both encouraged me to grow and learn, as well as mould my technical abilities in the lab.

I have enjoyed working with everyone in the Trinity Centre of Bioengineering. Thanks especially to Grainne for her constant help in performing general lab procedures and protocols as well as other post-doctoral research fellows throughout my time including Olivier, Raja and particularly Binu, whose guidance in rt-PCR has been invaluable. Another thank you goes to Simon for instructing me through much of my technical engineering work from the onset of this project. Further thanks go to the rest of the lab.

Thanks to everyone in the workshop, Michael Reilly and Paul Normoyle for technical assistance in manufacturing and computation respectively.

Finally, I could not overlook the huge support from my very patient parents whose unwavering support helped make this possible.

Contents

List of Figures

List of Tables

Nomenclature

g 1 gram is a unit of mass. It is equivalent to mass that 1 one-thousandth cubic metre of water holds.

kPa 1 Pascal is a unit of pressure that refers to the weight of 1 Newton acting over a 1 square metre area. 1 kPa refers to 1000 Pascals (Pa) of pressure.

O_2 Chemical symbol for oxygen molecule.

CHAPTER 1

Introduction

1.1 Joint damage and degeneration

A RTICULAR cartilage is a complex tissue that lines the edges of bones in diarthrodial joints (fig. 1.1). Defects in cartilage can arise either through traumatic overloading of the joint (e.g. sporting injuries) or pathogenically through a degenerative disease known as osteoarthritis (OA) [1,2]. The lesions that arise from such defects have adverse structural and biological effects that cause thinning of the tissue and a loss of mechanical integrity. To compound the issue, cartilage is avascular in nature as well as having a highly organised structure that make both natural and artificial repair of these defects difficult [3,4]. The low grade synovial inflammation (synovitis) that also occurs in both the early and late phases of OA also contributes to the progression of the disease. This induces a vicious circle that promotes further joint degradation.

For severe osteoartritic degeneration, the most common from of treatment is arthroplasty, in which joints are totally replaced by inorganic materials [5]. Various other surgical procedures exist that attempt to promote tissue repair and regeneration in milder forms of cartilage and joint degeneration [6]. For example, non-aggressive debridement of fibrous/osteoarthritic articular cartilage is deemed to be effective in relieving pain and restoring function in patients with traumatic and mildly degenerative lesions. The procedure

may be coupled with micro-fracturing of the subchondral bone layer in areas of partial or total cartilage loss. These micro punctures attempt to invoke a natural repair response by allowing blood to inflitrate from the underlying bone tissue and marrow. A more invasive method of repairing chondral and osteochondral defects is through the use of allografts and autografts. Mosaicplasty involves taking a number of osteochondral autografts from a donor site that are then re-implanted in the affected areas. Allografts from other patients can also be used [7]. Despite short-term success, all the aforementioned techniques have efficacy concerns relating to undesirable outcomes such as periosteal hypertrophy, delamination of the implant, arthofibrosis, disease transmission, immune rejection and ultimately implant or tissue regeneration failure [8]. In the case of microfracture, the repair tissue also tends to consist of fibrous cartilage, which does not have the biomechanical competence of the hyaline type that lines articulating joints.

The concern surrounding previous joint repair and regeneration procedures has lead to extensive research into alternative methods that either attempt to engineer or regenerate the tissue using novel approaches. Currently approved tissue engineering approaches include autologous cartilage implantation (ACI) and matrix-assisted ACI (MACI) [9]. In these procedures cartilage cells (extracted and expanded from the patient), termed chondrocytes, are surgically placed in the defect site; either alone, or within a biocompatible matrix material. Despite success in regenerating largely hyaline like cartilage, these approaches have associated limitations; an additional defect site is created in the patient on a non-load bearing cartilage region so that chondrocytes can be isolated from this tissue. Equally, there is an inability to obtain sufficient numbers of differentiated chondrocytes from this cartilage tissue, particularly in elderly and osteoarthritic patients.

Current research is, therefore, now exploring the potential of mesenchymal stem cells (MSCs) for joint tissue engineering and regenerative therapies due to their increased capacity to be isolated and expanded in large numbers as well as for their regenerative potential [10,11]. Attempting to engineer an osteo-inductive or chondro-inductive environment by combining these cells with 3-dimensional (3-D) scaffold structures and other external mechanical stimuli has become a potentially successful avenue of engineering cartilage and

osteochondral tissue [12]. The ability to control the differentiation of MSCs into specialised cell types will be central to unlocking their regenerative potential.
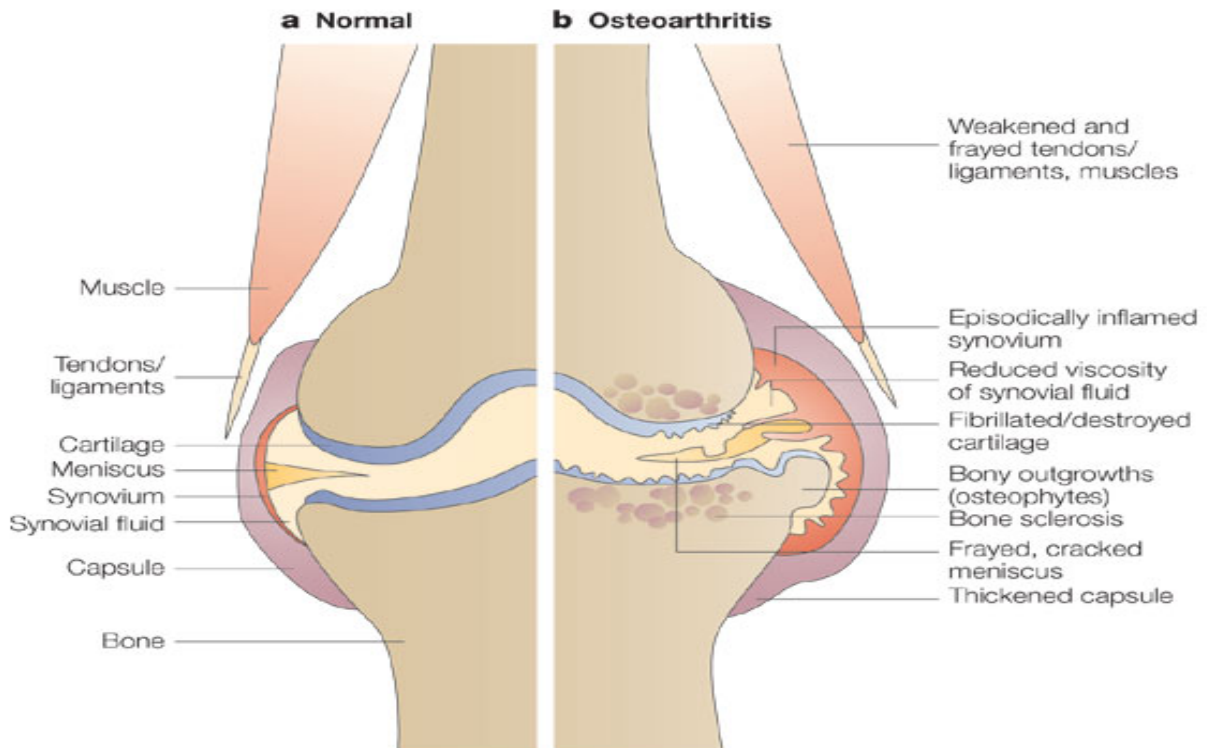
Figure 1.1 Knee anatomy in normal and osteoarthritic states. Taken from https://sciencebasedmedicine.org/.

1.2 MSC based osteochondral tissue engineering

MSCs have an affinity to differentiate into cell types specific to certain tissues such as cartilage and bone, which make them a promising cell source for osteochondral tissue engineering. Transforming Growth Factor-β_3 has been shown to promote chondrogenesis of MSCs[10,11,13–15]. TGF-β_3 primed MSCs are therefore widely used for cartilage tissue engineering purposes. A major challenge in MSC-based articular cartilage repair

therapies is the prevention of terminal differentiation in which chondrocytes, differentiated from MSCs, become hypertrophic, increase in size and progress along the endochondral pathway before terminally differentiating into bone forming cells [16,17]. This apparent obstacle in MSC-based articular cartilage tissue engineering has recently been realised as a potential advantage in both endochondral bone tissue engineering and osteochondral tissue engineering [18–20]. A means by which chondrogenesis and endochondral ossification could be modulated would potentially allow the formation of both stable cartilage, or endochondral bone; through either inhibiting, or promoting the endochondral pathway (EC) respectively. This opens the possibility of spatially directing MSCs towards either a stable hyaline phenotype or along an EC pathway to engineer osteochondral tissues by managing the potential shift from cartilage to endochondral bone (fig. 1.2).

Having established endochondral ossification as a promising approach for engineering osteochondral grafts, the challenge becomes spatially modulating the chondrogenic differentiation of MSCs. Current approaches to altering chondrogenic hypertrophy include the use of different oxygen culturing conditions [21] and biomechanical stimuli, such as substrate stiffness [22] and dynamic compression [23]; among other more biochemically focused approaches that will not be considered as part of this thesis.

Low oxygen has been shown to both enhance chondrogenesis [24,25] and suppress hypertrophy of MSCs [26]. Prolonged culture periods at high oxygen conditions can lead to the development of hypertrophic tissue within MSC laden constructs [17]. Biomechanical stimuli in combination with soluble cues have also shown to be promising in modulating both MSC fate and chondrogenic hypertrophy [27]. Ramos et al. recently demonstrated the potential of hydrogel stiffness to alter chondrocyte deposition of cartilage specific matrix components [28]. Other studies have highlighted the importance of hydrogel stiffness on MSC fate towards either adipogenic or osteogenic lineages [29]; but few studies have specifically focused on the role of such stimuli on both chondrogenesis and hypertrophy of MSCs. Dynamic compression (DC) has been identified as a regulator of MSC chondrogenesis [30] with the ability to both induce and enhance MSC chondrogenesis [31,32] in certain culture conditions as well as to suppress hypertrophy [22]. In contrast, other studies have

shown that osteogenic genes were upregulated when osteoblasts were subjected to 10 % dynamic compressive strain [33]. This suggests DC may have the potential to either enhance or suppress hypertrophy, possibly depending on the magnitude of the applied stimulus mimicking the differences in dynamic compressive strain within the respective tissues during articulation. Therefore the question remains how can oxygen tension, substrate stiffness and dynamic compression be combined and spatially regulated to modulate MSC chondrogenesis and hypertrophy in order to develop a strategy for engineering a viable osteochondral grafts.
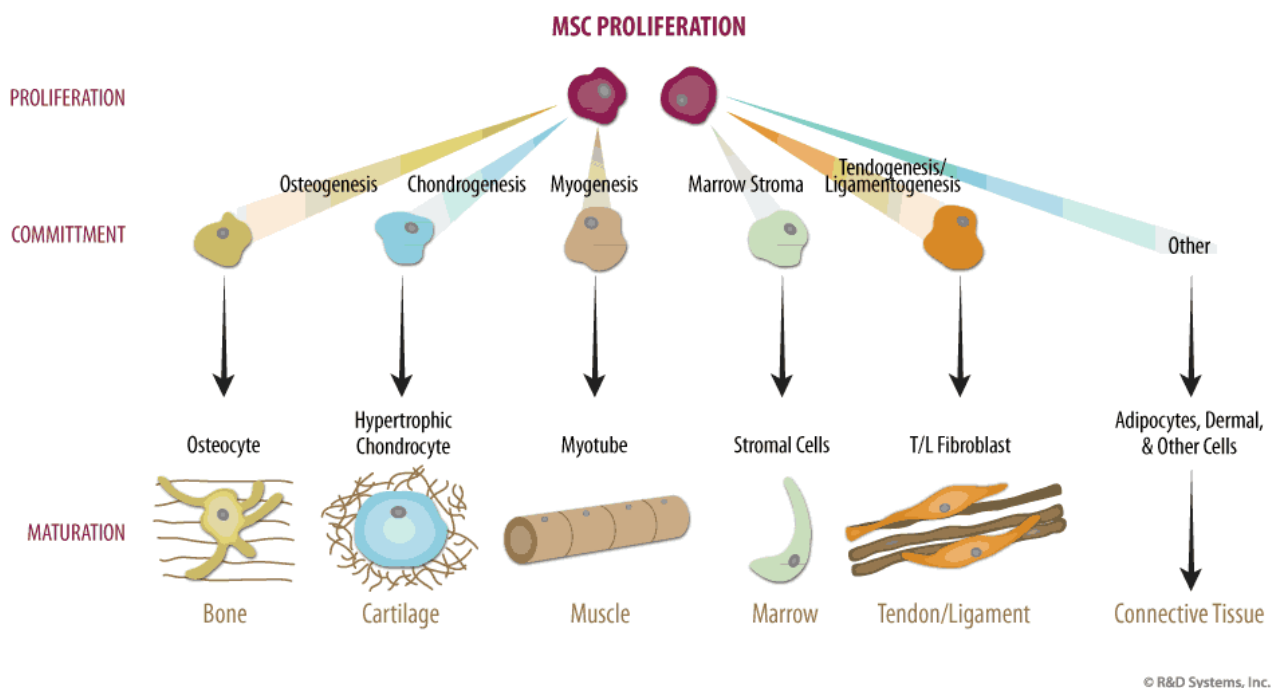
Figure 1.2 Differentiation pathways of stem cells derived from the mesenchyme. Taken from https://www.rndsystems.com/resources/.

1.3   Project aims and objectives

The overall objective of this thesis is to develop the precursor to an osteochondral graft by mechanically modulating chondrogenesis and hypertrophy of MSCs within a 3-dimensional hydrogel environment. Mechanical stimuli have been shown to be important for both the

initiation of chondrogenesis, and more recently have been implicated in the progression of MSC chondrogenesis towards either stable, hyaline-like cartilage or terminally-differentiated, hypertrophic cartilage that leads to bone formation through endochondral ossification. Mechanical stimuli are clearly a determining factor in both processes so the correct combination of these may alone provide a means of engineering an osteochondral graft from an engineered cartilage template.

It is hypothesised that by providing spatially defined environmental cues to hydrogel encapsulated MSCs it will be possible to engineer a zonally defined tissue consisting of a layer of stable articular cartilage overlaying a layer of hypertrophic cartilage.
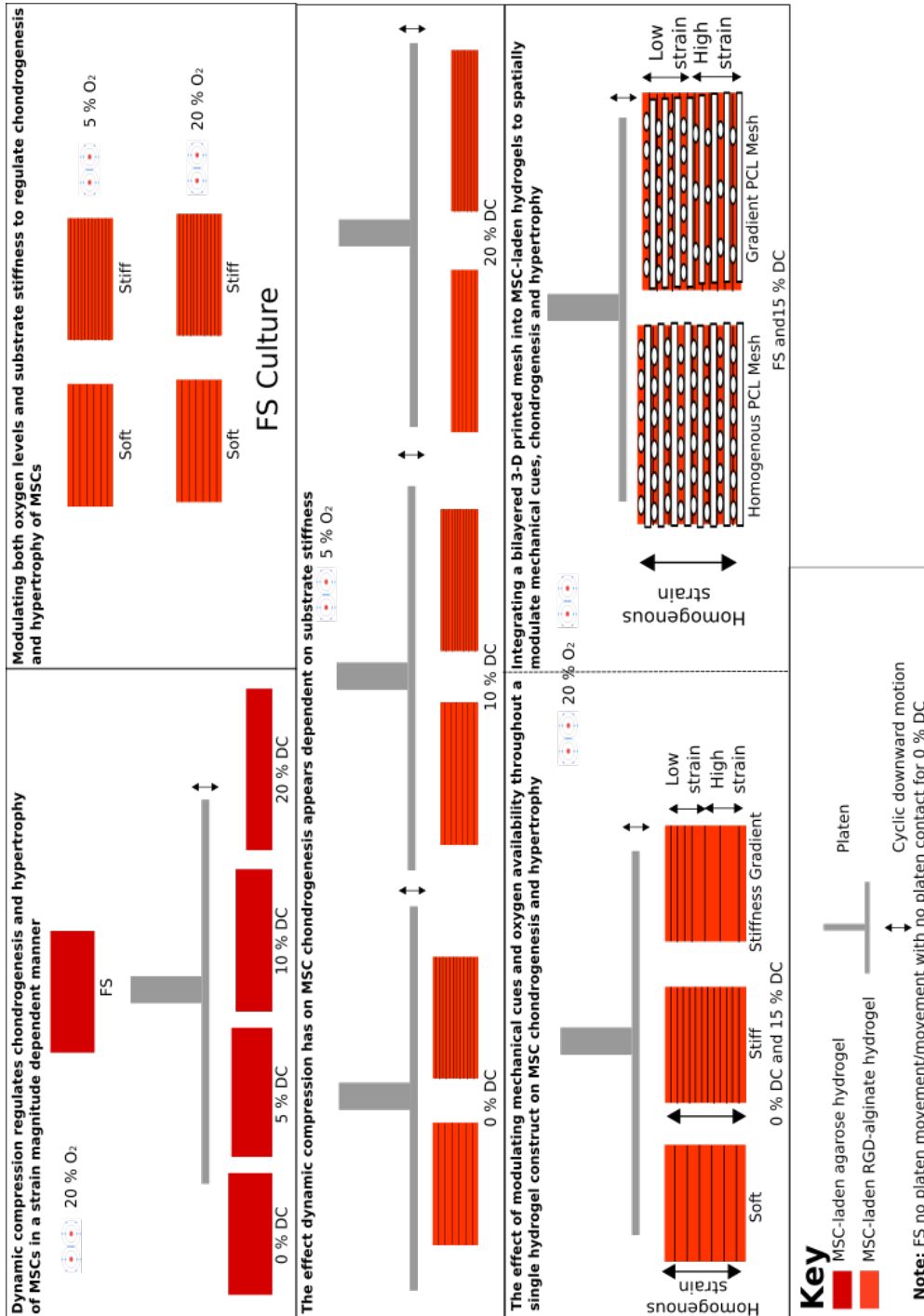
Figure 1.3 Full schematic of all thesis sub-objectives.

So considering both processes and in order to achieve this overall objective, the specific objectives of this thesis are:

1. Investigate the role that the magnitude of dynamic compression has on MSC chondrogenesis and progression along the endochondral pathway.
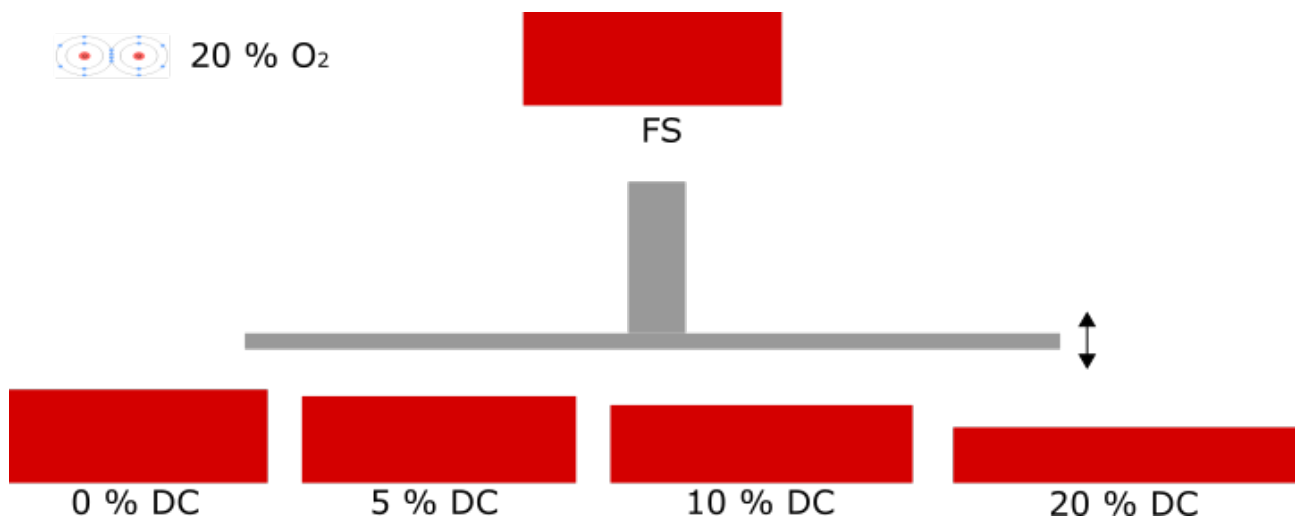
Figure 1.4a Sub-objective 1 schematic.

2. Determine the role of substrate stiffness and oxygen availability on the initiation and progression of chondrogenesis in MSCs.
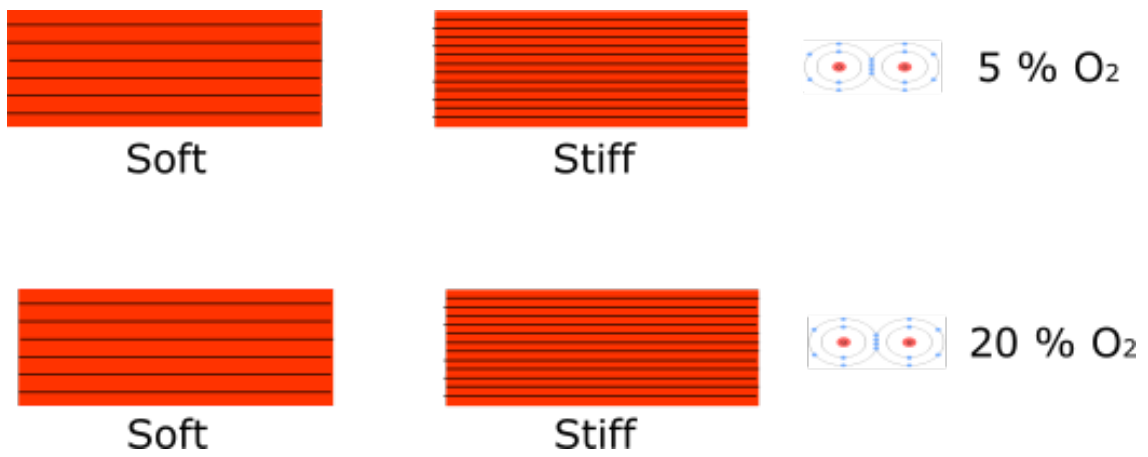
Figure 1.4b Sub-objective 2 schematic.

3. Explore the interaction between substrate stiffness and dynamic compression on the initiation and progression of MSC chondrogenesis.
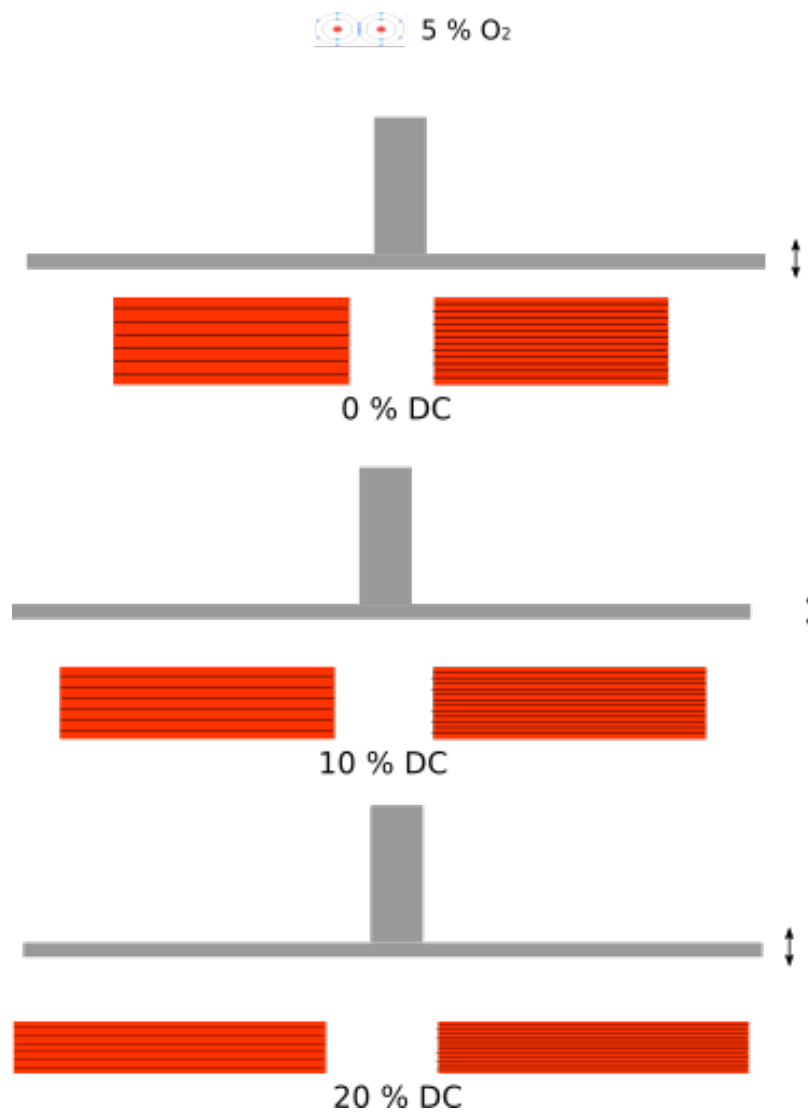
Figure 1.4c Sub-objective 3 schematic.

4. Biofabricate MSC-laden constructs with spatially defined mechanical properties to regulate MSC fate and promote the development of tissues destined for an osteochondral fate.
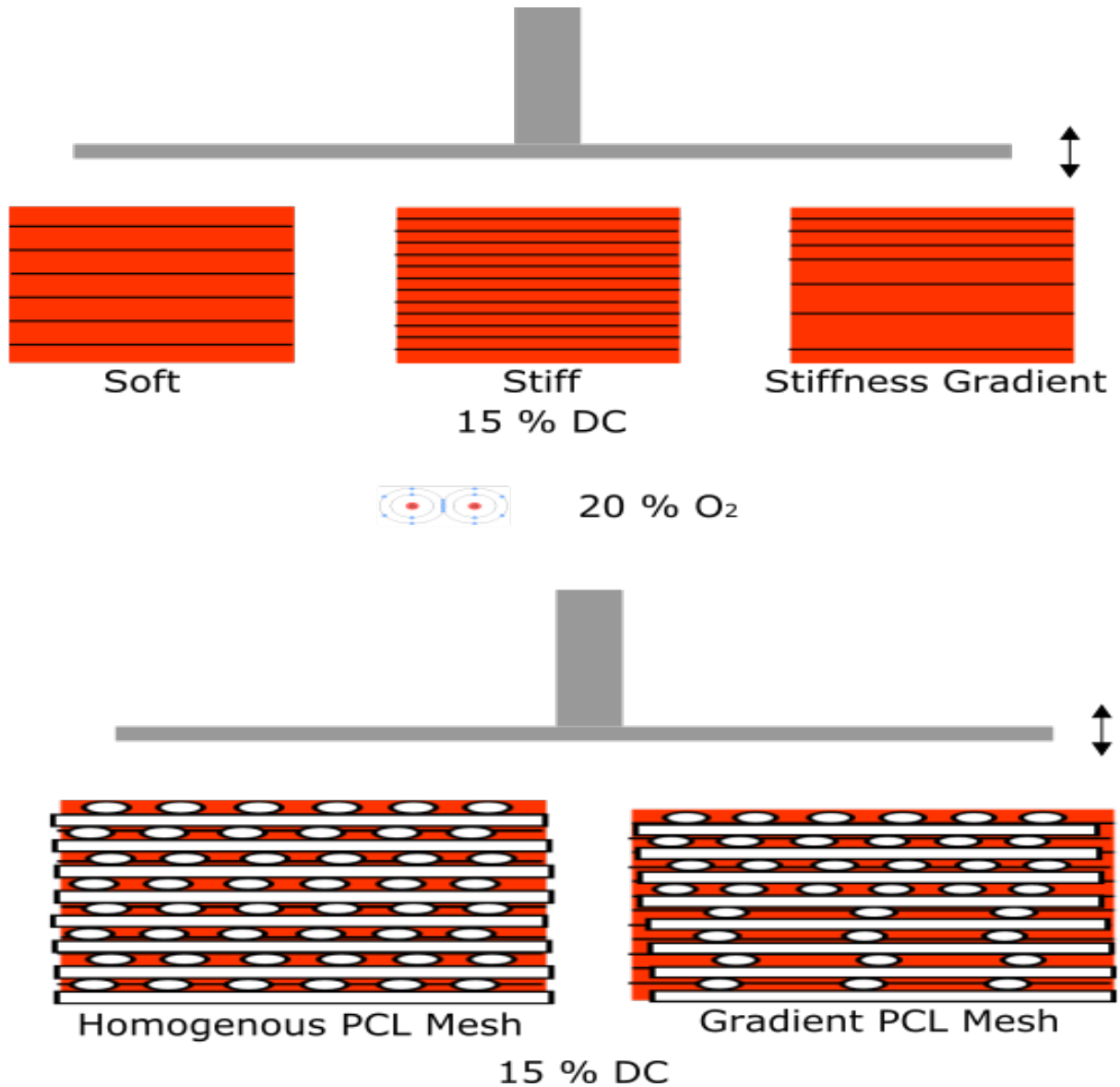
Figure 1.4d Sub-objective 4 schematic.

This can be achieved by modulating either substrate stiffness of the hydrogel or of an impregnated mesh within the hydrogel throughout the depth of the construct.

The overall aim being to spatially modulate the environmental cues developed within MSC-laden hydrogels in order to achieve the thesis global objective. Using a configuration such as the following:
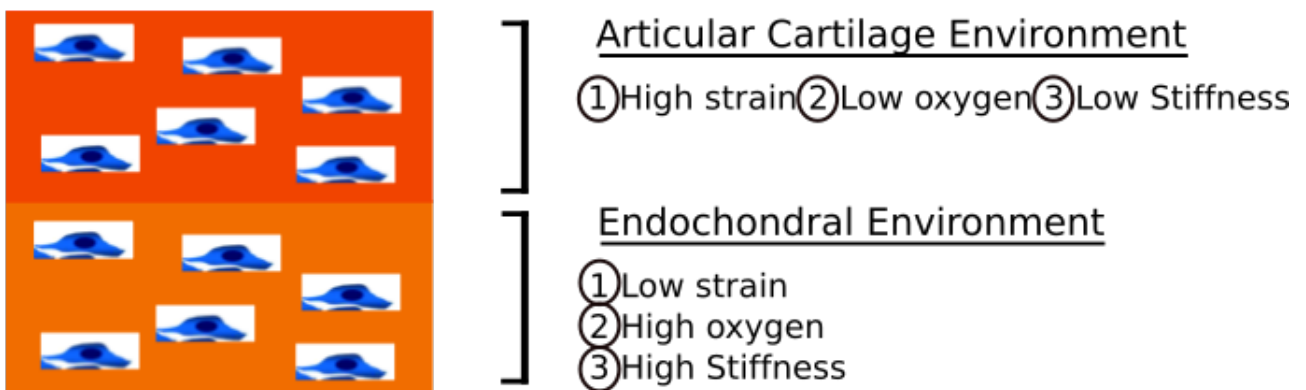
Figure 1.5 Modulating environmental cues to engineer MSCs with an osteochondral fate.

These mechanical variations can be achieved by spatially altering hydrogel stiffness alone or by spatially altering the stiffness of an impregnated 3-D printed mesh within the hydrogel and applying dynamic compression. Both avenues are explored in the last sub-objective.

CHAPTER 2

Literature Review

2.1 Composition, structure and mechanical properties of cartilage

ARTICULAR cartilage is a complex tissue consisting of an intricate anatomical structure. This structure provides the means by which cartilage can withstand its challenging biomechanical environment. Therefore there is a need to understand the composition and anatomical structure of articular cartilage as well as the biomechanical properties of the tissue.

2.1.1 Composition and structure of articular cartilage

The sparsely distributed cells in articular cartilage; named chondrocytes, account for less than 10 % of the tissue volume. This equates to a cell density of the order of five million per cm cubed in comparison to the typical density of a few hundred million per cm cubed found in other tissues throughout the body [34].

Despite their sparse distribution, chondrocytes produce, secrete and maintain the organic components that encompass the extracellular matrix of articular cartilage. The organic matrix contains a dense, fibrillar collagen type II network enmeshed in a concentrated solution of proteoglycans (PGs) [35,36]. The collagen content ranges from 10 to 30 % and the PG

content from 3 to 10 %, both by wet weight; the remaining 60 to 87 % comprises water, inorganic salts, and other small quantities of different matrix proteins, glycoproteins, and lipids [4]. Collagen fibrils and PGs are the structural components supporting the mechanical forces developed from applied loads [37,38]. It is the combination of these components with the interstitial fluid pressure produced by the containment of water in a tight organic matrix that provide the biomechanical properties of articular cartilage.

Collagen, the most abundant protein in the body, has a high level of structural organisation in articular cartilage that provides a fibrous ultrastructure for the tissue [4,35,39]. In general, this ultrastructure is heterogeneous in collagen fibril distribution, but layers within the tissue have been identified with a relatively homogenous distribution of these fibrils. The variation in collagen fibre orientation is mirrored by zonal variations of collagen content (fig. 2.1), which is greatest at the surface and remains relatively constant throughout the deeper zones [40]. This ultrastructure serves greatly in enhancing the biomechanical properties of articular cartilage by maximising interstitial fluid pressure support and minimising solid matrix stress within the tissue; the former being very important as collagen fibrils alone exhibits little resistance to compression due to their high slenderness ratio [41,42]. The fibrils can, however, resist high tensile loads, which again aid in the biomechanical behaviour of characteristics [43].

Cartilage PGs are large protein-polysaccharide molecules consisting of a protein core to which one or more glycosaminoglycans (GAGs) are attached [36]. Aggrecan consists of an approximately 200mm long protein core to with about 150 GAG chains are covalently attached to [36]. Keratan sulphate and chondroitin sulphate, the two sulphated GAGs found in articular cartilage, are polymer sequences of specific repeating disaccharide units.

The association of most PG monomers in native cartilage with hyaluronate constitutes the formation of PG aggregates (macromolecules). These aggregates form when up to a several hundred monomers non-covalently attach to a central hyaluronate core via the hyaluronic acid-binding region (HABR) [36]. The filamentous hyaluronic acid (HA) core molecule is a non-sulphated disaccharide chain. The attachment site between the HABR and the HA is stabilised by small glycoproteins; link proteins. It is widely accepted that PG aggregation

promotes immobilisation of the PGs within the collagen network, adding structural rigidity to the extracellular matrix [36,44,45].

Articular cartilage composes mainly of water when normalised to weight. Water consists of 80 % of the tissue with respect to wet weight with most concentrating at the surface of articular cartilage and this percentage decreases in a linear fashion with depth to roughly 65 % in the deep zone [46]. Many mobile cations are contained in the fluid mix of water and other soluble components that have a strong influence of the behaviour of articular cartilage [47–49]. The avascular nature of cartilage means that it depends on this balance of these fluid components for facilitating the diffusion of gases, nutrients and waste products between chondrocytes and the surrounding nutrient rich synovium [47,50,51]. Only a small percent of the fluid is intracellular while about 30 % is associated with the collagen fibrils [52]. This means that most of the fluid occupies the intermolecular space and is free to move when a load or pressure gradient is applied to the tissue. Theoretical and experimental analysis has shown that the interstitial fluid of cartilage pressurises considerably due to loading, potentially supporting most of the applied load under various transient or steady-state conditions [53]. During this loading process about 70 % of the fluid is removed from the tissue [54,55]. This movement is critical in controlling cartilage behaviour and joint lubrication as it has been shown that interstitial fluid load support plays a dominant role in regulating the frictional properties of cartilage; the understanding being that an elevated interstitial fluid load support correlates to a low friction coefficient [53].
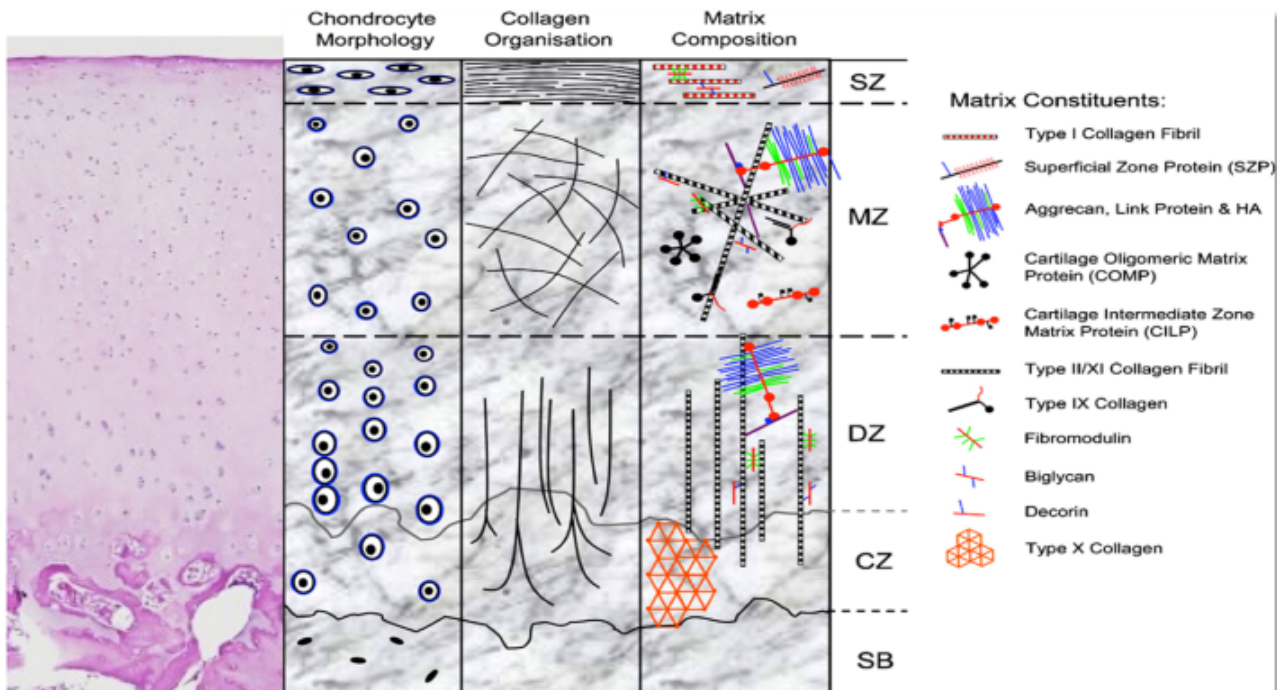
Figure 2.1 3-D Representation of the ultrastructural arrangement of the collagen network throughout the depth of articular cartilage. In the superficial tangential zone (STZ), collagen fibres are tightly woven into sheets arranged parallel to the articular surface. In the middle zone (MZ), randomly arranged fibrils are less densely packed to accommodate the high density of proteoglycans and water. The collagen fibrils of deep zone (DZ) form larger, radially orientated fibre bundles which cross the tidemark, enter the calcified zone (CZ), and anchor the tissue to the underlying bone (SB).

The properties and conformation of the PG aggregates are influenced by the chemical structure and interactions of the GAGs. The closed spaced sulphate and carboxyl groups on the GAG disaccharide units dissociate in solution, leaving fixed negative charges which create strong intra- and intermolecular charge repulsive forces. The inter-fibrillar space formed by the collagen network is extended and stiffened due to this charge repulsion. Mobile cations such as sodium and calcium are attracted to the anionic groups on the GAGs creating a substantial swelling pressure ranging from 0.5 to 3 MPa [56]. This swelling pressure is closely correlated to the GAG density and is resisted and balanced by tension in the collagen network, confining PGs to only 20 % of their free solution domain. Therefore, even in the absence of external loads, the collagen network is subject to a pre-stress [57].

When a stress is applied to the cartilage surface, deformation occurs primarily due to a change in the PG molecular domain. A sufficient external stress can cause an internal matrix pressure to exceed the swelling pressure, and liquid begins to exude from the tissue. As the fluid flows out the PG concentrations increases; this results in an increase in osmotic pressure, charge-charge repulsive force and compressive stress until equilibrium is achieved with the external stress. In addition, a change in a solution's pH or ion concentration will alter the PG intermolecular charge repulsive forces causing a change in the size of the aggregate domain. Therefore the osmotic swelling pressure associated with fixed charge density due to the ionic groups in the GAGs, as well as the bulk compressive stiffness of the PG aggregates trapped in the collagen network, are the two physiochemical properties of the PG that allow it to resist compression and complement the role in tension played by the collagen network [43,58].

2.1.2   Biomechanical properties of articular cartilage

Cartilage is defined as a viscoelastic material meaning that the mechanical response of the tissue to a constant load or deformation varies with time. Therefore a modelling the response of articular cartilage to mechanical loading must account for the combination of the viscous fluid and the elastic solid that encompass cartilage.

The two fundamental responses of a viscoelastic material under mechanical loading are creep and stress relaxation. The action of either a constant load or deformation determines creep or stress relaxation respectively. Generally, a rapid initial deformation followed by a slow (time-dependent) and progressively increasing deformation, known as creep, is the response of a viscoelastic solid until equilibrium is reached. In the instance of applying a constant deformation, a viscoelastic solid responds with a high initial stress followed by a slow and progressively decreasing stress required to maintain the deformation.

Articular cartilage has been shown to act as a viscoelastic solid primarily due to the flow of interstitial fluid [58,59], and in shear mainly because of the motion of long polymer chains such as collagen and PGs [58]. Biphasic viscoelastic theory describes the viscoelastic

behaviour of cartilage in response to interstitial fluid flow. The component due to macro-molecular motion is known as flow-independent (or intrinsic) and viscoelastic behaviour of the collagen-PG matrix [58].

Creep in articular cartilage is caused by exudation of the interstitial fluid. Shown in Figure is the biphasic creep response of articular cartilage in a one-dimensional confined compression test. The graph clearly highlights that following a constant force initiated at time t0, articular cartilage creeps until it reaches its equilibrium value; at which point the force is removed. Creep creases once the compressive stress within the solid matrix is enough to support the applied stress alone. Since the rate of creep is governed primarily by the rate of fluid exudation, it can be used to determine the permeability coefficient of the tissue. At equilibrium, no fluid flow occurs, indicating that the collagen-PG matrix intrinsic compressive modulus can be isolated from the equilibrium deformation. This has been found to range from 0.1 to 2.0 MPa [58].

Stress relaxation occurs when the stress begins to fall following an increase during a constant displacement rate of the tissue until a deformation d0 is reached. During this time, the stress continuously decreases until equilibrium is reached. The stress rise in the compression phase is related to fluid exudation, while stress relaxation is related to fluid redistribution within the porous matrix. This stress relaxation ceases when stress within the solid matrix reaches the intrinsic compressive modulus as described above [58].

2.1.3   In Vivo deformation of articular cartilage

The high levels of physiological loading experienced by cartilage lead to the significant deformations experienced within it. The varying magnitudes of physiological loads experienced in articular cartilage are generally reported within the lower and upper joint extremities [60,61]. By in large, the peak magnitudes of such loads are a function of the body weight of any given subject e.g. 2.5 to 4.9 x body weight in the hip during walking [61–63]; and 4 x body weight in the knee [64]. In the upper extremities peak magnitudes are almost

equivalent to body weight, e.g. 0.9 x body weight in the glen humeral joint during abduction [60].

In general, the loading regime in a di-arthrodial joint is cyclical and/or intermittent. The mean contact stresses produced by these loads during non-strenuous daily activities are in the region of 2 MPa, whilst strenuous activity can result in stresses approaching 6 MPa [62,65,66]. It is estimated that the largest contact stress in non-traumatic conditions is 12.6 MPa [67]; although in vivo measurements of femoral prostheses have measured contact stresses as high as 18 MPa [61]. These loads highlight the importance of the interstitial fluid in balancing these extremely high contact stresses. The high water content, low permeability and composition of articular allow this pressurization of the interstitial fluid in order to resist these large contact stresses.

Changes in cartilage thickness from 6 - 20 % have been reported for physiological loading levels of 1 to 5 x body weight [68]. This highlights the large intermittent mechanical environment that this tissue is subjected to and therefore must be of some consideration before either implanting inferior biomechanical constructs or cells that do not respond well to such stimulus.

2.2   Articular cartilage injury

The major need for cartilage tissue engineering, as outlined previously, is the inability of cartilage tissue to self-repair following injury. Defects in cartilage can arise either through overloading of the joint (e.g. sporting injuries) or pathogenically through a degenerative disease known as osteoarthritis (OA). Defects caused by such exist in three types; matrix disruption, partial thickness defects and full thickness defects.

Matrix disruption is generally the result of blunt trauma arising from incidents such as traffic collisions [12]. Sufficient but not extreme damage to the extracellular matrix (ECM)leads to the remaining viable chondrocytes increasing their synthetic activity to facilitate tissue repair.

Partial thickness defects (e.g. fissures, etc.) are disruption to the cartilage surface that do not penetrate the subchondral bone. For some unknown reason, nearby residing cells begin to proliferate immediately following the incident in a cellular attempt to fill the defect but terminate this activity before fully repairing the tissue.

Full thickness defects penetrate through the cartilage layer into the underlying subchondral bone. The normal wound healing response ensues as a fibrin clot fills this defect following damage. This injury is unique in the fact that it has access to bone marrow stem/progenitor cells, which can migrate to fill the defect [69,70]. The resulting repair tissue formed is generally an intermediary between fibro- and hyaline cartilage. The eventual degradation of this inferior tissue is thought to be due to its less stiff and more permeable characteristics [70].

Collectively it can be seen that each of these three defect types has an inability to fully repair in order to restore tissue function. Insufficient mechanical function of cartilage only leads to enhanced degeneration cartilage tissue and surrounding areas, such as the subchondral bone, during daily motion. This vicious circle of injury and degeneration is a major problem especially considering the lack of viable regenerative medicine strategies that exist to date.

The limited self-repair capacity of cartilage following injury may have a few explanations. Chondrocytes have a relatively low metabolic activity perhaps simply because these cells do not need to proliferate in order to maintain cartilage tissue [12]. Apart from full thickness defects, the limited access to stem/progenitor cells as well as the low density of chondrocytes within cartilage may mean very few cells occupy the defect site; thus preventing proliferation in an attempt to repair the tissue. In addition, cell adhesion is often prevented by proteoglycans present in cartilage tissue, further undermining the native repair process by inhibiting proliferation [71,72]. A combination of these factors may collectively impinge on the mechano-sensing mechanism of chondrocytes. This would lead to an inability of cells to respond to tissue damage, and explain the absence of an articular cartilage self-repair process. This lack of self-repair process coupled with repair procedures, which are either expensive or lack efficacy, make cartilage and joint degeneration a very large problem.

This degenerative state and lack of tissue function causes severe pain during articulation of the joint and can seriously debilitate a person's life. According to estimates from the National Institute of Arthritis and Musculoskeletal and Skin Diseases more than 20 million Americans currently suffer from OA [7]. Conservative estimates suggest that 35-40 million Europeans have OA. Statistical data from epidemiological studies suggest that arthritis is the number one condition associated with functional limitation and physical disability among US population aged 65 and older, in addition to affecting 30 % of the population [7]. It is expected that by 2030, 20 % of adults will have developed OA in Western Europe and North America. OA is an important cause of disability-adjusted-life years in both the developed and developing world [5]. Therefore, OA is expected to be a heavy economic burden on healthcare systems and community services in Europe, North America and the rest of the world as the population expands and the number of older people increases. 3 An effect means of solving this growing problem is therefore extremely important [7].

2.3 Cartilage tissue engineering

The development of a successful repair strategy for both chondral and osteochondral defects require the establishment of certain design criteria. Firstly, viable cells are needed to engineer the proteins necessary to recapitulate the structure and composition of articular cartilage or subchondral bone. Secondly, the proteins produced by these cells must be tissue and site specific in order to restore the structure of the required area. Thirdly, the ability to integrate firmly with the host tissue through either natural or artificial means is important. Finally, the strength to withstand the highly loaded, biomechanical environment of the joint is also a key factor.

In order to meet these design criteria, tissue engineering traditionally uses a triad combination of approaches:

- Viable cells used to produce site-specific matrix molecules.

- A 3-D biomaterial that provides a structural support and housing for the cells in which to form the desired tissue.

- Biochemical (growth factor) and/or mechanical (e.g. deformation) stimulus to encourage differentiation of the cells and the enhanced production of extracellular matrix.

Chondrocytes, the primary cell type within cartilage, have been the traditional source for viable cells. However, sourcing these cells creates an additional defect within the site of the patient or donor through an invasive surgery. Also there is the inability to obtain sufficient numbers of these cells from the biopsy obtained following surgery. In addition, when culture expanded in 2-D, chondrocytes have a tendency to de-differentiate toward a fibrotic phenotype producing collagen type I instead of the desired cartilage specific collagen type II [73]. Moreover when using expanded chondrocytes there can be an age related loss in yield, proliferation and chondrogenic capacity [74], and chondrocytes isolated from osteoarthritic patients exhibit reduced collagen synthesis and may have increased DNA damage [75,76]. These inadequacies in the use of chondrocytes have led to the idea of using mesenchymal stem cells (MSCs) as an alternative.
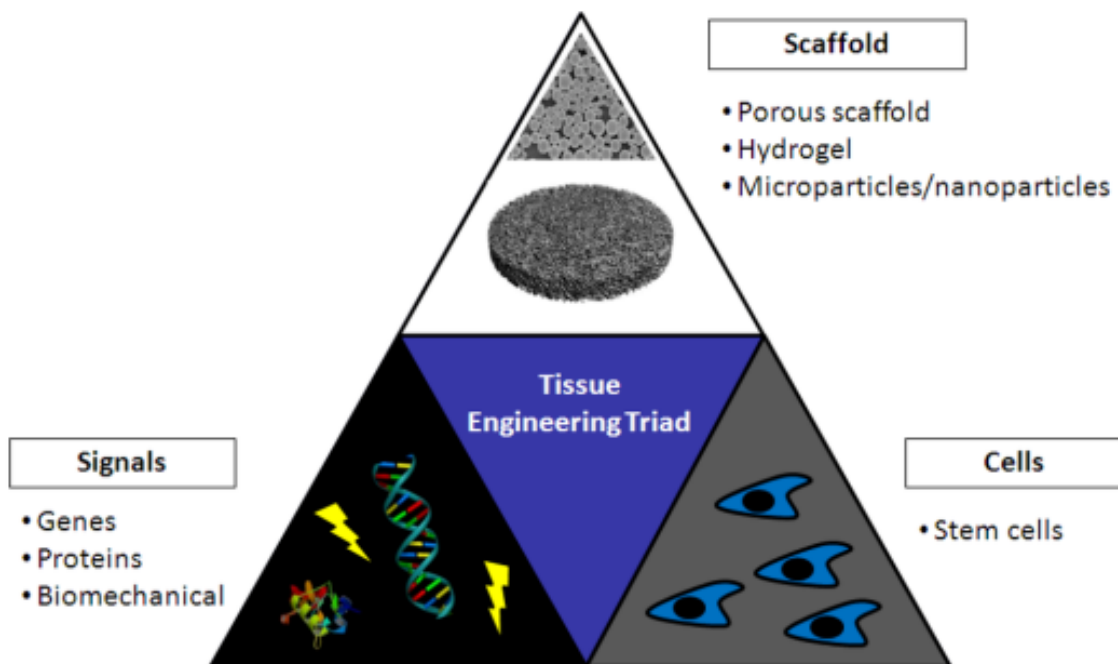
Figure 2.2 The traditional triad approach of tissue engineering. Taken from http://www.mdpi.com/.

2.3.1 Mesenchymal Stem Cells (MSCs)

Stem cells, in general, are undifferentiated cells capable of undergoing self-renewal and multi-lineage differentiation. Stem cells originate from embryonic and postnatal tissues. Embryonic stem cells can be derived from the blastocyst and are described as totipotent since they are capable of developing into lineages of all three embryonic germ layers; endoderm (liver, pancreas, thymus, thyroid and lung), mesoderm (bone, cartilage .muscle, heart and kidneys) or ectoderm (skin, brain eyes and neural tissue) [77]. However, much controversy surrounds the use of human embryonic stem cells. The many ethical issues and legal constraints surrounding their use make them an unattractive source of stem cells. An alternative source of stem cells is of postnatal origin, and of particular relevance to orthopaedics and other disciples are the mesenchymal stem/progenitor cells (MSCs) [78]. These are multipotent cells present in many adult mesenchymal tissues such as bone marrow, adipose tissue, muscle and synovial membrane [79].

The discovery that non-haematopoeitic MSCs of the bone marrow selectively adhered to plastic allowed for their isolation from the non-adherent haematopoeitic cells present in the bone marrow. These cells, when expanded on plastic, exhibit a homogenous population of cells with a spread, fibrotic morphology, which can form colonies during 2-D monolayer expansion. This gave rise to the original term of marrow stromal fibroblasts: known today as either mesenchymal stem cells (MSCs), mesenchymal stromal cells (MSCs) or mesenchymal progenitor cells (MPCs). Debate still remains as to whether these cells can be appropriately called stem cells [80–82]. Regardless they still exhibit some potency and can be differentiated down the adipogenic (fat), osteogenic (bone), chondrogenic (cartilage) and myogenic (muscle) lineages.

Bone-marrow derived MSCs have therefore good proliferative potential and possess the ability to differentiate into a range of tissues. It has been stated that only 0.001 - 0.01 % of cells resident in adult bone marrow comprise MSCs. Identification of a range of surface markers allows the characterisation of these cells [11]. Various techniques, such as flow cytometry and magnetic bead isolation, allow for the isolation of cells from the marrow population with the relevant surface markers pertaining to MSCs. Many researchers, however, continue to use the plastic adherence technique to isolate MSCs from the other cell populations within bone marrow aspirates.

2.3.2 Chondrogenic growth factors

Chondrogenic differentiation can be directed by different growth factors or cytokines. These include bone morphogenic proteins (BMPs) [83], members of the transforming growth factor-β(TGF-β) superfamily [14,84], fibroblast growth factors (FGFs) that can be also be used to increase proliferative potential during expansion, insulin like growth factor (IGF-1), Indian hedhehog and others [85]. The most widely used is TGF-β_1 or TGF-β_3. A timescale for the synthesis of a cartilage matrix as a result of TGF-β induced chondrogenesis is shown below. The synthesis of matrix components is divided into three stages: 0 - 6 days, 6 - 8 days

and 8 - 21 days, which relates to gene expression, protein synthesis, and both the synthesis and accumulation of glycosaminoglycan (GAG) [86]. While the use of growth factors to direct MSC chondrogenesis generally results in a reasonable cartilage template, it fails to meet the standards of chondrocyte laden biomaterials in terms of tissue deposition and mechanical properties [87]. Therefore further avenues, such as incorporating mechanical stimuli, need to be sought in order to enhance and improve the cartilage template produced.
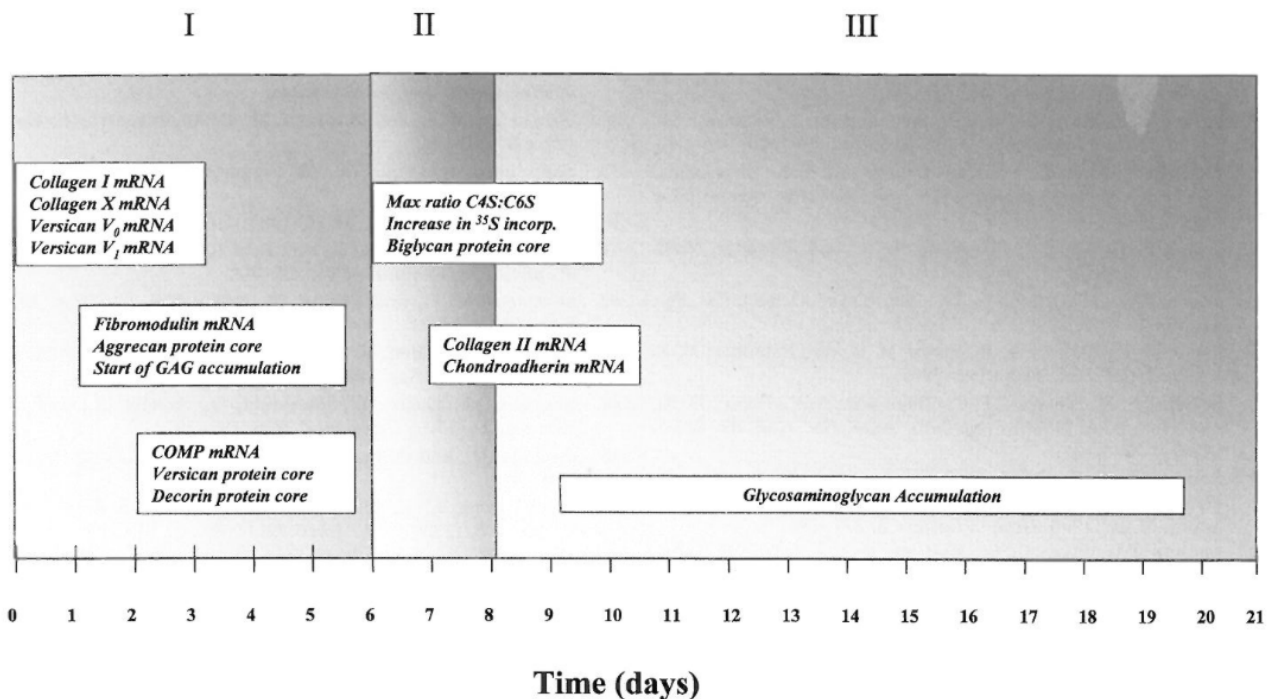
Figure 2.3 Defined events in chondrogenic differentiation of mesenchymal stem cells determined by the sequential expression of matrix components during pellet culture. [86]

2.3.3   Chondrocyte fate and differentiation

The process and stages of chondrogenesis *in vitro* can be directly related to how chondrocytes are derived in the early embryo from mesenchymal cells that migrate into presumptive skeletogenic sites [88]. The cells become tightly packed at these sites and form cell mass condensations that prefigure the future skeletal elements [89,90]. During

this process, the chondrogenically committed MSCs express extracellular matrix and cell adhesion molecules such as N-cadherin, N-CAM (Ncam1), tenascin C (Tnc), versican, and thrombospondin-4. Expression of mesenchymal and condensation markers are turned off by prechondrocytes that emerge in the centre of these condensations and start to express Col2a1 and other early cartilage markers.

A strong increase in cell proliferation and deposition of cartilage matrix are key indicators that prechondrocytes have overtly differentiated into fully committed and active chondrogenic cells. Col2a1 expression is upregulated and a different splice variant of the gene is produced (type IIB instead of type IIA [91]. The cells also start to express Agc1, Cartl1, the genes for the collagen types IX and XI, and other cartilage extracellular matrix components at high levels. These cells are referred to as chondroblasts rather than chondrocytes as they rapidly proliferate and build new tissue, rather than limiting their activity to maintaining the functional integrity of mature cartilage tissue [92].

During development of long bones, early chondroblasts in the metaphyses start to form columnar zones once the cells in the diaphyses have undergone prehypertrophy and proceed toward terminal maturation. Initially small and round, they become flattened and organized into parallel, longitudinal columns. They proliferate at the highest rate at the top of the columns (away from the primary ossification center) and progressively decrease their proliferation rate as they move down the columns [93]. They undergo irreversible growth arrest as they convert into prehypertrophic chondrocytes, one layer at a time, at the bottom of the columnar zone. The cells in the diaphyses, however, at the prehypertrophic stage, they contain higher levels of RNA for Col2a1, Agc1, and most other early cartilage matrix genes than chondroblasts, and sequentially activate the genes for the parathyroid hormone and parathyroid hormone-related peptide receptor (Pthr1), Ihh, and Col10a1. At the hypertrophic stage, they cease to express early cartilage matrix genes and also terminate expression of Pthr1 and Ihh. They upregulate expression of Col10a1 and activate the gene for the vascular endothelial growth factor (Vegf). This large shift in cell fate, and the mechanical cues regulating this, will be discussed further in subsequent sections [92,93].

This cascade of transcriptional factors is part of the process that results in the development

of articular cartilage or long bone tissue. There are a number of ways of detecting these stages as they occur. Genetically, real-time polymerase chain reaction can be used to detect select genes activated along the process and identify the state of the chondrogenic or hypertrophic development. Histology and immunohistolchemistry can be used to stain for specific cartilage and hypertrophic markers previously mentioned. Finally, constructs can be papain digested and biochemically tested for matrix components such as sGAG and collagen; or reconstituted with HCl and tested for calcium content, for example. These processes underpin the ways in which chondrogenesis and hypertrophy can be identified throughout culture in this thesis.
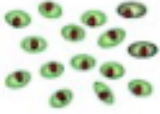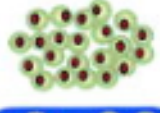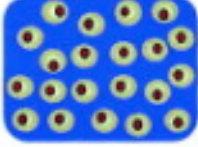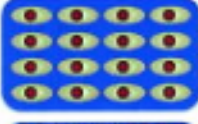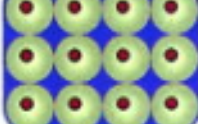
Figure 2.4 Schematic of the successive steps of the chondrocyte differentiation pathway as they occur during development of endochondral bones, highlighting major histological features, extracellular matrix markers, and regulatory markers expressed at each step.

2.3.4 Hydrogels supporting MSC chondrogenesis

Biomaterials are often used to assess cell metabolism and matrix synthesis under different conditions, with a view to create a functional tissue for implantation. As chondrocytes adopt a round 3-D morphology to maintain their phenotype, it is widely considered that this cell shape is preferred for chondrogenesis. Ideally, a biomaterial should be three-dimensional (3-D),

biogradeable, non-toxic both initially and following enzymatic degradation, non-immunogenic and easily manufactured [94]. Scaffolds must have both high porosity and permeability to permit the transport of nutrients and waste to and from cells located at the scaffold core. Scaffolds must be able to withstand biomechanical loading.

Hydrogels are a commonly used class of scaffold in many tissue engineering disciplines including that for cartilage. Hydrogel materials include agarose, alginate, chitosan, collagen, fibrin, poly(ethylene glycol), poly(vinyl alcohol) (PVA) and pluronics as examples [95]. They are beneficial in the fact that many have the potential to be formed in situ. The swelling nature of hydrogels also produces an aqueous environment for encapsulated cells that is comparable to soft tissues, such as cartilage, and the exchange of nutrients is facilitated by their high water content. They can also be combined with plastic, biocompatible scaffolding platforms. These platforms can be easily bioprinted and have the advantage of providing biomechanical integrity while also allowing the hydrogel within to provide the necessary cellular stimuli to direct differentiation.

2.3.4.1   Agarose hydrogel

Agarose, a linear polysaccharide extracted from marine red algae, is a thermosetting hydrogel that undergoes gelation in response to reduction in temperature due to hydrogen bonding of entangled chains that form the gel. Agarose has been extensively used for studies involving the addition of biomechanical stimuli in which gels are deformed. It is an attractive gel for these purposes due to its ability to withstand sustained mechanical loading as well as its strong chondrogenic potential.

The use of agarose in so called mechanobiology studies has particularly focussed on cyclical dynamic compression using both chondrocytes and MSCs [96–98]. Computational models have also been used to assess spatial variations in the local mechanical environment due to applied loads within the well-defined agarose, mechanobiology model [99,100].

2.3.4.2   Alginate hydrogel

Agarose is classically used in mechanobiology studies for the reasons above but lacks the required degradation to permit vascularisation and bone formation. Therefore while a good hydrogel candidate for mechanobiology studies involving chondrogeneis, it is not suitable for the bone layer in osteochondral tissue engineering approaches. Alginate has been extensively used for both chondrogenesis, endochondral ossification and osteogenesis. Therefore it would suit initial stages of osteochondral graft development with the long-term goal of using a biphasic hydrogel approach to recapitulate both the cartilage and bone layer.

Alginate is a naturally occurring anionic polymer typically obtained from brown seaweed. Its biocompatibility, low toxicity, relatively low cost, and mild gelation by addition of divalent cations, such as Ca^{2+}, make it suitable for use in many biomedical applications. In addition, there are several cross-linking methods for gelating alginate making it a versatile biomaterial; and also the structural similarity of alginate to extracellular matrices of living tissues allows its application in wound healing, delivery of bioactive agents such as small chemical drugs and proteins, and cell transplantation [101].

Alginate varies in molecular structure and as such it is important to understand the chemical constituents that encompass the biomaterial. D-mannuronate and the more recently discovered L-guluronate residue [102] are regarded as the major components of alginate. The use of magnesium and calcium salts in fractional precipitation showed that alginate is composed of copolymer blocks, which has a ratio of guluronate to mannuronate that varies depending on the natural source [103]. Alginate is now known to be a whole family of linear copolymers containing blocks of (1,4)-linked β-D-mannuronate (M) and α-L-guluronate (G) residues. The blocks are composed of consecutive G residues (GGGG), consecutive M residues (MMMM), and alternating G and M residues (GMGM). Different alginate extract sources have been shown to change the M and G contents as well as the length of each respective block, and more than 200 different alginates are currently undergoing manufacturer [104]. Divalent cations (e.g., Ca^{2+}) are only believed to cross-link the G-blocks of alginate in order to form a gelated alginate hydrogel. The composition (i.e., M/G ratio), sequence,

G-block length, and molecular weight are thus critical factors affecting the physical properties of alginate and its resultant hydrogels [105].

There are various ways to cross-link alginate chains to prepare gels. Thermal gelation and covalent crosslinking chemistry are among two of the three ways in which alginate gels can be formed. Thermal gelation can be problematic to work with in vitro despite its in vivo potential as an in situ forming gel. Covalent crosslinking involves the use of potentially toxic chemicals that can be hazardous to cell viability. Therefore, the last of the three options, ionic crosslinking has proven the most popular means of gelating alginate chains. Combining the viscous alginate solution with exogenous, ionic-crosslinking agents, such as divalent Ca^{2+} cations, solely allows binding of the guluronate blocks of the alginate chains enabling alginate gelation. Gelation using ionic agents binds the guluronate blocks of one polymer with adjacent guluronate polymer chains in of aformation of cross-linking known as the egg-box model [106]. Calcium chloride ($CaCl_2$) is one of the most frequently used agents to ionically cross-link alginate. The advantage of rapid gelation using calcium chloride is counteracted, in part, by poorly controlled gelation caused by high solubility of calcium chloride in aqueous solutions. Other solutions can be mixed with alginate in a syringe system to allow slow, controlled gelation. This, however, can lead to bubbles forming within the solution and therefore substantial loss of cells containing material during gel fabrication. Higher mechanical integrity and greater uniformity can, however, be achieved.

Chemically-modified alginates, which typically incorporate cell-binding peptides to enable greater cell-substrate interactions, provide a means to mimic native cell-matrix interactions in biomaterials that lack natural cell-matrix binding sites. Carbodiimide chemistry can be used to couple various cell-binding peptides via the carboxylic groups of the sugar residues in alginate chains. This attaches a cell-binding peptide as a side chain to the alginate polymer structure. Peptides including the sequence arginine-glycine-aspartic acid (RGD) have been extensively used as model adhesion ligands, due to the wide-spread presence of integrin receptors (e.g., $\alpha_v \beta_3$, $\alpha_5 \beta_1$) for this ligand on various cell types. Water-soluble carbodiimide chemistry can be used to couple these RGD peptides. A likely tissue-specific minimum concentration of RGD peptides in alginate gels is needed for the adhesion and growth of

cells. The affinity of the RGD peptides is also important as it can increase the potency of the peptide; thus lowering the effective concentration of peptide needed to change cellular adhesion. Cyclic peptides tend to have a greater potency than linear RGD peptides [101]

Alginate gels have been used across many tissue engineering disciplines. MSCs within alginate hydrogels have the ability to undergo chondrogenesis, myogenesis, adipogenesis and osteogenesis. The in situ gelation of alginate motivates its use as a delivery vehicle for endothelium cells to damaged areas of myocardium tissue. Alginate gels are also being to be used to assess how biomechanical stimuli affect stem cell fate due to the ease with which the stiffness of these hydrogels can be varied [29]. Both crosslinking density and polymeric concentration can be used to effect bulk stiffness of ionically crosslinked alginate gels.

There is a small area of debate surrounding the use of RGD-modified alginate gels in the context of cartilage tissue engineering. Some papers suggest peptide introduction alone to alginate chains is inhibitory to chondrogenesis [107]. The addition of higher RGD concentrations results in an enhanced inhibitory effect. Others suggest the incorporation of RGD-peptides in microcavity forming alginate gels to be beneficial [108]. Regardless of its effect on chondrogenesis, it is still a useful tool to possibly enhance the mechanosensing of matrix deformations through integrin binding complexes. These integrin complexes have been shown to be involved in multiple mechanotransduction mechanisms [109,110]. This suggests a benefit of RGD-peptide incorportation in tissue engineering experiments involving different biomechanical stimuli.

2.4   Hypertrophy in cartilage tissue engineering

Terminal differentiation of chondrocytes during MSC chondrogenesis presents both a tissue engineering challenge and opportunity. Over time MSCs tend to acquire hypertrophic properties owing to their terminal differentiation along the endochondral pathway leading to bone formation [111,112]. Cartilage tissue engineering seeks to stabilize the chondrogenic phenotype and suppress hypertrophy of chondrogenically-primed MSCs. Engineering

endochondral bone, however, leverages this mechanism by mimicking the process of long bone growth. An ability to modulate the process in different conditions and recapitulating these in a single construct could lead to the development of an osteochondral graft of both stable and hypertrophic cartilage respectively.

2.4.1 Characterisation of chondrogenic hypertrophy

Chondrogenic hypertrophy is characterised by a greater than 10-fold increase in cell volume, as well as ECM structural remodelling [113]. Cell function is affected by this dramatic expansion in cell volume [114]. Changes in intracellular and extracellular osmolarity; peripheral ECM degradation; and increasing number of organelles around the cell occur as a result of the explosive change in cell volume [115]. Images taken stereoelogically show osmotic swelling to be responsible for most of the cell volume increase. An increase in cytoplasmic concentration or a decrease in extracellular osmolarity can result in swelling that is followed by aquaporin-mediated movement of water to re-establish iso-osmotic conditions [116]. The abundance of proteoglycans coupled with their high negative fixed charge mean that these ECM molecules are the prime contributors to generation of osmotic pressure within cartilage. It remains unclear whether the expression of terminal markers results in increased cell volume or vice versa.

Chondrocyte hypertrophic differentiation is the gradual development process from chondrogenic differentiation to cartilage mineralization, which is characterized by a series of markers; each of which have their own function in the process of cartilage mineralization [117]. For example, the transcription factors, runt-related transcription factor 2 (RUNX2) and myocyte enhancer factor-2C (MEF2C), drive the expression of terminal differentiation markers, including matrix metalloproteinase 13 (MMP13), collagen type X (COLX) [118], Indian hedgehog (IHH) [119], alkaline phosphatase (ALP), and vascular endothelial growth factor (VEGF) [112,120], which all functionally contribute to endochondral ossification. Secreted MMP13 degrades COLII and AGC, key ECM components of functional cartilage

[121]; COLX serves as a framework for subsequent calcification through matrix vesicles (MV); ALP hydrolyses pyrophosphate (PPi) to inorganic phosphate (Pi) which, in the presence of calcium, forms hydroxyapatite [122]; and IHH induces the proliferation of non-hypertrophic chondrocytes [123].

Calcification of cartilage ECM originates at MV [124]. ECM mineralization to endochondral bone formation consists of three steps: (1) Hydroxyapatite crystals are formed inside the MV; (2) Hydroxyapatite crystals penetrate MV into the ECM; and (3) Endochondral ossification. The final stages of endochondral ossification include the degradation of the calcified matrix, VEGF-mediated vascular invasion of the calcified zone, and deposition of osteoid on the calcified trabeculae by osteoblasts, are all under the control of MMPs [125]. Development of MV depends on MMPs that can calcify the growth plate. Finally, calcification is substituted by endochondral bone. MMP13 binding to the MV membrane and cooperating with MMP9 could promote the release of VEGF in apoptotic chondrocytes, further accelerating the formation of vascularity in the growth plate [126].

2.4.2   Factors affecting chondrogenic hypertrophy

The use of pharmaceutical inhibitors to inhibit key pathways in MSC hypertrophy has been extensively used to enable a reduction in MSC hypertrophy. This, however, in clinical translation could lead to ectopic tissue formation caused by the uncontrolled release of these pharmaceutical factors to undesired sites. As an alternative, researchers have also tuned biomechanical stimuli within their tissue engineering approaches in order to alter MSC hypertrophy. Such factors include, oxygen tension as an environmental factor; substrate stiffness as an intrinsic mechanical factor defined as being directly sensed by the cells while not being externally applied; and finally extrinsic mechanical factors that require the use of external mediators, such as bioreactors, to deliver mechanical forces including dynamic compression. All of these conditions have the potential to be delivered and have been previously have shown to regulate MSC hypertrophy [21–23].

Bian et al. found that dynamic compressive loading increased the mechanical properties, as well as the glycosaminoglycan (GAG) and collagen contents of human BMSC-seeded hyaluronic acid hydrogel constructs in a seeding density dependent manner. Hypertrophic markers were shown to be significantly reduced and calcification was suppressed within these constructs [22]. This is one example of several papers that have linked dynamic compression with a suppression of MSC hypertrophy following TGF-βinduction chondrogenesis. The authors further reported that hydrogel properties such as polymeric density and crosslinking time that correlate with stiffness both affect the extent of chondrogenic hypertrophy. A low stiffness gel acted to accelerate hypertrophy based on greater calcium and collagen type X deposition [22]. In addition to these factors, normoxia has been shown to enhance late stage MSC hypertrophy. Hypoxia alternatively has been shown to delay hypertrophic development within chondrogenically primed MSCs [21].

Taken together this highlights the need to optimize environmental and biomechanical conditions in order to control MSC hypertrophy and endochondral ossification. All in all biomechanical stimuli clearly play a role in MSC hypertrophy. This is further evidence for investigating their use in engineering osteochondral grafts using MSCs.

2.4.3   Trophic effects of MSCs

Adult marrow-derived Mesenchymal Stem Cells (MSCs) are capable of dividing and their progeny are further capable of differentiating into one of several mesenchymal phenotypes such as osteoblasts, chondrocytes, myocytes, marrow stromal cells, tendon-ligament fibroblasts, and adipocytes. In addition, these MSCs secrete a variety of cytokines and growth factors that have both paracrine and autocrine activities. These secreted bioactive factors suppress the local immune system, inhibit fibrosis (scar formation) and apoptosis, enhance angiogenesis, and stimulate mitosis and differentiation of tissue-intrinsic reparative or stem cells. These effects, which are referred to as trophic effects, are distinct from the direct differentiation of MSCs into repair tissue. Several studies which tested the use of

MSCs in models of infarct (injured heart), stroke (brain), or meniscus regeneration models are reviewed within the context of MSC-mediated trophic effects in tissue repair [127].

MSCs do more than respond to stimuli and differentiate. It has been documented that newly committed progenitors synthesize a broad spectrum of growth factors and cytokines that have effects on cells in their vicinity [128]. The function (paracrine and autocrine) of the secreted bioactive factors can be either direct or indirect or even both. Direct by causing intracellular signalling or indirect by causing another cell in the vicinity to secrete the functionally active agent. This indirect action is referred to as trophic. Therefore MSCs can have two functions: MSCs can provide replacement units for expired cells in mesenchymal tissue, and MSCs can have trophic effects on cells in their vicinity without generating newly differentiated mesenchymal phenotypes. There are three distinct experimental tissue repair models in which the introduction of MSCs have dramatic effects without extensive differentiation of the therapeutic MSCsMyocardial Infarct, Strike and Meniscus Regeneration.

The brain is a complex, multi-cellular, multi- compartmented organ with its various layers and compartments nurtured by the vascular system. An interruption in vascular flow or blockade results in an injury response associated with the resulting ischemia. The cumulative effect of a vascular blockage, ischemia, and injury is summarily referred to as stroke. MSCs are capable of differentiating into neural elements and as such if introduced into an ischemic sector of the brain, may enable the restoration of pre-existing pathways or development of circumnavigating routes to re-establish neural components. Chopp and his collaborators, as well as others, have shown that MSCs can re-establish parts of coordinated function when introduced directly or systemically into the affected brain. MSC-mediated restoration of coordinated function in old rats suggested that MSCs do not differentiate into neurons or neuronal support cells and instead use an alternative mechanism [129,130]. It is proposed that the MSCs supply bioactive agents that inhibit scar formation, inhibit apoptosis, increase angiogenesis, and stimulate the action of intrinsic neural progenitor cells to regenerate functional neurological pathways (synaptogenesis, neurogenesis) with the resulting gain of coordinated function.

Several studies that administer MSCs in cardiac repair models show co-localisation of

cardaic markers with implanted MSCs. However, the therapeutic contribution of MSCs to increased heart function can be caused by multiple factors including: neo-vascularization, inhibition of scarring, decreased cardiomyocyte apoptosis, increased nerve sprouting, and direct differentiation into cardiomyocytes [131]. Despite most studies highlighting that he contribution of donor MSCs is through their differentiation into cardiomyocytes, most authors also acknowledge the extent to which heart function is restored cannot be solely attributed to this mechanism. Recent studies document the effects of transplanted MSCs expressing the pro-survival gene Akt1 [132]. The trophic effects of MSCs have been documented by Tang et al., who showed that MSCs implanted into ischemic myocardium simulated an increased production of vascular endothelial growth factor (VEGF), increased vascular density and blood flow, and decreased apoptosis, all of which were likely influenced by the secretion of bioactive molecules; the authors also present evidence that some MSCs differentiated directly into endothelial cells [133].

Finally, tearing of the meniscus lacks spontaneous repair and therefore requires therapeutic intervention. Studies by Frank Barry and colleagues detail the use of an adult goat model to document MSC-mediated regeneration of meniscus [134]. Surgical removal of the meniscus (in part combined with a severing of the anterior cruciate ligament) was followed by daily, 1 hour treadmill exercises after 2 weeks until after a month of such exercises, the goats were given an injection of 10 million autologous or allogeneic MSCs in a hyaluronan delivery vehicle or, as a control, given an injection of the hyaluronan delivery vehicle without cells. No restoration occurred in the control groups. In animals where meniscus was restored in appeared morphologically, histologically, and immunocytochemically indistinguishable from normal meniscus. Some pre-labeled MSCs could be observed in the new meniscus, but too few to account for the massive regeneration of this new tissue . It is thus interfered that the regenration of the meniscus was enabled by the secretion of bioactive agents inhibiting scarring and apoptosis at the cut surface, stimulated angiogenesis as well as host-derived reparative cells to proliferate and fabricate a new meniscus. Therefore the therapeutic role of MSCs is complex and is not solely attributed to their differentiation capacity as deemed by partial conclusions in the heart case,

punitive observations in the stroke model and a strong undocumented case in meniscus repair.

2.5   Oxygen tension as a regulator of MSC chondrogenesis

Cartilage tissue has a poor intrinsic repair capability due, in part, to its avascular nature. In vivo, cartilage resides in a low oxygen microenvironment and is exposed to hypoxic conditions of as low as 1 % oxygen [135]. Most in vitro tissue engineering strategies are performed within a 20 % oxygen environment, in conditions known as normoxia. Hypoxia is generally associated with oxygen levels below 2 % oxygen; other conditions below normoxic conditions of 20 % oxygen are generally termed low oxygen.

The ability of cells to sense and respond to changes in oxygen tension is vital for many physiological events [136]. Hypoxia-inducible factor (HIF-1) is a key transcriptional regulator of cellular responses to low ambient oxygen levels. HIF-1 is an oxygen-sensitive, dimeric complex composed of HIF-1α and HIF-1β subunits. During normoxia HIF-1α resides in the cytosol but is rapidly degraded by the ubiquitin-proteosome pathway. A reduced oxygen environment is one means of stabilising HIF-1α allowing HIF-1α to subsequently translocate to the nucleus and, in concert with HIF-1β, initiate the transcription of hypoxia-related genes such as vascular endothelial growth factor [137].

Expansion under hypoxia was reported to enhance the preservation of stemness and the subsequent differentiation potential of bone marrow-derived MSCs in vitro [138]. Another study highlighted the positive influence hypoxia (2 % O_2) has on chondrogenesis of rat bone marrow MSCs with increased Safarin-O staining and collagen type II deposition. It also demonstrated a link with HIF-1α nuclear translocation. Taken together hypoxia is a pro-chondrogenic stimulus [138].

2.5.1 Oxygen tension affecting MSC hypertrophy and endochondral ossification

During embryonic development, the permanent articular cartilage and the transient hypertrophic cartilage both arise from the same cartilaginous anlage. However, specific sets of stimuli drive these two hyaline cartilages into distinct differentiation programs. Attempts to identify the required stimuli to drive the formation of permanent articular cartilage have been largely unsuccessful to date. Recent studies suggested that oxygen levels might play a role in driving hypertrophic differentiation [139,140]. Interestingly, in the cartilage anlage, permanent articular cartilage is formed under hypoxic conditions, whereas hypertrophic differentiation of cartilage and subsequent endochondral ossification are associated with vascular invasion and, consequently, much higher levels of oxygen [141].

Various oxygen levels have linked low oxygen to a suppression of MSC hypertrophy such as Sheehy at el. in which differentiation at low oxygen (5 % O_2) of bone marrow-derived MSCs in both pellets and hydrogels was revealed to suppress markers of hypertrophy such as collagen X and alkaline phosphatase [21]. Similarly, Gawlitta et al. showed that the deposition of collagen type X in MSC aggregates was evidenced in both chondrogenically and hypertrophically stimulated cultures. However, mineralization was exclusively observed in hypertrophically stimulated, normoxic cultures [142]. Overall, the progression of hypertrophy was delayed in hypoxic compared with normoxic groups.

In a separate study conducted by Leijten et al., alternate 2.5 % O_2 levels enhanced the chondrogenesis of hMSCs micromass pellets in which GAG staining was more abundant throughout the construct in these low oxygen levels compared with lower staining concentrated predominantly in the core of the construct under normoxic conditions [141]. 2.5 % O_2 levels created a more hyaline-like, articular cartilage over the 35 day culture period as upregulation of hypertrophic markers of COLX, MMP13 and PANX3 in normoxia was severely suppressed in the 2.5 % O_2 levels. Switching of oxygen levels from low to high at the 3 week point for a period of 2 weeks decreased GAG accumulation, downregulated key chondrogenic markers and also downregulated markers particularly associated with articular cartilage,

including GREM, FRZB, DKK1 [141]. Furthermore, the study highlighted that with low oxygen pre-conditioning MSC-laden alginate implants in a 5 week, nude mouse subcutaneous model prevented the hypertrophic development of collagen type II; in contrast to the normoxia pre-implantation conditions that promoted both hypertrophy and vascular invasion [141].

Therefore hypoxia or low oxygen tends to suppress hypertrophy and generate a more hyaline-like, stable articular cartilage phenotype, while normoxia provides a hypertrophic stimulus that accelerates terminal differentiation and endochondral ossification. Appropriate use of oxygen conditions could allow models for the formation of either stable cartilage, endochondral bone formation or a switch between the two.

2.6   Cell shape

There are several studies presenting evidence that cell shape plays a role in MSC lineage commitment as well as the degree to which that commitment occurs. Several researchers have investigated the effect of spreading area and shape of stem cells cultured on both micro- and nano-patterned surfaces on differentiation lineage commitment while others have used hydrogels to present a more physiologically relevant 3-D environment. The basic motivation being connective tissue cells differ greatly in phenotype. Although they descend from a common mesenchymal stem cell (MSC) precursor, differentiated adipocytes are round and fat-laden [143,144], while osteoblasts vary from elongated to cuboidal, depending on their matrix deposition activity [145,146]. The shapes of these cells serve their specialized functions, while simultaneously driving their multicellular organization. A round, spherical shape allows for maximal lipid storage in adipose tissue, while cell spreading facilitates osteoblast matrix deposition during bone remodeling [147].

2.6.1   Regulating myogenic and chondrogenic differentiation

TGF-β_3 has been linked with both myogenesis and chondrogenesis. Therefore when culturing in TGF-β_3 supplemented media, there is the potential for a myogenic or chondrogenic lineage commitment switch [148]. This potential has been clearly demonstrated by Gao et al. when culturing MSCs in these conditions on micro-patterned surfaces of varying sizes. The contact surface area enabled or inhibited cellular spreading. MSCs that took on a flattened and spread cell shape were found to differentiate towards a myogenic lineage and exhibited higher Rac1 activity. In contrast, when cell spreading is prevented TGF-β_3 fails to activate Rac1 and instead leads to an upregulation in chondrogenic genes. Constitutive activation of Rac1 induced myogenic differentiation when MSCs were grown in non-differentiating medium, while inhibition of Rac1 activity was required but not sufficient for inducing chondrogenesis [148]. Cell-cell contact and the expression of the cell adhesion molecule N-cadherin were

found to be strongly correlated with myogenesis, with exposure to TGF-β_3 increasing the expression of N-cadherin only in the spread cells [148].
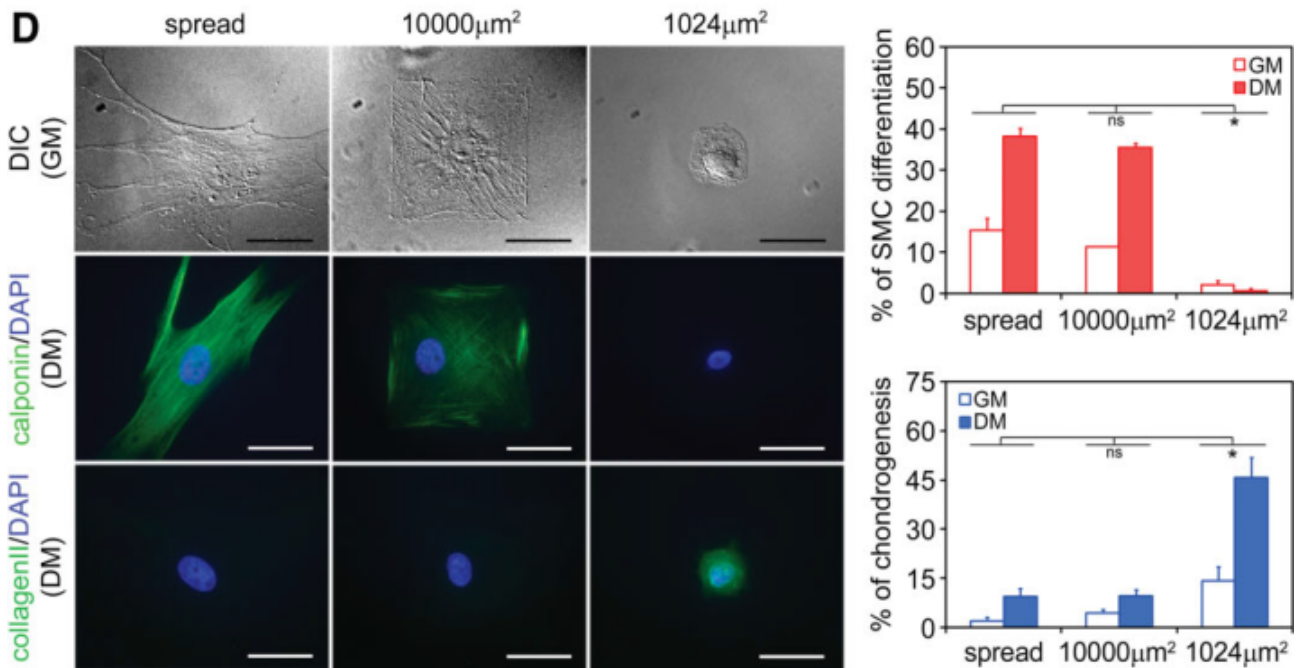
Figure 2.5 Cell shape mediated changes in differentiation using micro-patterned islands [148]. Cells were placed on islands of area 1,024 or 10,000 µm^2 in size and compared to cells allowed to spread in an unconstrained environment.

Tay et al. investigated the differentiation of hMSCs toward the myogenic lineage when these cells were cultured on thin PLGA films with micro-patterned fibronectin islands. Human MSCs cultured on micro-patterned surfaces in expansion medium were found to be highly elongated with small adhesive areas of approximately 2000 µm^2, whereas hMSCs cultured on unpatterned surfaces had flat morphologies with large adhesive areas of approximately 10,000 µm^2 [149]. Several hallmark neurogenesis (NeuroD1, nestin, GFAP, and MAP2) and myogenesis genes (GATA4, MyoD1, cTnT, and β-MHC) were upregulated in hMSCs on micropatterned surfaces in expansion medium, whereas osteogenic genes (alkaline phosphatase, RUNX2) were specifically downregulated or remained at normal levels [149].

Myogenic lineage proteins, such as cardiac myosin heavy chain (MHC), predominantly existed in hMSCs cultured on micropatterned surfaces. The enforced cell shape distortion resulted in the rearrangement of the cytoskeletal network and altered the shape of the nucleus, indicating the mechanical deformation of hMSCs translated into a biochemical response and ultimately contributed to specific differentiation toward a specific lineage, such as the myocardial lineage [149].

Even in the absence of soluble factors MSCs can begin to differentiate along specific lineages in response to topographical cues alone. Seeding hMSCs onto thin films of polylactic- co-glycolic acid (PLGA) printed with fibronectin lead to an up-regulation of mainly myogenic markers, but expression of neurogenic markers were also observed, due to a highly elongated shape over a small area [149]. Controls on non-patterned substrata adhered to the surface causing them to be thin and spread, which produced no increase in myogenic or neurogenic markers. This biochemical response was perceived to be due to large-scale rearrangements in cytoskeletal components and altered nucleus shape, which are enforced by modulation of cell morphology [149].

As well as directing stem cell fate in the absence of specific growth factors, cell shape also modulates biochemical mediation of differentiation in 3-D environments [150]. Free swelling culture of adipose stem cells (ASCs) within a collagen type I hydrogel in chondrogenic media initially induces chondrogenic gene expression, but this is suppressed by day 14. After blocking β-1 integrin in order to hinder cellular spreading, chondrogenic markers were promoted [150]. Blocking β-1 integrin, a key trans-membrane receptor that controls attachment to the cell and its ECM, causes a down-regulation in Rock-1 and -2 genes, producing a rounded cell shape, both of which are key factors in modulating chondrogenic differentiation. Therefore integrin binding is important in late stages of chondrogenic growth and can be regarded as a putative mechano-sensor in chondrogenically primed SCs [150].

Thorpe et al. found that in agarose hydrogels, cell adopted a round morphology and underwent chondrogenesis, while in fibrin hydrogel MSCs spread and expressed markers of myogenesis [151].

Arginine-glycine-aspartic acid (RGD) modified hydrogels, which support cell adhesion,

have also been used to systematically investigate the influence of cell shape and cell-matrix interactions on SC fate. It was found that interactions with the RGD-modified hydrogels promoted BMSC spreading in a density-dependent manner and involved in receptors. In the presence of media containing chondrogenic supplements, the RGD modified agarose gels inhibited the stimulation of sGAG formation, but disrupting the F-actin cytoskeleton with cytochalasin D could prevent this reduction in sGAG formation. In the presence of serum-supplemented media, however, osteogenic gene markers were enhanced. These results show that the cell shape effects stem cell differentiation and this depends on the biochemical composition of the microenvironment [107]. Other studies contract these findings by showing that culture in RGD-modified hydrogels produced significantly greater cartilage-specific gene up-regulation and ECM production than in pellet culture or unmodified poly(ethylene glycol) gels [152].

To add to all this, chondrocyte growth in 2D culture that stimulates a flattened cell shape leads to "de-differentiation" and a shift from a chondrogenic phenotype to a more fibroblastic phenotype [153]. The native shape of chondrocytes is retained in a 3D shape using pellet culture [154] or by encapsulation in a gel such as agarose or alginate [155]. Interestingly, chemical alteration of the actin cytoskeleton can partially restore some of the phenotypic changes [156,157] . In this light, a number of studies have shown that the differentiation of adult or embryonic stem cells into a chondrogenic phenotype requires a rounded cell shape, either through pellet (e.g., micromass) culture, or through the use of gel-based artificial encapsulation systems [14,158]. Indeed, chondrogenic markers were enhanced in round morphologies when directly comparing the cell and nuclear shape of bone-marrow derived MSCs [159].

2.6.2   Regulating osteogenesis and adipogenesis differentiation

Similarly to the use of TGF-β_3, a mixed osteo-adipo media can enable commitment of MSCs along both osteogenesis and adipogenesis in both 2-D and 3-D. A seminal paper in the field

of cell shape mediated differentiation by McBeath et al. was the first to demonstrate this influence of cell shape [160]. Human MSCs were seeded onto micro-patterned islands to again control the degree of cell spreading and then cultured in a mixed media containing both adipogenic and osteogenic factors. Cells on small islands took on a round shape and underwent adipogenesis, while cells on larger islands spread and underwent osteogenesis. Cell-shape mediated regulation of SC fate was found to depend on myosin generated cytoskeletal tension, with greater RhoA (a cytoskeletal re-organising enzyme) and ROCK (the downstream Rho effector) activity in spread cells compared to round cells [160]. Expressing dominant-negative RhoA was found to promote adipogenic differentiation, but only in rounded cells. The activation of the RhoA effector, ROCK, was also found to induce osteogenesis in hMSCs regardless of cell shape through myosin-actin generated tension [160]. These results highlight the importance of cytoskeletal tension, generated through the myosin-actin network integration, in mechanotransduction and in directing stem cell fate. The paper also points to the different mechanisms of cell shape influence on MSC differentiation in comparison to the follow-up study conducted by Gao et al. that demonstrated Rac1 playing a role in cell shape mechanotransduction as a means of SC fate switching [148]. These findings are supported by studies showing significant changes in the F-actin cytoskeleton and cellular mechanical properties during differentiation of MSCs into chondrocytes or osteoblasts.

Another more recent paper to examine the underlying mechanism of stem cell fate toward either osteogenesis or adipogenesis decoupled a very important additional stimulus that directs this commitment to either lineage; cellular traction [29]. Through a range of hydrogel biomaterials to decouple matrix interactions; hydrogel stiffness variations to identify structural effects; and hydrogel degradation to mediate cellular traction, it was shown that ultimately cellular traction directs osteogenesis not adhesion or matrix stiffness. Adhesion is, however, necessary to facilitate traction-mediated response but is not the ultimate cell fate mediator [29].

Author	2D or 3D	Cell Shape Control Mechanism	Outcomes
Gao et al. [148]	2D	micro-patterned surfaces of varying sizes	Round cells ↑ chondro, spead cells ↑ myo via Rac1
Tay et al. [149]	2D	micro-patterned surfaces of varying sizes	
Lu et al. [150]	2D vs 3D	Integrin blocking	Integrin blocking (round cell) ↓ osteo genes (Rock-1, Rock-2)
Thorpe et al. [151]	3D	Agarose vs. fibrin hydrogels	Agarose (round) ↑ chondro genes, Fibrin (spread) ↑ myo genes
Connelly et al. [107]	3D	Absence or presence of RGD ligands	Presence of RGD ↓ sGAG (chondro)
McBride et al. [159]	2D	Cell seeding density	Higher cell seeding density, more round cell shape, ↑ chondro gene expression (Sox9, Aggrecan)
McBeath et al. [160]	2D	micro-patterned surfaces of varying sizes	Round cells ↑ adipo, spead cells ↑ osteo via ROCK

Table 2.1 Summary of literature findings on MSC differentiation in response to cell shape.

2.6.3 Summary

The consistent tread in this cell shape story is that round cells enhance chondrogenesis or adipogenesis depending on on the type of growth factor supplementation. This is controlled

in part at least through the Rac1 pathway in the chondro-/myo-genesis fate switch or via the ROCK signalling pathway in the adipo-/osteo-genesis lineage commitment choice. Disrupting the integrin-mediated spread cell shape changes can also alter the expression of MSCs towards a chondrogenic lineage.

2.7   Substrate stiffness

In addition to the influence that an artificial ECM may have on cell shape, there is significant evidence that other physical properties of the ECM may also contribute to stem cell fate or lineage commitment. Cells that attach to a substrate have been shown to exert contractile forces, resulting in tensile stresses in the cytoskeleton [161]. Interestingly, the relationship between these forces and the mechanical stiffness, or elasticity, of the ECM can have a major influence on cellular behaviours such as migration [162], apoptosis [163], and proliferation [164].

2.7.1   2-D culture

Following these principals, more recent studies have been able to directly test the hypothesis that stem cell lineage specification can be determined by the mechanical properties of the ECM [165]. MSCs grown on variably compliant polyacrylamide gel were found to alter their properties in relation to the stiffness of the underlying substrate (i.e. stiffer substrates induced stiffer cells). Furthermore, the stiffness of the substrate defined MSC differentiation: soft substrates (0.1 - 1 kPa) that mimic the mechanical properties of brain tissue were found to be neurogenic, whereas substrates of intermediate stiffness (8 - 17 kPa) that mimic muscle were myogenic, and relatively stiff substrates (25 - 40 kPa) with bone-like properties were found to be osteogenic [165].

Similarly, the effective stiffness of the underlying substrate has been shown to regulate the differentiation of neural stem cells in certain stiffness ranges. Neural stem cells were cultured

on a synthetic, interfacial hydrogel substrate varying in moduli between 10 and 10,000 Pa [166]. Cell spreading, self-renewal, and differentiation were inhibited on soft substrates (10 Pa), whereas these cells proliferated on substrates with moduli of 100 Pa or greater and exhibited peak levels of a neuronal marker, beta-tubulin III, on substrates that had the approximate stiffness of brain tissue. Softer substrates ($\approx$ 100 - 500 Pa) promoted neuronal differentiation, whereas stiffer substrates ($\approx$ 1,000 - 10,000 Pa) led to glial differentiation.

2.7.2   3-D culture

2-D, gel coated environments provide a practical means of testing how cells respond to stiffness but fail to recapitulate the 3-D nature of physiological environments as is the niche with which most cells reside. While demonstrating very important stem cell fate decisions in response to substrate stiffness, they fail to provide a functional platform for current tissue engineering strategies.

With this in mind, Park et al. compared the explored the effect of substrate stiffness using polyacrylamide gels (PA), crosslinked with various concentrations of bis-acrylamide to produce stiffness values between 1 and 15 kPa [167]. These collagen-I coated gels were then compared to similarly coated stiff plastic conditions. This research demonstrated that stem cells (SCs) on soft 3-D substrates had less spreading, fewer stress fibers and lower proliferation rate than MSCs on stiff 2-D substrates. MSCs on stiff substrates had higher expression of SMC markers, α-actin and calponin-1; in contrast, MSCs on soft 3-D substrates had a higher expression of chondrogenic marker collagen-II and adipogenic marker lipoprotein lipase (LPL) [167]. TGF-β increased SMC marker expression on stiff 2-D substrates. However, TGF-β increased chondrogenic marker and suppressed adipogenic marker on the soft 3-D substrates, while adipogenic medium and soft substrates induced adipogenic differentiation effectively. All in all, these results highlight the increased propensity of MSCs cultured on stiff substrates to adopt a more spread morphology with greater number of stress fibres that together promote a myogenic phenotype. 3-D substrates, however,

reduce spreading, the number of stress fibres and proliferation creating a culture environment that promotes chondrogenesis in TGF-β supplemented conditions while adipogenesis is enhanced when using adipogenic medium in comparison to stiff 2-D conditions.
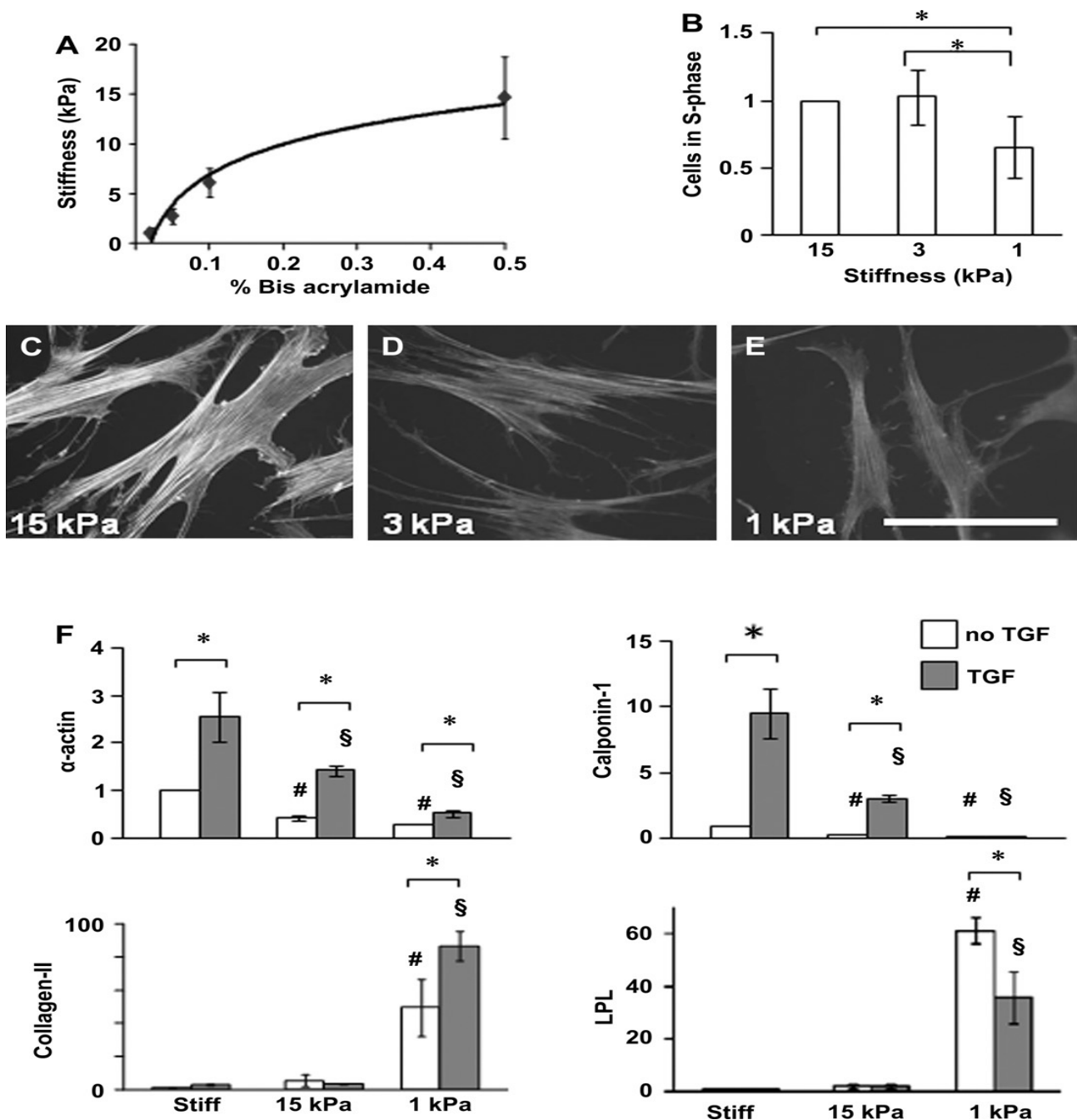
Figure 2.6 Modulation of MSC proliferation and differentiation by matrix stiffness. (A) Stiffness of PA gels using 6 % acrylamide and different bis-acrylamide concentrations. (B) MSCs were grown on PA gel for 1 day. Proliferation of MSCs on PA gels was quantified by BrdU incorporation. The number of cells in S phase for each sample was normalized to that on 15 kPa substrate to show fold-changes. * indicates significant difference ($P < 0.05$).(CeE) Phalloidin staining of F-actin after 1-day culture. (F) MSCs were grown on collagen-coated stiff substrates or PA gels for 2 days in the absence or presence of TGF-β, and lysed for qPCR analysis. *, # and & indicate significant differences [167].

Huebsch et al. demonstrated in a seminal study that to the fate of MSCs also depends on substrate rigidity in three-dimensional environments, with osteogenesis occurring predominantly in hydrogels with stiffness in the 11 - 30 kPa range, with adipogenesis observed on softer gels [29]. In contrast to previous two-dimensional work, cell fate was not correlated with morphology. Instead, stem cell differentiation was dictated by matrix stiffness irrespective of cell morphology because MSCs remained round in morphology independent of stiffness. In these circumstances, variations in substrate stiffness regulated integrin binding as well as reorganization of adhesion ligands on the nanoscale, both of which were traction dependent and correlated with osteogenic commitment of mesenchymal stem-cell populations. These results show that for the cell to differentiate towards osteogenesis it must be able to re-organise the adhesion mechanisms to the substrate that surround the cell [29]. It also suggested a selective window for which stiffness supports differentiation to various lineages as adipogenesis occurred in soft substrates < 11 kPa, osteogenesis occurred on intermediate substrates 11 - 30 kPa and no differentiation was observed in the mixed osteo-adipo media at substrate stiffness levels of 110 kPa.
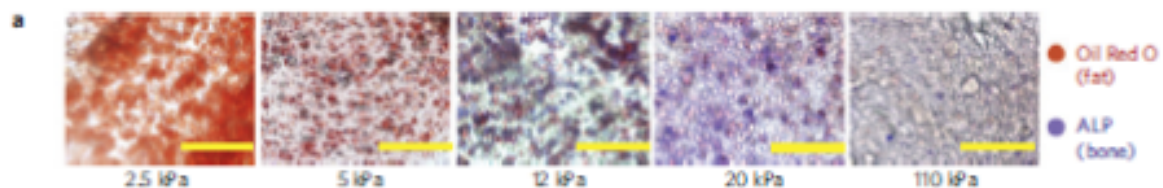
Figure 2.7 Stem cell fate response to changes in stiffness of 3-D RGD-modified alginate hydrogels [29].

In further studies, the manipulation of the stiffness of collagen-HA scaffolds in the range 1 to 10 kPa, using different amounts of the cross-linking agent 1-ethyl-3(3-dimethylaminopropyl) carbodi- imide (EDC), produced both neuronal cells and glial. Stem cells seeded on the softer gels (1 kPa) adopted a neuronal lineage whereas those in the stiffer gel (10 kPa) underwent glial differentiation [168]. This again shows, even in relatively small stiffness ranges, that cells

sense and actively respond to these cues in distinct and even marginally selective windows.

Another influential study went further to unravel the interplay between stiffness and adhesive ligand presentation by using a system of various polyacrylamide gel substrates that were coated with either of the following covalently bound tissue-specific ECM proteins: collagen I, collagen IV, laminin, or fibronectin [169]. Of the 16 gel-protein combinations investigated, osteogenic differentiation was found to occur significantly only on collagen I-coated gels with the highest modulus gel tested (80 kPa). Myogenic differentiation occurred on all gel-protein combinations that had stiffness values > 9 kPa but to varying extents as ascertained by MyoD1 expression. These results suggest that it is not stiffness alone that governs stem cell fate, but the mechano-transduction method is slightly more complicated in the fact that specific adhesion to the ECM is also a key factor.

Finally, not only substrate stiffness windows, but too viscoelasticity play a role in stem cell fate as demonstrated by the Mooney lab. By switching from covalent to ionic crosslinking of alginate chains, viscoelasticity could be introduced and stiffness was also varied in this system. As such, this approach found that cell spreading, proliferation, and osteogenic differentiation of mesenchymal stem cells (MSCs) are all enhanced in cells cultured in gels with faster relaxation. Strikingly, MSCs form a mineralized, collagen-1-rich matrix similar to bone in rapidly relaxing hydrogels with an initial elastic modulus of 17 kPa [170]. We also show that the effects of stress relaxation are mediated by adhesion-ligand binding, actomyosin contractility and mechanical clustering of adhesion ligands.

In terms of cartilage tissue engineering, few researchers have fully explored the interplay between substrate stiffness and chondrogenesis. Ramos et al. used soft collagen-I gels of different stiffness values, achieved by varying the collagen concentration, to demonstrate at the very least stiffness plays a role in determining the quantity of protein deposition by chondrocytes [28]. Aggrecan (Acan), type II collagen (Col2a1), and Sox9 was upregulated in the softer gels (both in monolayer and in 3D culture). Stiffer gels induced an organization of the actin cytoskeleton that correlated with the loss of a chondrocyte phenotype.

Collectively, these results highlight the importance of substrate stiffness values on stem cell fate decisions. It also shows that these interactions only occur in gels with viscoelasticity,

presentation of certain adhesive ligands and that enable traction-mediated remodelling of these ligands.

Author	2D or 3D	Substrate & Stiffness Ranges	Outcomes
Engler et al. [165]	2D	Polyacrylamide Gels (0.1 - 1, 8 - 17, 25 - 40 kPa)	Neuro 0.1 - 1kPa, Myo 8-17 kPa, Osteo 25 - 40 kPa
Saha et al. [166]	2D	IPN Synthetic Hydrogel (10 Pa - 10 kPa)	Glial differentiation at 10 kPa
Park et al. [167]	2D vs 3D	Plastic vs Polyacrylamide gels (1 - 15 kPa)	2D Myogenic, Soft 3D ↑ chondrogenesis
Huebsch et al. [29]	3D	RGD-Alginate hydrogels (2.5 kPa - 110 kPa)	Soft ↑ adipo, 12 - 20 kPa ↑ osteo, very stiff no tissue formation
Her et al. [168]	3D	Collagen-HA Scaffolds (1 and 10 kPa)	Neural soft, stiff ↑ glial
Rowlands et al. [169]	3D	Polyacrylamide gels with different ECM coatings (2 - 80 kPa)	↑ osteo 80 kPa, ↑ myo all $>$ 9 kPa but with ECM specific expression levels

Table 2.2 Summary of literature findings on MSC differentiation in response to substrate stiffness.

2.7.3 Summary

The culmination of these papers highlight that substrate stiffness can alter stem cell fate but the values at which alterations occur generally vary based on the biomaterial environment.

Firstly comparing the 2-D to the physiologically more relevant 3-D environment in glial differentiation, it is clear that neurogenesis occurs in soft substrates and glial differentiation takes place at around 10 kPa in both environments. In 2-D, neurogenesis has been measured on much softer substrates. This may simply be due to the fact that a 3-D substrate fails to support its own structure at such stiffness values. Myogenesis throughout also tends to occur at stiffness values above 9 kPa in both 2-D and 3-D environments. This can be seen in the seminal paper by Engler et al. as well as the interesting mix that was explored by Rowlands et al., of substrate stiffness and ECM incorporation. myogenesis was also shown to occur on very stiff plastic in the paper by Park et al., in which 2-D is poorly compared in a direct manner to a completely different 3-D environment. Chondrogenesis appears to occur on softer substrates, from this paper, however, when a more reasonable argument of comparing substrate stiffness of different values in 3-D alone was studied. Finally, it is osteogenesis in which the largest variation in substrate stiffness values based on the biomaterial environment occurs. With 25 - 40 kPa, 12 - 20 kPa and above 80 kPa accounting for osteogenesis in 2-D polyacrylamide gels, 3-D RGD-modified alginate gels and 3-D polyarcrylamide gels with different ECM coatings respectively. This taken together highlights that substrate stiffness augments differentiation in a biomaterial specific manner.

2.8 Dynamic compression as regulator of chondrogenesis

An important requirement for healthy cartilage homeostasis is mechanical loading. Spatially variable mechanical stimuli are generated within articular cartilage during normal physiological loading. Shear stress and high fluid flow is dominant at the surface whereas high hydrostatic pressure and low fluid flow occurs close to the tidemark in the deep zone. Dynamic compression plays a major role in initiating these stimuli. The cyclic, compressive deformation of cartilage, ranging from 6 - 20 % of its initial thickness, along with the inherent low permeability of the tissue provides the basic mechanisms for initiating these stimuli throughout the depth of the tissue. These stimuli are perceived and transduced

by chondrocytes and regulate cartilage maintenance and development. An individual understanding of how these mechanical factors affect chondrogenesis may hold the key to improving cartilage tissue engineering strategies both in vitro and in vivo.

2.8.1 Chondrocyte response

The biosynthetic activity of chondrocytes during in vitro culture has been shown to be dependent on both the biochemical and biophysical stimuli the cells experience. The application of appropriate levels of dynamic compressive loading to chondrocytes encapsulated in agarose hydrogels has been shown to enhance cartilage specific matrix production [171–175]. Furthermore, it has been shown that the temporal application of TGF-β_3 for up to 14 days prior to the initiation of dynamic compression culminates in the achievement of GAG content and equilibrium moduli surpassing that of native cartilage [176,177]. Integrin binding and cytoskeletal re-organisation has been proposed as a potential key mechanoreceptor in chondrocytes [178,179]. Villaneuva et al. demonstrated that dynamic loading of bovine chondrocytes only had an effect when negatively charged chondroitin sulfate adesive molecules were incorportated. These collectively point to the idea that cell-matrix interactions are important in transducing mechanical forces and enabling cells to respond to such stimuli.

2.8.2 Initiation and progression MSC chondrogenesis

Mechanical signals have been shown to be as effective as TGF-β_1 stimulation for inducing chondrogenesis of BMSCs. In this study [180], rabbit MSCs were suspended in agarose hydrogels and subjected to cyclic compressive loading in the presence or absence of TGF-β_1. Aggrecan and collagen type II gene expression were similar in the TGF-β group and the solely loaded group, while combining loading with TGF-β treatment promoted collagen type II gene expression more effectively than TGF-β_1 alone. Individually TGF-β_1 treatment and

cyclic compression were both shown to upregulate TGF-β_1 gene expression, suggesting that both stimuli induce chondrogenesis of bone marrow MSCs through a similar pathway [30]. In a follow up study, cyclic compressive loading also promoted gene expression and protein production of two transmembrane TGF-βreceptors essential for chondrogenesis of MSCs when TGF-βsignalling is involved [181]. This study also demonstrated that dynamic compression upregulated both Sox-9 and TGF-β_1 at the gene and protein level. The mechanical environment, within such compressed agarose hydrogels [30], determined by finite element modelling revealed that the hydrostatic pressure was low (0.1 kPa), while compressive strain was similar in magnitude to that shown to enhance the biosynthetic activity of mature chondrocytes [171,172,175]. Dynamic compressive loading has also been shown to regulate chondrogenic gene expression in human bone marrow-derived MSCs [31,182]. In the absence of chondrogenic growth factors, dynamic compression of MSCs embedded in alginate gels has been shown to down regulate collagen type II gene expression and upregulate aggrecan expression after 8 days [31]. Also in fibrin hydrogel system, chondrogenic gene markers of Sox9 and aggrecan were upregulated in the absence of soluble cues after being subjected to dynamic compression during longer loading periods. Inhibitors of the ERK1/2 pathway, abolished this induction and the cells displayed a more osteogenic phenotype as shown by ALP, Col I and Osteocalcin expression [183]. Dynamic loading of bovine MSCs embedded in agarose hydrogels has also been shown to increase aggrecan promoter activity in both the core and annulus of the constructs [97]. The same study demonstrated that sGAG accumulation was higher in dynamically compressed constructs but lower than constructs maintained in free swelling conditions in the presence of TGF-β_3. Similar studies using alternative loading regimes have also confirmed that while loading in the absence of TGF-β enhances sGAG accumulation, levels are again lower than that observed under free swelling conditions with TGF-β supplementation [184]. A more recent study has identified compressive principal strains as the key regulator of chondrogenesis in fibrin-polyurethane composite scaffolds enriched with human MSCs. Although dynamic uniaxial compression did not induce chondrogenesis, multiaxial loading by combined application of dynamic compression and interfacial shear induced significant

chondrogenesis at locations where all the three principal strains were compressive and had a minimum magnitude of 10 % suggesting a role of magnitude in regulating responses to dynamic compression [185].

A more complex pattern emerges when MSCs are subjected to simultaneous compression and TGF-β stimulation. The expression levels of aggrecan are reduced when MSCs are subjected to TGF-β_3 stimulation in addition to dynamic loading, when compared to the action of the former alone [92]. In a synthetic hydrogel, it has been shown that under intermittent and low frequency (0.3 Hz) dynamic loading coupled with TGF-β_1 stimulation, all cartilage- related markers (Sox9, aggrecan, collagen type II) were down-regulated, along with reduced aggrecan staining and no collagen type II staining [186]. Long-term studies have also revealed that cartilage matrix production by MSCs embedded in agarose hydrogels is reduced when mechanical stimulation is initiated at the onset of TGF-β induced chondrogenesis [31,32]. In contrast, cyclic compression enhances proteoglycan and collagen accumulation for MSCs embedded in hyaluronan-gelatin composites [187]. Such contradictory findings suggest that the interaction of MSCs with their surrounding matrix is critical to their response to loading. Related to this is the observation that the response of MSCs to dynamic compression in the presence of TGF-β_3 depends on when loading is initiated; application at early time-points (Day 8) decreases aggrecan gene expression, while loading at later time-points (Day 16) increases chondrogenic gene expression [188]. This suggests that the mechano-responsiveness of MSCs changes depending on the stage of chondrogenesis and the development of a pericellular matrix. Following 7 days of pre-culture in free swelling conditions in fibrin-polyurethane composite scaffolds, various mechanical loading protocols incorporating dynamic compression induced higher GAG synthesis and higher chondrocyte like gene expression [189]. The same authors have also demonstrated that the influence of mechanical loading depends on the TGF-β concentration of the culture medium, with a much stronger effect on chondrogenic gene expression observed at lower TGF-β_1 concentrations. When TGF-β_1 was absent from the medium, mechanical load stimulated mRNA expression and protein synthesis of TGF-β_1 and TGF-β_3 [189].

The combination of gradients in dynamic compression magnitude and oxygen availability

have previously been used to produce zonal articular cartilage [190]. By radially confining the bottom of MSC-laden hydrogels, oxygen levels were reduced in this zone. Application of dynamic compression produced higher strains in the top of radially confined constructs. A combination of oxygen and mechanical gradients produced a increase in cartilage specific matrix component production as well as suppression of hypertrophy and calcification throughout. The gradient presentation of oxygen and mechanical cues combined to produce an increase in proteoglycan-4 (lubricin) deposition toward the top surface of these tissues; a key GAG component of the superficial zone in articular cartilage [190].

2.8.3   MSC hypertrophy and endochondral ossification

Bian et al. found that dynamic compressive loading increased the mechanical properties, as well as the glycosaminoglycan (GAG) and collagen contents of human BMSC-seeded hyaluronic acid hydrogel constructs in a seeding density dependent manner and was also shown to significantly reduce the expression of hypertrophic markers and to suppress the degree of calcification in MSC-seeded hyaluronic acid hydrogels . They further reported that hydrogel properties such as polymeric density and crosslinking time that correlate with stiffness both affect the extent of chondrogenic hypertrophy. A low stiffness gel acted to accelerate hypertrophy based on greater calcium and collagen type X deposition [22].

Zhang et al. again highlighted the ability of dynamic compression to inhibit hypertrophy in comparison to free swelling conditions in small amounts of collagen type X were produced [23]. hMSCs seeded on PLCL/chitosan constructs were prevented from producing collagen type X following the application of 10 % dynamic compression in 20 % O_2 for 3 weeks following a 3 week delay period under free swelling conditions. This suppression was linked to the SMAD1/5/8 pathway through TGF-β notch signalling [23].

Steinmetz et al. highlighted the importance modulating the strain environment can have. Variation of hydrogel stiffness throughout the depth using altered UV exposure during photo-polymerisation provided the basis for modulating strain throughout the depth of

the tissue during dynamic compression [191]. This produced osteogenesis during early differentiation in areas of low strain and chondrogenesis in areas of high strain [191]. The switch between a chondrogenic and osteogenic fate based on strain magnitude may suggest its use in modulating hypertrophy and endochondral ossification also.

Author	Growth Factors	DC Protocol	Outcomes
Huang et al. [30]	Growth factor free or TGF-β	2 % Agarose 10 % DC 1Hz 4 hrs/day	DC induced chondro to similar levels as TGF-β
Huang et al. [181]	Growth factor free	2 % Agarose 15 % DC 1Hz 2 days	DC activates TGF-β signal transduction at early chondro
Campbell et al. [31]	Presence/absence 10 ng/ml TGF-β_3	Alginate 15 % DC 1 Hz 8 days	Chondro induced in absence of growth factor
Pelaez et al. [182]	Growth factor free	Fibrin (40, 60 & 80 mg/ml); DC 10 %; 0.1, 0.5 & 1 Hz	Fibrin supports compression induced chondro

Pelaez et al. [183]	TGF-β	As previous Pelaez et al. paper above	ERK1/2 inhibition switches chondro to osteo MSC response
Mauck et al. [97]	TGF-β		DC elevated sGAG levels
Kisiday et al. [184]	TGF-β		
Zahedmanesh et al. [185]	Growth factor free	Fibrin-polyurethane composite; minimum 10 %	Threshold dependent chondro induction by DC
Steinmetz et al. [186]	TGF-β_1	PEG-RGD hydrogel; 15 % DC 0.3 Hz	↓ chondro and osteo; DC inhibitory
Thorpe et al. [32]	TGF-β_3	2 % Agarose; 10 % DC	↓ chondro
Angele et al. [187]	TGF-β	DC 4 hrs/d	↑ chondro

Mouw et al. [188]	TGF-β_1	DC introduced at day 8	COL I & II ↑ with DC
Thorpe et al. [190]	TGF-β_3	Delayed 10 % DC 1 Hz 5 d/wk	↑ chondro
Zhang et al. [23]	TGF-β_3	10 % DC 1 Hz 5 d/wk	↓ hypertrophy
Steinmetz et al. [191]	TGF-β_3	15 % Global DC	High DC chondro, low DC osteo fate

Table 2.3 Summary of literature findings on MSC differentiation in response to dynamic compression.

2.8.4 Summary

These articles paint a confusing picture of the way in which dynamic compression affects chondrogenesis and hypertrophy. Initially it would appear dynamic compression has the power to induce chondrogenesis to similar levels of TGF-β yet this was not demonstrated in our laboratory. The prevailing trend is, however, that dynamic compression enhances chondrogenesis despite Steinmetz et al. contradicting these coherent findings. This may be due to the hydrogel or low frequency of stimulation used. Finally, dynamic compression being inhibitory to hypertrophy and low magnitudes enhancing osteogenesis present some insight into the diverse nature of dynamic compression in controlling MSC fate.

2.9   Cellular mechanics as a result of mechanical cues

It has been shown that chondrocyte deformation varies within the zonal structures of articular cartilage that exist throughout the depth of the tissue [192]. A study highlighted that chondrocytes in middle and deep zones experienced local strains of 15 %; a magnitude similar to the surface-surface or global strain experienced within the tissue. In the superficial zone, however, local strains increased to 19 %, which the authors proposed was due to a lower zonal stiffness of this layer.

A recent study highlighted the same is true for compression applied to chondrocytes within hydrogels of different stiffness values [193]. Here, aspect ratios of chondrocytes subjected to compression (10 % strain) were significantly higher in 4.5 % agarose hydrogels than 2 % agarose hydrogels. This reflected similar increasing compressive strains of beads with increasing gel concentration. This highlights that the stiffness of the substrate greatly affects the way in which compressive strains and/or stresses are transferred to the cell.

Another paper highlighted that chondrocytes response to dynamic loading depends also on the stiffness of the pericellular matrix (PCM) as well as the anisotropy of the extracellular matrix (ECM) [194]. This finite element model demonstrated a reduction in stress within the cell with increasing PCM stiffness despite higher stresses being developed within the PCM itself.

These findings highlight that the stiffness of the substrate and PCM are key to physically transferring dynamic compression from the macroscopic hydrogel level to the cellular environment.

2.10   Summary

Cartilage is a complex tissue that lines articulating joints. The intricate network the collagens that vary in orientation and quantity throughout the depth coupled with the swelling pressure of the interlinked network of proteoglycans cause a pre-stress in collagen fibres and a highly

hydrated environment with low tissue permeability that can pressurise under load. This enables cartilage to resist the high forces and deformations that result in the tissue during joint articulation. The low friction nature of its surface also provides ease of movement during joint articulation. A loss of structure through injury or osteoarthritis can lead to overloading of the joint and pain during motion.

Current strategies to treat these ailments are either expensive or lack efficacy. The most successful to date; matrix-assisted autologous cartilage implantation (MACI) relies too heavily on obtaining sufficient numbers of healthy chondrocytes, which can dedifferentiate in expansion, and it extends an additional defect site in a non-load bearing region to the patient. All in all, alternative cell sources to this otherwise successful tissue engineering strategy need to be found.

Mesenchymal stem cells provide that alternative as they can have the ability to proliferate, self-renew and differentiate into multiple cell lineages. Use of growth factors in vitro can direct their differentiation but mechanical factors have also been shown to be influence and enhance this process. MSC chondrogenesis through the use of soluble factors alone has yet to meet standards set by non-passaged chondrocytes but the incorporation of mechanical or other factors has substantial potential in closing the gap.

Hypertrophy during MSC chondrogenesis in vitro has also been a significant problem in cartilage tissue engineering, especially when using bone marrow-derived MSCs. In endochondral bone tissue engineering it has, however, been a benefit by providing a template that can survive in a hypoxic environment and direct bone regeneration. Little work has investigated how mechanical factors could be used to spatially modulate this process using mechanical factors in order to create an osteochondral graft. Low oxygen is widely accepted at enhancing chondrogenesis and suppressing hypertrophy. Certain stiffness windows have been shown to be influential for osteo-adipo, myo-chondro and neuronal-glial fate switches but little work has focussed on the initiation and progression of MSC chondrogenesis. Dynamic compression (DC) has been linked with both inducing and enhancing MSC chondrogenesis as well as suppressing hypertrophy yet little research has used it in osteochondral tissue engineering strategies.

2.11   Project objectives

These observations provided the basis for the overall objective of this thesis, which is to develop the precursor to an osteochondral graft by spatially modulating chondrogenesis and hypertrophy of MSCs within a 3-dimensional environment using a combination of mechanical stimuli. The specific objectives of this thesis are:

1. Investigate the role that the magnitude of dynamic compression has on MSC chondrogenesis and progression along the endochondral pathway.

2. Determine the role of substrate stiffness and oxygen availability on the initiation and progression of chondrogenesis in MSCs.

3. Explore the interaction between substrate stiffness and dynamic compression on the initiation and progression of MSC chondrogenesis.

4. Finally, biofabricate MSC-laden constructs with spatially defined mechanical properties to regulate MSC fate and promote the development of tissues destined for an osteochondral fate.

Based on knowledge gained from the literature, the following hypotheses can be made:

- A low magnitude of dynamic compression will enhance chondrogenesis and the progression along the endochondral pathway, while higher magnitudes will suppress

hypertrophy and endochondral ossification.

- Low oxygen tension and low substrate stiffness act synergestically to enhance chondrogenesis.

- The response of MSCs to dynamic compression depends on the stiffness of the local substrate.

- Spatially modulating the stiffness of MSC laden constructs leads to:

    1. Spatial changes in strain with the application of dynamic compression.

    2. Spatial changes in MSC differentiation, with hypertrophy proceeding in regions of low strain, and stable cartilage forming in regions of high strain.

CHAPTER 3

Dynamic compression regulates chondrogenesis and hypertrophy of MSCs in a strain magnitude dependent manner

3.1   Abstract

THE aim of this study was to explore how the magnitude of dynamic compressive loading influences chondrogenesis and hypertrophy of MSCs encapsulated within agarose hydrogels.   Bone marrow derived mesenchymal stem cells (MSCs) were seeded in agarose hydrogels and subjected to dynamic compressive loading following chondrogenic-preconditioning in 10ng/ml TGF-β_3, 5 % O_2.   Markers of chondrogenic and endochondral differentiation were assessed.   Dynamic compression (10 %) was found to enhance chondrogenesis as evident by enhanced deposition of collagen type II. Low and medium magnitudes of DC (5 and 10 % respectively) acted to enhance endochondral ossification, as evident by increased calcium deposition in comparison to non-compressed controls. This acceleration was inhibited at higher strain magnitudes with little effect on chondrogenesis.   The application of dynamic compression also improved the mechanical properties of the engineered tissues, which correlated with increases in calcium accumulation.   This highlights the importance of the magnitude of the dynamic

compression on chondrogenesis of mesenchymal stem cells ability to either promote a stable chondrogenic phenotype or to accelerate endochondral ossification.

Keywords – **MSCs, chondrogenesis, endochondral ossification, tissue engineering, hypertrophy, mechanotransduction**

3.2 Introduction

OSTEOARTHRITIS (OA) is a common, degenerative joint disease, affecting approximately 50 % of the population aged 60 years or older [195]. Due to its avascular nature, articular cartilage has a limited capacity to self-repair [196,197]. This has motivated the development of cell based therapies such as autologous chondrocyte implantation for the repair of cartilage defects [198,199]. A major limiting factor in extending the use of such therapies is obtaining sufficient numbers of differentiated autologous chondrocytes, particularly in elderly and more osteoarthritic patients. An age-related loss in chondrocyte yield, proliferation and functional capacity has been observed in culture expanded chondrocytes, while chondrocytes isolated from osteoarthritic patients exhibit reduced collagen type II synthesis. [200]. Mesenchymal stem cells (MSCs) are a promising alternative cell source for cartilage repair due to their enhanced ability to proliferate and self renew as well as their chondrogenic differentiation potential [10,11]. Chondrogenic differentiation of MSCs from different tissue sources has been shown in the presence of members of the transforming growth factor-β (TGF-β) superfamily [14,84,201–204]. While chondrogenesis of MSCs has been demonstrated in different three-dimensional scaffolds and hydrogels [189,205–209], it has been shown that matrix accumulation and the subsequent mechanical properties of MSC laden constructs are lower than those of chondrocyte seeded controls [206,208]. In addition, chondrogenically-primed MSCs have been shown to have a tendency to become hypertrophic, mineralise and convert into bone forming cells via the process of

endochondral ossification [17]. Therefore novel strategies are required to not only enhance MSC chondrogenesis but also to control their ultimate phenotype.

Chondrocytes generally respond to physiological levels of dynamic compressive loading through enhanced cartilage-specific macromolecule biosynthesis [96,210–213]. In addition, the application of appropriate levels of dynamic compressive loading to chondrocytes encapsulated in agarose hydrogels has been shown to enhance cartilage specific matrix production [171–175] with GAG content and equilibrium moduli surpassing that of native cartilage [176,177]. The effect of dynamic compressive loading on MSCs is more complicated. It has been demonstrated that dynamic compressive loading in the absence of TGF-β family members can increase chondrogenic gene expression [30,31,97,181,214,215] and stimulate the accretion of cartilage-like extra-cellular matrix (ECM) components relative to unloaded controls [97,184,214]. However, the combined effects of dynamic compression and chondrogenic growth factor supplementation on chondrogenesis of MSCs are generally more complex [31]. Dynamic compression in the presence of TGF-β has produced increases in both chondrogenic gene expression [30,31,97,181,214–216] and ECM secretion [187,215,216]. Other studies, however, indicate the contrary, with the combination of dynamic compression and TGF-β resulting in a down-regulation of chondrogenic gene-expression [31] and inferior ECM accumulation when compared to unloaded controls [32,184]. Our laboratory has demonstrated that loading MSCs following TGF-β mediated chondrogenesis was beneficial for chondrogenesis, while early loading initiated at the onset of differentiation was inhibitory [98]. Dynamic compression has been associated with the inhibition of MSC hypertrophy and progress along the endochondral pathway [22,23]. For example, Bian et al. found that dynamic compressive loading increased the mechanical properties, as well as the glycosaminoglycan (GAG) and collagen contents of human BMSC-seeded hyaluronic acid hydrogel constructs in a seeding density dependent manner. Loading was also shown to significantly reduce the expression of hypertrophic markers and to suppress the degree of calcification in MSC-seeded hyaluronic acid hydrogels [22]. In contrast, other studies have shown that mechanical loading can enhance endochondral ossification [217]

Oxygen tension also plays a key role in the initiation and progression of MSC

chondrogenesis. Low oxygen tension can enhance chondrogenesis of MSC cultures and has been shown to reduce hypertrophy. Therefore in order to develop a cartilage graft, low oxygen culturing conditions may be beneficial. During MSC-hydrogel culture, an oxygen gradient generally exists due to high cellular oxygen consumption at the periphery. Dynamic compression has been shown to reduce this gradient increasing oxygen availability within loaded MSC-laden constructs. Attempting to de-couple these two processes, may be beneficial for both enhancing chondrogenesis and modulating endochondral ossification.

While it is clear that mechanical cues can potentially enhance chondrogenesis of MSCs and modulate their phenotype stability, it remains unclear how this process is regulated by the magnitude of the applied load. Clearly endochondral ossification can proceed in a mechanically loaded environment; it does so during fracture healing [218], however it is clear that certain types of biophysical cues can also suppress hypertrophy of MSCs. The hypothesis of this study is that chondrogenesis and hypertrophy of MSCs is regulated by dynamic compression in a magnitude dependent manner. To test this hypothesis, MSC laden agarose hydrogels will be subjected to 3 weeks of either 0, 5, 10 or 20 % magnitudes of strain in unconfined dynamic compression at 20 % O_2 following the onset of chondrogenesis (3 weeks culture at 5 % O_2 in the presence of TGF-β_3). Therefore mechanical loading can potentially modulate chondrogenesis in two ways. Firstly by directly stimulating encapsulated MSCs, and secondly by altering oxygen availability within the construct.

3.3 Materials and Methods

3.3.1 Cell isolation, expansion and hydrogel encapsulation

MSCs were isolated from porcine femora and preserved in liquid nitrogen before later being thawed and expanded according to a modified method developed for human MSCs. MSCs were plated at a seeding density of 50,000 cells/cm^2 in high-glucose Dulbecco's modified eagles medium (4.5 mg/mL D-Glucose, 200 mM L-Glutamine; hgDMEM) supplemented with

10 % fetal bovine serum (FBS) and 2 % penicillin (100 μg/ml) - streptomycin (100 μg/ml); and expanded to passage two in a humidified atmosphere at 37 °C and 5 % CO_2.

MSCs were suspended in chondrogenic medium (CM), which consisted of hgDMEM supplemented with penicillin (100 μg /ml) and streptomycin (100 μg/ml), sodium pyruvate (100 μg/ml), L-proline (40 μg/ml), bovine serum albumin (1.5 mg/ml), linoleic acid (4.7 μg/ml), insulin-transferrin-selenium (10 μg/ml), L-ascorbic acid-2-phosphate (50 μg/ml), dexamethasone (100 nM) and 10 ng/mL TGF-β_3. The MSC suspension was subsequently mixed with 4 % agarose Type VII (dissolved in phosphate buffered saline) at a ratio of 1:1 at approximately 40 °C, to yield a final gel concentration of 2 % and a cell density of 20 million cells/ml. The agarose-cell suspension was cast in a stainless steel mould before being biopsy punched to produce cylindrical constructs (5 mm diameter, 2 mm thickness). Constructs were maintained separately in 12-well plates with 2 ml of chondrogenic medium in 5 % O_2. Medium was exchanged twice weekly and constructs were cultured in these conditions for 24 days.

3.3.2 Dynamic compression application

Dynamic compressive loading was applied to constructs, also in the presence of TGF-β_3, following this 24 day culture period. Dynamic compression (DC) was carried out in an incubator housed, custom-built compressive loading bioreactor as documented in Appendix A of this thesis. Uniaxial, unconfined compression was initiated using an electric linear actuator with 0.05 μm resolution (Zaber Technologies Inc., Vancouver, Canada). A 1000 g load cell (RDP Electronics Ltd, Wolverhampton, UK) attached to the actuator lead screw sensed the load applied. The system was controlled and data logged using Matlab (fig. 3.1). The dynamic compression protocol consisted of 0, 5, 10 and 20 % strain amplitude superimposed on a maximum 1 % preload at a frequency of 1 Hz employed for a period of 2 h/day and 4 days/week. 0 % loaded constructs were placed in the bioreactor culture dish while the platen displaced 0.1mm in both directions at the 1Hz cycle condition above the constructs

without the application of strain. This group provided a 0 % strain control that enabled the decoupling of oxygen and nutrient transport result of DC from the magnitude of the dynamic compressive strain stimulus. A normal free swelling control was maintained in 12-well plates at the same oxygen conditions. During each day of dynamic culture, all constructs were placed symmetrically within the bioreactor dish to prevent an uneven loading regime being established. Minimal media was used in the bioreactor culture dish to effectively cover the samples without allowing them to float when placing the platen in position before loading. Medium within the bioreactor culture dishes were changed every 2-3 days to account for this.

3.3.3 Mechanical testing

Constructs were mechanically tested (n = 4) in unconfined compression between impermeable platens using a standard materials testing machine with a 5 N load cell (Zwick Roell Z005, Herefordshire, UK) as previously described hydrated through immersion in a phosphate bufefred saline (PBS) bath maintained at room temperature. A preload of 0.01 N was applied to ensure that the construct surface was in direct contact with the impermeable loading platens. Stress relaxation tests were performed consisting of a ramp displacement of 10 µm/s up to 10 % strain, which was maintained until equilibrium was reached (roughly 30 minutes). This was followed by a dynamic test where cyclic strain amplitude of 1 % (10 - 11 % total strain) was applied for 10 cycles at 1 Hz. Constructs were then further used for biochemical analysis.

Measures used from this testing are Young's, Equilibrium and Dynamic Moduli respectively. Young's modulus highlights the elastic region of the stress-strain curve. It is calculated by using the stress at the peak force (directly following termination of the ramp phase) and dividing this by the strain performed (10 %). Equilibrium modulus highlights the viscoelastic properties of the construct by determining the stiffness of the solid matrix alone. It is calculated by using the stress at equilibrium having held the ramp strain for at least 30 minutes and dividing by the strain at equilibrium (10 %). Finally, the dynamic modulus

represents the elastic stiffness of the construct during dynamic motion. It is calculated by using the difference in peak and trough stresses after the cyclic/dynamic strain of 1 % is superimposed on the 10 % static strain and dividing this by the dynamic strain (1 %).
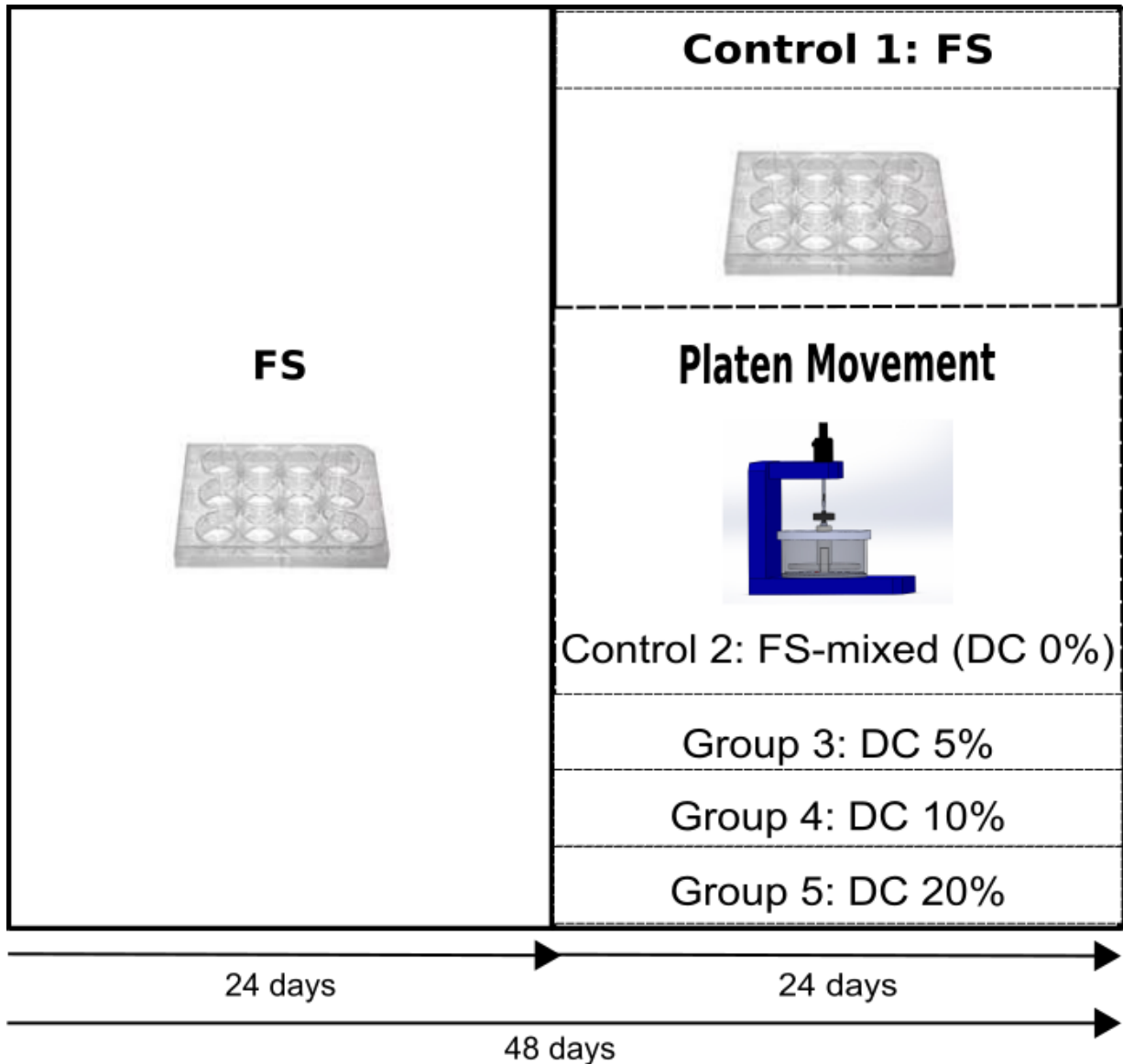
Figure 3.1 Study design and bioreactor schematic.

3.3.4   Biochemical content

The biochemical content of constructs (n = 3 or n = 4) was assessed at each time point. The wet mass of each construct half was recorded before being frozen at -85 ℃ for later analysis. Samples were digested with papain (125 µg/mL) in 0.1 M sodium acetate, 5 mM L-cysteine HCl, 0.05 M EDTA, pH 6.0 (all Sigma- Aldrich) at 60 ℃ under constant rotation for 18 h. DNA content was quantified using the Hoechst Bisbenzimide 33258 dye assay as previously described [219]. The proteoglycan content was estimated by quantifying the amount of sulfated glycosaminoglycan (sGAG) in constructs using the dimethylmethylene blue dyebinding assay (Blyscan, Biocolor Ltd., Carrickfergus, UK), with a shark chondroitin sulfate standard. Total collagen content was determined through measurement of the hydroxyproline content [220]. A hydroxyproline-to-collagen ratio of 1:7.69 was used.

The remaining halves of mechanically tested constructs were digested using 1M HCl at 60 ℃ under constant rotation for at least 18 hrs. Samples were subsequently centrifuged at 5000g to remove any sediment from the digest. Calcium chloride at the defined calcium content was diluted in 1M HCl to produce two standard stocks (100 and 20 µg/ml respectively), which were diluted further to produce the four high and three low standard points of the curve respectively. Calcium content was then determined relative to dye fluorescence in response to calcium concentration using a commercial sentinel calcium kit.

3.3.5   Histology and immunohistochemistry

Constructs (n = 2) were fixed in 4 % paraformaldehyde (Sigma-Aldrich), wax embedded and sectioned at 5 µm to produce a cross section perpendicular to the disk face. Sections were stained for sGAG with 1 % alcian blue 8GX (Sigma-Aldrich) in 0.1 M HCl; for collagen with picro-sirius red; and for calcium with alziran red. The deposition of collagen type I, type II and type X was identified through immunohistochemistry. Briefly, sections were quenched of peroxidase activity, rinsed with PBS before treatment with chondroitinase ABC (Sigma-Aldrich) in a humidified environment at 37 ℃. Slides were rinsed with PBS

and non-specific sites were blocked with goat serum (Sigma-Aldrich). Sections were then incubated overnight at 4 °C with the primary antibody; mouse monoclonal collagen type I antibody. (1:400; 1.4 mg/mL; Abcam, Cambridge, UK) or mouse monoclonal anti-collagen type II (1:100; 1 mg/mL; Abcam). After washing in PBS, sections were incubated for 1 h in the secondary antibody; anti-mouse IgG biotin antibody produced in goat (1:400; 1 mg/ mL; Sigma-Aldrich). Colour was developed using the Vectastain ABC reagent (Vectastain ABC kit, Vector Laboratories, Peterborough, UK) followed by exposure to peroxidase DAB substrate kit (Vector Laboratories). Negative and positive controls of porcine ligament, cartilage or growth plate were included for each batch. For both histology and immunohistochemistry images presented at high magnification from opposite annulus regions (left and right) and core (middle) as well as macroscopic images at low magnifications (corner).

3.3.6 Statistical analysis

Statistics were preformed using graphpad prism software package. Groups were analysed for significant differences using a general linear model for analysis of variance in the factor of loading magnitude. Tukey's test for multiple comparisons was used to compare conditions. Significance was accepted at a level of $p < 0.05$. Numerical and graphical results are presented as mean $\pm$ standard error from the mean.

3.4 Results

3.4.1 Agitation of the culture media within a bioreactor system may suppress chondrogenesis of MSCs

Platen movement during bioreactor culture will agitate the media and alter oxygen levels within MSC laden hydrogels. This may mask any effect of direct mechanical stimulation. The first experiment therefore compared how agitating the media, with 0 % strain applied to constructs (termed free swelling, FS-mixed) compared to FS controls in 12-well plates. 24 days of TGF-β_3 and low oxygen tension mediated chondrogenesis followed by these conditions for a further 24 days in normoxia provided the basis for these studies. Media agitation resulted in the reduction of collagen type II deposition and alcian blue staining (Fig 3.2 A,B). In addition, calcium deposition appeared somewhat reduced. Overall, staining was inhomogenous. Both GAG and collagen type II deposition in FS samples stained more intensely in one vertical side of the construct. Alternatively, FS-mixed groups had GAG and particularly collagen type II staining constricted mostly to the core. Alizarin red staining for calcium deposits was asymmetrical, being restricted to one side in the lateral direction (fig. 3.2A).

DNA content remained similar between FS controls and FS-mixed samples (fig. 3.2B). Chondrogenesis was, however, suppressed by the action of agitating the media as evident by a significant 19 % reduction in GAG production by FS-mixed samples compared to FS controls (fig. 3.2C). GAG per DNA was reduced, on average by 14 % but this difference was not significant (fig. 3.2D).
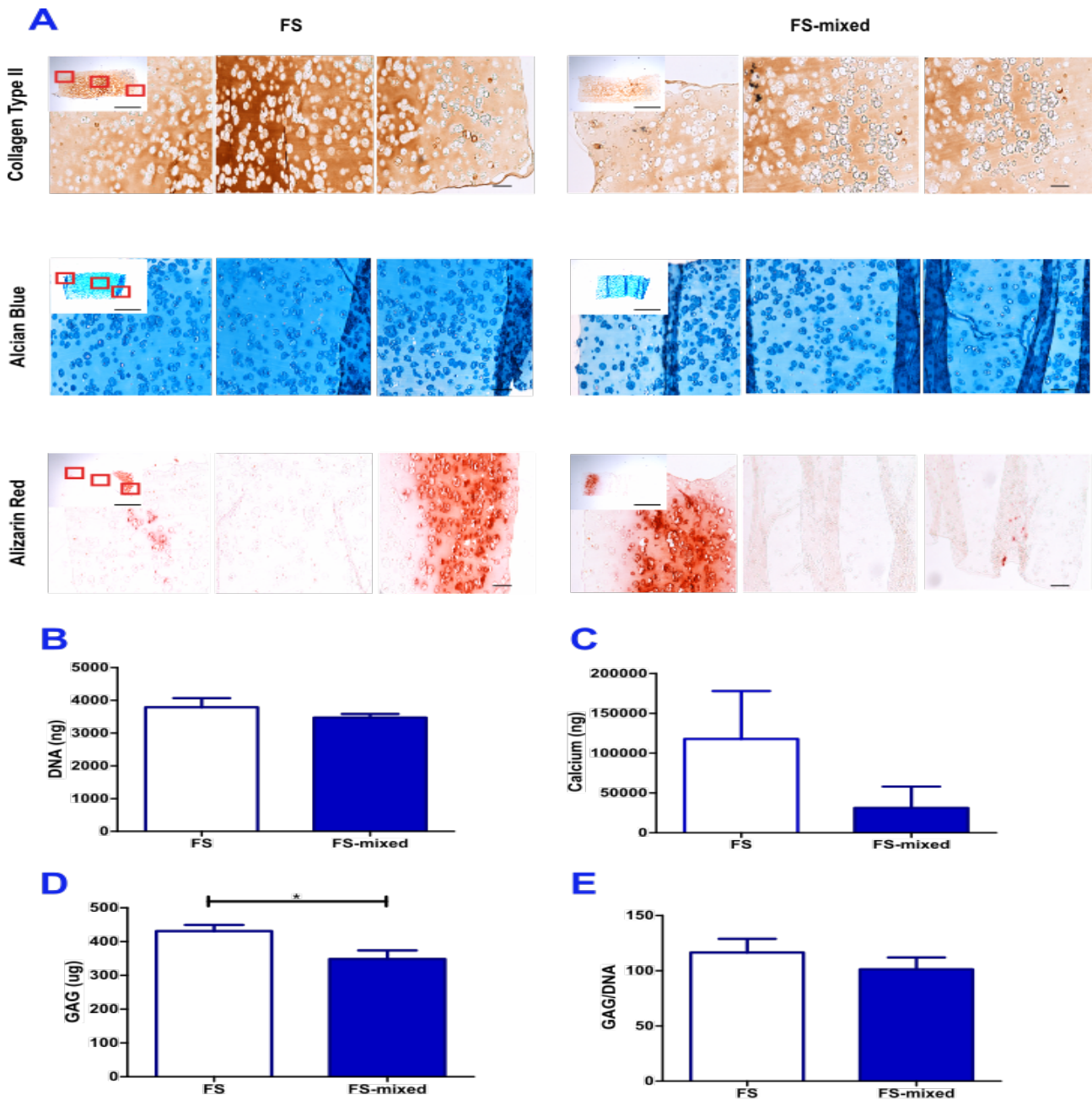
Figure 3.2 The influence agitating the media (FS-mixed) has on chondrogenesis in comparison to free swelling (FS) controls. 0 % strain was applied to FS-mixed samples within the bioreactor system. (A) Spatial presentation of immunohistochemical staining for collagen type II production, and histological staining with alcian blue for sulphated mucins, and with alizarin red for calcium deposits (n = 2). (B) DNA (ng), (C) calcium (ng) and (D) GAG (ug) and (E) GAG/DNA content of biochemically digested samples (n = 3 or 4). Scale bars: 500 μm (inset macro image) and 100 μm. * denotes p < 0.05 based on student t-test analysis

3.4.2 Dynamic compression enhances the functional development of cartilage grafts engineered using BMSCs

The second phase of this study sought to identify how dynamic compression influences MSC chondrogenesis. Having found that the media agitation action of the platen mildly suppressed chondrogenesis, all strained magnitudes were compared to the FS-mixed control (newly termed 0 % strain). Intermediate levels of DC compression (10% strain) were found to enhance type II collagen. Staining for collagen type X was, however, extremely low (fig. 3.3A).

Biochemically, DNA (fig. 3.3B) and GAG (fig. 3.3C) content in 10 % strained groups remained similar to 0 % controls. Mechanical testing indicated that functional development of cartilage grafts were greatly increased in 10 % strained samples (fig. 3D). This was based on the equilibrium modulus increasing from an average of 24.93 $\pm$ 2.64 kPa to 41.22 $\pm$ 0.70 kPa.
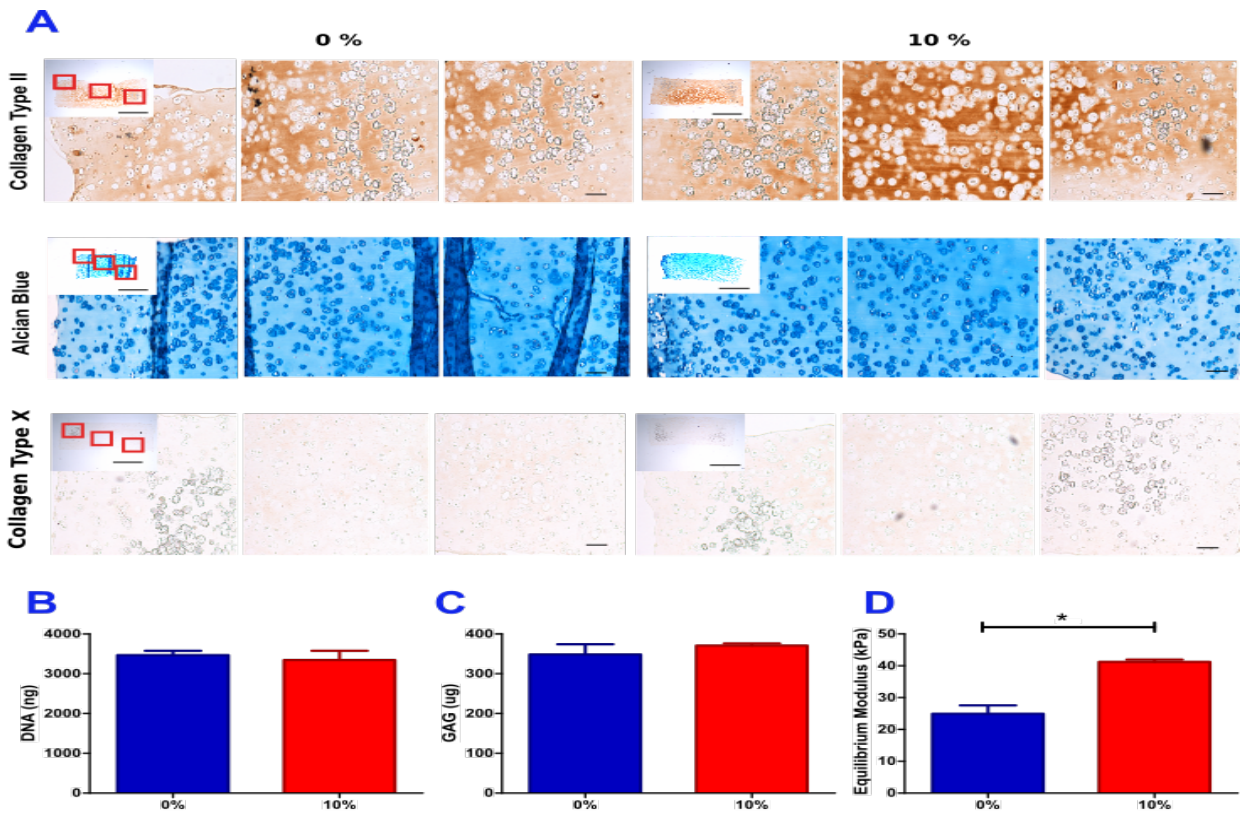
Figure 3.3 The influence conventional 10 % strain DC magnitude has on chondrogenesis in comparison to 0 % agitated controls. (A) Immunohistochemical staining for collagen type II production and histological staining with alcian blue for sulphated mucins and with alizarin red for calcium deposits (n = 2). (B) DNA, (C) GAG and (D) GAG/DNA content of biochemically digested samples (n = 4). Scale bars: 500 μm (inset macro image) and 100 μm. * denotes p < 0.05 based on 1-way ANOVA post-test analysis

3.4.3 Intermediate levels of DC promote hypertrophy and calcification of engineering cartilage

Having established the positive effect of DC at 10 % strain on chondrogenesis, the overall effect of DC at various magnitudes on hypertrophy and calcification of cartilage grafts was then determined. All tissues, irrespective of magnitude of applied dynamic compression, stained intensely for sGAG accumulation (fig. 3.4A). Control samples of 0 % strain with media agitation led to the production of calcified deposits asymmetrically within the tissue. Intermediate levels of DC acted to accelerate calcification of the cartilage graft as evident by increased alizarin red staining for calcium deposition in these constructs (fig. 3.4A). High levels of DC compression (20 % strain) appeared to reduce the development of calcified deposits.

Biochemically, there were no significant differences between controls and loaded groups in terms of GAG (fig. 3.4B) and collagen (fig. 3.4C) accumulation. Calcium production tended to increase in all dynamically compressed groups with a significant rise in 10 % strained samples of 81 % with respect to unloaded controls. At higher magnitudes of strain (20 %), this load induced increase in calcification was not observed. Mechanical testing indicated that functional development of cartilage grafts were greatly increased in 10 % strained samples , but not in samples subjected to 20 % strain.
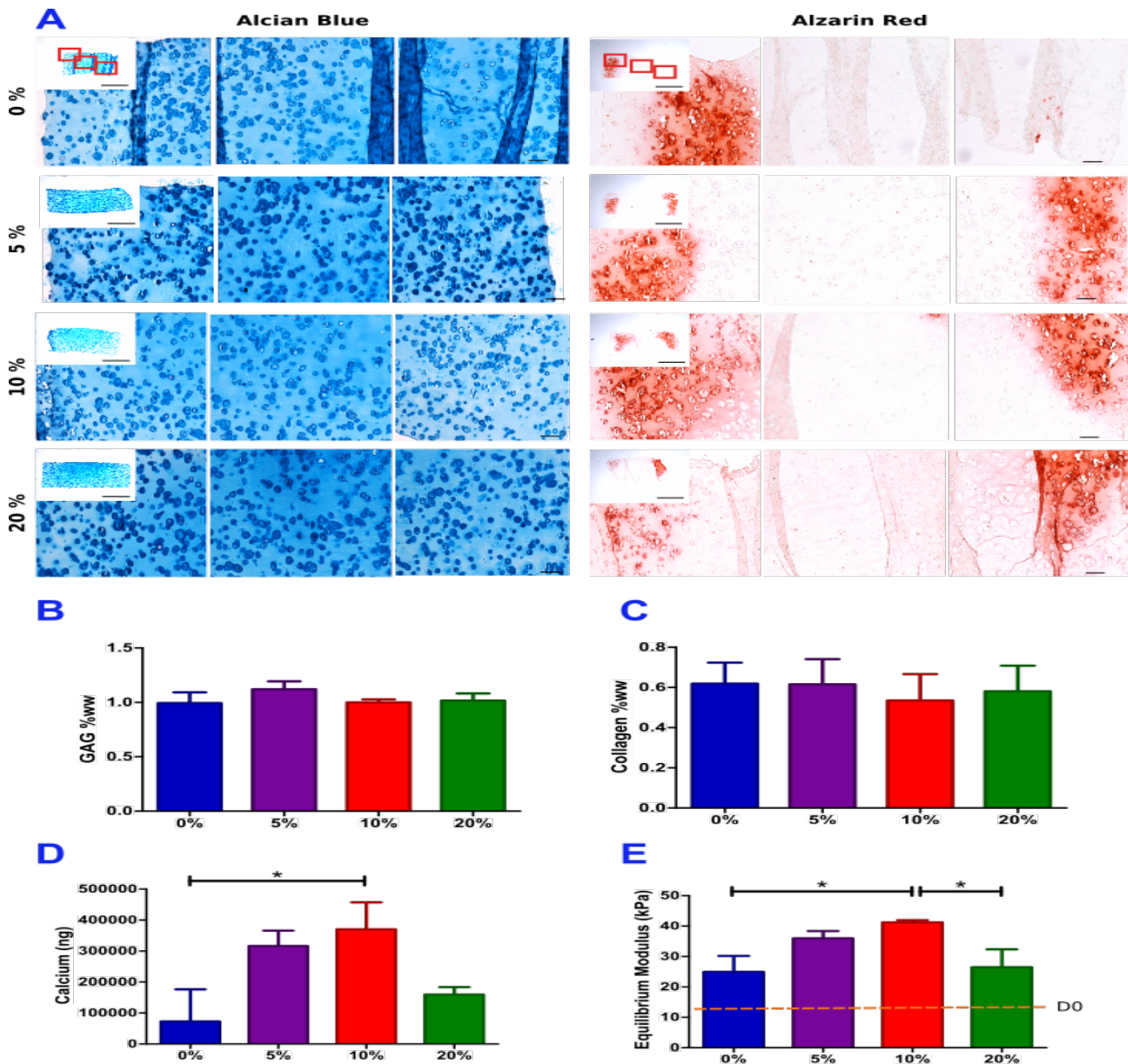
Figure 3.4 Effect different magnitudes of loading have on the progression of MSC chondrogenesis in cartilage grafts. (A) Histological staining for calcium deposition and sGAG accumulation with alizarin red for calcium deposits and with alcian blue for sulphated mucins respectively (n = 2). (B) GAG as a percentage of wet weight (% ww), (C) collagen % ww and (D) calcium content of biochemically digested samples (n = 3 or 4). (E) Equilibrium modulus of sample groups based on mechanical testing (n = 4). Scale bars: 500 μm (inset macro image) and 100 μm. * denotes $p < 0.05$ based on 1-way ANOVA post-test analysis

3.4.4 Increases in stiffness correlate with enhanced calcium accumulation in mechanically stimulated engineered tissues

Correlating increases in equilibrium modulus with deposition of collagen, GAG and calcium revealed a significant trend relationship between calcium deposition and the functional development of cartilage grafts (fig. 3.5C). This is based on a significant ($p = 0.0136$) Pearson's rank correlation coefficient of 0.4720 (fig. 3.5C). Whilst GAG also trends quite strongly it is not significant (fig. 3.5A). Comparing correlation coefficients, however, reveals a Fisher r-z transformation score of z = 0.67 between calcium and GAG correlations with Young's modulus indicating no statistical significance between these results. Similarly, a larger z-score between calcium and collagen correlations with Young's modulus also highlighted the same indication.
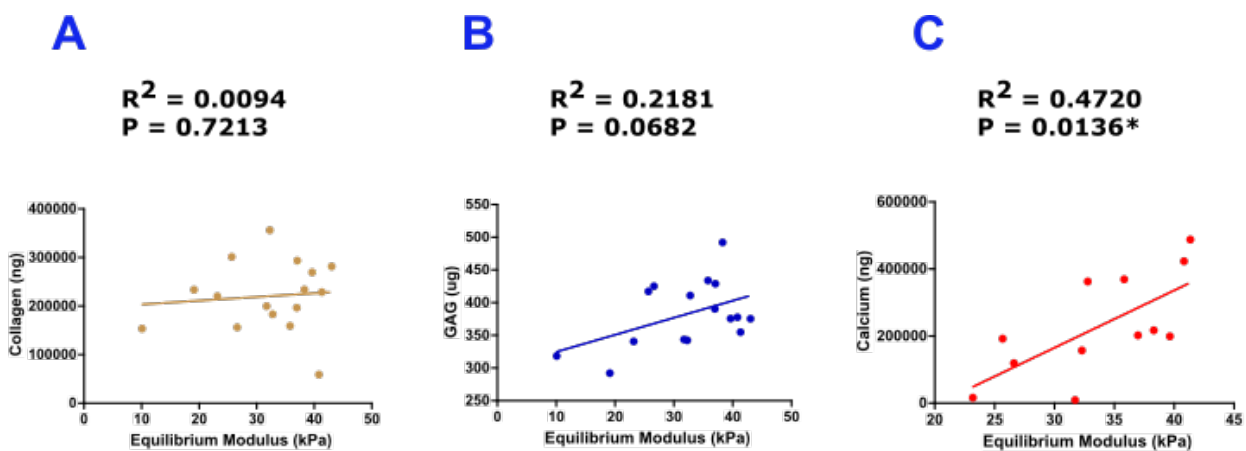
Figure 3.5 Correlating increases in equilibrium modulus with calcium deposition. Scatter plots of equilibrium modulus (kPa) against production of (A) collagen (ng), (B) GAG (µg) and (C) calcium (ng). Pearson coefficient, R^2 denotes fit of trend line. * denotes statistical confidence in trend, $p < 0.05$.

3.5 Discussion

The aim of this study was to test the hypothesis that chondrogenesis and hypertrophy of MSCs is regulated by DC in a magnitude dependent manner. The agitation of media during DC was found to suppress chondrogenesis in terms of sGAG production and collagen type II deposition. Therefore to test the effect of DC magnitude mechanically stimulated constructs were compared to controls in which the media was agitated by displacing the bioreactor platen but not compressing the tissue. While GAG and collagen production was found to be independent of DC, calcification was increased at low and intermediate DC magnitudes.

Media agitation alone was found to suppress chondrogenesis, likely due to the enhanced oxygen levels that this action creates within the construct. It is clear that oxygen tension plays an influential role in chondrogenesis. Low oxygen tension has been shown to enhance MSC chondrogenesis during hydrogel culture. In static culture, oxygen levels can drop from 20 % at the surface of the culture media to in the region of 15 - 17 % at the periphery of the MSC-laden hydrogel. On the other hand normoxic oxygen conditions during prolonged TGF-β mediated MSC chondrogenesis have enhanced the hypertrophic development of cartilage grafts towards bone formation. Witt et al. recently highlighted that dynamic compression also tends to increase oxygen tension within the centre of MSC laden hydrogels even over a relatively short, 30 minute loading period. Therefore, DC acts to both increase oxygen within cellular laden constructs as well as providing a mechanical stimulus to the cells. Platen movement without dynamic compression will increase oxygen availability at the periphery of the MSC-laden hydrogel. The gradients, produced by peripheral cellular consumption, that provide the pro-chondrogenic, lower oxygen environment in normoxia must therefore be reduced. Thus chondrogenesis is subsequently suppressed in normoxia by dynamic platen movement.

The application of a 10 % cyclic, compressive strain was found to enhance chondrogenesis. This is in agreement with DC enhancing both chondrogenesis and the resulting functional development of cartilage grafts is widely accepted in literature. Huang et al. have shown 10 % dynamic compression to have a positive effect on mechanical properties of the resulting

tissue despite failing to alter matrix composition [221]. In our laboratory, Thorpe et al. have shown the beneficial effects of dynamic compression on sGAG deposition applied 21 days following the onset of MSC differentiation [98]. Both researchers implemented a similar loading protocol of 10 % strain at 1Hz frequency. This research confirms clarification that dynamic compression has a beneficial effect on MSC chondrogenesis.

The application of 10 % dynamic compression was also found to increase calcium deposition, suggesting that this magnitude of loading was both pro-chondrogenic and promoted progression along the endochondral pathway. This is contrast with other findings in the literature. Bian et al. found dynamic compression downregulated hypertrophic markers and significantly suppressed calcification when MSC-laden hydrogels were maintained in hypertrophic culture conditions [22]. While no chemical catalyst of hypertrophy was used in this study, a switch from 5 % to 20 % O_2 was used to achieve a similar outcome. It should be noted Bian et al. initiated an intermediate loading magnitude of DC after day 3 and maintained cultures in normoxia throughout [22]. Zhang et al. recently highlighted suppression of hypertrophy through TGF-β notch signalling pathways mediated by DC [23]. The scaffold used during this experiment was coated with chitosan, which enables cellular attachment. This may have facilitated enhanced mechano-transduction of the smaller loading magnitude. Again normoxic conditions were used throughout. Differences in media supplementation conditions, scaffold or hydrogel composition and/or oxygen levels may go some way towards explains these discrepancies in findings.

The reduction in calcification at high strain magnitudes (20 %) is an important observation despite not being significant. Horner et al. have recently shown an increased suppression of calcification at increasing magnitudes of strain applied in the form of dynamic compression [222]. In their study increasing strain magnitude between 5, 10 and 20 % strain suppressed calcification with increasing effect. This study highlights a different trend as free-swelling controls (0 % strain) were not as heavily calcified. In the study conducted by Horner et al. osteogenic media was used, which therefore may enhance the potency of dynamic compression to provide a pro-chondrogenic stimuli.

3.6 Conclusion

DC has frequently been shown to enhance chondrogenesis. This study now extends its use to osteochondral tissue engineering. Strain dependent changes in calcification may allow the modulation of MSC chondrogenic progression towards either stable cartilage or bone formation through endochondral ossification. While this may be specific to the oxygen conditions within the system, it may become a useful tool for exploration in the field of osteochondral tissue engineering. In the next chapter, I will explore the way in which oxygen tension and substrate stiffness interact and effect MSC chondrogenesis within RGD-modified alginate hydrogels.

CHAPTER 4

Modulating both oxygen levels and substrate stiffness to regulate chondrogenesis and hypertrophy of MSCs

4.1 Abstract

THIS study aimed to understand how changing the stiffness of a 3-dimensional alginate hydrogel and the external oxygen tension influences MSC chondrogenesis. Bone marrow derived mesenchymal stem cells (MSCs) were seeded in RGD-modified alginate hydrogels ionically crosslinked using two different concentrations (10 mM and 100 mM) of calcium chloride ($CaCl_2$) to produce soft or stiff constructs. These MSC-laden hydrogels were then cultured at either 5 % or 20 % O_2 for 28 days. The Young's modulus of the alginate hydrogel increased from 4 to 15 kPa when the molarity of $CaCl_2$ was increased from 10 to 100 mM. After 14 days of culture, an upregulation of collagen type II gene expression was observed in soft hydrogels at both external oxygen tensions. In spite of this, no significant differences in total sGAG or collagen accumulation was in stiffer gels at either O_2 level over 28 days in culture. Furthermore, the softer gels remained weaker even after this 28 day culture period. Oxygen tension also had a negligible effect on total sGAG and collagen synthesis, yet dramatically altered spatial ECM deposition. At 20 % O_2, picrosirius red staining for collagen deposition was greater in both soft and stiff MSC-laden hydrogels, while at 5 % O_2 collagen type II was more more homogenously deposited and in greater quantity. Calcium

deposition was only evident on the extreme periphery of stiff hydrogels.Taken together this paper suggests that softer hydrogels cultured in 5 % O_2 tensions appear to be the most chondrogenic. The paper further highlights the correct combination of substrate stiffness and oxygen can both enhance or more evenly distribute cartilage-specific proteins with little effect on calcification over 28 days of culture.

Keywords – **MSCs, chondrogenesis, oxygen tension, substrate stiffness, tissue engineering, mechanotransduction**

4.2 Introduction

It is well established that, in addition to soluble factors, mechanical cues and other external, environmental factors can direct stem cell behaviour [160,223–226]. MSC fate, towards a given lineage, has been shown to be dependent on the stiffness ranges of the underlying substrate that reflected physiological and tissue-specific mechanical property ranges. Therefore MSCs on soft substrates (0.1 - 1 kPa) were found to be neurogenic, whereas on intermediate subsrate stiffness (8 - 17 kPa) MSCs underwent myogenesis, and relatively stiff substrates (25 - 40 kPa) produced osteogenesis in MSCs [165]. Stem cell fate has shown to be mediated by substrate stiffness in both 2-D and 3-D hydrogel environments. During 3-D hydrgoel culture, substrate stiffness has been shown to determine the osteo-adipo fate choice of MSCs with softer substrates supporting adipogenesis [29]. Conversely, osteogenesis occured in all other higher stiffness 3-D substrates, except those above 100kPa. Furthermore, a cell's ability to generate tension is important for allowing it to respond to changes in substrate stiffness. The incorporation of RGD-binging peptides allowed cells to generate tension, reorganise their surrounding integrin binding and ultimately switch their fate in response to substrate stiffness up to a given threshold. It is therefore clear substrate stiffness significantly influences MSC fate towards a range of tissue lineages.

The effect of substrate stiffness on MSC chondrogenesis is less clear. Park et al.

demonstrated that the fate of MSCs towards chondrogenesis depends on substrate stiffness with soft 3-D environments producing enhanced chondrogenesis, while MSCs on stiff 2-D substrates mainly underwent myogenesis. Park et al. further highlighted that MSCs in soft 3-D substrates had less spreading, had fewer stress fibers and a lower proliferation rate than MSCs on stiff 2-D plastic substrates [167]. The implication that soft substrates produce enhanced chondrogenesis was also made evident by Steward et al., in which it has shown that the total production of sGAG within the construct and excreted to the media was higher in soft agarose hydrogels [227].

Oxygen availability is another potent regulator of MSC fate, with low oxygen tension enhancing both stemness [138] during expansion and chondrogenesis during culture [141]. In addition, Ramos et al. indicates that any response to substrate stiffness, in chondrocytes at least, may be specific to the external oxygen tension. At low oxygen tension, stiffer collagen hydrogel networks produced a more chondrogenic response from chondrocytes with increased production of cartilage-specific matrix proteins, while the opposite was true at atmospheric external oxygen conditions. This suggests that the interplay between the two stimuli may also have an effect on MSC chondrogenesis, particularly in a physiologically relevant 3-D environment.

Therefore while it is clear that substrate stiffness plays a role in MSC differentiation, its exact role in regulating chondrogenesis in a 3-D hydrogel environment is less certain. Furthermore it is unknown whether the response of MSCs to altered oxygen environments depends on the stiffness of the substrate. This study therefore aims to understand how the interplay between substrate stiffness and external oxygen tension in a 3-D environment affects MSC chondrogenesis. The hypothesis of this study is that soft hydrogels promote a more chondrogenic phenotype; and that this is enhanced synergestically at low oxygen tension (5 % O_2). To test this hypothesis, MSCs will be encapsulated in RGD-modified alginate hydrogels of two different stiffness at both 5 % and 20 % O_2.

4.3   Materials and Methods

4.3.1   RGD incorporation and alginate preparation

RGD-modified methacrylated alginate was prepared by researchers in Eben Alsberg's laboratory and synthesized in a two-step reaction utilizing standard carbodiimide chemistry. Low-molecular-weight sodium alginate (37,000 g/mol) was prepared by irradiating Protanal LF 20/40 (196,000 g/mol; FMC Biopolymer, Philadelphia, PA) at a gamma dose of 5 Mrad. Twenty-five percent actual methacrylation of alginate carboxylic acid groups was performed as described previously [228]. Methacrylated alginate solutions (1 %, w/v) were prepared with 50mM of 2-(N-morpholino)- ethane sulfonic acid hydrate (Sigma, St. Louis, MO) buffer solution containing 0.5 M NaCl (Sigma) at pH 6.5, and sequentially mixed with N-hydroxysuccinimide (Sigma) and 1-ethyl-3-[3-(dimethylamino)propyl] carbodiimide (EDC; Sigma). The molar ratio of N-hydroxysuccinimide to EDC was 0.5:1.0, and the weight ratio of EDC to methacrylated alginate was 1.0:20.7. The Gly-Arg-Gly-Asp-Ser-Pro (Commonwealth Biotechnologies, Richmond, VA) amino acid peptide sequence was added to the methacrylated alginate solution at a weight ratio of 10 mg/g methacrylated alginate. After reacting for 24 h at 48 ℃, the reaction was stopped by addition of hydroxylamine (0.18 mg/mL; Sigma), and the solution was purified by dialysis against ultrapure deionized water (di-H_2O) (MWCO 3500; Spectrum Laboratories, Rancho Dominguez, CA) for 3 days, treated with activated charcoal (0.5 mg/100 mL, 50-200 mesh; Fisher, Pittsburgh, PA) for 30 min, filtered (0.22 mm filter), and lyophilized. Control methacrylated alginate was prepared in the same manner but without the presence of peptide.

The lyophilised alginate with RGD modification was then re-suspended in ultra pure water at 2.5 % before being filtered through a 45 μm mesh.

4.3.2   Cell isolation, expansion and hydrogel encapsulation

MSCs were isolated from porcine femora. Following isolation, Porcine MSCs were preserved in liquid nitrogen before later being thawed and expanded according to a modified method developed for human MSCs. MSCs were plated at a seeding density of 50,000 cells/cm^2 in high-glucose Dulbecco's modified eagles medium (4.5 mg/mL D-Glucose, 200 mM L-Glutamine; hgDMEM) supplemented with 10 % fetal bovine serum (FBS) and 2 % penicillin (100 µg/ml) - streptomycin (100 µg/ml); and expanded to passage two in a humidified atmosphere at 37 ℃ and 5 % CO_2.

MSCs were suspended in chondrogenic medium (CM), which consisted of hgDMEM supplemented with penicillin (100 µg /ml) and streptomycin (100 µg/ml), sodium pyruvate (100 µg/ml), L-proline (40 µg/ml), bovine serum albumin (1.5 mg/ml), linoleic acid (4.7 µg/ml), insulin-transferrin-selenium (10 µg/ml), L-ascorbic acid-2-phosphate (50 µg/ml), dexamethasone (100 nM) and 10 ng/mL TGF-β_3. The MSC suspension was subsequently mixed with 2.5 % RGD-modified alginate (dissolved in ultra pure water) at a ratio of 1:4 to yield a final gel concentration of 2 % RGD-modified alginate and a cell density of 20 million cells/ml. The alginate-cell suspension was cast in a agarose moulds (5 mm diamater by 2 mm deep) containing either 100 mM or 10 mM $CaCl_2$. A slab and solution, containing a similar $CaCl_2$ concentration, was placed on top of and around moulds containing 20 samples respectively. This housing was then incubated for 30 minutes. Constructs were maintained separately in 12-well plates with 2 ml of chondrogenic medium in 5 % or 20 % O_2. Medium was exchanged twice weekly and constructs were cultured in these conditions for 28 days.

4.3.3   Mechanical testing

Constructs were mechanically tested (n = 4) in unconfined compression between impermeable platens using a standard materials testing machine with a 5 N load cell (Zwick Roell Z005, Herefordshire, UK) as previously described hydrated through immersion in a PBS bath maintained at room temperature. A preload of 0.01 N was applied to ensure that

the construct surface was in direct contact with the impermeable loading platens. Stress relaxation tests were performed consisting of a ramp displacement of 10 µm/s up to 10 % strain, which was maintained until equilibrium was reached (roughly 30 minutes). This was followed by a dynamic test where cyclic strain amplitude of 1 % (10 - 11 % total strain) was applied for 10 cycles at 1 Hz. Constructs were then further used for biochemical analysis.

4.3.4 RNA isolation and real-time reverse transcriptase polymerase chain reaction (rt-PCR)

Cell lysate for RNA isolation was prepared at day 14 of culture by lysing MSC laden hydrogels (n = 4 gels/group) using RLT lysis buffer (Qiagen, UK) supplemented with 10 µl β-mercaptoethanol (Sigma-Aldrich, Ireland), before homogenising with a pestle, flash-freezing in liquid N_2 and storing at -85 ℃. Control MSCs were typsinised from 80 - 90 % confluent flasks, lysed in a similar manner and homogenised using a pipette before being flash-frozen and stored at -50 ℃ also. At the time of isolation, lysates were thawed and homogenized using a QIAshredder column (Qiagen, UK) and total RNA was isolated and purified using the RNeasy mini kit (Qiagen, UK) as per the suggested manufacturer protocol. Purity and yield of RNA was quantified using a NanoDrop Spectrophotometer (Labtech International, Uckfield, UK). For cDNA preparation, 314 ng total RNA per sample were reverse transcribed into cDNA per 50 µl of reaction volumes using a high capacity reverse transcription cDNA kit (Applied Biosystems, Paisley, UK) as per manufacturer's instructions. Quantitative PCR was performed in an ABI 7500 sequence detection system (Applied Biosystems, Paisley, UK) using SYBR select master mix (Applied Biosystems, Paisley, UK) for evaluating the expression of aggrecan (ACAN), α-smooth muscle actin (ACTA), collagen type II (COL2A1), collagen type X (COL10A1) and Glyceraldehyde-3- phosphate dehydrogenase (GAPDH) genes. Porcine specific primer sequences that were used for amplification of these genes are listed in Table 4.1. Comparative Threshold (Ct) data were analysed using the $\Delta\Delta$Ct method with an average of GAPDH and ACTB as the endogenous control [229]. Relative

expression of the genes is presented as fold changes relative to the control group.

4.3.5 Biochemical content

The biochemical content of constructs (n = 3 or n = 4) was assessed at each time point. The wet mass of each construct half was recorded before being frozen at -85 °C for later analysis. Samples were digested with papain (125 µg/mL) in 0.1 M sodium acetate, 5 mM L-cysteine HCl, 0.05 M EDTA, pH 6.0 (all Sigma- Aldrich) at 60 °C under constant rotation for 18 h. DNA content was quantified using the Hoechst Bisbenzimide 33258 dye assay as previously described [219]. The proteoglycan content was estimated by quantifying the amount of sulfated glycosaminoglycan (sGAG) in constructs using the dimethylmethylene blue dyebinding assay (Blyscan, Biocolor Ltd., Carrickfergus, UK), with a shark chondroitin sulfate standard. Total collagen content was determined through measurement of the hydroxyproline content [220]. A hydroxyproline-to-collagen ratio of 1:7.69 was used.

The remaining halves of mechanically tested constructs were digested using 1M HCl at 60 °C under constant rotation for at least 18 hrs. Samples were subsequently centrifuged at 5000g to remove any sediment from the digest. Calcium chloride at the defined calcium content was diluted in 1M HCl to produce two standard stocks (100 and 20 µg/ml respectively), which were diluted further to produce the four high and three low standard points of the curve respectively. Calcium content was then determined relative to dye fluorescence in response to calcium concentration using a commercial sentinel calcium kit.

4.3.6 Histology and immunohistochemistry

Constructs (n = 2) were fixed in 4 % paraformaldehyde (Sigma-Aldrich), wax embedded and sectioned at 5 um to produce a cross section perpendicular to the disk face. Sections were stained for sGAG with 1 % alcian blue 8GX (Sigma-Aldrich) in 0.1 M HCl; for collagen with picro-sirius red; and for calcium with alziran red. The deposition of collagen type I,

Gene name	Gene symbol	Forward/Reverse Sequence
Glyceraldehyde-3-phosphate dehydrogenase	GAPDH	STTTAACTCTGGCAAAGTGG/ GAACATGTAGACCATGTAGTG
Actin, Beta	ACTB	GCGGGCATCCACGAAACTA/ TGTTGGCGTAGAGGTCCTT
Smooth muscle aortic alpha-actin	ACTA	CAAAAGAGGAATCCTGACC/ CATTGTAGAAAAGAGTGGTGC
Aggrecan	ACAN	GACCACTTTACTCTTGGTG/ CATTGTAGAAAGAGTGGTGC
Collagen type 2, alpha-1	COL2A1	CGACGACATAATCTGTGAAG/ TCCTTTGGGTCCTACAATATC
Collagen type 10, alpha-1	COL10A1	GTAGGTGTTTGGTATTGCTC/ GAGCAATACCAAACACCTAC

Table 4.1 Primer sequences used for rt-PCR.

type II and type X was identified through immunohistochemistry. Briefly, sections were quenched of peroxidase activity, rinsed with PBS before treatment with chondroitinase ABC (Sigma-Aldrich) in a humidified environment at 37 °C. Slides were rinsed with PBS and non-specific sites were blocked with goat serum (Sigma-Aldrich). Sections were then incubated overnight at 4 °C with the primary antibody; mouse monoclonal collagen type I antibody. (1:400; 1.4 mg/mL; Abcam, Cambridge, UK) or mouse monoclonal anti-collagen type II (1:100; 1 mg/mL; Abcam). After washing in PBS, sections were incubated for 1 h in the secondary antibody; anti-mouse IgG biotin antibody produced in goat (1:400; 1 mg/ mL; Sigma-Aldrich). Colour was developed using the Vectastain ABC reagent (Vectastain ABC kit, Vector Laboratories, Peterborough, UK) followed by exposure to peroxidase DAB substrate kit (Vector Laboratories). Negative and positive controls of porcine ligament, cartilage or growth plate were included for each batch. For both histology and immunohistochemistry images presented at high magnification from opposite annulus regions (left and right) and core (middle) as well as macroscopic images at low magnifications (corner).

4.3.7   Statistical analysis

Statistics were preformed using graphpad prism software package. Groups were analyzed for significant differences using a general linear model for analysis of variance with factors of substrate stiffness and oxygen availability examined. Tukey's test for multiple comparisons was used to compare conditions. Significance was accepted at a level of $p < 0.05$. Numerical and graphical results are presented as mean $\pm$ standard error from the mean.

4.4 Results

4.4.1 Altering substrate stiffness in alginate hydrogels by varying ionic crosslinking concentration

It has been previously shown that changing concentrations of ionic crosslinking solutions allow alginate gels of varying stiffnesses to be formed. Reducing the concentration of $CaCl_2$ from 100 mM to 10 mM was found to reduce the Young's modulus of a cell-free RGD-alginate hydrogel from 15 to 5 kPa (Cell-free; $p < 0.01$, fig. 4.1A). The equilibrium modulus was also found to reduce from 9 to 4 kPa (Cell-laden; fig. 4A,B). The differences between the stiffness of the 10 mM and 100 mM $CaCl_2$ crosslinked gels was less dramatic when MSCs were incorporated into the construct. From this point onwards, the 10 mM $CaCl_2$ crosslinked RGD-modified alginate hydrogels are termed soft, while 100mM $CaCl_2$ crosslinked gels are termed stiff.
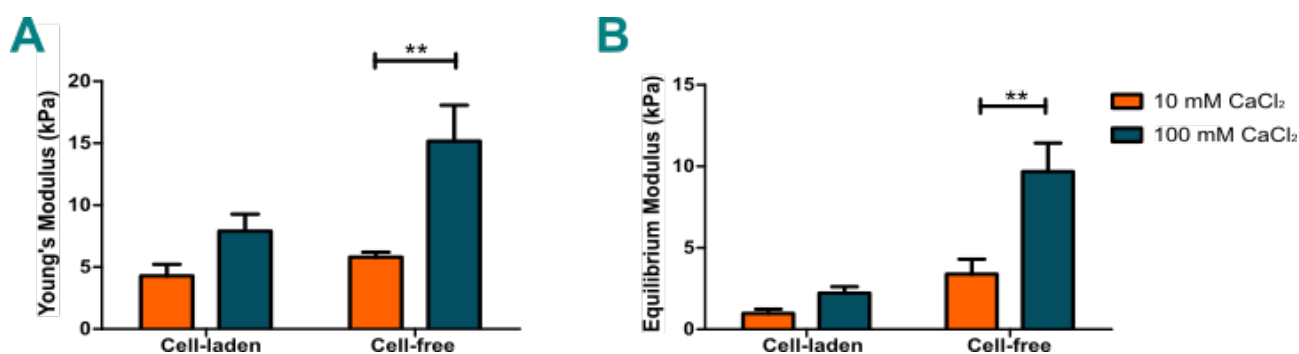
Figure 4.1 Altering substrate stiffness of alginate hydrogels by varying molarity of calcium chloride. (A) Young's modulus (kPa) and (B) equilibrium modulus (kPa) of 2mm high by 5mm diameter RGD-modified alginate hydrogels subjected to 10 % ramp strain and hold mechanical testing protocol. Cell-laden or cell-free alginate hydrogels were crosslinked with 10 mM (orange bars) or 100 mM (dark teal bars) calcium chloride for 30 minutes. ** denotes p $<$ 0.01 based on one-way ANOVA post-test analysis

4.4.2 Soft hydrogels provide enhanced biological cues for chondrogenesis

In general, soft hydrogels provided a more chondrogenic environment for MSCs, as evident by higher expression of type II collagen (COL2A1; $p < 0.05$; fig. 4.2). α-smooth muscle actin, a marker of myogenesis, was more highly expressed in MSC-laden stiff hydrogels at 5 % O_2 culture conditions (ACTA; $p < 0.001$; fig. 4.2). Aggrecan (ACAN), another key marker of chondrogenesis, was expressed at similar levels in all groups, as was type X collagen (COL10A1), a marker of hypertrophy.
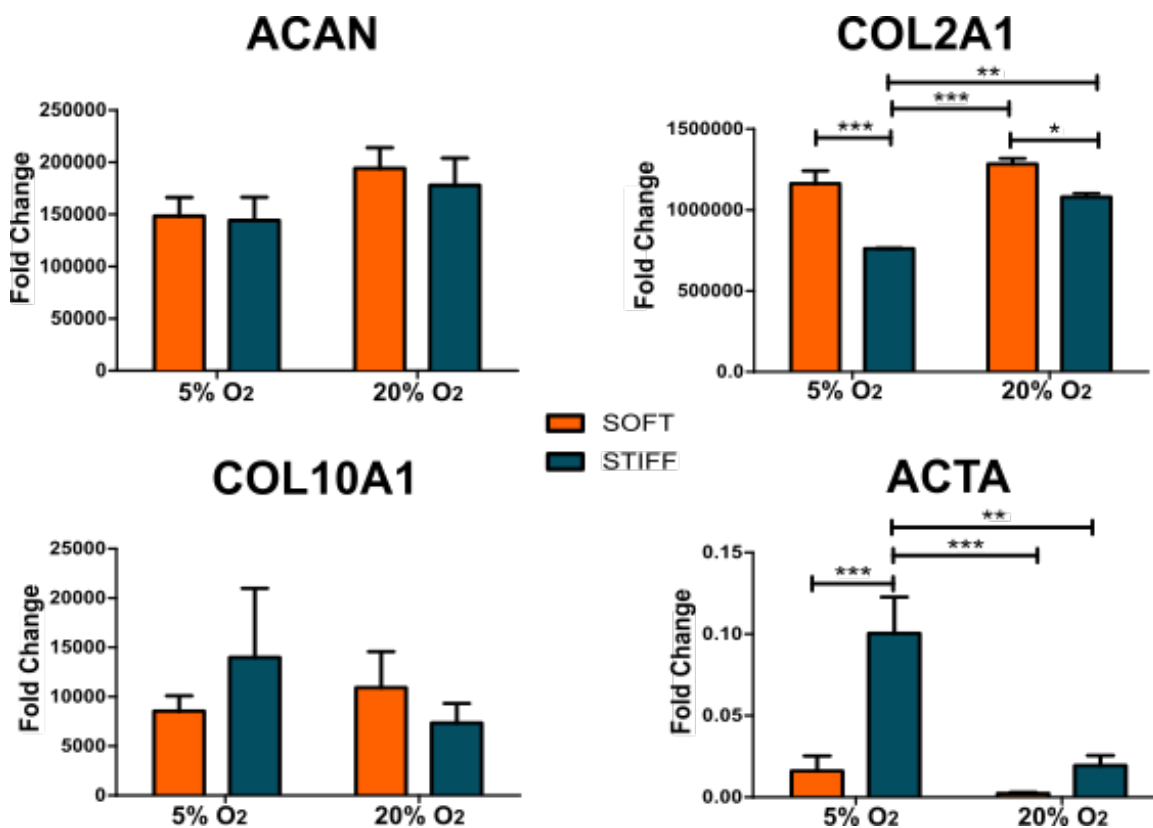
Figure 4.2 Soft hydrogels promote enhanced chondrogenic gene expression after 14 days of culture in chondrogenic conditions. Fold change gene expression in comparison to trypsinised MSCs during expansion of aggrecan (ACAN), collagen type II (COL2A1), collagen type X (COL10A1) and α-smooth muscle actin (ACTA) of MSCs in soft and stiff alginate hydrogels cultured at 5 % or 20 % O_2 for 14 days (n = 4). *, **, *** denotes $p < 0.05, 0.01, 0.001$ respectively based on one-way ANOVA post-test analysis

4.4.3 Stiff hydrogels promote the development of a more mechanically functional cartilage tissue

A small reduction in DNA levels was observed in all groups over 28 days in culture ($p < 0.05$; fig. 4.3A). GAG levels were comparable across groups (fig. 4.3C), which agrees with aggrecan gene expression at day 14 (ACAN; fig. 4.2). In normoxic culture conditions (20 % O_2) stiff hydrogels promote the development of a more mechanically functional cartilage tissue ($p < 0.01$; fig.4.3G,H) as well as increased collagen production (fig. 4.3D) in comparison to all other groups. Similarly GAG and collagen quantities normalised to

DNA content highlighted no significant differences (fig. 4.3E,F). Low levels of calcium were observed in all constructs, with a trend towards greater accumulation in the stiffer gels (fig. 4.3B).
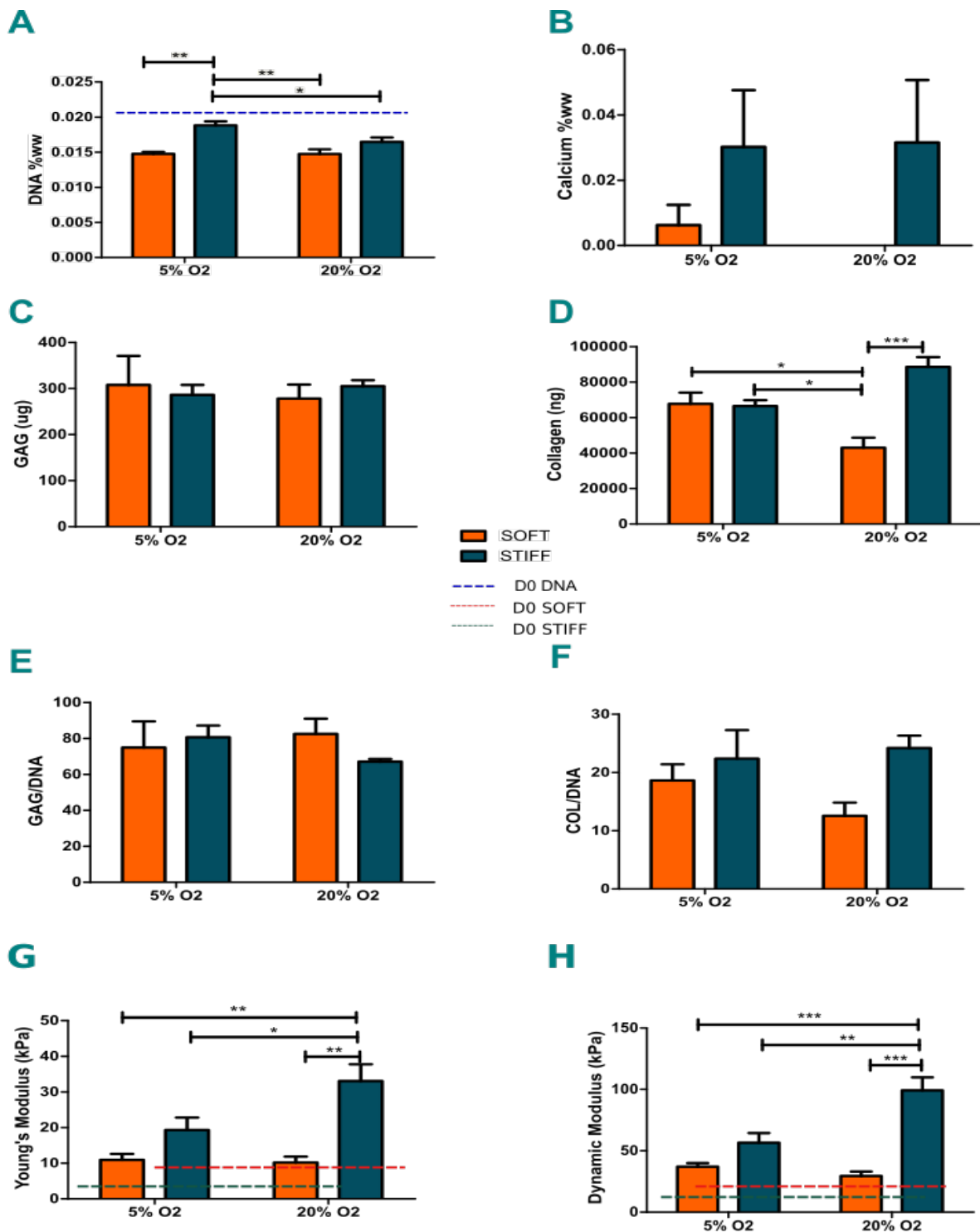
Figure 4.3 Biochemical content of MSCs in soft and stiff alginate hydrogels cultured at 5 % or 20 % O$_2$ after 28 days in TGF-β_3 culture conditions. (A) DNA and (B) calcium content both as a percentage of wet weight, (C) GAG (μg) and (D) collagen (ng) content, (E) GAG/DNA and (F) COL/DNA, and finally (G) Young's modulus and (H) dynamic modulus of RGD-modified hydrogels both soft and stiff cultured at 5 or 20 % O$_2$ (n = 4). *, **, *** denotes p < 0.05, 0.01, 0.001 respectively based on one-way ANOVA post-test analysis

4.4.4 Both external oxygen levels and hydrogel stiffness influence spatial tissue deposition

Tissue deposition after 28 days of culture was analysed histologically using a dual aldehyde fuchsin - alcian blue stain to detect sulphated glycosaminoglycans (dark blue or purple) from residual alginate (light blue), picrosirius red to stain for collagen production and alzarin red to highlight calcium deposits, while collagen type II accumulation was immunohistochemically detected (fig. 4.4).

GAG deposition appeared similar throughout with large amount of sGAG being deposited in all constructs. Picrosirius red staining highlighted a slightly different spatial distribution of collagen proteins. Collagen was distributed more homogenously in constructs cultured at 5 % O_2, both soft and stiff, while the majority of collagen deposited in constructs of both stiffness values cultured at 20 % O_2 was restricted to the core (Picrosirius Red; fig. 4.4). Deposits of calcium, visualised using alzarin red staining, appeared very low in quantity and only occurred in the extreme periphery of stiff hydrogels across both oxygen conditions (Alziarin Red; fig. 4.4). Finally, collagen type II deposition was enhanced at 5 % O_2 conditions in soft hydrogels (Collagen Type II; fig. 4.4). Again suggesting soft hydrogels are slightly more chondrogenic. Spatial distributions in collagen type II were more homogenously deposited in both stiffness conditions cultured at 5 % O_2, while collagen type II was constricted to the core in these conditions at 20 % O_2 culturing conditions.
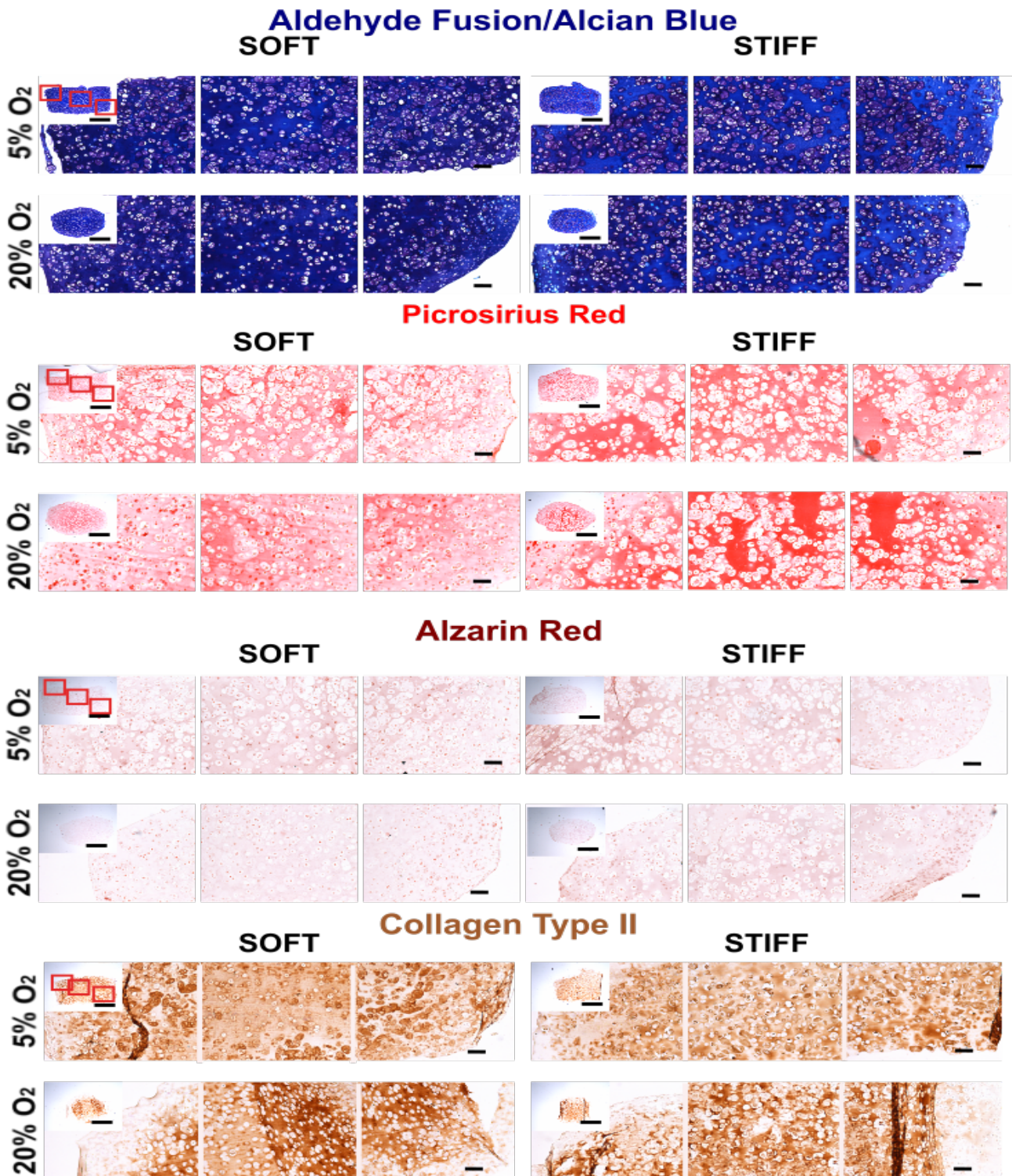
Figure 4.4 Histological view of tissue produced in soft and stiff alginate hydrogels cultured at 5 % or 20 % O$_2$ after 28 days in TGF-β_3. Pictorial representation of the combined aldehyde fuchsin/alcian blue stain to highlight sGAG (dark purple) and residual alginate (light blue), pircosirius stain for non-specific collagens (red), alzarin solution to depict calcium deposition (dark red) and immunohistochemistry for collagen type II strained with DAB (brown). Scale bars: 500 µm (inset macro image) and 100 µm.

4.5 Discussion

This study aimed to understand how the interplay between substrate stiffness and external oxygen tension in a 3-D environment affects MSC chondrogenesis. The results demonstrate that by simply reducing ionic $CaCl_2$ crosslinking concentration the substrate stiffness of a RGD-modified alginate hydrogel can be reduced by at least 50 %. This reduction in substrate stiffness resulted in increased type II collagen gene expression. While substrate stiffness did not alter sGAG accumulation, stiffer substrates promoted higher levels of collagen synthesis overall and resulted in the development of stiffer tissues. These constructs also showed early signs of calcification; especially at 20 % 0_2. Oxygen availability also influenced the spatial development of the engineered tissues, with type II collagen deposition restricted to the core at 20 % O_2. Therefore a combination of soft substrate stiffness and low O_2 appears to promote the development of hyaline-like cartilage, while stiff hydrogels maintained at normoxia promote collagen deposition and a progression along the endochondral pathway.

The ability to alter substrate stiffness by reducing $CaCl_2$ concentration from 100 mM to 10 mM proved reasonably effective. Varying crosslinking concentration or molarity in ionically crosslinked alginate hydrogels has previously been used as an effective way of varying the substrate stiffness of the resulting 3-D hydrogel. Huebsch et al. was able to produce hydrogels with a large range of stiffness, namely 2.5 - 110 kPa [29]. This was achieved by changing calcium concentration of the crosslinking solution from 6.25 - 50 mM. The final percentage of alginate obtained was lower (1.5 %) and was crosslinked by vigorously mixing calcium sulphate into the alginate-cell suspension. In our case, the more rapid $CaCl_2$ solution was used. This may account for the smaller range that could be achieved. Also the method in question, which relies on external entry of the crosslinking solution may be less potent. Nevertheless, a significantly large range of stiffness was possible by lowering $CaCl_2$ concentration from 100 mM to 10 mM.

As evident by enhanced collagen type II expression, soft hydrogels appear to enhance MSC chondrogenesis. This is in agreement with the findings of Park et al., who cultured MSCs on both hydrogels of different stiffness values and stiff plastic. PCR after day 2 of

culture in 1 kPa hydrogels deomstrated an enhancment in type II collagen expression in comparison to MSCs cultured in stiffer hydrogels (15 kPa) or stiff plastic controls [167]. The opposite was also true for α-smooth muscle actin with stiff and 15 kPa hydrogel conditions enhancing its expression in MSCs particularly at 20 % O_2 external oxygen tension. This is further evidence that soft hydrogels irrespective of external oxygen tension tend to enhance MSC chondrogenesis.

The potential of MSCs to generate more tension and re-organise their surrounding extracellular matrix may have allowed higher cell viability in stiff hydrogel constructs after 28 days. It may also have influenced their ability to sense changes in substrate stiffness. Trends of higher sGAG accumulation in 5 % O_2 and soft hydrogels exposed to 20 % O_2 were not significant. So too were trends of increased collagen production in stiff hydrogels cultured in both external O_2 conditions. This may have been due to the small window of substrate stiffness variation. Perhaps a larger reduction in substrate stiffness is needed to have a substantial and significant effect on MSC chondrogenesis in terms of sGAG production in quantitative terms at least. Engler et al. pointed to this by not characterising groups on a single close average value but a range of substrate stiffness values [165]. Therefore when examining how substrate stiffness effects MSC potential to differentiate into a given tissue, a technique capable of manipulating substrate stiffness across a wide range is necessary. Despite this mechanical functionality of the developed tissue was enhanced for stiff hydrogels in 20 % O_2 culture conditions. This may be linked to the increases in collagen production or potentially the low amount of calcium produced solely within these constructs. The link with collagen content enhancing mechanical properties was first made by Mauck et al., in which functionally more mature tissues had a higher collagen content [208].

Collagen type II deposition appearing throughout the construct highlights the enhancing effect of 5 % O_2 on MSC chondrogenesis. The deposition of increased collagen and calcium in stiff hydrogels failing to correlate with collagen type II deposition, and being irrespective of external oxygen, suggest that stiffer hydrogels are perhaps less chondrogenic and have tendencies towards other fate decisions including hypertrophy. Bian et al. demonstrated that MSCs in hydrogels of increasing substrate stiffness tended to produce more calcium in the

construct periphery [230]. Soft hydrogels did alternatively produce more collagen type II and chondroitin sulphate [230].

4.6   Conclusion

This study shows that soft hydrogels tend to enhance MSC chondrogenesis. It also highlights that even slight alterations in substrate stiffness can have an effect of MSC chondrogenesis, calcification and the functional development of the tissue. Spatial distribution of tissue-specific protein deposition are also highly effected by the external oxygen tension.   All of this must be considered before designing an optimum biomaterial and environment for MSC chondrogenesis, especially when attempting to engineer spatially complex tissues such as the bone-cartilage interface. The next chapter will study how substrate stiffness interacts with dynamic compression to affect MSC chondrogenesis and hypertrophy.

CHAPTER 5

The effect dynamic compression has on MSC chondrogenesis is dependent on substrate stiffness

5.1 Abstract

THIS study aimed to determine (1) the effect of substrate stiffness on both early MSC chondrogenesis and (2) the response of MSCs undergoing chondrogenesis to dynamic compression. Bone marrow derived mesenchymal stem cells (MSCs) were seeded in soft or stiff RGD-modified alginate hydrogels and cultured, initially in free-swelling culture for 5 days before subsequent application of dynamic compression for a further 5 days at varying strain magnitudes (0, 10 and 20 %). All constructs were maintained culture conditions at 5% O_2. Soft hydrogels promoted enhanced early MSC chondrogenesis with increased GAG deposition at day 5 and the upregulation of the chondrogenic gene markers ACAN and COL2A1. The application of dynamic compression had no effect on early MSC chondrogenesis in soft hydrogels, irrespective of the magnitude of strain. In contrast, dynamic compression enhanced early MSC chondrogenesis in stiff hydrogels with the expression of the hypertrophic marker COL10A1 modulated in a strain-dependent manner. This study confirms that soft hydrogels provide a more permissive environment for early MSC chondrogenesis. In such environments additional stimuli, such as dynamic compression, cannot further enhance chondrogenesis. Dynamic compression does, however, enhance

early MSC chondrogenesis in stiff hydrogels with the progression towards hypertrophy appearing to depend on the strain magnitude.

Keywords – **MSCs, chondrogenesis, substrate stiffness, dynamic compression, tissue engineering, mechanotransduction**

5.2   Introduction

Diverse mechanical cues have been shown to have an effect on MSC chondrogenesis [31,97,109,167,182]. In the previous chapter of this thesis, it was demonstrated that soft hydrogels enhance early chondrogenesis, while stiff hydrogels facilitate the development of a more mechanically functional tissue. Understanding and tailoring substrate stiffness in a physiologically relevant 3-D environment is an important factor for MSC chondrogenesis. It also plays a factor in other MSC differentiation pathways and is dependent on the stress relaxation and stiffness range chosen [29,165,170]. In addition to substrate stiffness, dynamic compression is known to be a key regulator of MSC chondrogenesis [23,31,97,151,182]. Dynamic compression can both induce and enhance MSC chondrogenesis [30,98]. The way in which diverse cues such as dynamic compression and substrate stiffness interact is, however, still largely unclear. So too is how this interaction is dependent on the magnitude of the mechanical strain.

It has previously been shown that the response of MSCs to hydrostatic pressure and dynamic compression is dependent on the stiffness of the local substrate [227,231]. These studies highlighted that MSC chondrogenesis was only enhanced by the application of either mechanical stimuli in stiffer hydrogels; highlighting the importance of substrate stiffness on mechanotransduction. Furthermore, a study has recently highlighted that the magnitude of dynamic compression plays a role in the hypertrophic response of MSCs to dynamic compression [232]. Here only relatively low levels of loading reduced accumulation of hypertrophic deposits based on collagen type X staining. This highlights that not only the act

of dynamic compression is important, but also the means by which it is applied; particularly for MSC hypertrophy.

Strain transmission from the hydrogel to the cell would appear to be dependent on the stiffness of the given hydrogel [193]. With this in mind, it may be a potential benefit to explore the response of MSCs to altered magnitudes of dynamic compression depends on the stiffness of the local substrate. The objective of this study is to understand how substrate stiffness in hydrogels impacts MSC chondrogenesis and to determine if substrate stiffness alters the response of MSCs subjected to dynamic compression. The hypotheses of this study are that the stiffness of the surrounding hydrogel substrate will impact how the magnitude of dynamic compression modulates MSC chondrogenesis and hypertrophy. More specifically, soft hydrogels will inhibit mechanotransduction in MSCs producing no response to dynamic compression, while enhancing MSC chondrogenesis in free-swelling culture. Alternatively stiff hydrogels will enable MSCs to modulate their behaviour based on different magnitudes of applied dynamic compression. This in turn will produce enhanced MSC chondrogenesis alongside modulated MSC hypertrophy in response to dynamic compression and the corresponding magnitude of strain.

5.3   Materials and Methods

5.3.1   RGD incorporation and alginate preparation

RGD-modified methacrylated alginate was prepared by researchers in Eben Alsberg's laboratory and synthesized in a two-step reaction utilizing standard carbodiimide chemistry. Low-molecular-weight sodium alginate (37,000 g/mol) was prepared by irradiating Protanal LF 20/40 (196,000 g/mol; FMC Biopolymer, Philadelphia, PA) at a gamma dose of 5 Mrad. Twenty-five percent actual methacrylation of alginate carboxylic acid groups was performed as described previously [228]. Methacrylated alginate solutions (1 %, w/v) were prepared with 50mM of 2-(N-morpholino)- ethane sulfonic acid hydrate (Sigma, St. Louis,

MO) buffer solution containing 0.5 M NaCl (Sigma) at pH 6.5, and sequentially mixed with N-hydroxysuccinimide (Sigma) and 1-ethyl-3-[3-(dimethylamino)propyl] carbodiimide (EDC; Sigma). The molar ratio of N-hydroxysuccinimide to EDC was 0.5:1.0, and the weight ratio of EDC to methacrylated alginate was 1.0:20.7. The Gly-Arg-Gly-Asp-Ser-Pro (Commonwealth Biotechnologies, Richmond, VA) amino acid peptide sequence was added to the methacrylated alginate solution at a weight ratio of 10 mg/g methacrylated alginate. After reacting for 24 h at 48 °C, the reaction was stopped by addition of hydroxylamine (0.18 mg/mL; Sigma), and the solution was purified by dialysis against ultrapure deionized water (di-H_2O) (MWCO 3500; Spectrum Laboratories, Rancho Dominguez, CA) for 3 days, treated with activated charcoal (0.5 mg/100 mL, 50-200 mesh; Fisher, Pittsburgh, PA) for 30 min, filtered (0.22 mm filter), and lyophilized. Control methacrylated alginate was prepared in the same manner but without the presence of peptide.

The lyophilised alginate with RGD modification was then re-suspended in ultra pure water at 2.5 % before being filtered through a 45 μm mesh.

5.3.2   Cell isolation, expansion and hydrogel encapsulation

MSCs were isolated from porcine femora. Following isolation, Porcine MSCs were preserved in liquid nitrogen before later being thawed and expanded according to a modified method developed for human MSCs. MSCs were plated at a seeding density of 50,000 cells/cm^2 in high-glucose Dulbecco's modified eagles medium (4.5 mg/mL D-Glucose, 200 mM L-Glutamine; hgDMEM) supplemented with 10 % fetal bovine serum (FBS) and 2 % penicillin (100 μg/ml) - streptomycin (100 μg/ml); and expanded to passage two in a humidified atmosphere at 37 °C and 5 % CO_2.

MSCs were suspended in chondrogenic medium (CM), which consisted of hgDMEM supplemented with penicillin (100 μg /ml) and streptomycin (100 μg/ml), sodium pyruvate (100 μg/ml), L-proline (40 μg/ml), bovine serum albumin (1.5 mg/ml), linoleic acid (4.7 μg/ml), insulin-transferrin-selenium (10 μg/ml), L-ascorbic acid-2-phosphate (50 μg/ml),

dexamethasone (100 nM) and 10 ng/mL TGF-β_3. The MSC suspension was subsequently mixed with 2.5 % RGD-modified alginate (dissolved in ultra pure water) at a ratio of 1:4 to yield a final gel concentration of 2 % RGD-modified alginate and a cell density of 20 million cells/ml. The alginate-cell suspension was cast in a agarose moulds (5 mm diamater by 2 mm deep) containing either 100 mM or 10 mM CaCl$_2$. A slab and solution, containing a similar CaCl$_2$ concentration, was placed on top of and around moulds containing 20 samples respectively. This housing was then incubated for 30 minutes. Constructs were maintained separately in 12-well plates with 2 ml of chondrogenic medium in 5 % O$_2$. Medium was exchanged twice weekly and constructs were cultured in these conditions for 5 days.

5.3.3   Biochemical content

The biochemical content of constructs (n = 3 or n = 4) was assessed at each time point. The wet mass of each construct half was recorded before being frozen at -85 °C for later analysis. Samples were digested with papain (125 µg/mL) in 0.1 M sodium acetate, 5 mM L-cysteine HCl, 0.05 M EDTA, pH 6.0 (all Sigma- Aldrich) at 60 °C under constant rotation for 18 h. DNA content was quantified using the Hoechst Bisbenzimide 33258 dye assay as previously described [219]. The proteoglycan content was estimated by quantifying the amount of sulfated glycosaminoglycan (sGAG) in constructs using the dimethylmethylene blue dyebinding assay (Blyscan, Biocolor Ltd., Carrickfergus, UK), with a shark chondroitin sulfate standard. Total collagen content was determined through measurement of the hydroxyproline content [220]. A hydroxyproline-to-collagen ratio of 1:7.69 was used.

The remaining halves of mechanically tested constructs were digested using 1M HCl at 60 °C under constant rotation for at least 18 hrs. Samples were subsequently centrifuged at 5000g to remove any sediment from the digest. Calcium chloride at the defined calcium content was diluted in 1M HCl to produce two standard stocks (100 and 20 µg/ml respectively), which were diluted further to produce the four high and three low standard points of the curve respectively. Calcium content was then determined relative to dye fluorescence in response

to calcium concentration using a commercial sentinel calcium kit.

5.3.4 Histology and immunohistochemistry

Constructs (n = 2) were fixed in 4 % paraformaldehyde (Sigma-Aldrich), wax embedded and sectioned at 5 um to produce a cross section perpendicular to the disk face. Sections were stained for sGAG with 1 % alcian blue 8GX (Sigma-Aldrich) in 0.1 M HCl; for collagen with picro-sirius red; and for calcium with alziran red. The deposition of collagen type I, type II and type X was identified through immunohistochemistry. Briefly, sections were quenched of peroxidase activity, rinsed with PBS before treatment with chondroitinase ABC (Sigma-Aldrich) in a humidified environment at 37 °C. Slides were rinsed with PBS and non-specific sites were blocked with goat serum (Sigma-Aldrich). Sections were then incubated overnight at 4 °C with the primary antibody; mouse monoclonal collagen type I antibody. (1:400; 1.4 mg/mL; Abcam, Cambridge, UK) or mouse monoclonal anti-collagen type II (1:100; 1 mg/mL; Abcam). After washing in PBS, sections were incubated for 1 h in the secondary antibody; anti-mouse IgG biotin antibody produced in goat (1:400; 1 mg/ mL; Sigma-Aldrich). Colour was developed using the Vectastain ABC reagent (Vectastain ABC kit, Vector Laboratories, Peterborough, UK) followed by exposure to peroxidase DAB substrate kit (Vector Laboratories). Negative and positive controls of porcine ligament, cartilage or growth plate were included for each batch. For both histology and immunohistochemistry images presented at high magnification from opposite annulus regions (left and right) and core (middle) as well as macroscopic images at low magnifications (corner)

5.3.5 Dynamic compression application

Dynamic compressive loading was applied to constructs also supplied with chondrogenic medium following a 5 day culture period. Dynamic compression (DC) was carried out in an incubator housed, custom-built compressive loading bioreactor. Uniaxial, unconfined

compression was initiated using an electric linear actuator with 0.05 µm resolution (Zaber Technologies Inc., Vancouver, Canada). A 1000 g load cell (RDP Electronics Ltd, Wolverhampton, UK) attached to the actuator lead screw sensed the load applied. The system was controlled and data logged using Matlab. The dynamic compression protocol consisted of 0, 10 and 20 % strain amplitude superimposed on a maximum 1 % preload at a frequency of 1 Hz employed for a period of 5 days for 2 h/day at 5 % O_2. 0 % loaded constructs were agitated without the application of compressive strain as previously stated. Medium was exchanged 2 - 3 times weekly.

5.3.6 RNA isolation and real-time reverse transcriptase polymerase chain reaction (rt-PCR)

Immediately following the application of the final DC cycle, MSC laden RGD-modified alginate hydrogels were lysed (n = 5 gels/group) using RLT lysis buffer (Qiagen, UK) supplemented with 10 µl β-mercaptoethanol (Sigma-Aldrich, Ireland), before homogenising with a pestle, flash-freezing in liquid N_2 and storing at -85 °C. At the time of isolation, lysates were thawed and homogenized using a QIAshredder column (Qiagen, UK) and total RNA was isolated and purified using the RNeasy mini kit (Qiagen, UK) as per the suggested manufacturer protocol. Purity and yield of RNA was quantified using a NanoDrop Spectrophotometer (Labtech International, Uckfield, UK). For cDNA preparation, 250 ng total RNA per sample were reverse transcribed into cDNA per 50 µl of reaction volumes using a high capacity reverse transcription cDNA kit (Applied Biosystems, Paisley, UK) as per manufacturer's instructions. Quantitative PCR was performed in an ABI 7500 sequence detection system (Applied Biosystems, Paisley, UK) using SYBR select master mix (Applied Biosystems, Paisley, UK) for evaluating the expression of aggrecan (ACAN), α-smooth muscle actin (ACTA), collagen type II (COL2A1), collagen type X (COL10A1) and Glyceraldehyde-3- phosphate dehydrogenase (GAPDH) genes. Porcine specific primer sequences that were used for amplification of these genes are listed in Table 5.1. Comparative Threshold (Ct) data were analysed using the $\Delta\Delta$Ct

method with an average of GAPDH and ACTB as the endogenous control [229]. Relative expression of the genes is presented as fold changes relative to the control group.

5.3.7 Statistical analysis

Statistics were preformed using graphpad prism software package. Groups were analysed for significant differences using a general linear model for analysis of variance with factors of substrate stiffness, dynamic compression magnitude and interactions between these factors examined. Tukey's test for multiple comparisons was used to compare conditions. Significance was accepted at a level of $p < 0.05$. Numerical and graphical results are presented as mean $\pm$ standard error from the mean.

Gene name	Gene symbol	Forward/Reverse Sequence
Glyceraldehyde-3-phosphate dehydrogenase	GAPDH	STTTAACTCTGGCAAAGTGG/ GAACATGTAGACCATGTAGTG
Actin, Beta	ACTB	GCGGCATCCACGAAACTA/ TGTTGGCGTAGAGGTCCTT
Smooth muscle aortic alpha-actin	ACTA	CAAAAGAGGAATCCTGACC/ CATTGTAGAAAGAGTGGTGC
Aggrecan	ACAN	GACCACTTACTCTTGGTG/ CATTGTAGAAAGAGTGGTGC
Collagen type 2, alpha-1	COL2A1	CGAGGACATAATCTGTGAAG/ TCCTTTGGGTCCTACAATATC
Collagen type 10, alpha-1	COL10A1	GTAGGTGTTTGGTATTGCTC/ GAGCAATACCAAACACCTAC

Table 5.1 Primer sequences used for rt-PCR.

5.4   Results

5.4.1   Soft hydrogels enhance early chondrogenesis

The stiffness of 3-D RGD-modified alginate hydrogels was varied using the same method as in chapter 4. It was found that after 5 days of free-swelling (FS) culture MSCs produced significantly more GAG/DNA in soft RGD-alginate hydrogels than those in stiff hydrogels ($p < 0.05$, fig. 5.1A). MSCs encapsulated in soft hydrogels secreted twice the levels of GAG than those in stiff hydrogels. There was no difference in collagen synthesis between the groups (fig. 5.1B). There was significantly more GAG deposition in the periphery of soft MSC-laden constructs as depicted by purple, aldehyde stained GAGs in this region of the hydrogel(Soft; fig. 5.1C). This GAG deposition in soft constructs also appeared to extend past the pericellular region surrounding the cells. In contrast, GAG staining was reduced in stiff MSC-laden constructs and constricted to the extreme periphery (Stiff; fig. 5.1C). Collagen type II staining appeared similar in both soft and stif hydrogels (fig. 5.1D), with only weak staining observed after 5 days of culture.
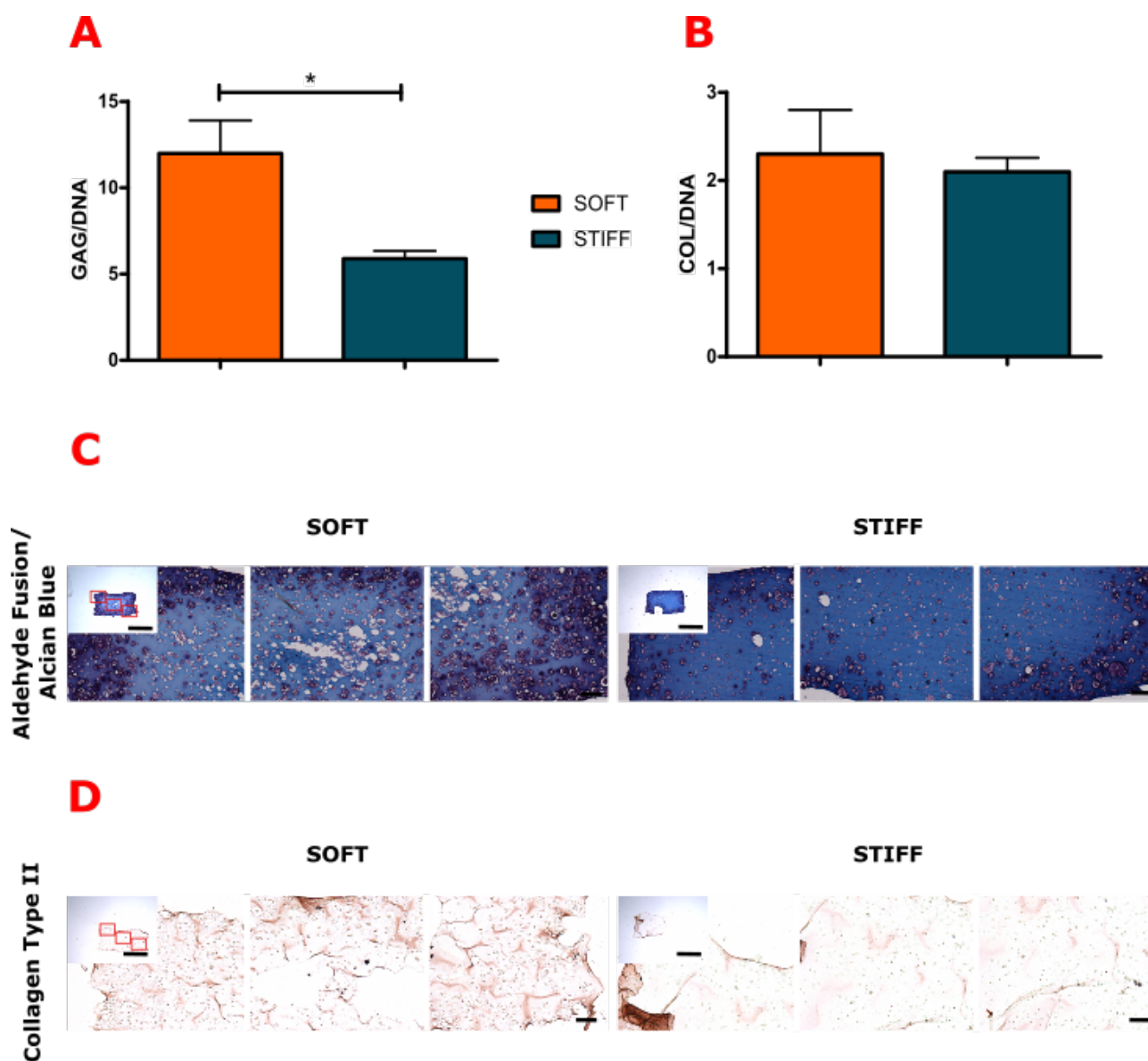
Figure 5.1 Soft hydrogels are more chondrogenic in short term culture than stiff MSC laden hydrogels Comparing chondrogenic response of MSC laden hydrogels in soft and stiff 3-D constructs. Biochemical content of soft and stiff constructs including (A) GAG per DNA content (GAG/DNA) and (B) collagen per DNA content (COL/DNA). (C) Images of histological sections stained with both aldehyde fuchsin and alcian blue to highlight sulphated GAG content. (D) Immunohistochemical staining for collagen type II on sections of both soft and stiff constructs.

After a 5 days in FS culture constructs were placed in a bioreactor for a further 5 days of culture. It was found that soft MSC-laden hydrogels promote a significantly more chondrogenic environment for MSCs. This is evident by significantly higher aggrecan (ACAN) and type II collagen (COL2A1) expression (1.5 and 3.3 increases respectively; fig. 5.2). Large increases in type X collagen (10.5 fold increase; fig. 5.2), a marker of hypertrophy were observed in softer hydrogels. No change in α-smooth muscle actin was observed (fig. 5.2).
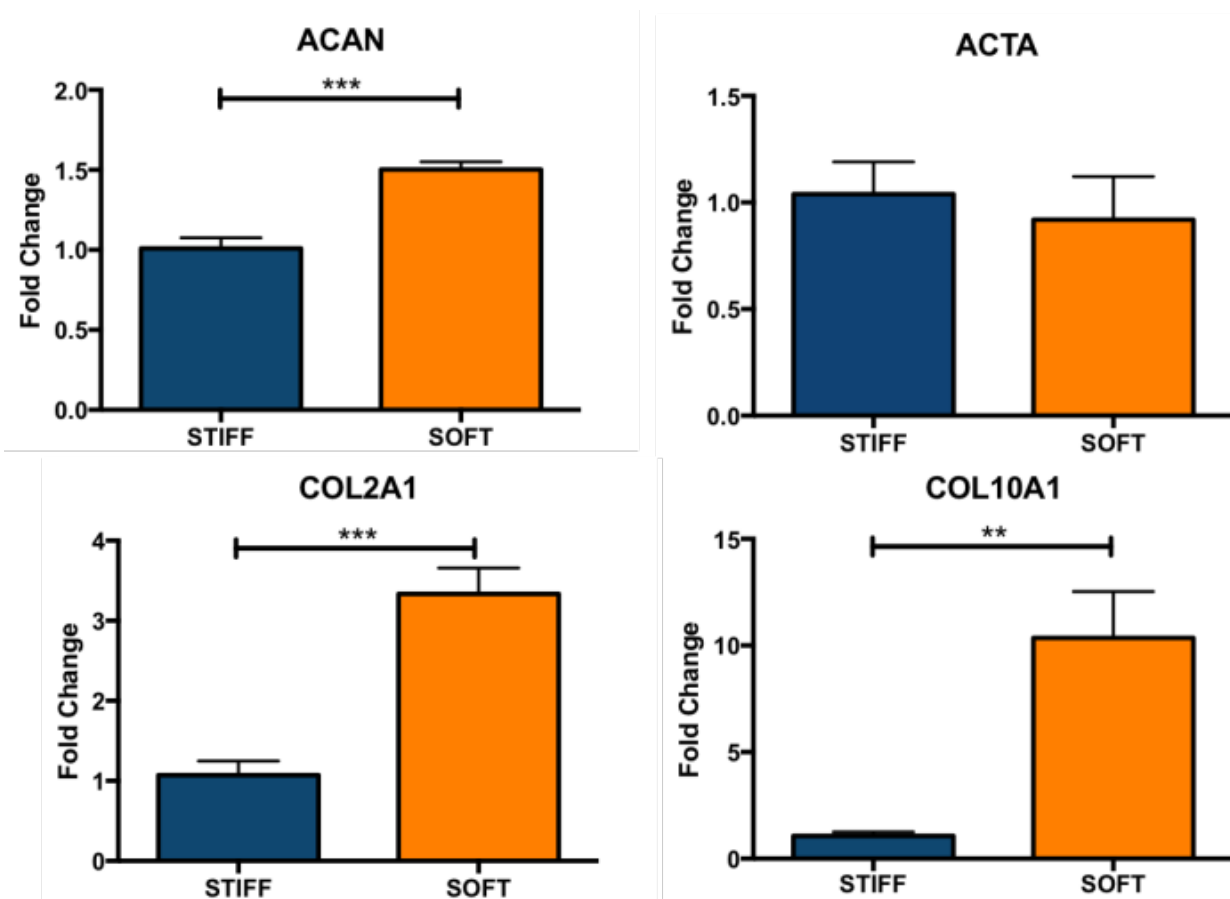
Figure 5.2 Soft hydrogels promote enhanced chondrogenic gene expression after a further 5 days of culture in FS-mixed bioreactor conditions. Fold change gene expression of aggrecan (ACAN), type II collagen (COL2A1), type X collagen (COL10A1) and α-smooth muscle actin (ACTA) of MSCs in soft hydrogels relative to stiff counterparts; both cultured at 5 % O_2 for 10 days (5 days FS culture followed by 5 days in FS-mixed bioreactor culture; n = 4). **, *** denotes $p < 0.01, 0.001$ respectively based on t-test analysis

5.4.2 Dynamic compression does not enhance chondrogenesis of MSCs encapsulated in soft hydrogels

Significant increases, relative to FS-mixed (0 % DC) conditions, in α-smooth muscle actin (ACTA) were observed at high magnitudes of dynamic compression (20 % strain) in soft MSC-laden hydrogels (ACTA; fig. 5.3) but otherwise loading had no effect on MSC chondrogenesis or hypertrophy. Dynamic compression did not significantly alter expression of aggrecan (ACAN), type II collagen (COL2A1) and type X collagen (COL10A1) relative gene expression (fig. 5.3).
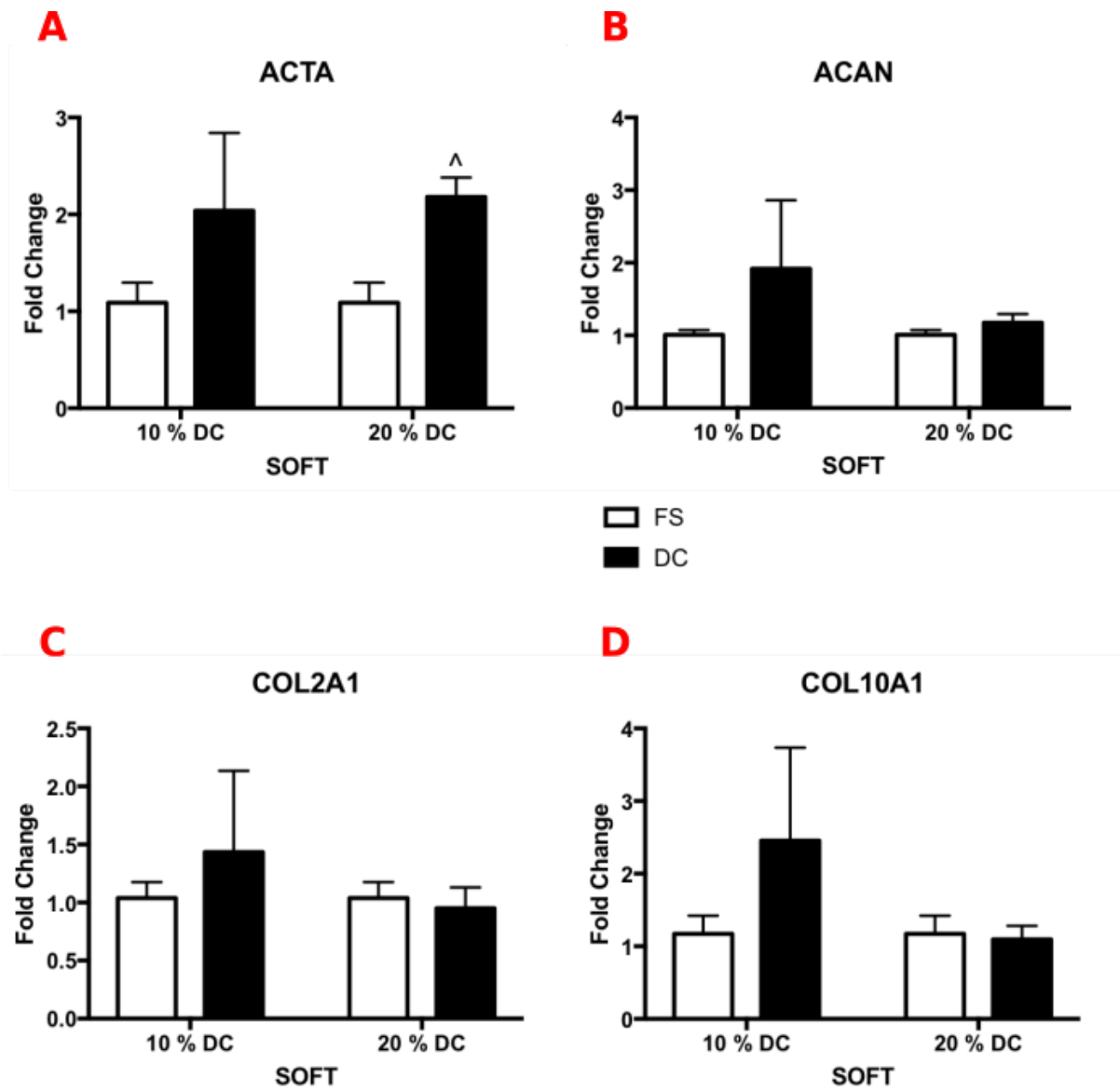
Figure 5.3 MSCs fail to respond to dynamic compression in soft hydrogels Fold change gene expression of aggrecan (ACAN), type II collagen (COL2A1), type X collagen (COL10A1) and α-smooth muscle actin (ACTA) of MSCs in soft hydrogels cultured at 5 % O_2 for 5 days in dynamically compressed bioreactor culture (10 and 20 % strain) relative to 0 % strain (n = 4). ˆ denotes $p < 0.05$ with respect to 0 % strain. **, *** denotes $p < 0.01$, 0.001 between groups respectively based on t-test statistical analysis

5.4.3 Dynamic compression enhances chondrogenesis in stiff hydrogels while regulating hypertrophy in a strain dependent manner

Dynamic compression at medium strain magnitudes (10 %) significantly enhanced aggrecan (ACAN) and type II collagen (COL2A1) gene expression (fig. 5.4), while α-smooth muscle actin (ACTA) and type X collagen expression were enhanced following the application of either 10 % or 20 % dynamic compression. Significantly lower increases in type X collagen were observed following the application of 20 % DC compared to 10 % suggesting a strong strain dependence on the hypertrophy of MSCs within stiff, dynamically compressed hydrogels (COL10A1; fig. 5.4). Two-way ANOVA results indicate p values < 0.0001 for analysing variation in loading, loading magnitude and interactions between the two factors for COLX gene expression.
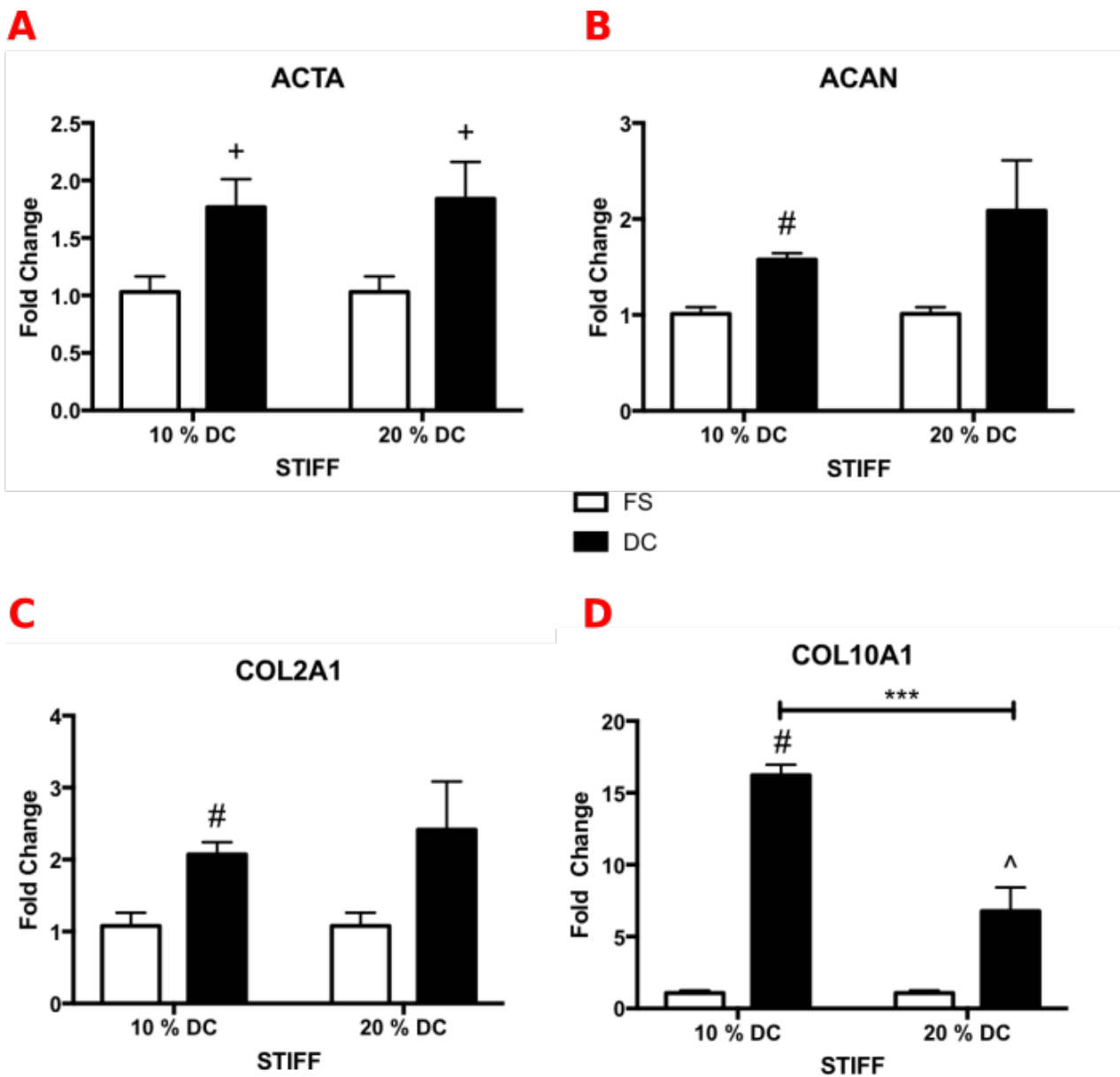
Figure 5.4 MSC chondrogenesis is enhanced by dynamic compression in stiff hydrogels while hypertrophy is strain dependent Gene expression of aggrecan (ACAN), type II collagen (COL2A1), type X collagen (COL10A1) and α-smooth muscle actin (ACTA) of MSCs in stiff hydrogels cultured at 5 % O$_2$ for 5 days in dynamically compressed bioreactor culture (10 and 20 % strain) relative to 0 % strain (n = 4). ˆ, +, # denotes $p < 0.05$ with respect to 0 % strain. *** denotes $p < 0.001$ between groups respectively based on t-test statistical analysis

5.5 Discussion

This study sought to determine the effect of substrate stiffness on MSC chondrogenesis; as well as how substrate stiffness impacts MSC chondrogenesis and hypertrophy in response to different magnitudes of dynamic compression. In agreement with the findings of chapter 4, the results demonstrate that soft hydrogels enhance early stage MSC chondrogenesis. This was demonstrated by enhanced GAG production at day 5 and an upregulation in aggrecan and type II collagen gene expression at day 10. When subjected to dynamic compression, MSC chondrogenesis was unaltered in soft hydrogels. In contrast, MSC chondrogenesis was enhanced by the application of dynamic compression in stiff hydrogels. Type X collagen expression in stiff hydrogels also depended on the magnitude of the applied strain. Therefore soft hydrogels appear to support enhanced chondrogenesis, but within such constructs MSCs apear less responsive to the application of dynamic compression.

Soft hydrogels promoting enhanced chondrogenesis agrees with findings in chapter 4 of this thesis. Results from both this and the previous chapter show that MSCs cultured in soft hydrogels undergo robust chondrogenesis, as evident by at GAG production by day 5 of culture and gene expression data at day 10 and day 14. Increased type II collagen expression at day 10 in soft hydrogels can be related to increased collagen type II production at day 14 of MSCs in soft hydrogels. Together these findings highlight that soft hydrogels benefit early MSC chondrogenesis, supporting the findings of other studies.

Despite soft hydrogels enhancing MSC chondrogenesis applying dynamic compression to these constructs did not further accelerate MSC chondrogenesis. This may suggest that adequate levels of mechanical stimulation is transduced in soft hydrogels to promote a beneficial chondrogenic response [192]. Soft hydrogels promote robust early chondrogenesis, leading to the formation of a stiff pericellular matrix [194]. Therefore the soft nature of the matrix may not be able to superimpose adequate levels of deformation on a potentially stress shielding stiff pericellular environment. For this reason a higher strain magnitude was chosen in the experimental design to test this theory. Even high strain magnitudes (20 %) produce no change in chondrogenic gene expression. Therefore soft hydrogels in combination with

appropriate levels of TGF-β_3 stimulation (10 ng/ml) appropriate an environment ideally suited for MSC chondrogenesis, in which no addition cue, such as dynamic compression, is able to have an effect.

In contrast, dynamic compression enhanced MSC chondrogenesis in stiff hydrogels. One possible explanation for this is that greater strain transmission to cells occurs in stiffer hydrogels [192]. It may also be that a stiff hydrogel promotes reduced MSC chondrogenesis and therefore a less stiff pericellular matrix [194]. In combination with enhanced strain transmission this may allow for the transduction of a greater and more beneficial level of mechanical stimulus.

Increases in type X collagen gene expression in response to both strain magnitudes (10 and 20 %) suggest that hypertrophy is regulated by dynamic compression in stiff hydrogels. The lower levels of type X collagen gene expression at high strain magnitudes (20 %) provide support for the hypothesis that hypertrophy is regulated by the magnitude of dynamic compression. A study from Bryant et al. highlighted similar changes in chondrocyte response to dynamic compression based on changes in crosslinking density and the associated alterations in substrate stiffness [233].

High strain magnitudes reducing hypertrophic responses of MSCs to dynamic compression is largely a new concept. Recent studies from Horner et al. have found similar findings when human MSCs were cultured on electrospun 3-D scaffolds in osteogenic media. In these conditions, a magnitude dependent reduction in osteogenic markers (COL1A1, SPARC, RUNX2) as well as an upregulation in chondrogenic markers (ACAN, COL2A1, SOX9) [222] was also witnessed. A reduction in calcium deposition was also dependent on the strain magnitude of applied dynamic compression.

5.6   Conclusion

This study confirms that soft hydrogels enhance MSC chondrogenesis. It also demonstrates that MSC response to dynamic compression is both substrate stiffness and strain magnitude

dependent. Dynamic compression enhancing MSC chondrogenesis only occured in stiff hydrogels. High strains produced less robust increases in type X collagen suggesting that hypertrophy is dependent on the magnitude of dynamic compression. This could provide a platform for modulating MSC chondrogenesis in order to produce an osteochondral, tissue-engineered construct. In the next chapter will explore the effect of spatially modulating substrate stiffness throughout the depth of a hydrogel on MSC chondrogenesis with and without the application of dynamic compression.

CHAPTER 6

The effect of modulating mechanical cues and oxygen availability throughout a single hydrogel construct on MSC chondrogenesis and hypertrophy

6.1 Abstract

THIS study explored how altering local substrate stiffness affected MSC chondrogenesis within 3-D hydrogels. The influence of superimposing dynamic compression on these MSC laden hydrogels was also assessed. The goal of this study was to engineer a bi-layered hydrogel, with one layer primed to undergo endochondral ossification and the second layer supporting stable chondrogenesis. Bone marrow derived mesenchymal stem cells (MSCs) were seeded in RGD-modified alginate hydrogels ionically crosslinked using a layered casting mould that contained different concentrations (10 mM and 100 mM) of calcium chloride ($CaCl_2$) to produce local changes in substrate stiffness throughout the depth. Chondrogenesis in these gradient hydrogels was compared to homogenous soft and stiff constructs. No bulk changes in ECM accumulation were observed between groups following 21 days of culture at 5 % O_2. A further 5 days in bioreactor culture (0 and 15 % strain) led to enhanced MSC chondrogenesis in stiff hydrogels. Dynamic compression enhanced chondrogenesis in soft hydrogels, but not in stiff or gradient constructs... It also implies

greater control of local strain magnitudes and substrate stiffness over time is needed in order to spatially control MSC chondrogenesis and hypertrophy.

Keywords – **MSCs, chondrogenesis, hypertrophy, substrate stiffness, dynamic compression, gradient**

6.2   Introduction

Full thickness defects on the articulating joint surface penetrate through the cartilage layer into the underlying subchondral bone. These defects can lead to joint pain, reduced joint function and ultimately osteoarthritis. Tissue engineering is a promising approach for regenerating osteochondral tissues, and usually involves the presentation of different biochemical cues, cell types, and physical cues in a spatially defined manner. A bi-layered strategy that incompasses two distinct, spatially defined regions is the most common approach [234,235]. A typical approach involving the combination of a stiff layer of inorganic mineralised matrix (e.g., hydroxyapatite and β-tricalcium phosphate) that represents the subchondral bone is topped with a soft polymeric layer (e.g., poly(lactic-co- glycolic acid), collagen, agarose, etc.) representing the cartilage region [236]. Other approaches have employed the same scaffold chemistry in both layers and instead varied the physical properties (e.g., pore structure) [237] and/or the biochemical cues (e.g., tissue-specific ECM-analogs [238], growth factors [239], or genes [240]). More recently, however, a mechanical approach to alter the fate of MSCs in a layered hydrogel to develop an osteochondral precursor was developed by Steinmetz et al. [191]. Here, changing both the substrate stiffness throughout the depth and applying dynamic compression resulted in MSC chondrogenesis in the top soft layer and osteogenesis in the bottom stiff layer when dynamically compressed. This study sought to explore whether a similar approach could be used to spatially regulate endochondral ossification to engineer an osteochondral construct.

This thesis has identified that soft hydrogels promote enhanced MSC chondrogenesis,

high strain magnitudes of dynamic compression can potentially suppress hypertrophy, and low oxygen conditions enhance spatial and cartilage-specific protein deposition. Steinmetz et al. showed an alteration of substrate stiffness throughout the depth also altered local dynamic compressive strain magnitudes [191]. Differences in oxygen availability should also be considered. Therefore modulating these parameters throughout the depth of a osteochondral sized construct may enable a simpler approach to spatially direct MSC differentiation.

The overall objective of this study is to determine the effect of spatially defining the local mechanical environment in terms of substrate stiffness and dynamic compression, as well as oxygen availability, in order to modulate MSC chondrogenesis and hypertrophy for osteochondral tissue engineering. It is hypothesised that the bottom of osteochondral constructs during culture will provide lower oxygen levels (Schematic; fig. 5.1) that are potentially beneficial for MSC chondrogenesis. The application of dynamic compression at low strain magnitudes on a stiff hydrogel may enhance the endochondral pathway of chondrogenically-primed MSCs. Finally, a soft cartilage layer will enable both an ideal environment for MSC chondrogenesis but will also allow the formation of higher strain magnitudes that have been shown previously in this thesis to suppress hypertrophy.

6.3   Materials and Methods

6.3.1   RGD incorporation and alginate preparation

RGD-modified methacrylated alginate was prepared by researchers in Eben Alsberg's laboratory and synthesized in a two-step reaction utilizing standard carbodiimide chemistry. Low-molecular-weight sodium alginate (37,000 g/mol) was prepared by irradiating Protanal LF 20/40 (196,000 g/mol; FMC Biopolymer, Philadelphia, PA) at a gamma dose of 5 Mrad. Twenty-five percent actual methacrylation of alginate carboxylic acid groups was performed as described previously [228]. Methacrylated alginate solutions (1 %, w/v) were prepared with 50mM of 2-(N-morpholino)- ethane sulfonic acid hydrate (Sigma, St. Louis,

MO) buffer solution containing 0.5 M NaCl (Sigma) at pH 6.5, and sequentially mixed with N-hydroxysuccinimide (Sigma) and 1-ethyl-3-[3-(dimethylamino)propyl] carbodiimide (EDC; Sigma). The molar ratio of N-hydroxysuccinimide to EDC was 0.5:1.0, and the weight ratio of EDC to methacrylated alginate was 1.0:20.7. The Gly-Arg-Gly-Asp-Ser-Pro (Commonwealth Biotechnologies, Richmond, VA) amino acid peptide sequence was added to the methacrylated alginate solution at a weight ratio of 10 mg/g methacrylated alginate. After reacting for 24 h at 48 °C, the reaction was stopped by addition of hydroxylamine (0.18 mg/mL; Sigma), and the solution was purified by dialysis against ultrapure deionized water (di-H_2O) (MWCO 3500; Spectrum Laboratories, Rancho Dominguez, CA) for 3 days, treated with activated charcoal (0.5 mg/100 mL, 50-200 mesh; Fisher, Pittsburgh, PA) for 30 min, filtered (0.22 mm filter), and lyophilized. Control methacrylated alginate was prepared in the same manner but without the presence of peptide.

The lyophilised alginate with RGD modification was then re-suspended in ultra pure water at 2.5 % before being filtered through a 45 µm mesh.

6.3.2   Cell isolation, expansion and hydrogel encapsulation

MSCs were isolated from porcine femora. Following isolation, Porcine MSCs were preserved in liquid nitrogen before later being thawed and expanded according to a modified method developed for human MSCs. MSCs were plated at a seeding density of 50,000 cells/cm^2 in high-glucose Dulbecco's modified eagles medium (4.5 mg/mL D-Glucose, 200 mM L-Glutamine; hgDMEM) supplemented with 10 % fetal bovine serum (FBS) and 2 % penicillin (100 µg/ml) - streptomycin (100 µg/ml); and expanded to passage two in a humidified atmosphere at 37 °C and 5 % CO_2.

MSCs were suspended in chondrogenic medium (CM), which consisted of hgDMEM supplemented with penicillin (100 µg /ml) and streptomycin (100 µg/ml), sodium pyruvate (100 µg/ml), L-proline (40 µg/ml), bovine serum albumin (1.5 mg/ml), linoleic acid (4.7 µg/ml), insulin-transferrin-selenium (10 µg/ml), L-ascorbic acid-2-phosphate (50 µg/ml),

dexamethasone (100 nM) and 10 ng/mL TGF-β_3. The MSC suspension was subsequently mixed with 2.5 % RGD-modified alginate (dissolved in ultra pure water) at a ratio of 1:4 to yield a final gel concentration of 2 % RGD-modified alginate and a cell density of 20 million cells/ml. The alginate-cell suspension was cast in a agarose moulds (5 mm diamater by 2 mm deep) containing either 100 mM or 10 mM $CaCl_2$ or a layer of both. A slab and solution, containing a similar $CaCl_2$ concentration, was placed on top of and around moulds containing 20 samples respectively. For layered moulds, a 10 mM $CaCl_2$ slab was placed on top as well 10 mM $CaCl_2$ solution pipetted around the housing.This housing was then incubated for 30 minutes. Constructs were maintained separately in 12-well plates with 2 ml of chondrogenic medium in 5 % O_2. Medium was exchanged twice weekly and constructs were cultured in these conditions for 21 days.
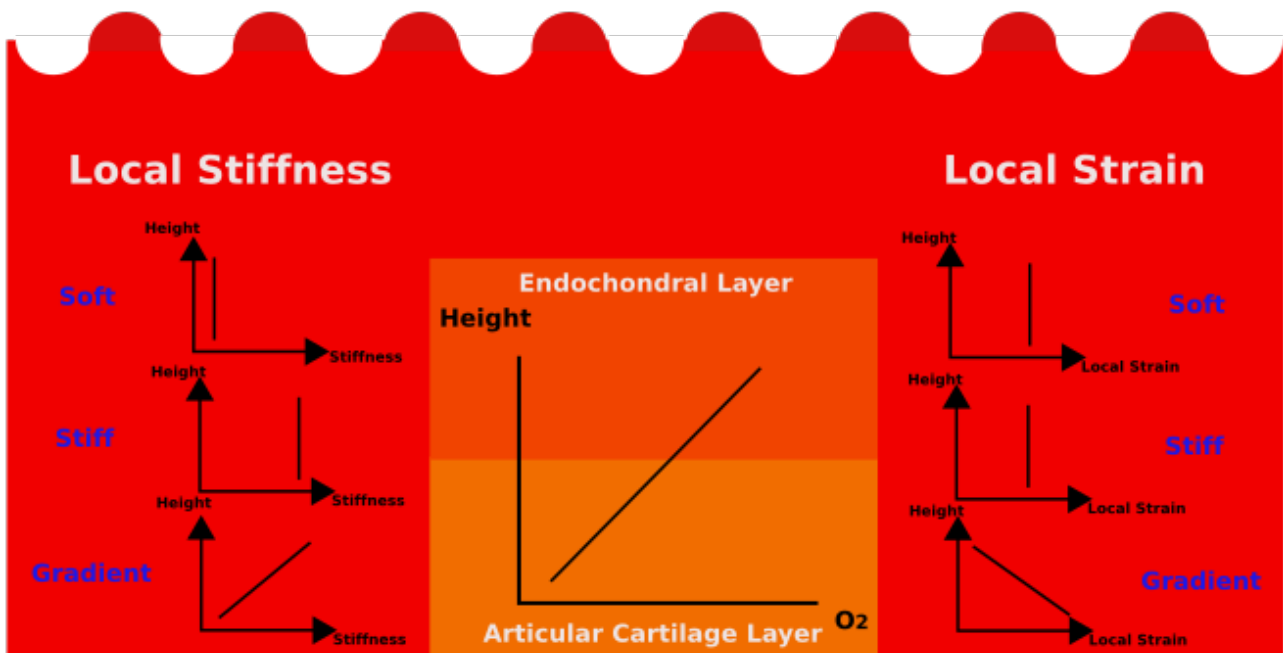
Figure 6.1 Schematic of experimental design. Visual representation of intended ways of altering local oxygen tension, substrate stiffness and strain magnitude under dynamic compression throughout the depth of experimental groups.

6.3.3 Biochemical content

The biochemical content of constructs (n = 3 or n = 4) was assessed at day 0 and day 21. The wet mass of each construct half was recorded before being frozen at -85 °C for later analysis. Samples were digested with papain (125 µg/mL) in 0.1 M sodium acetate, 5 mM L-cysteine HCl, 0.05 M EDTA, pH 6.0 (all Sigma- Aldrich) at 60 °C under constant rotation for 18 h. DNA content was quantified using the Hoechst Bisbenzimide 33258 dye assay as previously described [219]. The proteoglycan content was estimated by quantifying the amount of sulfated glycosaminoglycan (sGAG) in constructs using the dimethylmethylene blue dyebinding assay (Blyscan, Biocolor Ltd., Carrickfergus, UK), with a shark chondroitin sulfate standard. Total collagen content was determined through measurement of the hydroxyproline content [220]. A hydroxyproline-to-collagen ratio of 1:7.69 was used.

6.3.4 Histology and immunohistochemistry

Constructs (n = 2) were fixed in 4 % paraformaldehyde (Sigma-Aldrich), wax embedded and sectioned at 5 um to produce a cross section perpendicular to the disk face. Sections were stained for sGAG with 1 % alcian blue 8GX (Sigma-Aldrich) in 0.1 M HCl; for collagen with picro-sirius red; and for calcium with alziran red. The deposition of collagen type I, type II and type X was identified through immunohistochemistry. Briefly, sections were quenched of peroxidase activity, rinsed with PBS before treatment with chondroitinase ABC (Sigma-Aldrich) in a humidified environment at 37 °C. Slides were rinsed with PBS and non-specific sites were blocked with goat serum (Sigma-Aldrich). Sections were then incubated overnight at 4 °C with the primary antibody; mouse monoclonal collagen type I antibody. (1:400; 1.4 mg/mL; Abcam, Cambridge, UK) or mouse monoclonal anti-collagen type II (1:100; 1 mg/mL; Abcam). After washing in PBS, sections were incubated for 1 h in the secondary antibody; anti-mouse IgG biotin antibody produced in goat (1:400; 1 mg/ mL; Sigma-Aldrich). Colour was developed using the Vectastain ABC reagent (Vectastain ABC kit, Vector Laboratories, Peterborough, UK) followed by exposure to peroxidase DAB substrate

kit (Vector Laboratories). Negative and positive controls of porcine ligament, cartilage or growth plate were included for each batch. For both histology and immunohistochemistry images presented at high magnification from top and bottom regions including the both sides of the annulus and space between (left,right and middle for respective depth) as well as macroscopic images at low magnifications (corner).

6.3.5 Strain mapping using cell-tracking and digital image correlation (DIC)

The fiducial markers were created by fluorescent staining of MSC DNA. Samples were cut into semi-cylindrical sections, fixed with 4 % paraformaldehyde (Sigma-Aldrich) and immersed in 1 ml phenol-free DMEM with 1:100 10 ng/ml DAPI at room temperature to allow diffuchsin of the dye into the MSC-laden hydrogels and reaction with the cellular DNA. These samples were tested in unconfined compression in a custom made stainless steel compression rig that was designed to sit on the stage of an inverted fluorescent Olympus IX 51 microscope equipped with a 100 W xenon arc lamp, a DAPI filter cube and a 0.4 NA Universal Plan Super Apochromat 4 objective (Mason Technology, Dublin, Ireland). The semi-cylindrical MSC-laden hydrogels were bathed in phenol-red free DMEM in a testing chamber with a glass microscopic slide window at its base, sandwiched between two Perspex loading platens with its rectangular cross section facing down toward the microscope objective; enabling the visualisation of the cells during testing. 15 % strain, ramp compression was manually applied to the articular surface of test specimens by advancement of a micrometer gauge attached to the remaining Perspex platen (Mitutoyo, Radionics, Dublin, Ireland; resolution 0.01 mm). Images were taken before and after compression. The intra cellular or hydrogel displacement field was calculated using the digital image correlation software VIC 2D 2009 (Correlated Solutions, Columbia, SC, USA).

6.3.6   Dynamic compression application

Dynamic compressive loading was applied to constructs also supplied with chondrogenic medium following a 21 day culture period. Dynamic compression (DC) was carried out in an incubator housed, custom-built compressive loading bioreactor. Uniaxial, unconfined compression was initiated using an electric linear actuator with 0.05 µm resolution (Zaber Technologies Inc., Vancouver, Canada). A 1000 g load cell (RDP Electronics Ltd, Wolverhampton, UK) attached to the actuator lead screw sensed the load applied. The system was controlled and data logged using Matlab. The dynamic compression protocol consisted of 0, 10 and 20 % strain amplitude superimposed on a maximum 1 % preload at a frequency of 1 Hz employed for a period of 5 days for 2 h/day. 0 % loaded constructs were agitated without the application of compressive strain as previously stated. Medium was exchanged 2 - 3 times weekly.

6.3.7   RNA isolation and real-time reverse transcriptase polymerase chain reaction (rt-PCR)

Immediately following the application of the final DC cycle, MSC laden RGD-modified alginate hydrogels were lysed (n = 4 gels/group) using RLT lysis buffer (Qiagen, UK) supplemented with 10 µl β-mercaptoethanol (Sigma-Aldrich, Ireland), before homogenising with a pestle, flash-freezing in liquid N_2 and storing at -85 ℃. At the time of isolation, lysates were thawed and homogenized using a QIAshredder column (Qiagen, UK) and total RNA was isolated and purified using the RNeasy mini kit (Qiagen, UK) as per the suggested manufacturer protocol. Purity and yield of RNA was quantified using a NanoDrop Spectrophotometer (Labtech International, Uckfield, UK). For cDNA preparation, 200 ng total RNA per sample were reverse transcribed into cDNA per 40 µl of reaction volumes using a high capacity reverse transcription cDNA kit (Applied Biosystems, Paisley, UK) as per manufacturer's instructions. Quantitative PCR was performed in an ABI 7500 sequence detection system (Applied

Biosystems, Paisley, UK) using SYBR select master mix (Applied Biosystems, Paisley, UK) for evaluating the expression of aggrecan (ACAN), α-smooth muscle actin (ACTA), collagen type II (COL-2), collagen type X (COL10A1) and Glyceraldehyde-3- phosphate dehydrogenase (GAPDH) genes. Porcine specific primer sequences that were used for amplification of these genes are listed in Table 4.1. For relative gene expression, ΔCt values with GAPDH as the endogenous control were used to calculate relative gene expression as $2^{\Delta Ct}$. Comparative Threshold (Ct) data were analysed using the $\Delta\Delta$Ct method with an average of GAPDH and ACTB as the endogenous control [229]. Relative expression of the genes is also presented as either fold changes relative to the control group.

6.3.8 Statistical analysis

Statistics were preformed using graphpad prism software package. Groups were analysed for significant differences using a general linear model for analysis of variance with factors of hydrogel stiffness and dynamic versus free swelling culture conditions examined. Tukey's test for multiple comparisons was used to compare conditions. Significance was accepted at a level of $p < 0.05$. Numerical and graphical results are presented as mean $\pm$ standard error from the mean.

Gene name	Gene symbol	Forward Sequence	Reverse Sequence
Glyceraldehyde-3-phosphate dehydrogenase	GAPDH	STTTAACTCTGGCAAAGTGG/	GAACATGTAGACCATGTAGTG
Actin, Beta	ACTB	GCGGGCATCCACGAAACTA/	TGTTGGGCGTAGAGGTCCTT
Aggrecan	ACAN	GACCACTTTACTCTTGGTG/	CATTGTAGAAAAGAGTGGTGC
Collagen type 2, alpha-1	COL2A1	CGACGACATAATCTGTGAAG/	TCCTTTGGGTCCTACAATATC
SRY (Sex Determining Region Y)-Box-9	SOX9	CAGACCCTTGAGGAGACTTAG/	GTTCGAGTTGCCTTTAGTG
Collagen type 10, alpha-1	COL10A1	GTAGGTGTTTGGTATTGCTC/	GAGCAATACCAAAACACCTAC
Runt-related transcription factor-2	RUNX2	CCAACAGAGGCATTAAGG/	CCAAAAGAAGTTTTGCTGAC

Table 6.1 Primer sequences used for rt-PCR.

6.4 Results

6.4.1 Effect of spatially altering substrate stiffness through the depth of alginate hydrogels on MSC chondrogenesis

Reducing the concentration of $CaCl_2$ from 100 mM in stiff gels to 10 mM in soft gels was found to reduce the Young's modulus of a 4mm high, MSC-laden RGD-alginate hydrogel from $\approx$ 20 to $\approx$ 8 kPa (p $<$ 0.05, fig. 6.1A). Introducing a casting mould, which contained depth defined layers of $CaCl_2$, to crosslink MSC-laden, RGD-modified alginate hydrogels in a gradient fashion produced a construct with an intermediate bulk stiffness (Gradient; fig. 6.1A). Changes in substrate stiffness had no effect on the viability of MSCs over 21 days of culture in the presence of TGF-β_3 (fig. 6.1B). To assess spatial changes in cartilage specific ECM deposition, the engineeered tissues were sectioned into two halves to determine the composition of the top (endochondral region) and bottom (articular cartilage region) of the construct. No spatial differences in cartilage specific ECM synthesis was observed in the top/osteochondral and bottom/cartilage region of the MSC-laden hydrogels. This was evident by no changes in GAG or collagen production as normalised to DNA content (fig. 6.1C,D). Surprisingly, no differences in chondrogenesis was observed between soft and stiff hydrogels by day 21 of culture.
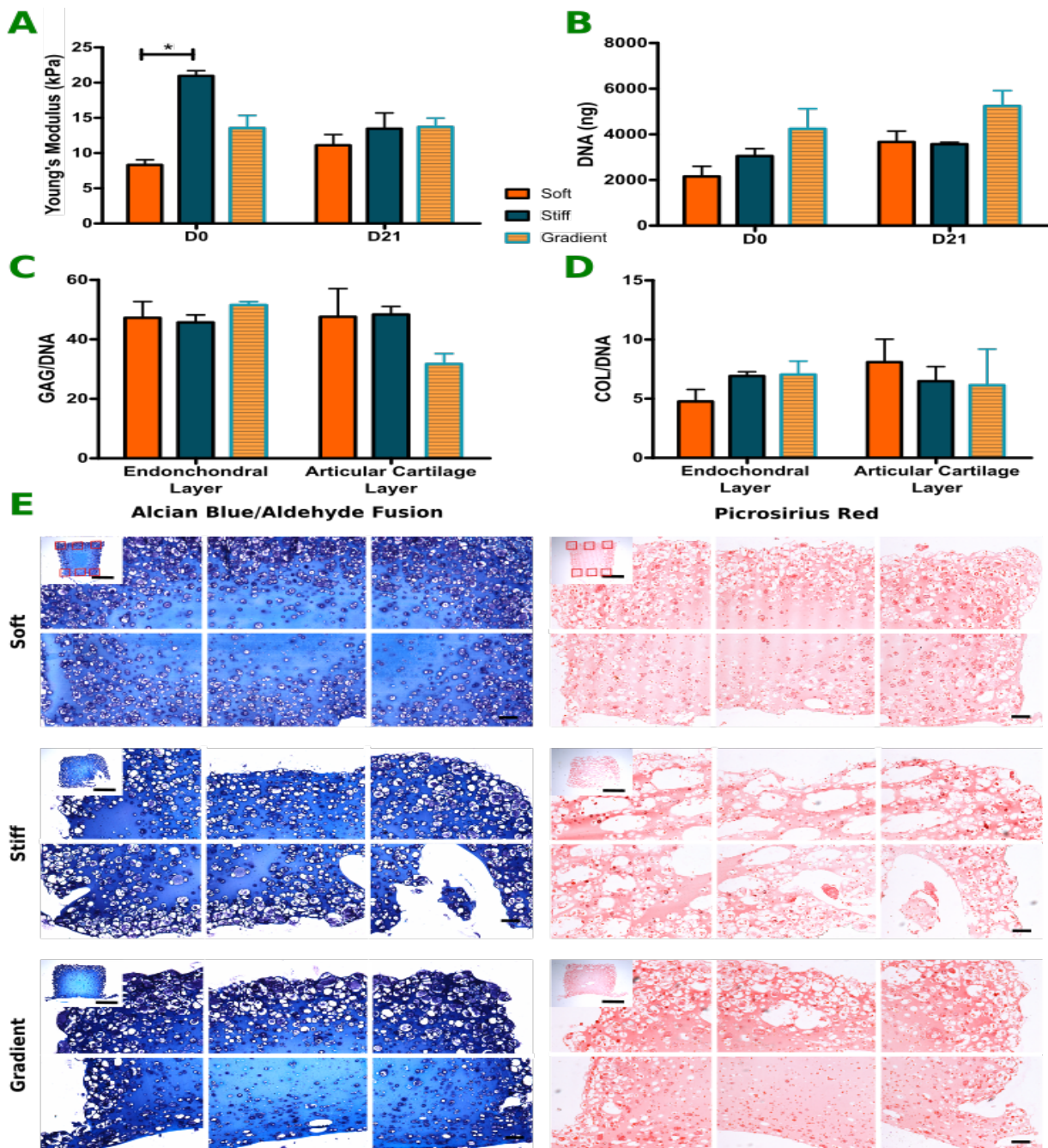
Figure 6.2 Altering substrate stiffness in MSC laden hydrogels. (A) Young's modulus (kPa) of 4 mm high by 5 mm diameter soft, stiff and gradient MSC-laden RGD-modified alginate hydrogels subjected to 10 % ramp strain mechanical testing protocol at day 0 and day 21. (B) DNA content, (C) GAG content normalised to DNA content (GAG/DNA) and (C) collagen content normalised to DNA content (COL/DNA) of samples at day 0 and after 21 days culture in the presence of TGF-β_3. * denotes $p < 0.05$ based on one-way ANOVA post-test analysis.

6.4.2 The effects of spatially altering substrate stiffness on the local strain magnitudes developed within MSC-laden hydrogels subject to cyclic dynamic compression

Initially after cell seeding, a largely homogenous strain field was observed throughout the depth of soft MSC laden hydrogels subjected to unconfined compression (fig. 5.3). Conversely, high local compressive strains within the core and radially decreasing strain magnitudes in the periphery were observed in 'stiff' hydrogels. This suggests inhomogenous cross-linking of the stiff RGD-modified alginate hydrogels. Additionally, a linear increase of local compressive strains from top to bottom was observed throughout the depth of 'gradient' constructs.

These strain fields were altered by tissue deposition over the course of 21 days of free-swelling culture. The top and bottom of soft hydrogels stiffened, lowered the local compressive strains and producing a central area experiencing high compressive strains when subjected to externally applied compression. Alternatively, a more homogenous strain pattern was observed in stiff hydrogels, despite some areas of stress concentration. Finally, some evidence of increasing compressive strain magnitude with decreasing height was observed from the extreme top of the construct; yet overall the local compressive strain field was more homogenous in nature.
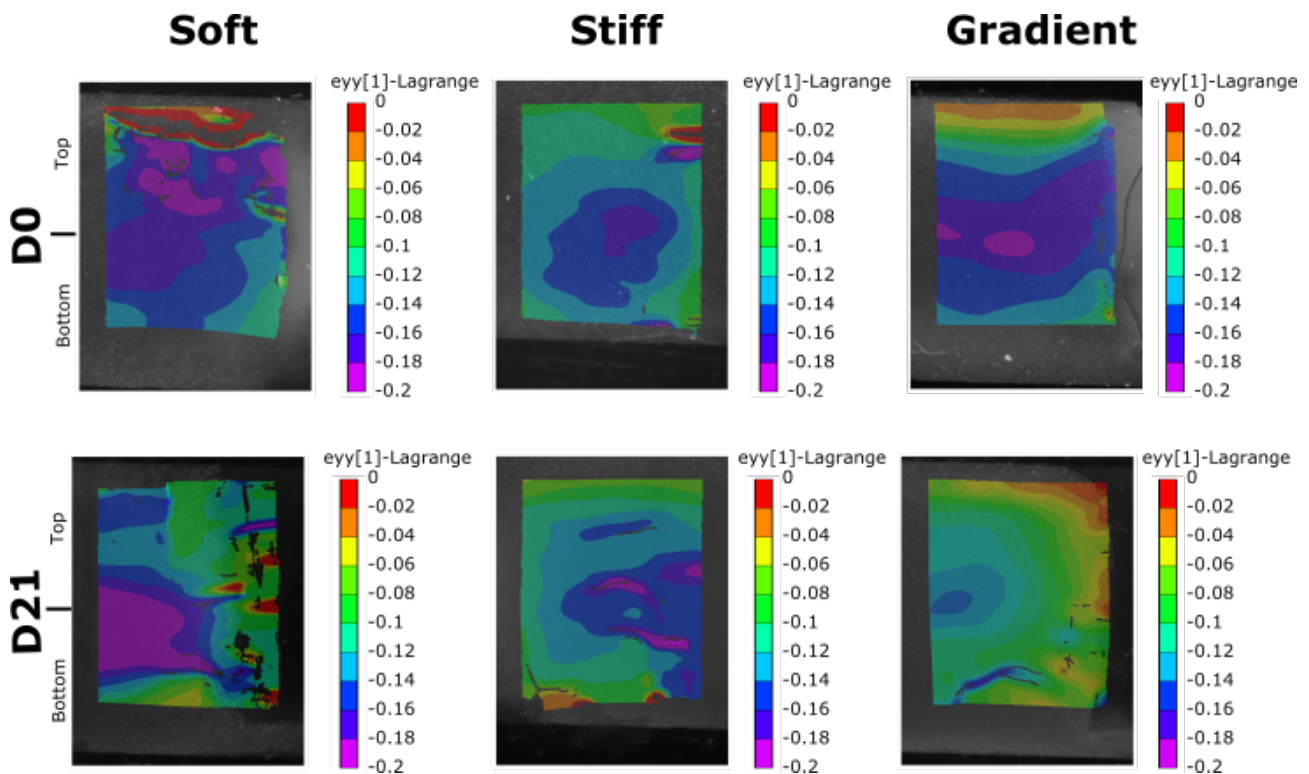
Figure 6.3 Digital image correlation analysis (DIC) to determine effect of substrate stiffness gradient on local strain magnitudes. DIC analysis to compute local strains of these MSC-laden hydrogels subjected to 15 % ramp strain indicative of dynamic compressive loading cycle. DAPI-stained MSCs were tracked in fixed constructs before and after loading. Vic2D software was then used to calculate local strain magnitudes shown in soft, stiff and gradient hydrogels at day 0 and 21 of culture.

6.4.3   Late MSC chondrogenesis is enhanced in stiff hydrogels

The expression of a number of chondrogenic and endochondral genes were assessed after 28 days in culture following an additional 5 days of bioreactor culture (0 % strain) at 20 % O_2. At this later time point, the expression of a number of chondrogenic genes was higher in stiff hydrogels.This is evident by increased aggrecan (ACAN) and type II collagen (COL2A1) expression in both the top and bottom of constructs in comparison to both soft and gradient hydrogels (fig. 6.3A,B). SOX9 relative expression also revealed an increase in mRNA levels in stiff hydrogels when compared to soft counterparts only within the top of the construct (TOP; $p < 0.001$, fig. 6.3C).
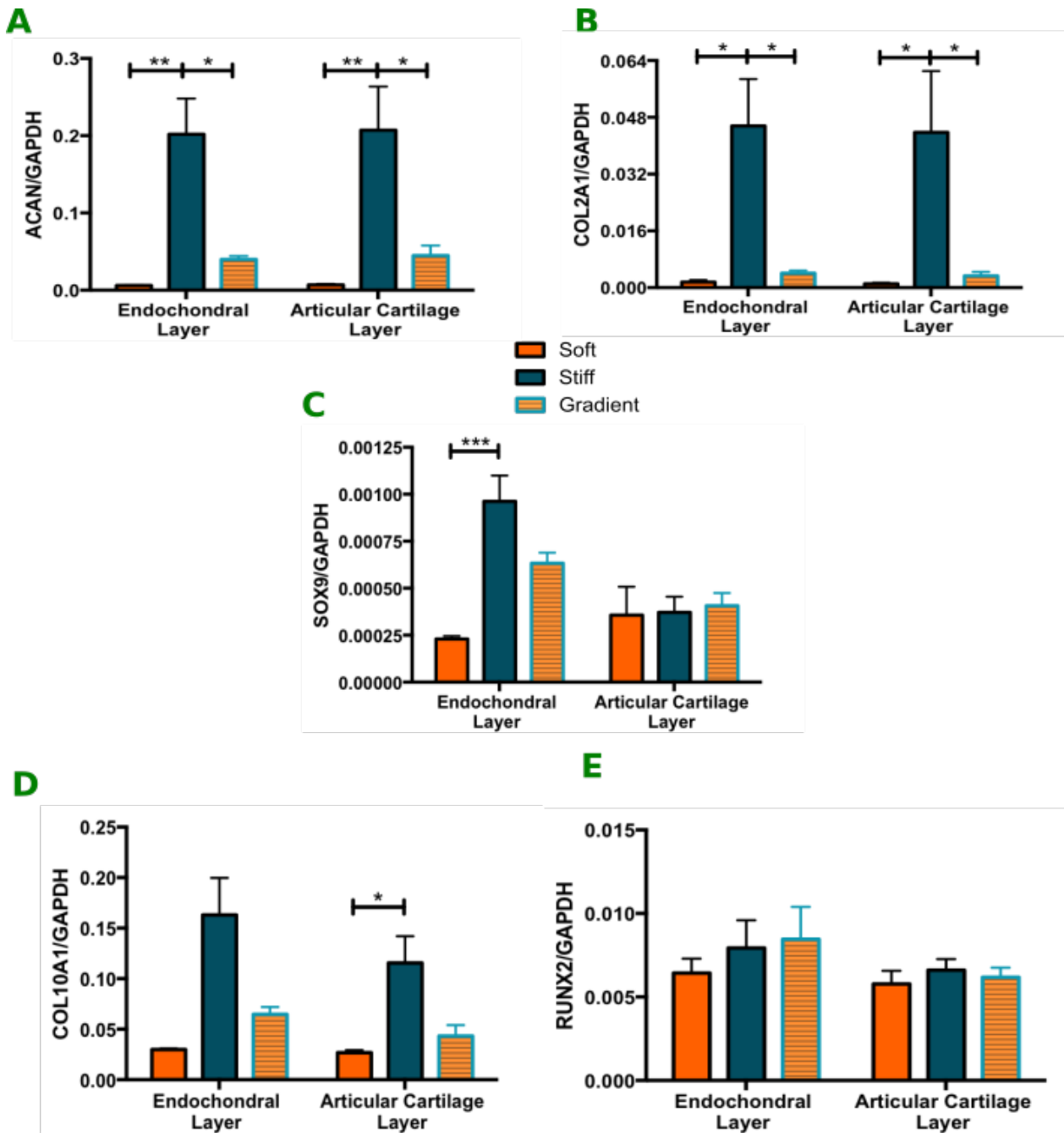
Figure 6.4 Late MSC chondrogenesis is enhanced in stiff hydrogels. Relative gene expression aggrecan (ACAN), type II collagen (COL2A1), SRY (Sex Determining Region Y)-Box-9 (SOX9), Runt-related transcription factor-2 (RUNX2) and type X collagen (COL10A1) from MSCs encapsulated in the articular cartilage and endochondral layers of soft, stiff and gradient hydrogels cultured at 21 % O_2 for a further 5 days in FS-mixed bioreactor conditions (n = 4). *,**,*** denotes $p < 0.05, 0.01, 0.001$ between groups respectively based on one-way ANOVA post-test analysis

6.4.4 Dynamic compression enhances late MSC chondrogenesis in stiff hydrogels

Dynamic compression (15 % strain) enhances late (day 28) MSC chondrogenesis in soft hydrogels as evident by enhanced fold change in aggrecan (ACAN) expression in the endochondral and articular cartilage layers with respect to 0 % strain controls ($p < 0.0001$, fig. 6.4A). Soft hydrogels also produced greater fold changes in aggrecan gene expression than both stiff and gradient hydrogels with the application of dynamic compression(15 % DC). No changes were observed in type II collagen (COL2A1) and SOX9 expression (fig. 6.4B,C). Dynamic compression upregulated type X collagen (COL10A1) in both layers of soft hydrogels and in the articular cartilage region of gradient hydrogels (fig. 6.4D). Soft hydrogels also had greater upregulation of type X collagen expression yet lower expression of RUNX2 than both stiff and gradient hydrogels (fig. 6.4D,E). Dynamic compression down regulated RUNX2 expression in stiff hydrogels in the articular cartilage region in both soft and stiff hydrogels as well as in the endochondral region of soft hydrogels (fig. 6.4E).
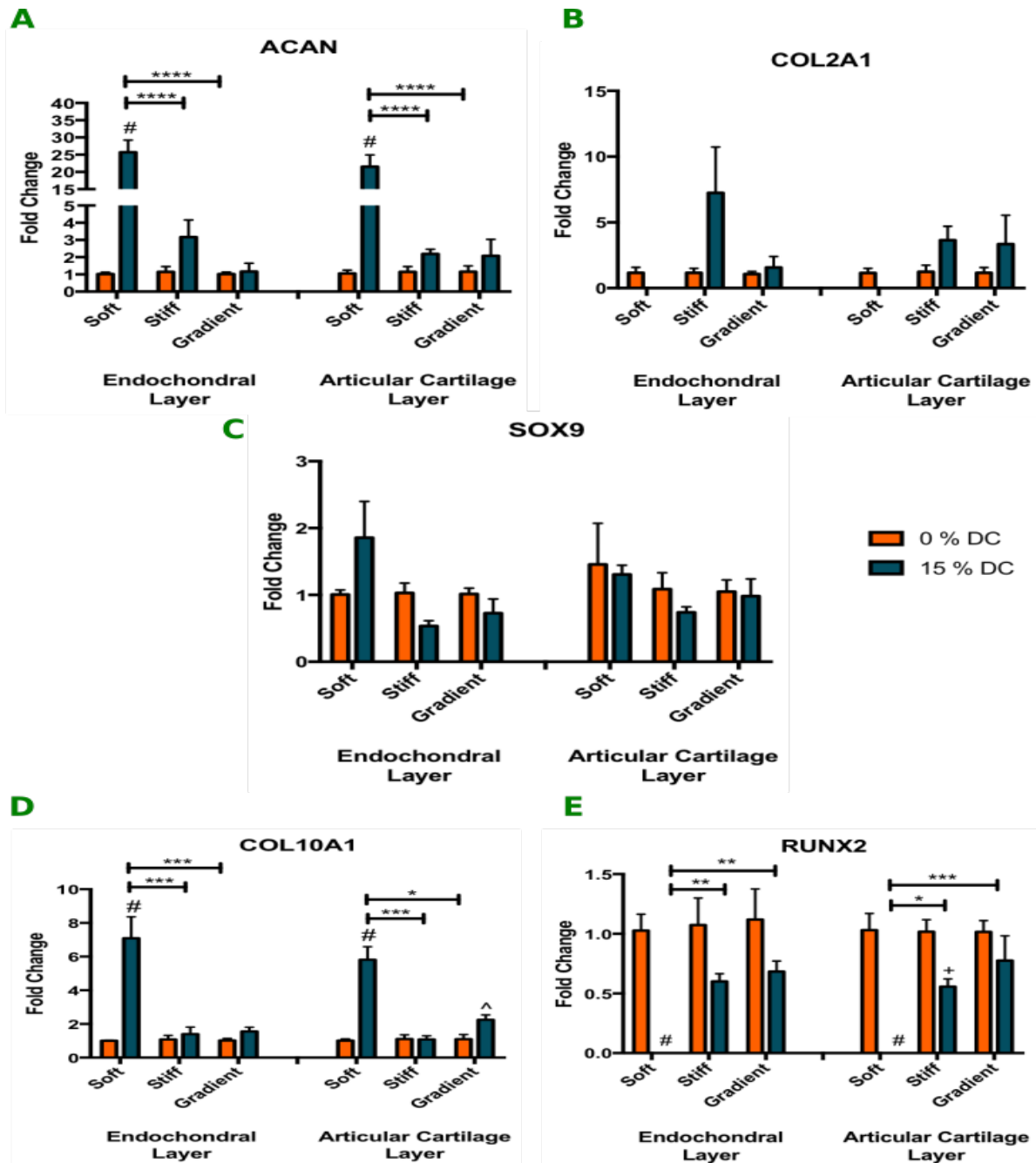
Figure 6.5 Dynamic compression enhances late MSC chondrogenesis. Fold change in the gene expression of strained (15 %) constructs normalised against unstrained (0 %) constructs for genes including aggrecan (ACAN), type II collagen (COL2A1), SRY (Sex Determining Region Y)-Box-9 (SOX9), Runt-related transcription factor-2 (RUNX2) and type X collagen (COL10A1) from MSCs in soft, stiff and gradient hydrogels cultured at 21 % O_2 for a further 5 days in FS-mixed bioreactor conditions (n = 4). ¸ +, # denotes p < 0.05, 0.01, 0.001 between strained constructs and controls respectively *,**,***,**** denotes p < 0.05, 0.01, 0.001, 0.0001 between groups respectively based on ONE-WAY ANOVA post-test analysis

Analysing spatial differences alone between the respect layers highlights no significant spatial differences in all groups for the given array of genes (fig. 6.5). Overall, type X collagen does tend to downregulate in the articular layer of all groups with the application of dynamic compression (15 % strain), while aggrecan and type II collagen tend to be upregulated in the articular layer of gradient hydrogels when dynamically compressed also.
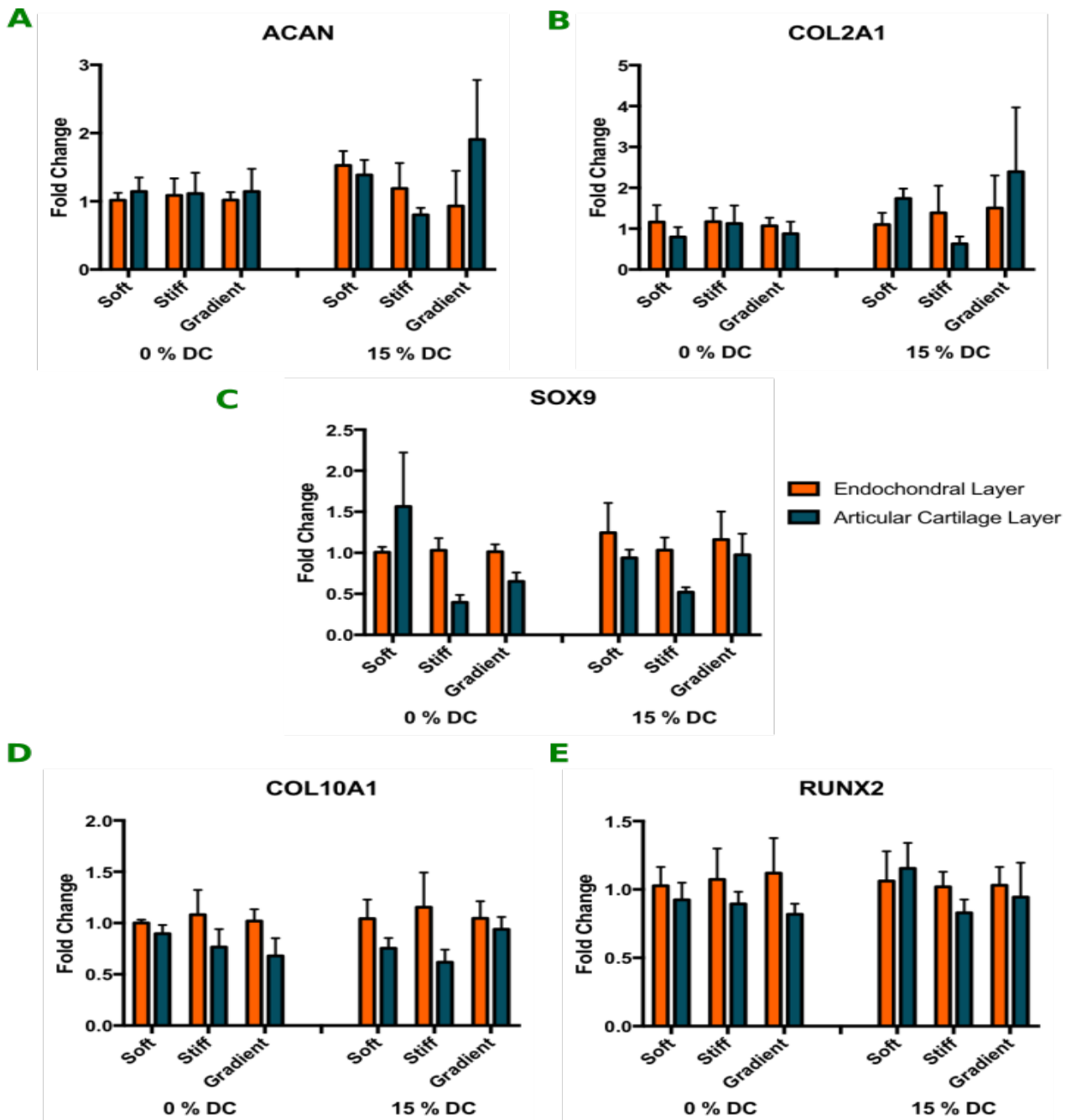
Figure 6.6 Overall no spatial alterations in MSC response to mechanical cues throughout the depth in all hydrogels. Fold change in the gene expression of the articular cartilage layer normalised against the endochondral layer for genes including aggrecan (ACAN), type II collagen (COL2A1), SRY (Sex Determining Region Y)-Box-9 (SOX9), Runt-related transcription factor-2 (RUNX2) and type X collagen (COL10A1) from MSCs in soft, stiff and gradient hydrogels cultured at 21 % O_2 for a further 5 days in FS-mixed bioreactor conditions (n = 4).

6.5   Discussion

This study aimed to modulate the mechanical environment throughout the depth of a MSC-laden hydrogel in order to provide a means of spatially enhancing MSC chondrogenesis and modulating MSC hypertrophy. It was found that the stiffness of an RGD-alginate hydrogel could be altered by varying the concentration of $CaCl_2$ within layers of the agarose casting slab. This alteration of substrate stiffness modulated the mechanical response of the substrate to mechanical deformation. Higher strains were developed in layers crosslinked with lower concentrations of $CaCl_2$, while the opposite was true for layers crosslinked with 100 mM $CaCl_2$. Unlike previous findings during early MSC culture, enhanced MSC chondrogenesis as evident by increases in SOX9, aggrecan (ACAN) and type II collagen (COL2A1) was observed in stiffer hydrogels at later timepoints , with the net effect being no changes in ECM deposition. Again the application of dynamic compression (15 % strain) to homogenously stiff hydrogels enhanced MSC chondrogenesis. An upregulation in COL10A1 and a downregulation in RUNX2 was observed in soft hydrogels, while RUNX2 was downregulated in the articular cartilage region of stiff hydrogels. This presents a complicated interaction of spatial altering environmental cues on MSC chondrogenesis and hypertrophy.

A reduction in $CaCl_2$ concentration from 100 mM to 10 mM between layers within the agarose casting mould proved an effective means of lowering the bulk substrate stiffness of gradient hydrogels. This highlights the versatile nature of altering substrate stiffness based on external crosslinking concentration. While the initial substrate stiffness was altered, this was not maintained throughout the 21 day culture period prior to the application of dynamic compression. This highlights the problem tissue deposition and remodelling pose for defining how substrate stiffness effects the response of MSC differentiation to delayed mechanical loading.

A gradient of crosslinking in RGD-modified alginate hydrogels lead to an initially well defined linear modulation of the local strain magnitudes with depth. In regions of 100 mM $CaCl_2$ crosslinking, local compressive strains were smaller in magnitude, with a linear increase in strain observed throughout the depth of the construct towards regions of 10

mM CaCl$_2$ crosslinking. This effective means of altering local strain magnitudes diminished over the 21 day culture period prior to loading application. This agrees with computational studies conducted by Steinmetz el al. in which models predicted a similar trend of high strains in regions of lower stiffness and/or crosslinking [191]. Constructs crosslinked with a singular CaCl$_2$ concentration did, however, present with variations in local strain magnitude under compression. The local variations in substrate stiffness that produce this would locally alter MSC differentiation. Whether this is an artefact of the image correlation process or a clarification of local changes in substrate stiffness is unclear. If the latter is true, the taller nature of these hydrogels would be responsible. The resulting increase in surface area would therefore allow the more rapid means of CaCl$_2$ crosslinking to create a stiffer periphery that prevents penetration of the crosslinking agent into the centre. The consequence being a softer core and inhomogenous substrate stiffness within the constructs.

Interestingly, this study highlighted that stiff hydrogels enhance markers of MSC chondrogenesis at later timepoints. This is in contrast to previous studies in this thesis that indicate soft hydrogels enhance early MSC chondrogenesis. Those earlier studies showed enhanced GAG production at day 5, and increased chondrogenic gene expression at day 10 and 14. Here, relative gene expression of ACAN and COL2A1 is increased in the top and bottom of stiff constructs in comparison to soft and gradient hydrogels. This implies a shift from enhanced MSC chondrogenesis at early stages in soft hydrogels to delayed increases in chondrogenesis in stiff hydrogels (see fig. 6.1) at latter stages of typical in vitro culture. This may be due to cell-ECM matrix interactions becoming more important to MSC chondrogenesis over time [241]. Alternatively, the loss of bulk stiffness over time in stiff hydrogels may suggest a degradation of the alginate matrix that produces a softening of the local cellular environment, which enables enhanced MSC chondrogenesis.

Enhancement in chondrogenesis was observed in soft hydrogels with the application of dynamic compression (15 % strain). Despite increases in aggrecan (ACAN) and type II collagen (COL2A1) with the application of dynamic compression in stiff hydrogels not being significant, it still highlights the responsiveness of MSCs embedded in stiff hydrogels to mechanical stimuli. Perhaps a shift in chondrogenesis is the key to regulating the response to

mechanical cues. A less than optimum chondrogenic environment (e.g. in terms of stiffness) may be directed towards a more pro-chondrogenic environment with the application of the correct stimuli, such as dynamic compression.

Finally, the effect of gradient hydrogels on both the spatial progression of MSC chondrogenesis and hypertrophy was less than originally hypothesised. This was evident by little or no changes in spatial MSC chondrogenesis and hypertrophy. This may be due to the loss of an overall stiffness gradient throughout the culturing period. In addition, the local strain magnitudes appeared much larger in both the soft and gradient hydrogel at day 21. This may be adversely impacting MSC chondrogenesis or at least limiting the benefit of applying dynamic compression. In a recent dynamic compression magnitude study, Horner et al. too found a threshold dynamic compressive strain (15 %), above which no enhancing effect on MSC chondrogenesis occured [222]. Variations in the strain field due to inhomogenous cross-linking or changes in local substrate stiffness may initiate dynamic loading at varying magnitudes above and below that threshold locally within the construct and therefore altering the expression of global MSC chondrogenesis.

6.6 Conclusion

Here, stiff hydrogels enhanced late MSC chondrogenesis possibly due to delayed chondrogenesis occuring in this hydrogel because of a softening of the gel and/or cell-PCM interactions over time. Gradient hydrogels here produce no spatial enhancement or modulation of MSC chondrogenesis and hypertrophy respectively but maintenance of a true gradient in substrate stiffness throughout the depth of constructs was not achieved. Controlling this in a hydrogel system over time may provide the basis for further development of engineered osteochondral constructs. In the next chapter, I will use a 3-D bioprinted mesh PCL lattice to incorporate a gradient in local strain magnitudes alone within a stiff hydrogel and assess the spatial effect on MSC chondrogenesis and hypertrophy.

CHAPTER 7

Integrating a bilayered 3-D printed mesh into MSC-laden hydrogels to spatially modulate mechanical cues, chondrogenesis and hypertrophy

7.1   Abstract

T HIS study aimed to alter local strain magnitudes within a MSC-laden hydrogel with the goal of spatially modulating MSC chondrogenesis and hypertrophy to engineer the precursor to an osteochondral-like tissue. Gradient mesh PCL lattice structures were 3-D bioprinted with a gradient of fibre spacing throughout the construct. This enabled the alteration of local strain magnitudes in both the mesh alone and when coupled with a MSC-laden hydrogel. Bone-marrow MSCs were then seeded in a homogenous and gradient mesh containing stiff RGD-modified alginate hydrogel. 21 days after culture with TGF-β_3 at 5 % O_2 to initiate robust chondrogenesis, dynamic compression was applied (15 % strain) at 21 % O_2 for a further 21 days. It was found that gradient constructs enhanced GAG deposition in the constructs under the application of dynamic compression. This correlates with regions of lower local compressive strain magnitudes. Calcification in the softer bottom of constructs was suppressed with the application of dynamic compression, although this was not statistically significant. This study highlights the ability to control the local mechanical

environment using a bioprinted polymeric lattice structure, and also suggests this enables a certain control of MSC chondrogenesis and hypertrophy.

Keywords – **MSCs, chondrogenesis, hypertrophy, dynamic compression, PCL mesh, local strain**

7.2   Introduction

Mechanical cues are known to affect MSC fate. The previous chapter attempted to spatially modulate MSC chondrogenesis and hypertrophy by controlling substrate stiffness and through the application of dynamic compression. Despite promising results, this method failed to produce consistent gradients in mechanical cues through the depth of MSC laden hydrogels. In this chapter, I will explore an alternative means of spatially altering the local strain magnitudes within a stiff MSC-laden hydrogel, with the goal of providing the mechanical cues necessary to enhance MSC chondrogenesis and modulate hypertrophy.

3-D printing polymer scaffolds have been used to mechanically reinforce cells laden hydrogels [242]. This has enabled the tissue engineering of anatomically accurate and mechanically functional constructs. Rapid prototype technology has also enabled the co-deposition of a polymer frame alongside cell laden bioinks, which facilitates functional and tuneable mechanical properties [242]. Spatial control of the polymer frame can enable the modulation of mechanical properties throughout the depth of a construct [243]. This fused deposition modelling technology may therefore provide an adequate framework, in which the local strain magnitudes of strain within an MSC-laden hydrogel under dynamic compression, could be modulated by altering the diameter and/or spacing of polymeric supports.

The objective of this study is to design a polymer (PCL) scaffolding mesh that can modulate the local magnitudes of strain within a MSC-laden hydrogel under dynamic compression. I then sought to determine if associated changes in local dynamic strain magnitudes will spatially alter MSC chondrogenesis and hypertophy. It is hypothesised

that altering scaffold design (fibre spacing) throughout the depth will cause larger hydrogel compressive strains in areas of higher PCL fibre spacing under the application of dynamic compression. It is further hypothesised that dynamic compression will enhance MSC chondrogenesis in large osteochondral-sized hydrogels and that hypertrophy will be suppressed in areas experiencing high strain magnitudes.

7.3   Materials and Methods

7.3.1   RGD incorporation and alginate preparation

RGD-modified methacrylated alginate was prepared by researchers in Eben Alsberg's laboratory and synthesized in a two-step reaction utilizing standard carbodiimide chemistry. Low-molecular-weight sodium alginate (37,000 g/mol) was prepared by irradiating Protanal LF 20/40 (196,000 g/mol; FMC Biopolymer, Philadelphia, PA) at a gamma dose of 5 Mrad. Twenty-five percent actual methacrylation of alginate carboxylic acid groups was performed as described previously [228]. Methacrylated alginate solutions (1 %, w/v) were prepared with 50mM of 2-(N-morpholino)- ethane sulfonic acid hydrate (Sigma, St. Louis, MO) buffer solution containing 0.5 M NaCl (Sigma) at pH 6.5, and sequentially mixed with N-hydroxysuccinimide (Sigma) and 1-ethyl-3-[3-(dimethylamino)propyl] carbodiimide (EDC; Sigma). The molar ratio of N-hydroxysuccinimide to EDC was 0.5:1.0, and the weight ratio of EDC to methacrylated alginate was 1.0:20.7. The Gly-Arg-Gly-Asp-Ser-Pro (Commonwealth Biotechnologies, Richmond, VA) amino acid peptide sequence was added to the methacrylated alginate solution at a weight ratio of 10 mg/g methacrylated alginate. After reacting for 24 h at 48 °C, the reaction was stopped by addition of hydroxylamine (0.18 mg/mL; Sigma), and the solution was purified by dialysis against ultrapure deionized water (di-H_2O) (MWCO 3500; Spectrum Laboratories, Rancho Dominguez, CA) for 3 days, treated with activated charcoal (0.5 mg/100 mL, 50-200 mesh; Fisher, Pittsburgh, PA) for 30 min, filtered (0.22 mm filter), and lyophilized. Control methacrylated alginate was prepared in the

same manner but without the presence of peptide.

The lyophilised alginate with RGD modification was then re-suspended in ultra pure water at 2.5 % before being filtered through a 45 µm mesh.

7.3.2   Scaffold mesh 3-d bioprinting

PCL scaffolds were fabricated using the 3D Discovery multi-head bioprinting system purchased from Regen Hu, Switzerland. 45,000 D average molecular weight PCL was melted at slightly higher temperatures of 68 °C and 3D Bioprinted through a 30 gauge needle at a pressure of 4 MPa. Scaffolds were fabricated to have a diameter of 12 mm to and were built to have a height of 4.88 mm. Fibre spacing was offset by 0.1 mm between layers to facilitate bending and lower bulk moduli. In homogenous scaffolds fibre spacing was increased from 1 mm to 1.5 mm after a quarter height before repeating this deposition pattern; again to enable the production of a weaker mesh (fig. 7.1). Gradient scaffolds had fibre spacing tapered in each quarter from 1, 1.5, 2 and finally to 3 mm spacings (fig. 7.1).
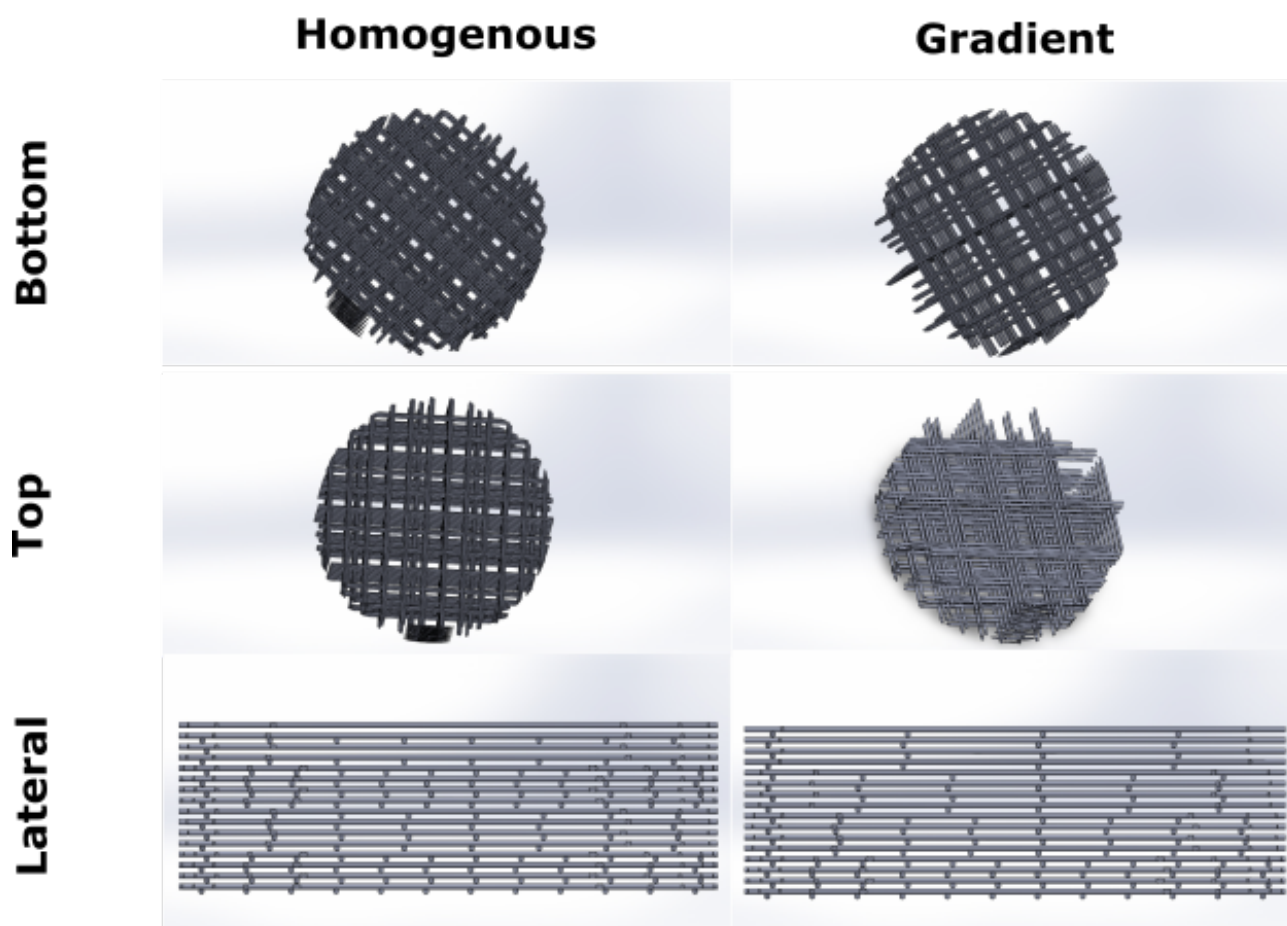
Figure 7.1 Ideal scaffold design and geometry.

7.3.3   Cell isolation, expansion and hydrogel encapsulation

MSCs were isolated from porcine femora. Following isolation, Porcine MSCs were preserved in liquid nitrogen before later being thawed and expanded according to a modified method developed for human MSCs. MSCs were plated at a seeding density of 50,000 cells/cm^2 in high-glucose Dulbecco's modified eagles medium (4.5 mg/mL D-Glucose, 200 mM L-Glutamine; hgDMEM) supplemented with 10 % fetal bovine serum (FBS) and 2 % penicillin (100 µg/ml) - streptomycin (100 µg/ml); and expanded to passage two in a humidified atmosphere at 37 °C and 5 % CO$_2$.

MSCs were suspended in chondrogenic medium (CM), which consisted of hgDMEM supplemented with penicillin (100 μg /ml) and streptomycin (100 μg/ml), sodium pyruvate (100 μg/ml), L-proline (40 μg/ml), bovine serum albumin (1.5 mg/ml), linoleic acid (4.7 μg/ml), insulin-transferrin-selenium (10 μg/ml), L-ascorbic acid-2-phosphate (50 μg/ml), dexamethasone (100 nM) and 10 ng/mL TGF-β_3. The MSC suspension was subsequently mixed with 2.5 % RGD-modified alginate (dissolved in ultra pure water) at a ratio of 1:4 to yield a final gel concentration of 2 % RGD-modified alginate and a cell density of 20 million cells/ml. The alginate-cell suspension was cast in an agarose mould (12 mm diameter by 5 mm deep) containing 100 mM $CaCl_2$ with the incorporation of either a homogenous or gradient mesh within the construct.A slab and solution, containing a 100 mM $CaCl_2$ concentration, was placed on top of and around moulds containing 12 samples respectively. This housing was then incubated for 30 minutes. Constructs were maintained separately in 12-well plates with 2 ml of chondrogenic medium in 5 % O_2. Medium was exchanged twice weekly and constructs were cultured in these conditions for 21 days.

7.3.4   Dynamic compression application

Dynamic compressive loading was applied to constructs also supplied with chondrogenic medium following a 21 day culture period. Dynamic compression (DC) was carried out in an incubator housed, custom-built compressive loading bioreactor. Uniaxial, unconfined compression was initiated using an electric linear actuator with 0.05 μm resolution (Zaber Technologies Inc., Vancouver, Canada). A 1000 g load cell (RDP Electronics Ltd, Wolverhampton, UK) attached to the actuator lead screw sensed the load applied. The system was controlled and data logged using Matlab. The dynamic compression protocol consisted of 15 % strain amplitude superimposed on a maximum 1 % preload at a frequency of 1 Hz employed for a period of 3 weeks, 5 days/week and 2 h/day (fig. 7.2). FS controls constructs were housed in the bioreactor dish without any media agitation (fig. 7.2). Medium was exchanged 2 - 3 times weekly.
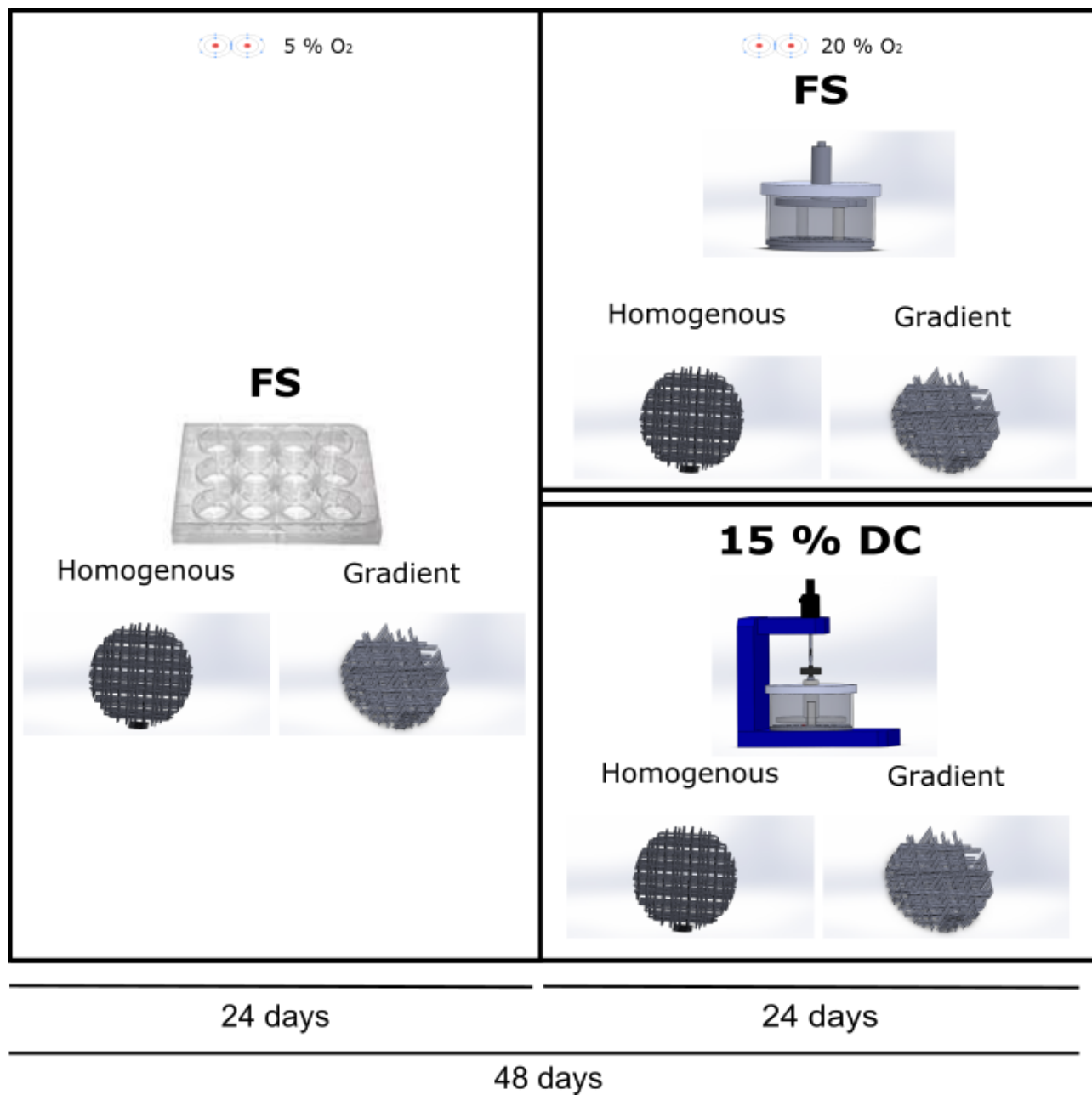
Figure 7.2 Schematic of study design.

7.3.5   Biochemical content

The biochemical content of constructs (n = 3 or n = 4) was assessed at day 0 and day 21. The wet mass of each construct half was recorded before being frozen at -85 °C for later analysis. Samples were digested with papain (125 µg/mL) in 0.1 M sodium acetate, 5 mM L-cysteine HCl, 0.05 M EDTA, pH 6.0 (all Sigma- Aldrich) at 60 °C under constant rotation for 18 h. DNA content was quantified using the Hoechst Bisbenzimide 33258 dye assay as previously described [219]. The proteoglycan content was estimated by quantifying the amount of sulfated glycosaminoglycan (sGAG) in constructs using the dimethylmethylene blue dyebinding assay (Blyscan, Biocolor Ltd., Carrickfergus, UK), with a shark chondroitin sulfate standard. Total collagen content was determined through measurement of the hydroxyproline content [220]. A hydroxyproline-to-collagen ratio of 1:7.69 was used.

7.3.6   Histology and immunohistochemistry

Constructs (n = 2) were fixed in 4 % paraformaldehyde (Sigma-Aldrich), wax embedded and sectioned at 5 and 10 µm to produce a cross section perpendicular to the disk face. Sections were stained for sGAG with 1 % alcian blue 8GX (Sigma-Aldrich) in 0.1 M HCl; for collagen with picro-sirius red; and for calcium with alziran red. The deposition of collagen type I, type II and type X was identified through immunohistochemistry. Briefly, sections were quenched of peroxidase activity, rinsed with PBS before treatment with chondroitinase ABC (Sigma-Aldrich) in a humidified environment at 37 °C. Slides were rinsed with PBS and non-specific sites were blocked with goat serum (Sigma-Aldrich). Sections were then incubated overnight at 4 °C with the primary antibody; mouse monoclonal collagen type I antibody. (1:400; 1.4 mg/mL; Abcam, Cambridge, UK) or mouse monoclonal anti-collagen type II (1:100; 1 mg/mL; Abcam). After washing in PBS, sections were incubated for 1 h in the secondary antibody; anti-mouse IgG biotin antibody produced in goat (1:400; 1 mg/ mL; Sigma-Aldrich). Colour was developed using the Vectastain ABC reagent (Vectastain ABC kit, Vector Laboratories, Peterborough, UK) followed by exposure to peroxidase DAB substrate

kit (Vector Laboratories). Negative and positive controls of porcine ligament, cartilage or growth plate were included for each batch. For both histology and immunohistochemistry images presented at high magnification from top and bottom regions including the both sides of the annulus and space between (left,right and middle for respective depth) as well as macroscopic images at low magnifications of both the left and right side of the scaled-up constructs (left and right corner).

7.3.7 Statistical analysis

Statistics were preformed using graphpad prism software package. Groups were analysed for significant differences using a general linear model for analysis of variance with factors of scaffold design and dynamic versus free swelling culture conditions examined. Tukey's test for multiple comparisons was used to compare conditions. Significance was accepted at a level of $p < 0.05$. Numerical and graphical results are presented as mean $\pm$ standard error from the mean.

7.4   Results

7.4.1   Scaffold design influences mechanical properties and the local strain environment within composite alginate-PCL constructs

Macroscopic images highlight differences in fibre spacing throughout the depth of the scaffold (fig. 7.1A). The gradient mesh structure showed a greater fibre spacing in the lower region (Bottom; fig. 7.1A), while spacing was the same in the top regions of both mesh structures. From these images, the average fibre diameter of the 3-D printed meshs was calculated using ImageJ as 134 μm, with little difference observed between each mesh design (fig. 7.1B). The overall effect of producing a gradient mesh was to significantly reduce the bulk Young's modulus of the hydrogel-mesh construct and this was maintained throughout 21 days of culture.
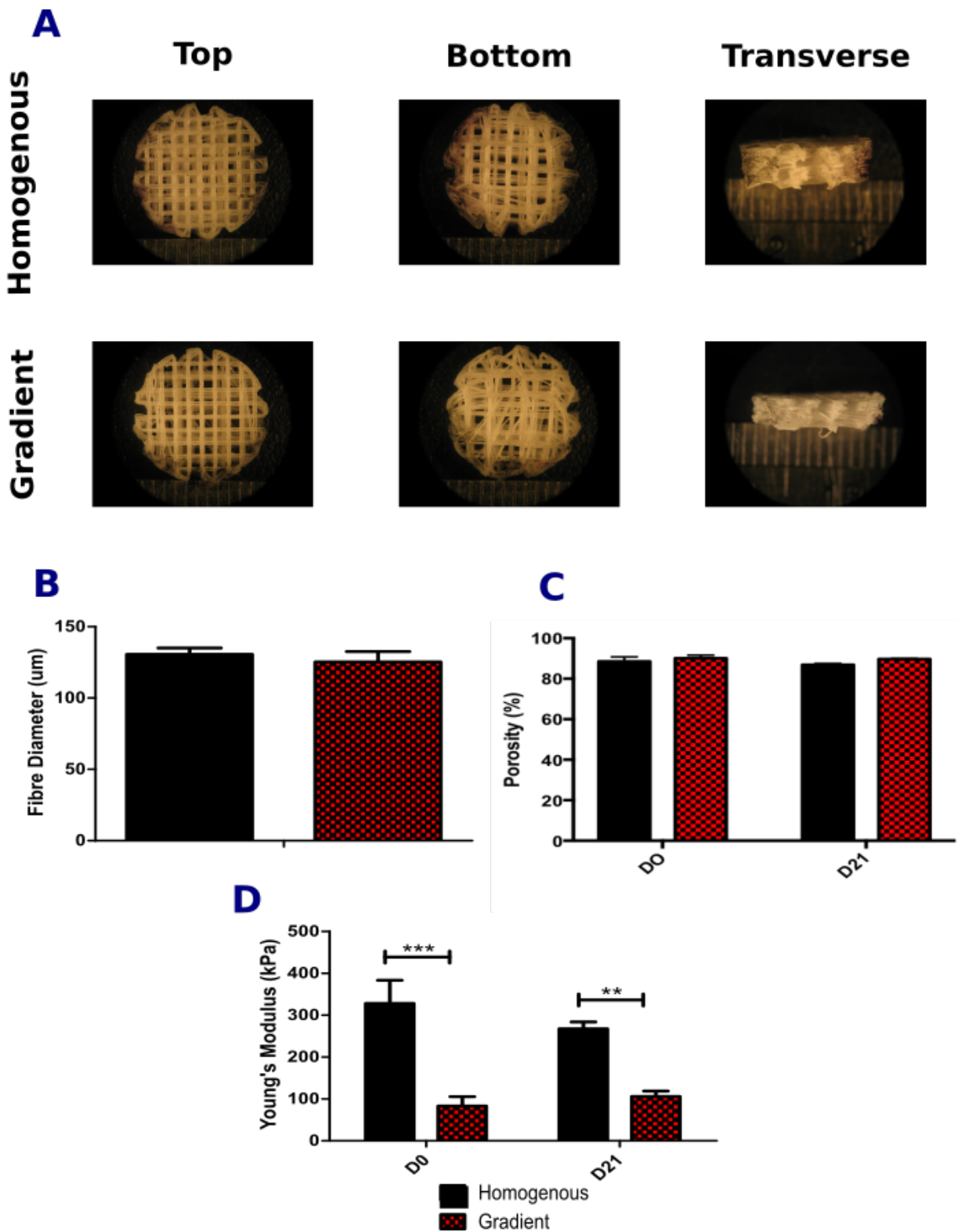
Figure 7.3 Stereomacroscopic characterisation of both mesh designs. (A) Top, bottom and lateral stereomacroscopic images of homogenous and gradient mesh designs. (B) ImageJ characterisation of fibre diameter. (C) Young's modulus of hydrogel-mesh constructs of both homogenous and gradient design at day 0 and day 21 in culture.

The application of a ramp compressive strain (15 %) to the gradient mesh-hydrogel construct produced considerable local strains variations (fig. 7.2). Within the gradient PCL-alginate construct, compressive strains appeared greatest at the bottom, particularly in the cellular region (fig. 7.2). Conversely, the homogenous PCL-alginate construct produced smaller spatial variations in local strain magnitudes. These may again be due to an artefact of digital image correlation for these structures. Conversely inhomogenous crosslinking of a scaled up construct. A similar pattern develops in hydrogel-free PCL mesh lattices (fig. 7.2), in which higher strains are developed in the filaments of gradient mesh structures under the application of a ramp compressive strain (15 %).
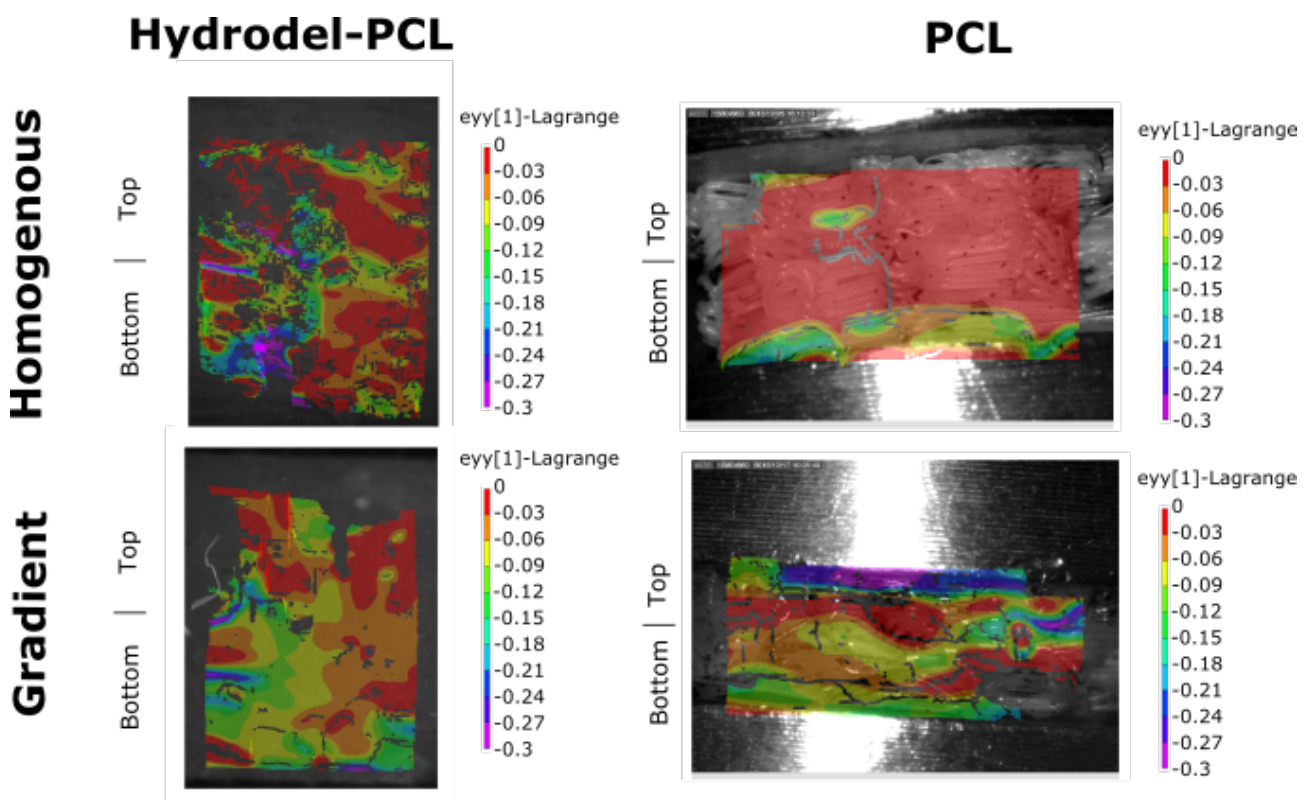
Figure 7.4 Digital image correlation analysis (DIC) to determine effect of different meshing designs on local strain magnitudes. DIC analysis to compute local strains of these MSC-laden mesh-hydrogel constructs and dotted mesh alone constructs subjected to a 15 % ramp strain indicative of dynamic compressive loading cycle. DAPI-stained MSCs were tracked in fixed constructs before and after loading. Mesh alone constructs were dotted were ink using a brush. Vic2D software was then used to calculate local strain magnitudes shown.

7.4.2 Dynamic compression enhances MSC chondrogenesis in constructs containing a mesh gradient

A small reduction in DNA levels from cell seeding levels was observed in all groups following 42 days of culture (fig. 7.3A). DNA levels were higher in constructs containing a gradient mesh construct in comparison to those with a homogenous mesh during free-swelling culture conditions (FS; $p < 0.05$, fig. 7.3A). Total biochemical content was used as the main outcome measure as the aim was to engineer a tissue, not assess biological changes in MSC differentiation. Stimulation of constructs using dynamic compression (15 % strain) resulted in the production of greater GAG levels in gradient meshed constructs compared to homogenous constructs subjected to dynamic compression (15 % DC; $p < 0.05$, fig. 7.3B). Similarly analysis of collagen content highlighted higher levels within gradient PCL constructs with the application of dynamic compression (15 % DC; $p < 0.05$, fig. 7.3C). Quantification of biochemical content in top and bottom cut sections revealed no significant spatial changes in DNA (fig. 7.3D) and collagen content (fig. 7.3F), while the application of dynamic compression (15 % DC) significantly increased GAG production in the top of constructs relative to FS controls of the same region (TOP; $p < 0.05$, fig. 7.3E). This highlights the ability of dynamic compression to enhance MSC chondrogenesis in gradient meshed constructs in a spatially defined manner.
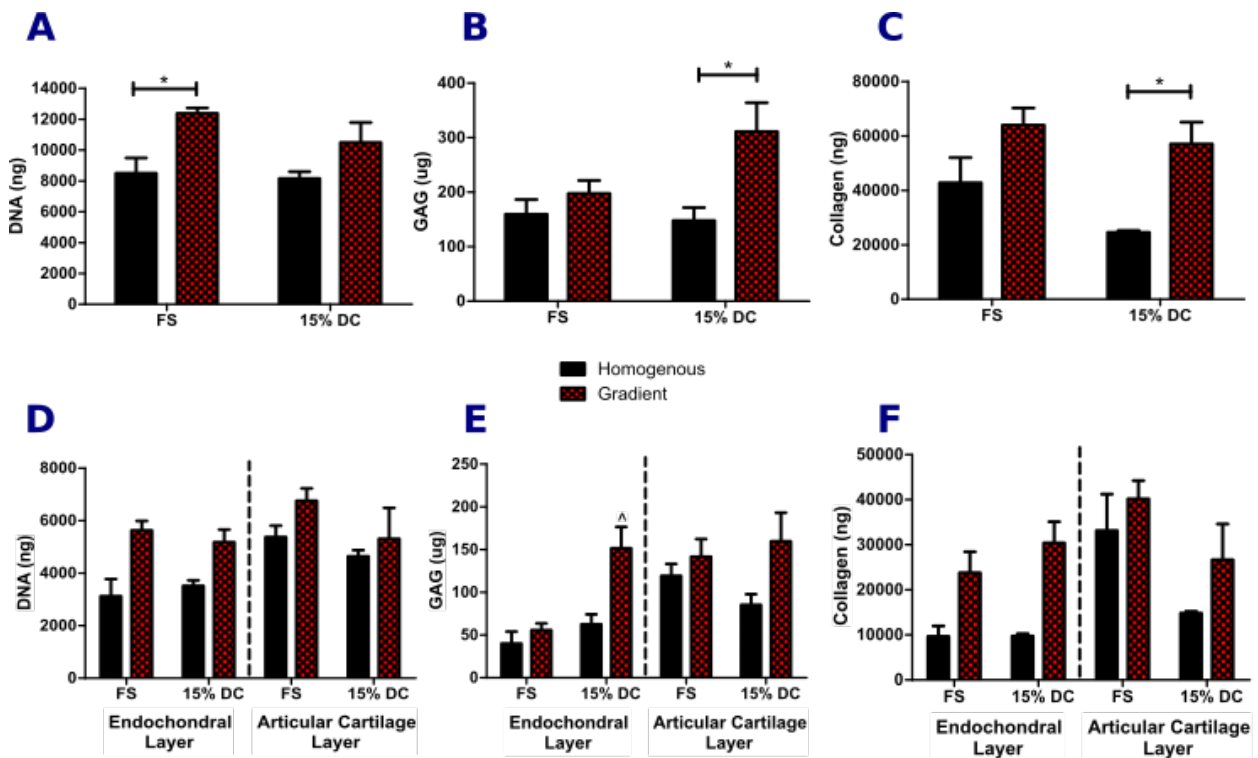
Figure 7.5 Gradient meshed constructs have a greater chondrogenic response to dynamic compression. (A) DNA, (B) GAG, and (C) non-specific collagen content of homogenous and gradient meshed constructs in FS and 15 % dynamic compressive strain culturing conditions. Spatial changes of these (D) DNA, (E) GAG, and (F) non-specific collagen contents in the top and bottom sections of homogenous and gradient meshed constructs cultured in FS and 15 % dynamic compressive strain conditions (n = 4). *,^ denotes $p < 0.05$ based on one-way ANOVA post-test analysis between groups or construct type respectively.

Histology highlights the difference in GAG staining top and bottom in gradient hydrogels during FS culture (fig. 7.4). It is evident that the application of dynamic compression produces increased GAG synthesis in pockets throughout the top of the constructs. Collagen type II staining reveals greater type II collagen production in gradient hydrogels, with little observed effect of dynamic compression (fig. 7.4).
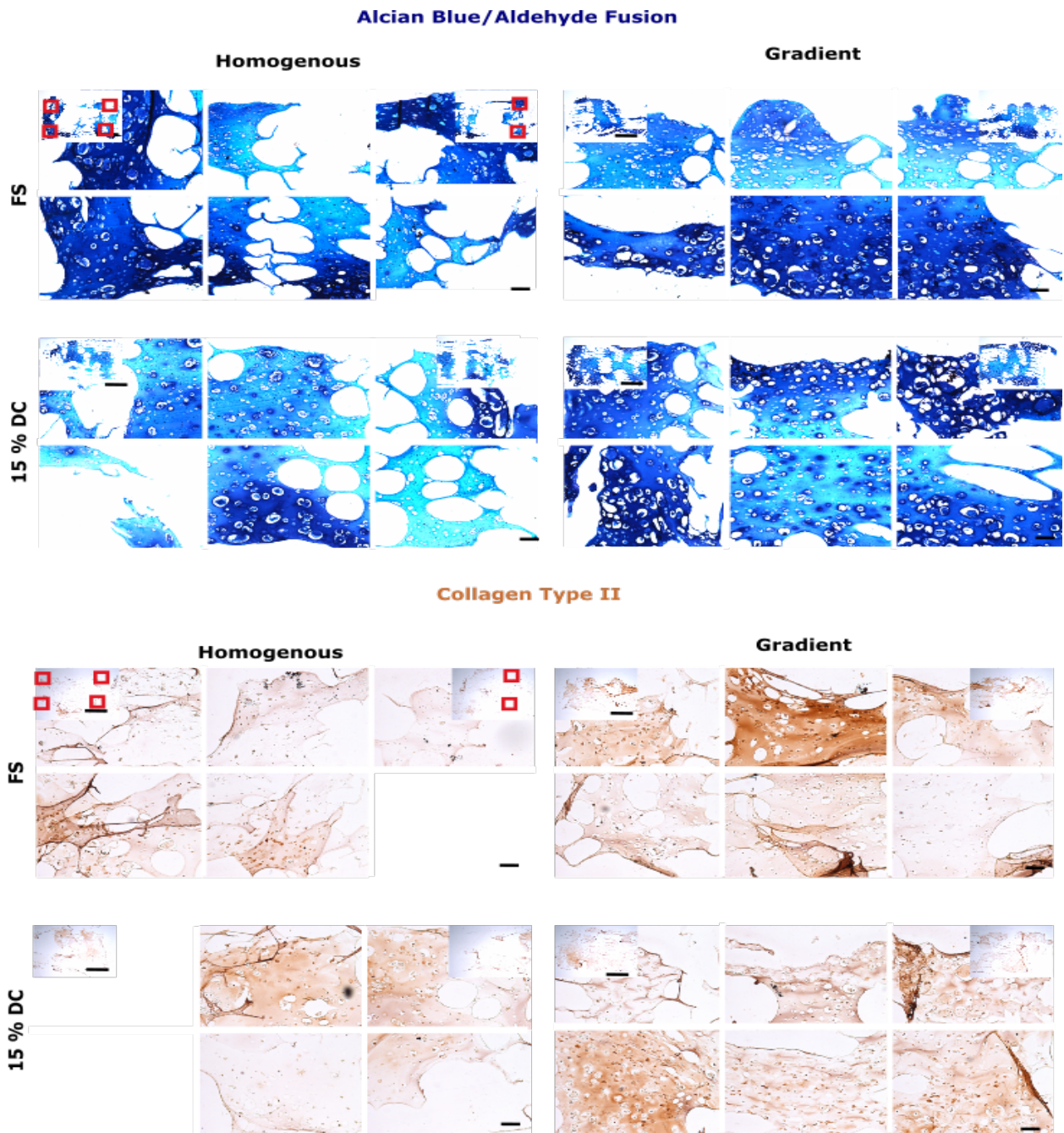
Figure 7.6 Visual representation of tissue content within MSC-laden hydrogel-mesh constructs subjected to 15 % dynamic compression. Spatial changes (left, middle and centre within top and bottom sections) in the combined aldehyde fuchsin/alcian blue stain to highlight sGAG (dark purple) and residual alginate (light blue); and immunohistochemistry stain for collagen type II strained with DAB (brown) (n = 2). Scale bars: 500 µm (inset macro image) and 100 µm.

7.4.3 Dynamic compression reduces hypertrophy in a spatially defined manner in constructs containing a mesh gradient

No changes in absolute calcium production was observed between both meshed constructs in either FS or dynamic compression conditions (fig. 7.5A). Similarly, differences in spatial content between top and bottom sections of these constructs revealed no significant alterations in any conditions (fig. 7.5B). Spatial observations did, however, reveal a trend towards a reduction in calcium in the bottom of all constructs under FS conditions. Trends also implied this spatial modulation was only maintained in gradient meshed constructs as there little difference in the mean content of the top and bottom of dynamically compressed (15 % strain) homogenous meshed constructs (fig. 7.5C).
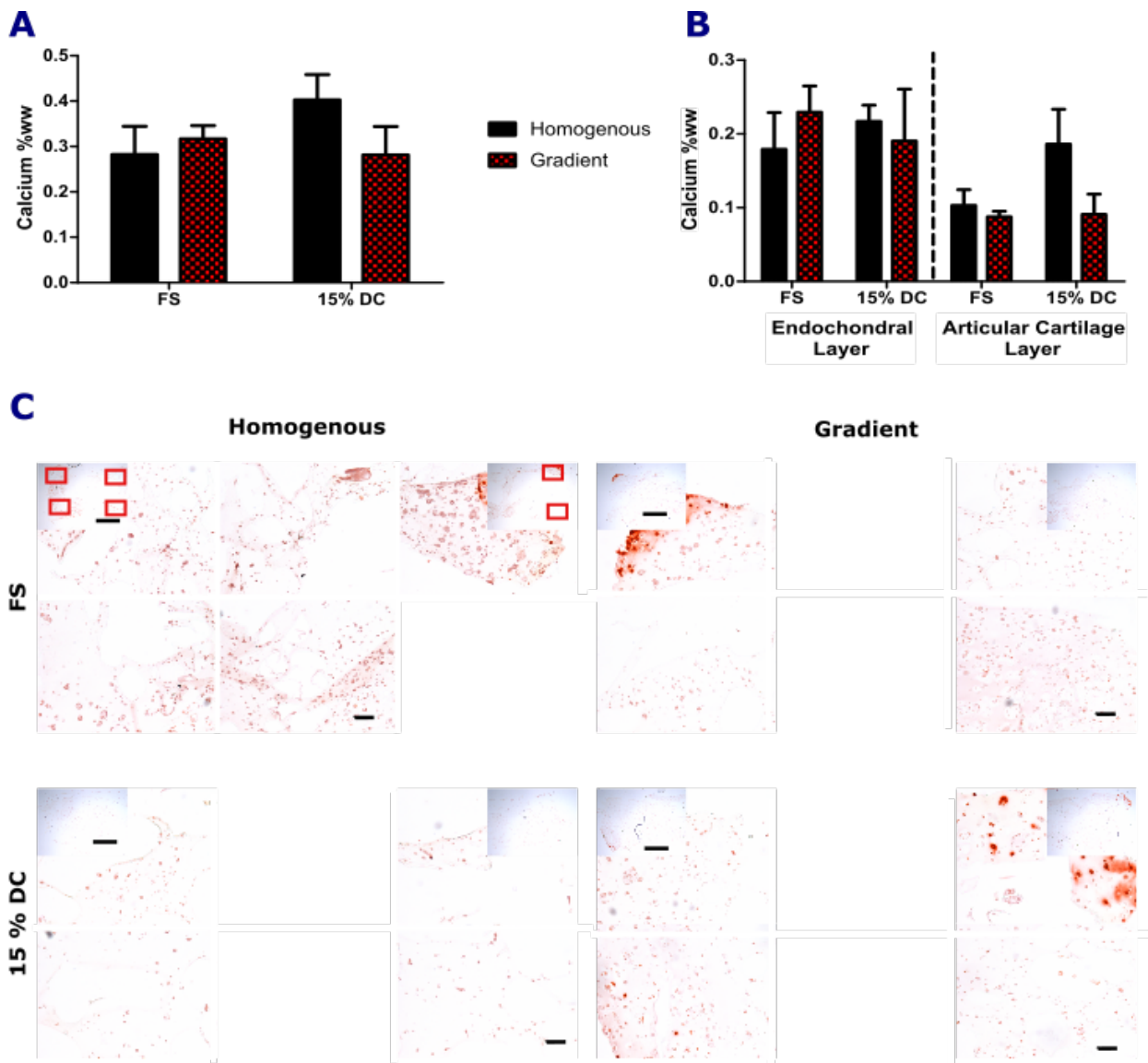
Figure 7.7 Calcium content of MSC-laden MSC-laden, gradient meshed or homogenous meshed, RGD-alginate hydrogels subjected to dynamic compression. (A) Total calcium content and **(B)** spatial calcium content (top and bottom) of homogenous and gradient meshed constructs subjected to FS or 15 % dynamic compressive strain conditions. **(C)** Spatial changes (left, middle and centre within top and bottom sections) in the alizarin red stain to highlight calcium deposits (dark red) (n = 2). Scale bars: 500 µm (inset macro image) and 100 µm.

7.4.4 Overall effect of spatially defined mechanical cues on MSC chondrogenesis and hypertrophy

When comparing a homogenous alginate-PCL construct subjected to dynamic compression with a similar construct that has a gradient of mechanical cues, it is evident that GAG content (μg) is higher in all regions of gradient hydrogels (GAG; fig. 7.6). Collagen content is significantly higher in the endonchondral region of gradient constructs where strains are expected to be lower (fig. 7.6). Finally, no change in calcium production between constructs in each of the layers. However, the lowest mean calcium content is in the loaded gradient construct in the articular region as hypothesised despite no significant change (fig. 7.6). This suggests a reduction of hypertrophy and endochondral ossification by higher local strain magnitudes.
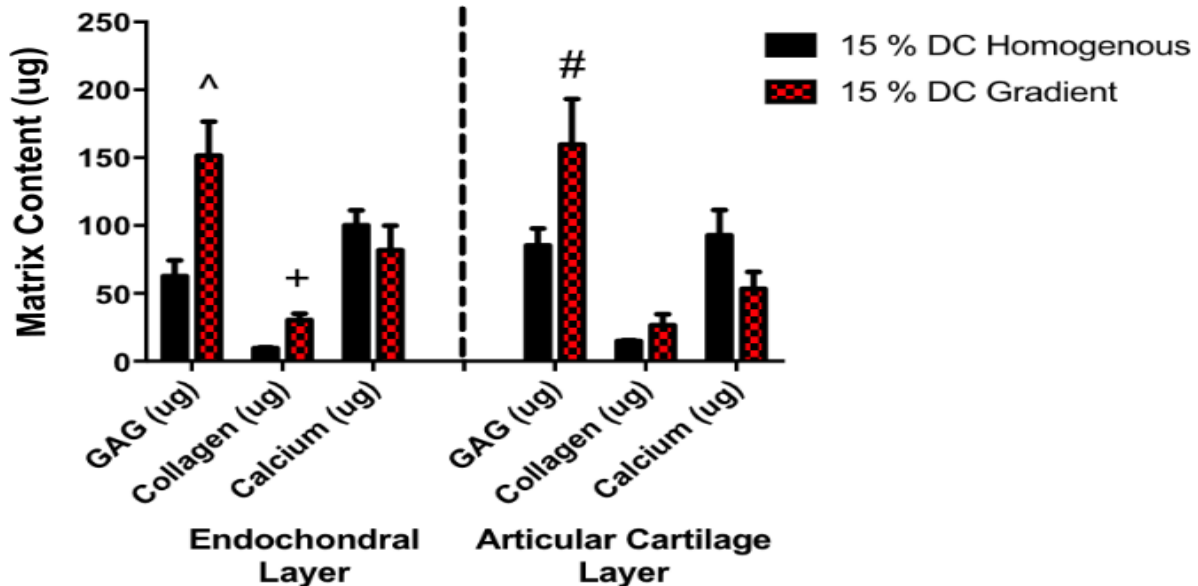
Figure 7.8 Differences in tissue composition of loaded alginate-PCL constructs. Summary of differences in GAG (μg), collagen (μg) and calcium (μg) contents between homogenous and gradient alginate-PCL constructs subjected to dynamic compression (15 % strain) in the articular cartilage and endochondral layer (n = 4). ˆ, +, # denotes $p < 0.05, 0.01, 0.001$ based on t-test analysis between loaded homogenous and gradient constructs.

7.5 Discussion

The aim of this study was to determine whether alterations in local strain magnitudes have the potential to spatially influence MSC chondrogenesis and hypertrophy within an alginate hydrogel. The use of 3-D bioprinting techniques enabled the fabrication of honeycomb, mesh-like, PCL lattices, wherein altering fibre spacing throughout the depth proved an effective means of spatially controlling mechanical deformation. A mesh with a layered gradient of fibre spacing produced higher local strain magnitudes in areas of high fibre spacing. This produced a similar gradient within a hydrogel impregnated with this mesh lattice. GAG production was also enhanced in gradient mesh lattices following the application of dynamic compression (15 % strain), mainly due to large increases in ECM production in the top of the construct where local strains were lower. Finally, no statistical change in MSC hypertrophy was observed despite trends in calcium content and alizarin red staining showing less calcium production in the bottom (articular cartilage region) of dynamically compressed hydrogel-gradient lattice structures.

Scaffold design altering the local mechanical environment of a construct is a relatively novel concept. Changes in pore architecture have, however, been used to successfully change bulk mechanical properties in printed structures [243]. In this study a change in fibre spacing, effectively altering macro-pore size, produced similar changes in mechanical properties. Here, higher fibre spacing reduced local mechanical properties similar to pore size reducing bulk mechanical characteristics. This translated effectively to altering deformations when coupled with a hydrogel. Small variations in the local strain fields are likely due to stress concentrations of particular fibre junctions. These were unlikely to have any masking or detrimental effect.

The stiff hydrogel and gradient-mesh lattice construct acted to enhance MSC chondrogenesis when subjected to dynamic compression (15 % strain). This was particularly evident in the top of these constructs; the area in which low local strains would be developed under dynamic compression. Low strains enhancing MSC chondrogenesis in stiff hydrogels has been shown in chapter 5 of this thesis, in which low strains upregulated type II collagen

and aggrecan gene expression. Additionally, Horner et al. have shown similar results with dynamic compression magnitudes approaching 15 % strain enhancing MSC chondrogenesis, while 20 % strain magnitudes suppress this phenomena to levels of lower strains [222].

Finally, it was found that the introduction of a gradient of local strain magnitudes had no significant effect on MSC hypertrophy and calcification is surprising. Horner et al. showed a progressive decrease in MSC calcification with increasing dynamic compression strain magnitudes [222]. Trends in this study did seem to show a spatial modulation in MSC hypertrophy in gradient mesh-hydrogel constructs with lower calcification in higher dynamically compressed regions. This highlights that further optimisation of the lattice mesh structure is needed to find a design that presents strains in a locally defined manner. Additionally, cell number may have inhibited the induction of significant MSC hypertrophy and endochondral ossification. Future studies should consider the inclusion of biochemical factors known to accelerate hypertrophy, where the effects of dynamic compression might become more pronounced.

7.6 Conclusion

This study provides further indication that low strains enhance MSC chondrogenesis in stiff hydrogels and also implies that altering local strain magnitudes can induce spatial changes in both MSC chondrogenesis and hypertrophy. It highlights the need for subsequent research to consider the local strain field of the deformed construct when applying mechanical stimuli *in vitro* or implanting within a load bearing environment *in vivo*.

CHAPTER 8

Discussion

8.1 Overview

THE inability of articular cartilage, and other tissues, to spontaneously repair areas of damaged tissue has lead the establishment of an interdisciplinary effort that seeks to find a means of regenerating tissue within these defects. Surgical techniques alone, such as microfracture, mosaicplasty and arthoroplasty for joint diseases including osteoarthritis, fail to restore full, long-term function to the joint. Therefore tissue engineering was developed to combine principles of engineering and the life sciences for the development of biological substitutes to replace, repair and restore tissue and function to damaged sites.

Multipotent mesenchymal stem cells (MSCs) have been identified as a potential cell source capable of producing tissue for many applications. Biochemical induction of MSCs towards a particular tissue lineage is a powerful means of directing differentiation along chondrogenic, osteogenic and myogenic pathways. This alone, however, is insufficient to achieve adequate levels of tissue production and organisation when compared with native tissues. Therefore, tissue engineering seeks to combine different cell sources with a variety of biomaterials, as well as numerous external mechanical and environmental cues, to tissue engineer functional grafts for specific applications.

Specifically for osteochondral tissue engineering, in which a cartilage defect penetrates

the underlying subchondral bone, modulating endochondral ossification of a cartilage template is a promising engineering strategy for developing osteochondral tissue [21,244]. It has been shown that creating bone from a cartilage template enables MSCs to withstand the development of hypoxia during bone formation in a critical sized bone defect [245]. It has also recently been shown that dynamic compression can suppress hypertrophy and subsequent endochondral ossification that can follow chondrogenesis of bone-marrow derived MSCs. Therefore this thesis seeks to control MSC chondrogenesis and hypertrophy by modulating mechanical cues in order to find a mechanical means of producing osteochondral tissue.

The overall objective of this thesis is to develop the precursor to an osteochondral graft by mechanically modulating chondrogenesis and hypertrophy of MSCs within a 3-dimensional hydrogel environment. This was achieved by applying dynamic compression to cartilage tissue that was engineered through the encapsulation of bone marrow derived MSCs in three-dimensional hydrogel constructs. Oxygen availability, substrate stiffness and magnitude of dynamic compression were varied throughout. The studies which comprise this thesis have demonstrated that MSC-laden hydrogels are responsive to both substrate stiffness, oxygen availability and dynamic compression. Furthermore, the response to dynamic compression is dependent on factors such as substrate stiffness and magnitude of the applied dynamic compression.

It was demonstrated that dynamic compression of MSC-laden agarose hydrogels enhanced MSC chondrogenesis as well as changing MSC hypertrophy in a magnitude dependent manner (Chapter 3). For the purposes of utilising this principle for osteochondral tissue engineering and allowing the development of bone tissue, RGD-modified alginate hydrogels were subsequently used. Having produced a means of forming soft and stiff versions of this hydrogel, it was found that soft MSC-laden alginate hydrogels promote enhanced chondrogenesis, while stiff hydrogels increase collagen production; and spatial distributions were altered by both oxygen tension and substrate stiffness (Chapter 4). Following on from this, it was found the response of MSCs to dynamic compression in these hydrogels in substrate stiffness dependent; no observed response in soft hydrogels, enhanced MSC chondrogenesis at moderate strains (10 %) in stiff hydrogels and a reduction

of MSC hypertrophy (compared to lower strain magnitudes) at high strains (20 %) (Chapter 5). Using these principles, to develop a mechanical means of developing osteochondral grafts, it was hypothesised initial spatial alterations in substrate stiffness, coupled with different oxygen availability and local changes in dynamic compressive strain magnitude could be used to create osteochondral-like tissue. It was found that while regions of specific substrate stiffness in a gradient hydrogel performed similarly to the corresponding region in a homogenous hydrogel of similar stiffness, the final profile of tissue-specific gene expression was not completely osteochondral in nature (Chapter 6). Finally, using mechanics alone to vary local strain magnitudes, it was found that low strains enhance MSC chondrogenesis and high strains tend to reduce MSC hypertrophy producing a very immature osteochondral-like tissue (Chapter 7).

This thesis has identified the way in which MSCs respond to mechanical cues and oxygen availability as well as the interdependence of these stimuli on MSC chondrogenesis and hypertrophy. Both MSC chondrogenesis and endochondral ossification following from MSC hypertrophy are selectively mechano-responsive. The differentiation state of the cell, mechanical environment over time and spatial presentation of the stimuli are important in each condition.

8.2 Modulators of MSC chondrogenesis

8.2.1 Substrate stiffness

One of the principle findings of this thesis is that the stiffness of RGD-modified alginate hydrogels directs MSC chondrogenesis. Soft MSC-laden hydrogels appear to stimulate enhanced chondrogenesis at early time points of culture. This is evident by increased GAG synthesis at day 5 and an upregulation in chondrogenic markers at day 10 and day 14. Park et al. demonstrated a similar upregulation in gene expression within MSCs encapsulated in a stiff 3-D hydrogel [167]. Despite alterations in gene expression at day 14 in chapter

4 based on encapsulation within a soft substrate, no overall changes in GAG deposition occurred at day 28. This suggests that soft hydrogels provide an environment ideal for MSC chondrogenesis yet perhaps culture with TGF-β_3 supplementation is more potent than substrate stiffness within the range presented.

An interesting shift towards stiff hydrogels enhancing MSC chondrogenesis at later timepoints (day 28) was observed in chapter 6. These stiff hydrogels softened over time based on bulk mechanical properties. This may be due to degradation of the alginate matrix. This presents a mechanism for softening the local substrate environment, which may explain the induction of an enhanced chondrogenic environment. Therefore changes in substrate stiffness over time may be very important in defining the overall effect substrate stiffness has on MSC chondrogenesis. Degradation mediated changes in MSC fate between osteogenesis and adipogenesis have previously been observed [246]. This is therefore a relevant consideration for assessing the effects of substrate stiffness over time in a tissue engineering construct.

The response of MSCs to dynamic compression is dependent on the stiffness of the MSC-laden hydrogel and perhaps more importantly the differentiation state of the cell. Dynamic compression provides an additional chondrogenic stimulus. Therefore dynamic compression may be more effective at enhancing MSC chondrogenesis within environments that provide a less robust chondrogenic cue to cells. In chapter 5 it was found that dynamic compression only enhances chondrogenesis in stiff MSC-laden hydrogels. These stiff hydrogels, however, provided a less robust chondrogenic environment than soft hydrogels. In chapter 6 dynamic compression upregulated markers of chondrogenesis within soft hydrogels while stiff hydrogels promoted an increased expression in chondrogenic gene markers.

This presents a conflicting picture of the effect substrate stiffness has on the response of MSCs to dynamic compression. Dynamic compression having a larger effect on MSCs in a less chondrogenic environment has previously been observed in most initial studies that incorporated dynamic compression into studies involving MSC chondrogenesis. This corroborates previous findings from Steward et al., which highlighted that stiff hydrogels are more responsive to dynamic compression in terms of MSC chondrogenesis than a more

chondrogenic soft construct [109].Therefore the differentiation state of the cell may play a crucial role in the response of MSCs to dynamic compression and this is strongly dependent on substrate stiffness and degradation of the substrate.

8.2.2   Magnitude of dynamic compression

A principle finding of this thesis is that MSC chondrogenesis depends on the magnitude of dynamic compression. Consistently, a moderate magnitude of dynamic compression enhanced MSC chondrogenesis. This is evident by moderate strains (10 %) enhancing MSC chondrogenesis in stiff hydrogels and GAG deposition increasing significantly in the endochondral layer of gradient alginate-PCL constructs where local magnitudes of strain were lower.

Moderate strains (10 %) enhancing MSC chondrogenesis is consistent with findings in literature. Thorpe et al. showed that dynamic compression at similar magnitudes enhanced GAG production [98] and altered MSC fate towards a chondrogenic phenotype [151]. Huang et al. showed increases in mechanical properties with dynamic compression despite no changes in matrix specific protein deposition [221] as seen in chapter 3.

8.2.3   Oxygen availability

Complex gradients in O_2 develop in MSC-laden constructs producing much lower oxygen availability in the core of a hydrogel than is externally available. Changes in external oxygen availability spatially altered the secretion of cartilage-specific matrix components in both chapter 4 and 7. Low oxygen availability (5 %) produced more homogenous ECM deposition of cartilage-specific matrix components in chapter 4 and tended to enhance GAG deposition in the articular cartilage region of MSC-laden alginate-PCL constructs. Despite these spatial changes no overall effect of oxygen availability was observed on bulk GAG deposition or genetic markers of chondrogenesis. This may be again due to the ideal chondrogenic

environment provided by the hydrogel and TGF-β_3 supplemented culture.

8.3 Modulators of MSC hypertrophy

8.3.1 Magnitude of dynamic compression

This thesis presents key findings to suggest that dynamic compression regulates MSC hypertrophy in a magnitude dependent manner. High strain magnitudes (20 %) lower MSC hypertrophy and calcification in comparison to lower strain magnitudes. This reflects recent findings by Horner et al. that highlighted a suppression of MSC hypertrophy with increasing strain magnitude up to 20 % strain [222].

Bian et al. also presented data of dynamic compression suppressing MSC hypertrophy [22]. In addition, Zhang et al. have highlighted a suppression of MSC hypertrophy with the application of moderate strains in a hydrogel that promotes hypertrophy[23]. These studies also present a FS control that promotes hypertrophy or osteogenesis. In contrast, the FS environment in this thesis is pro-chondrogenic. Therefore the effect the magnitude of dynamic compression has on MSC hypertrophy seems to be dependent on the environment within which dynamic compression is applied.

8.4 Experimental considerations

8.4.1 Magnitude of dynamic compression

The dynamic compression protocol employed in this thesis consisted of different strain magnitudes (0, 5, 10 and 20 %) applied at 1 Hz for a period of 5 days/week for a given number of weeks. Much evidence suggests that 1 Hz may be the optimum dynamic compression frequency for chondrogenesis of MSCs. Huang et al. found that 1 Hz dynamic compression

applied after TGF-β_3 stimulation increased construct stiffness when compared to 0.1 Hz [221]. The magnitude of dynamic compression applied resembles that presented by Horner et al. in which these magnitudes of dynamic compression had no detrimental effect on MSCs [222]. The dynamic compression bioreactor set-up did have the ability to log force signals from the load cell. These were not used to generate force-displacement curves as this is generally not a conventional measurement employed in dynamic compression bioreactor systems used for tissue engineering purposes.

8.4.2 Substrate Stiffness

Throughout this thesis substrate stiffness has been varied by altering $CaCl_2$ concentration. This has proven effective but latter analysis for larger constructs using digital image correlation has revealed possible changes in local substrate stiffness. This is based on variations in the local strain field when constructs are compressed. This is unlikely to be the case in the standard 5 mm $\oslash$ x 2 mm high construct as this is commonly used by other research groups in many of their studies. It does, however, highlight that MSC differentiation could be adversely affected. Changes in substrate stiffness would undoubtedly affect MSC differentiation of response to dynamic compression.

8.4.3 Oxygen availability

This thesis utilised high oxygen availability (20 %) to stimulate hypertrophic induction of MSCs in FS or unstrained culture. This appeared to insufficiently stimulate hypertrophy in this culture system as dynamic compression initiated without strain application (0 %), thought to enhance oxygen transport, tended to reduce calcification. In addition, no significant effect of oxygen availability was observed on calcification.

8.4.4   Biomaterial choice

The studies in this thesis utilised agarose and alginate for three-dimensional MSC culture. Hydrogels have many advantages over scaffold types which include uniform cell seeding throughout the construct and shape stability. Additionally, both the stiffness and permeability of these gels can be controlled through alterations in their constituent concentrations or exogenous crosslinking agents for alginate. Both are natural polymers that permit MSC chondrogenesis. Importantly, the properties of both hydrogels were tailored to permit the application of deformation loading in and around the physiological range progressively after encapsulation.

8.4.5   Time points

The thesis used a free swelling period usually in the range of 21 - 24 days before stimulating the constructs with dynamic compression with a further 5 or 21 - 24 days. The free swelling period is an appropriate time to enable robust chondrogenesis and allow a large delay before initiating the loading stimulus. Shorter free swelling periods of 5 days were also used in Chapter 5 to assess the impact of substate stiffness and dynamic compression at shorter periods to determine if the same magnitude dependent effect occurred. Dynamic compression being applied for 5 days/week over the course of 21 or indeed 4 days/week over 24 days reflects largely on the long loading durations used in literature. While 4 days/week over 24 days is uncommon, this was used for practical purposes and still maintains a similar amount of total loading to the standard 5 days/week over 21 days protocol. Shorter durations of 5 loading days generally are used to determine morphogenesis based on biological effects of gene transcription. This principle was applied throughout this thesis.

Studies not involving loading had a longer duration of 28 days. This was to allow possible hypertrophy to develop as this is only occurs in mature constructs.

Comparing these time points would involve comparing free swelling times of 21 and 24 days; experiments of 28 days including loading with thus in the absence of loading; loading

stimuli of 5 days; and loading stimuli of 21 - 24 days. This leaves the short free swelling period of 5 days as a standalone result with no comparable.

CHAPTER 9

Conclusion

9.1 Main Results

THE overall objective of this thesis was to develop an osteochondral graft by mechanically modulating chondrogenesis and hypertrophy of MSCs within a 3-dimensional hydrogel environment. To this end, oxygen availability, substrate stiffness and dynamic compression were modulated in MSC-laden agarose and RGD-modified alginate hydrogels. The main conclusions from this thesis are as follows:

- MSC chondrogenesis is enhanced by moderate strains, while MSC hypertrophy and endochondral ossification is regulated in a magnitude dependent manner with low strains enhancing endochondral ossification as evident by increases in calcification.

- Oxygen availability affects the spatial deposition of cartilage-specific proteins with 5 % O_2 producing a more homogenous construct, while 20 % O_2 restricted most protein deposition to the core of the engineered tissue.

- Soft MSC-laden hydrogels provide a more chondrogenic environment for early MSC

chondrogenesis, yet stiff counterparts begin to converge and approach this state by enhancing late MSC chondrogenesis.

- The effect of dynamic compression is dependent on the stiffness of the local substrate. Stiff MSC-laden hydrogels enable mechanotransduction to a greater degree than soft alginate hydrogels.

- Spatial alterations in mechanics and oxygen availability throughout the depth of the construct can produce alterations in MSC chondrogenesis and hypertrophy. Greater optimisation of the environment and mechanics presented in this thesis is needed to fully regulate MSC chondrogenesis in a spatially defined manner.

This thesis demonstrates that MSC chondrogenesis and hypertrophy are dependent on oxygen availability as well as mechano-regulated. Understanding the response of MSCs to environmental and mechanical stimuli in a physiologically relevant 3-dimensional environment will improve our knowledge of mechanobiology, our ability to engineer functional tissue, and our design of bioprinted tissue constructs.

9.2   Future Directions

This thesis has provided significant insights into the mechanoregulation of MSCs. It also lays the foundations for new research. Suggestions of where that might be are as follows:

- MSC hypertophy was modulated in this research by the magnitude of dynamic compression. Overall levels of hypertrophy were, however, rather low. Therefore following the production of a cartilage template, dynamic compression should be

initiated in a more hypertrophic environment. Possibly the use of hypertrophic media during loading periods could highlight its true potential to suppress hypertrophy with increasing potency at greater strain magnitudes.

- A greater understanding of the means by which dynamic compression regulates MSC chondrogenesis as well as hypertrophy could provide the basis for a biochemical counterpart for osteoarthritis therapies.

- The convergence in chondrogenic potential of soft and stiff MSC-laden hydrogels is interesting. A mechanobiology investigation into the pathway or physical mechanism through which this occurs could be insightful.

- By re-crosslinking hydrogels with depth dependent changes in substrate stiffness directly before initiating dynamic compression, a greater effect of the applied stimuli may be evident.

- Printing 3-D constructs with a higher degree of spatial control over mechanical cues may enable the formation of osteochondral constructs that have an enhanced control of MSC differentiation towards an osteochondral fate.

Bibliography

[1] J.A. Buckwalter and H.J. Mankin. Articular cartilage: degeneration and osteoarthritis, repair, regeneration, and transplantation. *Instructional course lectures*, 47:487–504, 1998.

[2] A. Mobasheri. The future of osteoarthritis therapeutics: Emerging biological therapy. *Current Rheumatology Reports*, 15(12), 2013.

[3] H.J. Mankin. The response of articular cartilage to mechanical injury. *Journal of Bone and Joint Surgery - Series A*, 64(3):460–466, 1982. cited By (since 1996)624.

[4] V.C. Mow, C. S. Proctor, and M. A. Kelly. Biomechanics of articular cartilage. *Basic biomechanics of the musculoskeletal system*, 1(9):31–57, 1989.

[5] S. Kurtz, K. Ong, E. Lau, F. Mowat, and M. Halpern. Projections of primary and revision hip and knee arthroplasty in the united states from 2005 to 2030. *Journal of Bone and Joint Surgery - Series A*, 89(4):780–785, 2007.

[6] G. Bentley, J.S. Bhamra, P.D. Gikas, J.A. Skinner, R. Carrington, and T.W. Briggs. Repair of osteochondral defects in joints-how to achieve success. *Injury*, 44(SUPPL.1):S3–S10, 2013.

[7] W. Brehm, B. Aklin, T. Yamashita, F. Rieser, T. Trub, R. P. Jakob, and P. Mainil-Varlet. Repair of superficial osteochondral defects with an autologous scaffold-free cartilage construct in a caprine model: implantation method and short-term results. *Osteoarthr. Cartil.*, 14(12):1214–1226, Dec 2006.

[8] S. Marlovits, P. Zeller, P. Singer, C. Resinger, and V. Vecsei. Cartilage repair: Generations of autologous chondrocyte transplantation. *European Journal of Radiology*, 57(1):24–31, 2006.

[9] W. Bartlett, J.A. Skinner, C.R. Gooding, R.W.J. Carrington, A.M. Flanagan, T.W.R. Briggs, and G. Bentley. Autologous chondrocyte implantation versus matrix-induced autologous chondrocyte implantation for osteochondral defects of the knee. a prospective, randomised study. *Journal of Bone and Joint Surgery - Series B*, 87(5):640–645, 2005.

[10] A.I. Caplan. Mesenchymal stem cells. *Journal of Orthopaedic Research*, 9(5):641–650, 1991.

[11] M.F. Pittenger, A.M. Mackay, S.C. Beck, R.K. Jaiswal, R. Douglas, J.D. Mosca, M.A. Moorman, D.W. Simonetti, S. Craig, and D.R. Marshak. Multilineage potential of adult human mesenchymal stem cells. *Science*, 284(5411):143–147, 1999.

[12] J.S. Temenoff and A.G. Mikos. Review: Tissue engineering for regeneration of articular cartilage. *Biomaterials*, 21(5):431–440, 2000.

[13] R.S. Tuan, G. Boland, and R. Tuli. Adult mesenchymal stem cells and cell-based tissue engineering. *Arthritis Research and Therapy*, 5(1):32–45, 2003.

[14] B. Johnstone, T.M. Hering, A.I. Caplan, V.M. Goldberg, and J.U. Yoo. In vitro chondrogenesis of bone marrow-derived mesenchymal progenitor cells. *Experimental Cell Research*, 238(1):265–272, 1998.

[15] N. Indrawattana, G. Chen, M. Tadokoro, L.H. Shann, H. Ohgushi, T. Tateishi, J. Tanaka, and A. Bunyaratvej. Growth factor combination for chondrogenic induction from human mesenchymal stem cell. *Biochemical and Biophysical Research Communications*, 320(3):914–919, 2004.

[16] M.B. Mueller, M. Fischer, J. Zellner, A. Berner, T. Dienstknecht, L. Prantl, R. Kujat, M. Nerlich, R.S. Tuan, and P. Angele. Hypertrophy in mesenchymal stem cell

chondrogenesis: Effect of tgf- isoforms and chondrogenic conditioning. *Cells Tissues Organs*, 192(3):158–166, 2010.

[17] T. Vinardell, E.J. Sheehy, C.T. Buckley, and D.J. Kelly. A comparison of the functionality and in vivo phenotypic stability of cartilaginous tissues engineered from different stem cell sources. *Tissue Engineering - Part A*, 18(11-12):1161–1170, 2012.

[18] C. Scotti, B. Tonnarelli, A. Papadimitropoulos, A. Scherberich, S. Schaeren, A. Schauerte, J. Lopez-Rios, R. Zeller, A. Barbero, and I. Martin. Recapitulation of endochondral bone formation using human adult mesenchymal stem cells as a paradigm for developmental engineering. *Proceedings of the National Academy of Sciences of the United States of America*, 107(16):7251–7256, 2010.

[19] P. Janicki, P. Kasten, K. Kleinschmidt, R. Luginbuehl, and W. Richter. Chondrogenic pre-induction of human mesenchymal stem cells on -tcp: Enhanced bone quality by endochondral heterotopic bone formation. *Acta Biomaterialia*, 6(8):3292–3301, 2010.

[20] Eric Farrell, Sanne K. Both, Kathrin I. Odörfer, Wendy Koevoet, Nicole Kops, Fergal J. O'Brien, Robert J. Baatenburg de Jong, Jan A. Verhaar, Vincent Cuijpers, John Jansen, Reinhold G. Erben, and Gerjo JVM van Osch. In-vivo generation of bone via endochondral ossification by in-vitro chondrogenic priming of adult human and rat mesenchymal stem cells. *BMC Musculoskeletal Disorders*, 12(1):1–9, 2011.

[21] E. J. Sheehy, T. Vinardell, C. T. Buckley, and D. J. Kelly. Engineering osteochondral constructs through spatial regulation of endochondral ossification. *Acta Biomater*, 9(3):5484–5492, Mar 2013.

[22] L. Bian, D.Y. Zhai, E.C. Zhang, R.L. Mauck, and J.A. Burdick. Dynamic compressive loading enhances cartilage matrix synthesis and distribution and suppresses hypertrophy in hmsc-laden hyaluronic acid hydrogels. *Tissue Engineering - Part A*, 18(7-8):715–724, 2012.

[23] T. Zhang, F. Wen, Y. Wu, G. S. Goh, Z. Ge, L. P. Tan, J. H. Hui, and Z. Yang. Cross-talk between TGF-beta/SMAD and integrin signaling pathways in regulating hypertrophy of mesenchymal stem cell chondrogenesis under deferral dynamic compression. *Biomaterials*, 38:72–85, Jan 2015.

[24] Y. Xu, P. Malladi, M. Chiou, E. Bekerman, A. J. Giaccia, and M. T. Longaker. In vitro expansion of adipose-derived adult stromal cells in hypoxia enhances early chondrogenesis. *Tissue Eng.*, 13(12):2981–2993, Dec 2007.

[25] M. C. Ronziere, E. Perrier, F. Mallein-Gerin, and A. M. Freyria. Chondrogenic potential of bone marrow- and adipose tissue-derived adult human mesenchymal stem cells. *Biomed Mater Eng*, 20(3):145–158, 2010.

[26] M. Hirao, N. Tamai, N. Tsumaki, H. Yoshikawa, and A. Myoui. Oxygen tension regulates chondrocyte differentiation and function during endochondral ossification. *J. Biol. Chem.*, 281(41):31079–31092, Oct 2006.

[27] S. Chen, P. Fu, R. Cong, H. Wu, and M. Pei. Strategies to minimize hypertrophy in cartilage engineering and regeneration. *Genes Dis*, 2(1):76–95, Mar 2015.

[28] P. Sanz-Ramos, G. Mora, M. Vicente-Pascual, I. Ochoa, C. Alcaine, R. Moreno, M. Doblare, and I. Izal-Azcarate. Response of sheep chondrocytes to changes in substrate stiffness from 2 to 20 Pa: effect of cell passaging. *Connect. Tissue Res.*, 54(3):159–166, 2013.

[29] N. Huebsch, P.R. Arany, A.S. Mao, D. Shvartsman, O.A. Ali, S.A. Bencherif, J. Rivera-Feliciano, and D.J. Mooney. Harnessing traction-mediated manipulation of the cell/matrix interface to control stem-cell fate. *Nature Materials*, 9(6):518–526, 2010.

[30] C.-Y.C. Huang, K.L. Hagar, L.E. Frost, Y. Sun, and H.S. Cheung. Effects of cyclic compressive loading on chondrogenesis of rabbit bone-marrow derived mesenchymal stem cells. *Stem Cells*, 22(3):313–323, 2004.

[31] J.J. Campbell, D.A. Lee, and D.L. Bader. Dynamic compressive strain influences chondrogenic gene expression in human mesenchymal stem cells. *Biorheology*, 43(3-4):455–470, 2006.

[32] S.D. Thorpe, C.T. Buckley, T. Vinardell, F.J. O'Brien, V.A. Campbell, and D.J. Kelly. Dynamic compression can inhibit chondrogenesis of mesenchymal stem cells. *Biochemical and Biophysical Research Communications*, 377(2):458–462, 2008.

[33] K. K. Papachroni, D. N. Karatzas, K. A. Papavassiliou, E. K. Basdra, and A. G. Papavassiliou. Mechanotransduction in osteoblast regulation and bone disease. *Trends Mol Med*, 15(5):208–216, May 2009.

[34] R.A. Stockwell. The cell density of human articular and costal cartilage. *Journal of Anatomy*, 101(4):753–763, 1967.

[35] D.R. Eyre. Collagen: Molecular diversity in the body's protein scaffold. *Science*, 207(4437):1315–1322, 1980.

[36] H. Muir. Proteoglycans as organizers of the intercellular matrix. *Biochemical Society Transactions*, 11(6):613–622, 1983.

[37] H. Silyn-Roberts and N.D. Broom. Fracture behaviour of cartilage-on-bone in response to repeated impact loading. *Connective Tissue Research*, 24(2):143–156, 1990.

[38] M.B. Schmidt, V.C. Mow, L.E. Chun, and D.R. Eyre. Effects of proteoglycan extraction on the tensile behavior of articular cartilage. *Journal of Orthopaedic Research*, 8(3):353–363, 1990.

[39] I.C. Clarke. Articular cartilage: a review and scanning electron microscope study. 1. the interterritorial fibrillar architecture. *Journal of Bone and Joint Surgery - Series B*, 53(4):732–750, 1971.

[40] H. Lipshitz, R. Etheredge III, and M.J. Glimcher. In vitro wear of articular cartilage. i. hydroxyproline, hexosamine, and amino acid composition of bovine articular cartilage

as a function of depth from the surface; hydroxyproline content of the lubricant and the wear debris as a measure of wear. *Journal of Bone and Joint Surgery - Series A*, 57(4):527–534, 1975.

[41] L.A. Setton, W. Zhu, and V.C. Mow. The biphasic poroviscoelastic behavior of articular cartilage: Role of the surface zone in governing the compressive behavior. *Journal of Biomechanics*, 26(4-5):581–592, 1993.

[42] R. Krishnan, S. Park, F. Eckstein, and G.A. Ateshian. Inhomogeneous cartilage properties enhance superficial interstitial fluid support and frictional properties, but do not provide a homogeneous state of stress. *Journal of Biomechanical Engineering*, 125(5):569–577, 2003.

[43] V.C. Mow, S.C. Proctor, and A. Ratcliffe. Structure and function of articular cartilage and meniscus. *Basic orthopaedic biomechanics*, V.C. Mow and W.C. Hayes. Philadelpia, PA; London, Lea and Febiger:113–117, 1997.

[44] T.E. Hardingham and H. Muir. Hyaluronic acid in cartilage and proteoglycan aggregation. *Biochemical Journal*, 139(3):565–581, 1974. cited By (since 1996)18.

[45] V.C. Hascall. Interaction of cartilage proteoglycans with hyaluronic acid. *Journal of Supramolecular and Cellular Biochemistry*, 7(1):101–120, 1977.

[46] H. Lipshitz, R. Etheredge III, and M.J. Glimcher. Changes in the hexosamine content and swelling ratio of articular cartilage as functions of depth from the surface. *Journal of Bone and Joint Surgery - Series A*, 58(8):1149–1153, 1976.

[47] F.C. Linn and L. Sokoloff. Movement and composition of interstitial fluid of cartilage. *Arthritis and rheumatism*, 8:481–494, 1965.

[48] W.M. Lai, J.S. Hou, and V.C. Mow. A triphasic theory for the swelling and deformation behaviors of articular cartilage. *Journal of Biomechanical Engineering*, 113(3):245–258, 1991.

[49] W.Y. Gu, W.M. Lai, and V.C. Mow. A mixture theory for charged-hydrated soft tissues containing multi- electrolytes: Passive transport and swelling behaviors. *Journal of Biomechanical Engineering*, 120(2):169–180, 1998.

[50] A. Maroudas. Biophysical chemistry of cartilaginous tissues with special reference to solute and fluid transport. *Biorheology*, 12(3-4):233–248, 1975.

[51] M.B. Albro, R.E. Banerjee, R. Li, S.R. Oungoulian, B. Chen, A.P. del Palomar, C.T. Hung, and G.A. Ateshian. Dynamic loading of immature epiphyseal cartilage pumps nutrients out of vascular canals. *Journal of Biomechanics*, 44(9):1654–1659, 2011.

[52] P.A. Torzilli, D.E. Rose, and D.A. Dethmers. Equilibrium water partition in articular cartilage. *Biorheology*, 19(4):519–537, 1982.

[53] G.A. Ateshian. The role of interstitial fluid pressurization in articular cartilage lubrication. *Journal of Biomechanics*, 42(9):1163–1176, 2009.

[54] M. Hlavacek and J. Novak. The role of synovial fluid filtration by cartilage in lubrication of synovial joints-iii. squeeze-film lubrication: Axial symmetry under low loading conditions. *Journal of Biomechanics*, 28(10):1193–1198, 1995.

[55] G.A. Ateshian. A theoretical formulation for boundary friction in articular cartilage. *Journal of Biomechanical Engineering*, 119(1):81–86, 1997.

[56] A. Maroudas. Balance between swelling pressure and collagen tension in normal and degenerate cartilage. *Nature*, 260(5554):808–809, 1976.

[57] L.A. Setton, H. Tohyama, and V.C. Mow. Swelling and curling behaviors of articular cartilage. *Journal of Biomechanical Engineering*, 120(3):355–361, 1998.

[58] V.C. Mow, M.H. Holmes, and W.M. Lai. Fluid transport and mechanical properties of articular cartilage: A review. *Journal of Biomechanics*, 17(5):377–394, 1984. cited By (since 1996)370.

[59] W.M. Lai and V.C. Mow. Drag-induced compression of articular cartilage during a permeation experiment. *Biorheology*, 17(1-2):111–123, 1980.

[60] N.K. Poppen and P.S. Walker. Forces at the glenohumeral joint in abduction. *Clinical Orthopaedics and Related Research*, NO. 135:165–170, 1978.

[61] W.A. Hodge, R.S. Fijan, K.L. Carlson, R.G. Burgess, W.H. Harris, and R.W. Mann. Contact pressures in the human hip joint measured in vivo. *Proceedings of the National Academy of Sciences of the United States of America*, 83(9):2879–2883, 1986.

[62] T.D. Brown and D.T. Shaw. In vitro contact stress distributions in the natural human hip. *Journal of Biomechanics*, 16(6):373–384, 1983.

[63] A.E. Anderson, B.J. Ellis, S.A. Maas, C.L. Peters, and J.A. Weiss. Validation of finite element predictions of cartilage contact pressure in the human hip joint. *Journal of Biomechanical Engineering*, 130(5), 2008.

[64] H. Kurosawa, T. Fukubayashi, and H. Nakajima. Load-bearing mode of the knee joint: Physical behavior of the knee joint with or without menisci. *Clinical Orthopaedics and Related Research*, NO 149:283–290, 1980.

[65] A.M. Ahmed and D.L. Burke. In-vitro measurement of static pressure distribution in synovial joints - part i: Tibial surface of the knee. *Journal of Biomechanical Engineering*, 105(3):216–225, 1983.

[66] H.H. Huberti and W.C. Hayes. Patellofemoral contact pressures. the influence of q-angle and tendofemoral contact. *Journal of Bone and Joint Surgery - Series A*, 66(5):715–724, 1984.

[67] L.S. Matthews, D.A. Sonstegard, and J.A. Henke. Load bearing characteristics of the patello-femoral joint. *Acta Orthopaedica*, 48(5):511–516, 1977.

[68] T. Macirowski, S. Tepic, and R.W. Mann. Cartilage stresses in the human hip joint. *Journal of Biomechanical Engineering*, 116(1):10–18, 1994.

[69] R.D. Coutts, R.L. Sah, and D. Amiel. Effects of growth factors on cartilage repair. *Instructional course lectures*, 46:487–494, 1997.

[70] J.A. Buckwalter. Articular cartilage: Injuries and potential for healing. *Journal of Orthopaedic and Sports Physical Therapy*, 28(4):192–202, 1998.

[71] E.B. Hunziker. Articular cartilage repair: Are the intrinsic biological constraints undermining this process insuperable? *Osteoarthritis and Cartilage*, 7(1):15–28, 1999. cited By (since 1996)216.

[72] E.B. Hunziker and E. Kapfinger. Removal of proteoglycans from the surface of defects in articular cartilage transiently enhances coverage by repair cells. *Journal of Bone and Joint Surgery - Series B*, 80(1):144–150, 1998. cited By (since 1996)66.

[73] P. D. Benya and J. D. Shaffer. Dedifferentiated chondrocytes reexpress the differentiated collagen phenotype when cultured in agarose gels. *Cell*, 30(1):215–224, Aug 1982.

[74] A. Barbero, S. Grogan, D. Schafer, M. Heberer, P. Mainil-Varlet, and I. Martin. Age related changes in human articular chondrocyte yield, proliferation and post-expansion chondrogenic capacity. *Osteoarthr. Cartil.*, 12(6):476–484, Jun 2004.

[75] T. Tallheden, C. Bengtsson, C. Brantsing, E. Sjogren-Jansson, L. Carlsson, L. Peterson, M. Brittberg, and A. Lindahl. Proliferation and differentiation potential of chondrocytes from osteoarthritic patients. *Arthritis Res. Ther.*, 7(3):R560–568, 2005.

[76] T. Aigner, S. Soder, P. M. Gebhard, A. McAlinden, and J. Haag. Mechanisms of disease: role of chondrocytes in the pathogenesis of osteoarthritis–structure, chaos and senescence. *Nat Clin Pract Rheumatol*, 3(7):391–399, Jul 2007.

[77] L. Duplomb, M. Dagouassat, P. Jourdon, and D. Heymann. Concise review: embryonic stem cells: a new tool to study osteoblast and osteoclast differentiation. *Stem Cells*, 25(3):544–552, Mar 2007.

[78] J. J. Minguell, A. Erices, and P. Conget. Mesenchymal stem cells. *Exp. Biol. Med. (Maywood)*, 226(6):507–520, Jun 2001.

[79] A. I. Caplan and S. P. Bruder. Mesenchymal stem cells: building blocks for molecular medicine in the 21st century. *Trends Mol Med*, 7(6):259–264, Jun 2001.

[80] P. Bianco, P. G. Robey, and P. J. Simmons. Mesenchymal stem cells: revisiting history, concepts, and assays. *Cell Stem Cell*, 2(4):313–319, Apr 2008.

[81] A. I. Caplan. All MSCs are pericytes? *Cell Stem Cell*, 3(3):229–230, Sep 2008.

[82] A. I. Caplan. Why are MSCs therapeutic? New data: new insight. *J. Pathol.*, 217(2):318–324, Jan 2009.

[83] B. Schmitt, J. Ringe, T. Haupl, M. Notter, R. Manz, G. R. Burmester, M. Sittinger, and C. Kaps. BMP2 initiates chondrogenic lineage development of adult human mesenchymal stem cells in high-density culture. *Differentiation*, 71(9-10):567–577, Dec 2003.

[84] G.D. Palmer, A. Steinert, A. Pascher, E. Gouze, J.-N. Gouze, O. Betz, B. Johnstone, C.H. Evans, and S.C. Ghivizzani. Gene-induced chondrogenesis of primary mesenchymal stem cells in vitro. *Molecular Therapy*, 12(2):219–228, 2005.

[85] B. de Crombrugghe, V. Lefebvre, R. R. Behringer, W. Bi, S. Murakami, and W. Huang. Transcriptional mechanisms of chondrocyte differentiation. *Matrix Biol.*, 19(5):389–394, Sep 2000.

[86] F. Barry, R. E. Boynton, B. Liu, and J. M. Murphy. Chondrogenic differentiation of mesenchymal stem cells from bone marrow: differentiation-dependent gene expression of matrix components. *Exp. Cell Res.*, 268(2):189–200, Aug 2001.

[87] R. L. Mauck, X. Yuan, and R. S. Tuan. Chondrogenic differentiation and functional maturation of bovine mesenchymal stem cells in long-term agarose culture. *Osteoarthr. Cartil.*, 14(2):179–189, Feb 2006.

[88] V. "Lefebvre and P. " Smits. "Transcriptional control of chondrocyte fate and differentiation". *"Birth Defects Res. C Embryo Today"*, 75(3):200–212, Sep 2005.

[89] B. K. "Hall and T. " Miyake. "All for one and one for all: condensations and the initiation of skeletal development". *Bioessays*, 22(2):138–147, Feb 2000.

[90] A. M. "DeLise, L. Fischer, and R. S. " Tuan. "Cellular interactions and signaling in cartilage development". *"Osteoarthr. Cartil."*, 8(5):309–334, Sep 2000.

[91] L. J. " "Sandell. "In situ expression of collagen and proteoglycan genes in notochord and during skeletal development and growth". *"Microsc. Res. Tech."*, 28(6):470–482, Aug 1994.

[92] P. "Smits, P. Li, J. Mandel, Z. Zhang, J. M. Deng, R. R. Behringer, B. de Crombrugghe, and V. " Lefebvre. "The transcription factors L-Sox5 and Sox6 are essential for cartilage formation". *"Dev. Cell"*, 1(2):277–290, Aug 2001.

[93] P. "Smits, P. Dy, S. Mitra, and V. " Lefebvre. "Sox5 and Sox6 are needed to develop and maintain source, columnar, and hypertrophic chondrocytes in the cartilage growth plate". *"J. Cell Biol."*, 164(5):747–758, 2004.

[94] R. Cancedda, B. Dozin, P. Giannoni, and R. Quarto. Tissue engineering and cell therapy of cartilage and bone. *Matrix Biol.*, 22(1):81–91, Mar 2003.

[95] J. Elisseeff, C. Puleo, F. Yang, and B. Sharma. Advances in skeletal tissue engineering with hydrogels. *Orthod Craniofac Res*, 8(3):150–161, Aug 2005.

[96] M.D. Buschmann, Y.A. Gluzband, A.J. Grodzinsky, J.H. Kimura, and E.B. Hunziker. Chondrocytes in agarose culture synthesize a mechanically functional extracellular matrix. *Journal of Orthopaedic Research*, 10(6):745–758, 1992.

[97] R.L. Mauck, B.A. Byers, X. Yuan, and R.S. Tuan. Regulation of cartilaginous ecm gene transcription by chondrocytes and mscs in 3d culture in response to dynamic loading. *Biomechanics and Modeling in Mechanobiology*, 6(1-2):113–125, 2007.

[98] S.D. Thorpe, C.T. Buckley, T. Vinardell, F.J. O'Brien, V.A. Campbell, and D.J. Kelly. The response of bone marrow-derived mesenchymal stem cells to dynamic compression following tgf-3 induced chondrogenic differentiation. *Annals of Biomedical Engineering*, 38(9):2896–2909, 2010.

[99] P. M. Freeman, R. N. Natarajan, J. H. Kimura, and T. P. Andriacchi. Chondrocyte cells respond mechanically to compressive loads. *J. Orthop. Res.*, 12(3):311–320, May 1994.

[100] E. G. Lima, L. Bian, K. W. Ng, R. L. Mauck, B. A. Byers, R. S. Tuan, G. A. Ateshian, and C. T. Hung. The beneficial effect of delayed compressive loading on tissue-engineered cartilage constructs cultured with TGF-beta3. *Osteoarthr. Cartil.*, 15(9):1025–1033, Sep 2007.

[101] K. Y. Lee and D. J. Mooney. Alginate: properties and biomedical applications. *Prog Polym Sci*, 37(1):106–126, Jan 2012.

[102] F. G. FISCHER and H. DORFEL. Polyuronic acids in brown algae. *Hoppe-Seyler's Z. Physiol. Chem.*, 302(4-6):186–203, Dec 1955.

[103] A. Haug and O. Smidsrod. FFractionation of alginic acid by precipitation with calcium and magnesium ions. *Acta Chem Scand.*, 13:601–603, 1959.

[104] H. H. Tonnesen and J. Karlsen. Alginate in drug delivery systems. *Drug Dev Ind Pharm*, 28(6):621–630, Jul 2002.

[105] M. George and T. E. Abraham. Polyionic hydrocolloids for the intestinal delivery of protein drugs: alginate and chitosan–a review. *J Control Release*, 114(1):1–14, Aug 2006.

[106] I. Braccini and S. Perez. Molecular basis of C(2+)-induced gelation in alginates and pectins: the egg-box model revisited. *Biomacromolecules*, 2(4):1089–1096, 2001.

[107] J.T. Connelly, A.J. Garcia, and M.E. Levenston. Interactions between integrin ligand density and cytoskeletal integrity regulate bmsc chondrogenesis. *Journal of Cellular Physiology*, 217(1):145–154, 2008.

[108] Y. Yao, L. Zeng, and Y. Huang. The enhancement of chondrogenesis of ATDC5 cells in RGD-immobilized microcavitary alginate hydrogels. *J Biomater Appl*, 31(1):92–101, Jul 2016.

[109] A. J. Steward, D. R. Wagner, and D. J. Kelly. Exploring the roles of integrin binding and cytoskeletal reorganization during mesenchymal stem cell mechanotransduction in soft and stiff hydrogels subjected to dynamic compression. *J Mech Behav Biomed Mater*, 38:174–182, Oct 2014.

[110] C. Ciobanasu, B. Faivre, and C. Le Clainche. Integrating actin dynamics, mechanotransduction and integrin activation: the multiple functions of actin binding proteins in focal adhesions. *Eur. J. Cell Biol.*, 92(10-11):339–348, 2013.

[111] T. Hennig, H. Lorenz, A. Thiel, K. Goetzke, A. Dickhut, F. Geiger, and W. Richter. Reduced chondrogenic potential of adipose tissue derived stromal cells correlates with an altered tgf receptor and bmp profile and is overcome by bmp-6. *Journal of Cellular Physiology*, 211(3):682–691, 2007.

[112] M.B. Mueller and R.S. Tuan. Functional characterization of hypertrophy in chondrogenesis of human mesenchymal stem cells. *Arthritis and Rheumatism*, 58(5):1377–1388, 2008.

[113] P.G. Bush, C.A. Parisinos, and A.C. Hall. The osmotic sensitivity of rat growth plate chondrocytes in situ; clarifying the mechanisms of hypertrophy. *Journal of Cellular Physiology*, 214(3):621–629, 2008.

[114] P.-H.G. Chao, A.C. West, and C.T. Hung. Chondrocyte intracellular calcium, cytoskeletal organization, and gene expression responses to dynamic osmotic loading. *American Journal of Physiology - Cell Physiology*, 291(4):C718–C725, 2006.

[115] E.J. Mackie, L. Tatarczuch, and M. Mirams. The skeleton: A multi-functional complex organ. the growth plate chondrocyte and endochondral ossification. *Journal of Endocrinology*, 211(2):109–121, 2011.

[116] F. Wang and Y. Zhu. Aquaporin-1: A potential membrane channel for facilitating the adaptability of rabbit nucleus pulposus cells to an extracellular matrix environment. *Journal of Orthopaedic Science*, 16(3):304–312, 2011.

[117] C.A. Hellingman, W. Koevoet, and G.J.V.M. Van Osch. Can one generate stable hyaline cartilage from adult mesenchymal stem cells? a developmental approach. *Journal of Tissue Engineering and Regenerative Medicine*, 6(10):e1–e11, 2012.

[118] M.A. Arnold, Y. Kim, M.P. Czubryt, D. Phan, J. McAnally, X. Qi, J.M. Shelton, J.A. Richardson, R. Bassel-Duby, and E.N. Olson. Mef2c transcription factor controls chondrocyte hypertrophy and bone development. *Developmental Cell*, 12(3):377–389, 2007.

[119] C.A. Yoshida, H. Yamamoto, T. Fujita, T. Furuichi, K. Ito, K.-I. Inoue, K. Yamana, A. Zanma, K. Takada, Y. Ito, and T. Komori. Runx2 and runx3 are essential for chondrocyte maturation, and runx2 regulates limb growth through induction of indian hedgehog. *Genes and Development*, 18(8):952–963, 2004.

[120] T.-G. Kwon, X. Zhao, Q. Yang, Y. Li, C. Ge, G. Zhao, and R.T. Franceschi. Physical and functional interactions between runx2 and hif-1 induce vascular endothelial growth factor gene expression. *Journal of Cellular Biochemistry*, 112(12):3582–3593, 2011.

[121] A.J. Fosang, K. Last, V. Knauper, G. Murphy, and P.J. Neame. Degradation of cartilage aggrecan by collagenase-3 (mmp-13). *FEBS Letters*, 380(1-2):17–20, 1996.

[122] H.C. Anderson. Matrix vesicles and calcification. *Current rheumatology reports*, 5(3):222–226, 2003.

[123] C.C. Van Donkelaar and R. Huiskes. The pthrp-ihh feedback loop in the embryonic growth plate allows pthrp to control hypertrophy and ihh to regulate proliferation. *Biomechanics and Modeling in Mechanobiology*, 6(1-2):55–62, 2007.

[124] J.P. Iannotti, S. Naidu, Y. Noguchi, R.M. Hunt, and C.T. Brighton. Growth plate matrix vesicle biogenesis: The role of intracellular calcium. *Clinical Orthopaedics and Related Research*, pages 222–229, 1994.

[125] N. Ortega, D.J. Behonick, and Z. Werb. Matrix remodeling during endochondral ossification. *Trends in Cell Biology*, 14(2):86–93, 2004.

[126] N. Ortega, D. Behonick, D. Stickens, and Z. Werb. How proteases regulate bone morphogenesis. *Annals of the New York Academy of Sciences*, 995:109–116, 2003.

[127] A. I. "Caplan and J. E. " Dennis. "Mesenchymal stem cells as trophic mediators". *"J. Cell. Biochem."*, 98(5):1076–1084, Aug 2006.

[128] S. E. "Haynesworth, M. A. Baber, and A. I. " Caplan. "Cytokine expression by human marrow-derived mesenchymal progenitor cells in vitro: effects of dexamethasone and IL-1 alpha". *"J. Cell. Physiol."*, 166(3):585–592, Mar 1996.

[129] J. "Chen, Y. Li, M. Katakowski, X. Chen, L. Wang, D. Lu, M. Lu, S. C. Gautam, and M. " Chopp. "Intravenous bone marrow stromal cell therapy reduces apoptosis and promotes endogenous cell proliferation after stroke in female rat". *"J. Neurosci. Res."*, 73(6):778–786, Sep 2003.

[130] Y. "Li, J. Chen, C. L. Zhang, L. Wang, D. Lu, M. Katakowski, Q. Gao, L. H. Shen, J. Zhang, M. Lu, and M. " Chopp. "Gliosis and brain remodeling after treatment of stroke in rats with marrow stromal cells". *"Glia"*, 49(3):407–417, Feb 2005.

[131] H. N. "Pak, M. Qayyum, D. T. Kim, A. Hamabe, Y. Miyauchi, M. C. Lill, M. Frantzen, K. Takizawa, L. S. Chen, M. C. Fishbein, B. G. Sharifi, P. S. Chen, and R. " Makkar. "Mesenchymal stem cell injection induces cardiac nerve sprouting and increased

tenascin expression in a Swine model of myocardial infarction". *"J. Cardiovasc. Electrophysiol."*, 14(8):841–848, Aug 2003.

[132] A. A. "Mangi, N. Noiseux, D. Kong, H. He, M. Rezvani, J. S. Ingwall, and V. J. " Dzau. "Mesenchymal stem cells modified with Akt prevent remodeling and restore performance of infarcted hearts". *"Nat. Med."*, 9(9):1195–1201, Sep 2003.

[133] Y. L. "Tang, Q. Zhao, Y. C. Zhang, L. Cheng, M. Liu, J. Shi, Y. Z. Yang, C. Pan, J. Ge, and M. I. " Phillips. "Autologous mesenchymal stem cell transplantation induce VEGF and neovascularization in ischemic myocardium". *"Regul. Pept."*, 117(1):3–10, Jan 2004.

[134] J. M. "Murphy, D. J. Fink, E. B. Hunziker, and F. P. " Barry. "Stem cell therapy in a caprine model of osteoarthritis". *"Arthritis Rheum."*, 48(12):3464–3474, Dec 2003.

[135] J. C. Haselgrove, I. M. Shapiro, and S. F. Silverton. Computer modeling of the oxygen supply and demand of cells of the avian growth cartilage. *Am. J. Physiol.*, 265(2 Pt 1):497–506, Aug 1993.

[136] M. C. Brahimi-Horn and J. Pouyssegur. Hypoxia in cancer cell metabolism and pH regulation. *Essays Biochem.*, 43:165–178, 2007.

[137] G. L. Semenza. HIF-1, O(2), and the 3 PHDs: how animal cells signal hypoxia to the nucleus. *Cell*, 107(1):1–3, Oct 2001.

[138] M. Kanichai, D. Ferguson, P. J. Prendergast, and V. A. Campbell. Hypoxia promotes chondrogenesis in rat mesenchymal stem cells: a role for AKT and hypoxia-inducible factor (HIF)-1alpha. *J. Cell. Physiol.*, 216(3):708–715, Sep 2008.

[139] J. C. Leijten, L. S. Moreira Teixeira, E. B. Landman, C. A. van Blitterswijk, and M. Karperien. Hypoxia inhibits hypertrophic differentiation and endochondral ossification in explanted tibiae. *PLoS ONE*, 7(11):e49896, 2012.

[140] K. Morita, T. Miyamoto, N. Fujita, Y. Kubota, K. Ito, K. Takubo, K. Miyamoto, K. Ninomiya, T. Suzuki, R. Iwasaki, M. Yagi, H. Takaishi, Y. Toyama, and T. Suda. Reactive oxygen species induce chondrocyte hypertrophy in endochondral ossification. *J. Exp. Med.*, 204(7):1613–1623, Jul 2007.

[141] J. Leijten, N. Georgi, L. Moreira Teixeira, C. A. van Blitterswijk, J. N. Post, and M. Karperien. Metabolic programming of mesenchymal stromal cells by oxygen tension directs chondrogenic cell fate. *Proc. Natl. Acad. Sci. U.S.A.*, 111(38):13954–13959, Sep 2014.

[142] D. Gawlitta, M. H. van Rijen, E. J. Schrijver, J. Alblas, and W. J. Dhert. Hypoxia impedes hypertrophic chondrogenesis of human multipotent stromal cells. *Tissue Eng Part A*, 18(19-20):1957–1966, Oct 2012.

[143] H. Green and O. Kehinde. Sublines of mouse 3t3 cells that accumulate lipid. *Cell*, 1(3):113–116, 1974.

[144] F.M. Gregoire, C.M. Smas, and H.S. Sul. Understanding adipocyte differentiation. *Physiological Reviews*, 78(3):783–809, 1998.

[145] A.E. Grigoriadis, J.N.M. Heersche, and J.E. Aubin. Differentiation of muscle, fat, cartilage, and bone from progenitor cells present in a bone-derived clonal cell population: Effect of dexamethasone. *Journal of Cell Biology*, 106(6):2139–2151, 1988.

[146] V.I. Sikavitsas, J.S. Temenoff, and A.G. Mikos. Biomaterials and bone mechanotransduction. *Biomaterials*, 22(19):2581–2593, 2001.

[147] A.M. Parfitt. Age-related structural changes in trabecular and cortical bone: Cellular mechanisms and biomechanical consequences. *Calcified Tissue International*, 36(1 Supplement):S123–S128, 1984.

[148] L. Gao, R. McBeath, and C.S. Chen. Stem cell shape regulates a chondrogenic versus myogenic fate through rac1 and n-cadherin. *Stem Cells*, 28(3):564–572, 2010. cited By (since 1996)121.

[149] C. Y. Tay, H. Yu, M. Pal, W. S. Leong, N. S. Tan, K. W. Ng, D. T. Leong, and L. P. Tan. Micropatterned matrix directs differentiation of human mesenchymal stem cells towards myocardial lineage. *Exp. Cell Res.*, 316(7):1159–1168, Apr 2010.

[150] Z. F. Lu, B. Zandieh Doulabi, C. L. Huang, R. A. Bank, and M. N. Helder. Beta1 integrins regulate chondrogenesis and rock signaling in adipose stem cells. *Biochem. Biophys. Res. Commun.*, 372(4):547–552, Aug 2008.

[151] S. D. Thorpe, C. T. Buckley, A. J. Steward, and D. J. Kelly. European Society of Biomechanics S.M. Perren Award 2012: the external mechanical environment can override the influence of local substrate in determining stem cell fate. *J Biomech*, 45(15):2483–2492, Oct 2012.

[152] D. S. Hwang, S. B. Sim, and H. J. Cha. Cell adhesion biomaterial based on mussel adhesive protein fused with RGD peptide. *Biomaterials*, 28(28):4039–4046, Oct 2007.

[153] H. Holtzer, J. Abbott, J. Lash, and S. Holtzer. The loss of phenotypic traits by differentiated cells in vitro. dedifferentiation of cartilage cells. *Proc. Natl. Acad. Sci. U.S.A.*, 46(12):1533–1542, Dec 1960.

[154] J. Abbott and H. Holtzer. The loss of phenotypic traits by differentiated cells. 3. The reversible behavior of chondrocytes in primary cultures. *J. Cell Biol.*, 28(3):473–487, Mar 1966.

[155] P. D. Benya and J. D. Shaffer. Dedifferentiated chondrocytes reexpress the differentiated collagen phenotype when cultured in agarose gels. *Cell*, 30(1):215–224, Aug 1982.

[156] P. Newman and F. M. Watt. Influence of cytochalasin D-induced changes in cell shape on proteoglycan synthesis by cultured articular chondrocytes. *Exp. Cell Res.*, 178(2):199–210, Oct 1988.

[157] N. C. Zanetti and M. Solursh. Induction of chondrogenesis in limb mesenchymal cultures by disruption of the actin cytoskeleton. *J. Cell Biol.*, 99(1 Pt 1):115–123, Jul 1984.

[158] G. M. Hoben and K. A. Athanasiou. Use of staurosporine, an actin-modifying agent, to enhance fibrochondrocyte matrix gene expression and synthesis. *Cell Tissue Res.*, 334(3):469–476, Dec 2008.

[159] S. H. McBride and M. L. Knothe Tate. Modulation of stem cell shape and fate A: the role of density and seeding protocol on nucleus shape and gene expression. *Tissue Eng Part A*, 14(9):1561–1572, Sep 2008.

[160] R. McBeath, D.M. Pirone, C.M. Nelson, K. Bhadriraju, and C.S. Chen. Cell shape, cytoskeletal tension, and rhoa regulate stem cell lineage commitment. *Developmental Cell*, 6(4):483–495, 2004.

[161] D. E. Ingber. The mechanochemical basis of cell and tissue regulation. *Mech Chem Biosyst*, 1(1):53–68, Mar 2004.

[162] W. H. Guo, M. T. Frey, N. A. Burnham, and Y. L. Wang. Substrate rigidity regulates the formation and maintenance of tissues. *Biophys. J.*, 90(6):2213–2220, Mar 2006.

[163] X. M. Wang, S. F. Yu, and Z. P. Yang. Apoptosis of osteoclast-like cells induced by alendronate is related to Fas gene expression. *Chin J Dent Res*, 3(2):26–32, Aug 2000.

[164] E. Hadjipanayi, R. A. Brown, and V. Mudera. Interface integration of layered collagen scaffolds with defined matrix stiffness: implications for sheet-based tissue engineering. *J Tissue Eng Regen Med*, 3(3):230–241, Mar 2009.

[165] A.J. Engler, S. Sen, H.L. Sweeney, and D.E. Discher. Matrix elasticity directs stem cell lineage specification. *Cell,* 126(4):677–689, 2006.

[166] K. Saha, A. J. Keung, E. F. Irwin, Y. Li, L. Little, D. V. Schaffer, and K. E. Healy. Substrate modulus directs neural stem cell behavior. *Biophys. J.*, 95(9):4426–4438, Nov 2008.

[167] J. S. Park, J. S. Chu, A. D. Tsou, R. Diop, Z. Tang, A. Wang, and S. Li. The effect of matrix stiffness on the differentiation of mesenchymal stem cells in response to TGF-Î. *Biomaterials*, 32(16):3921–3930, Jun 2011.

[168] G.J. Her, H.-C. Wu, M.-H. Chen, M.-Y. Chen, S.-C. Chang, and T.-W. Wang. Control of three-dimensional substrate stiffness to manipulate mesenchymal stem cell fate toward neuronal or glial lineages. *Acta Biomaterialia*, 9(2):5170–5180, 2013.

[169] A.S. Rowlands, P.A. George, and J.J. Cooper-White. Directing osteogenic and myogenic differentiation of mscs: Interplay of stiffness and adhesive ligand presentation. *American Journal of Physiology - Cell Physiology*, 295(4):C1037–C1044, 2008.

[170] O. Chaudhuri, L. Gu, D. Klumpers, M. Darnell, S.A. Bencherif, J.C. Weaver, N. Huebsch, H.-P. Lee, E. Lippens, G.N. Duda, and D.J. Mooney. Hydrogels with tunable stress relaxation regulate stem cell fate and activity. *Nature Materials*, 15(3):326–334, 2016.

[171] M.D. Buschmann, Y.A. Gluzband, A.J. Grodzinsky, and E.B. Hunziker. Mechanical compression modulates matrix biosynthesis in chondrocyte/agarose culture. *Journal of Cell Science*, 108(4):1497–1508, 1995.

[172] D.A. Lee and D.L. Bader. Compressive strains at physiological frequencies influence the metabolism of chondrocytes seeded in agarose. *Journal of Orthopaedic Research*, 15(2):181–188, 1997.

[173] D.A. Lee, T. Noguchi, M.M. Knight, L. O'Donnell, G. Bentley, and D.L. Bader. Response of chondrocyte subpopulations cultured within unloaded and loaded agarose. *Journal of Orthopaedic Research*, 16(6):726–733, 1998.

[174] D.A. Lee, T. Noguchi, S.P. Frean, P. Lees, and D.L. Bader. The influence of mechanical loading on isolated chondrocytes seeded in agarose constructs. *Biorheology*, 37(1-2):149–161, 2000.

[175] R.L. Mauck, M.A. Soltz, C.C.B. Wang, D.D. Wong, P.-H.G. Chao, W.B. Valhmu, C.T. Hung, and G.A. Ateshian. Functional tissue engineering of articular cartilage through

dynamic loading of chondrocyte-seeded agarose gels. *Journal of Biomechanical Engineering*, 122(3):252–260, 2000.

[176] O. Demarteau, D. Wendt, A. Braccini, M. Jakob, D. Schäfer, M. Heberer, and I. Martin. Dynamic compression of cartilage constructs engineered from expanded human articular chondrocytes. *Biochemical and Biophysical Research Communications*, 310(2):580–588, 2003.

[177] E.G. Lima, L. Bian, K.W. Ng, R.L. Mauck, B.A. Byers, R.S. Tuan, G.A. Ateshian, and C.T. Hung. The beneficial effect of delayed compressive loading on tissue-engineered cartilage constructs cultured with tgf-β_3. *Osteoarthritis and Cartilage*, 15(9):1025–1033, 2007.

[178] S.J. Millward-Sadler and D.M. Salter. Integrin-dependent signal cascades in chondrocyte mechanotransduction. *Annals of Biomedical Engineering*, 32(3):435–446, 2004.

[179] D.R. Haudenschild, D.D. D'Lima, and M.K. Lotz. Dynamic compression of chondrocytes induces a rho kinase-dependent reorganization of the actin cytoskeleton. *Biorheology*, 45(3-4):219–228, 2008.

[180] C. Y. Huang, K. L. Hagar, L. E. Frost, Y. Sun, and H. S. Cheung. Effects of cyclic compressive loading on chondrogenesis of rabbit bone-marrow derived mesenchymal stem cells. *Stem Cells*, 22(3):313–323, 2004.

[181] C.-Y.C. Huang, P.M. Reuben, and H.S. Cheung. Temporal expression patterns and corresponding protein inductions of early responsive genes in rabbit bone marrow-derived mesenchymal stem cells under cyclic compressive loading. *Stem Cells*, 23(8):1113–1121, 2005.

[182] D. Pelaez, C.-Y. Charles Huang, and H.S. Cheung. Cyclic compression maintains viability and induces chondrogenesis of human mesenchymal stem cells in fibrin gel scaffolds. *Stem Cells and Development*, 18(1):93–102, 2009.

[183] D. Pelaez, N. Arita, and H.S. Cheung. Extracellular signal-regulated kinase (erk) dictates osteogenic and/or chondrogenic lineage commitment of mesenchymal stem cells under dynamic compression. *Biochemical and Biophysical Research Communications*, 417(4):1286–1291, 2012.

[184] J.D. Kisiday, D.D. Frisbie, C.W. McIlwraith, and A.J. Grodzinsky. Dynamic compression stimulates proteoglycan synthesis by mesenchymal stem cells in the absence of chondrogenic cytokines. *Tissue Engineering - Part A*, 15(10):2817–2824, 2009.

[185] H. Zahedmanesh, M. Stoddart, P. Lezuo, C. Forkmann, M.A. Wimmmer, M. Alini, and H. Van Oosterwyck. Deciphering mechanical regulation of chondrogenesis in fibrin-polyurethane composite scaffolds enriched with human mesenchymal stem cells: A dual computational and experimental approach. *Tissue Engineering - Part A*, 20(7-8):1197–1212, 2014.

[186] N.J. Steinmetz and S.J. Bryant. The effects of intermittent dynamic loading on chondrogenic and osteogenic differentiation of human marrow stromal cells encapsulated in rgd-modified poly(ethylene glycol) hydrogels. *Acta Biomaterialia*, 7(11):3829–3840, 2011.

[187] P. Angele, D. Schumann, M. Angele, B. Kinner, G. Englert, R. Hente, B. Füchtmeier, M. Nerlich, C. Neumann, and R. Kujat. Cyclic, mechanical compression enhances chondrogenesis of mesenchymal progenitor cells in tissue engineering scaffolds. *Biorheology*, 41(3-4):335–346, 2004.

[188] J.K. Mouw, J.T. Connelly, C.G. Wilson, K.E. Michael, and M.E. Levenston. Dynamic compression regulates the expression and synthesis of chondrocyte-specific matrix molecules in bone marrow stromal cells. *Stem Cells*, 25(3):655–663, 2007.

[189] Z. Li, L. Kupcsik, S.-J. Yao, M. Alini, and M.J. Stoddart. Chondrogenesis of human bone marrow mesenchymal stem cells in fibrin-polyurethane composites. *Tissue Engineering - Part A*, 15(7):1729–1737, 2009.

[190] S.D. Thorpe, T. Nagel, S.F. Carroll, and D.J. Kelly. Modulating gradients in regulatory signals within mesenchymal stem cell seeded hydrogels: A novel strategy to engineer zonal articular cartilage. *PLoS ONE*, 8(4), 2013.

[191] N. J. Steinmetz, E. A. Aisenbrey, K. K. Westbrook, H. J. Qi, and S. J. Bryant. Mechanical loading regulates human MSC differentiation in a multi-layer hydrogel for osteochondral tissue engineering. *Acta Biomater*, 21:142–153, Jul 2015.

[192] F. Guilak, A. Ratcliffe, and V.C. Mow. Chondrocyte deformation and local tissue strain in articular cartilage: A confocal microscopy study. *Journal of Orthopaedic Research*, 13(3):410–421, 1995.

[193] D.L. Zignego, A.A. Jutila, M.K. Gelbke, D.M. Gannon, and R.K. June. The mechanical microenvironment of high concentration agarose for applying deformation to primary chondrocytes. *Journal of Biomechanics*, 47(9):2143–2148, 2014.

[194] Enda P. Dowling, William Ronan, and J. Patrick McGarry. Computational investigation of in situ chondrocyte deformation and actin cytoskeleton remodelling under physiological loading. *Acta Biomaterialia*, 9(4):5943 – 5955, 2013.

[195] J.M. Hootman and C.G. Helmick. Projections of us prevalence of arthritis and associated activity limitations. *Arthritis and Rheumatism*, 54(1):226–229, 2006.

[196] A.J. Sophia Fox, A. Bedi, and S.A. Rodeo. The basic science of articular cartilage: Structure, composition, and function. *Sports Health*, 1(6):461–468, 2009.

[197] H.J. Mankin. The response of articular cartilage to mechanical injury. *Journal of Bone and Joint Surgery - Series A*, 64(3):460–466, 1982.

[198] M. Brittberg, A. Lindahl, A. Nilsson, C. Ohlsson, O. Isaksson, and L. Peterson. Treatment of deep cartilage defects in the knee with autologous chondrocyte transplantation. *New England Journal of Medicine*, 331(14):889–895, 1994.

[199] L. Peterson, H.S. Vasiliadis, M. Brittberg, and A. Lindahl. Autologous chondrocyte implantation: A long-term follow-up. *American Journal of Sports Medicine*, 38(6):1117–1124, 2010.

[200] A. Barbero, S. Grogan, D. Schäfer, M. Heberer, P. Mainil-Varlet, and I. Martin. Age related changes in human articular chondrocyte yield, proliferation and post-expansion chondrogenic capacity. *Osteoarthritis and Cartilage*, 12(6):476–484, 2004.

[201] M. Iwasaki, K. Nakata, H. Nakahara, T. Nakase, T. Kimura, K. Kimata, A.I. Caplan, and K. Ono. Transforming growth factor-1 stimulates chondrogenesis and inhibits osteogenesis in high density culture of periosteum-derived cells. *Endocrinology*, 132(4):1603–1608, 1992.

[202] A.M. Mackay, S.C. Beck, J.M. Murphy, F.P. Barry, C.O. Chichester, and M.F. Pittenger. Chondrogenic differentiation of cultured human mesenchymal stem cells from marrow. *Tissue Engineering*, 4(4):415–428, 1998.

[203] K. Nishimura, L.A. Solchaga, A.I. Caplan, J.U. Yoo, V.M. Goldberg, and B. Johnstone. Chondroprogenitor cells of synovial tissue. *Arthritis and Rheumatism*, 42(12):2631–2637, 1999.

[204] J.U. Yoo, T.S. Barthel, K. Nishimura, L. Solchaga, A.I. Caplan, V.M. Goldberg, and B. Johnstone. The chondrogenic potential of human bone-marrow-derived mesenchymal progenitor cells. *Journal of Bone and Joint Surgery - Series A*, 80(12):1745–1757, 1998.

[205] R.M. Coleman, N.D. Case, and R.E. Guldberg. Hydrogel effects on bone marrow stromal cell response to chondrogenic growth factors. *Biomaterials*, 28(12):2077–2086, 2007.

[206] I.E. Erickson, A.H. Huang, C. Chung, R.T. Li, J.A. Burdick, and R.L. Mauck. Differential maturation and structure-function relationships in mesenchymal stem cell- and chondrocyte-seeded hydrogels. *Tissue Engineering - Part A*, 15(5):1041–1052, 2009.

[207] J.D. Kisiday, P.W. Kopesky, C.H. Evans, A.J. Grodzinsky, C.W. McIlwraith, and D.D. Frisbie. Evaluation of adult equine bone marrow- and adipose-derived progenitor cell chondrogenesis in hydrogel cultures. *Journal of Orthopaedic Research*, 26(3):322–331, 2008.

[208] R.L. Mauck, X. Yuan, and R.S. Tuan. Chondrogenic differentiation and functional maturation of bovine mesenchymal stem cells in long-term agarose culture. *Osteoarthritis and Cartilage*, 14(2):179–189, 2006.

[209] C.G. Williams, T.K. Kim, A. Taboas, A. Malik, P. Manson, and J. Elisseeff. In vitro chondrogenesis of bone marrow-derived mesenchymal stem cells in a photopolymerizing hydrogel. *Tissue Engineering*, 9(4):679–688, 2003.

[210] T. Davisson, S. Kunig, A. Chen, R. Sah, and A. Ratcliffe. Static and dynamic compression modulate matrix metabolism in tissue engineered cartilage. *Journal of Orthopaedic Research*, 20(4):842–848, 2002.

[211] A.J. Grodzinsky, M.E. Levenston, M. Jin, and E.H. Frank. Cartilage tissue remodeling in response to mechanical forces. *Annual Review of Biomedical Engineering*, 2(2000):691–713, 2000.

[212] Y.J. Kim, R.L.Y. Sah, A.J. Grodzinsky, A.H.K. Plaas, and J.D. Sandy. Mechanical regulation of cartilage biosynthetic behavior: Physical stimuli. *Archives of Biochemistry and Biophysics*, 311(1):1–12, 1994.

[213] M.J. Palmoski and K.D. Brandt. Effects of static and cyclic compressive loading on articular cartilage plugs in vitro. *Arthritis and Rheumatism*, 27(6):675–681, 1984.

[214] S.-H. Park, Y.S. Woo, W.P. Sin, S.Y. Sang, H.C. Byung, R.P. So, K. Park, and B.-H. Min. An electromagnetic compressive force by cell exciter stimulates chondrogenic differentiation of bone marrow-derived mesenchymal stem cells. *Tissue Engineering*, 12(11):3107–3117, 2006.

[215] V. Terraciano, N. Hwang, L. Moroni, B.P. Hyung, Z. Zhang, J. Mizrahi, D. Seliktar, and J. Elisseeff. Differential response of adult and embryonic mesenchymal progenitor cells to mechanical compression in hydrogels. *Stem Cells*, 25(11):2730–2738, 2007.

[216] I.C. Bonzani, J.J. Campbell, M.M. Knight, A. Williams, D.A. Lee, D.L. Bader, and M.M. Stevens. Dynamic compressive strain influences chondrogenic gene expression in human periosteal cells: A case study. *Journal of the Mechanical Behavior of Biomedical Materials*, 11:72–81, 2012.

[217] N. Ohashi, A.G. Robling, D.B. Burr, and C.H. Turner. The effects of dynamic axial loading on the rat growth plate. *Journal of Bone and Mineral Research*, 17(2):284–292, 2002.

[218] L.E. Claes and C.A. Heigele. Magnitudes of local stress and strain along bony surfaces predict the course and type of fracture healing. *Journal of Biomechanics*, 32(3):255–266, 1999.

[219] Y. J. Kim, R. L. Sah, J. Y. Doong, and A. J. Grodzinsky. Fluorometric assay of DNA in cartilage explants using Hoechst 33258. *Anal. Biochem.*, 174(1):168–176, Oct 1988.

[220] W. Kafienah and T. J. Sims. Biochemical methods for the analysis of tissue-engineered cartilage. *Methods Mol. Biol.*, 238:217–230, 2004.

[221] A. H. Huang, M. J. Farrell, M. Kim, and R. L. Mauck. Long-term dynamic loading improves the mechanical properties of chondrogenic mesenchymal stem cell-laden hydrogel. *Eur Cell Mater*, 19:72–85, Feb 2010.

[222] C. B. Horner, K. Hirota, J. Liu, M. Maldonado, B. H. Park, and J Nam. Magnitude-Dependent and Inversely-related Osteogenic/Chondrogenic Differentiation of Human Mesenchymal Stem Cells Under Dynamic Compressive Strain. *J Tissue Eng Regen Med*, Sep, 2016.

[223] A. R. Cameron, J. E. Frith, and J. J. Cooper-White. The influence of substrate creep on mesenchymal stem cell behaviour and phenotype. *Biomaterials*, 32(26):5979–5993, Sep 2011.

[224] M. Guvendiren and J. A. Burdick. Stiffening hydrogels to probe short- and long-term cellular responses to dynamic mechanics. *Nat Commun*, 3:792, 2012.

[225] S. Khetan, M. Guvendiren, W. R. Legant, D. M. Cohen, C. S. Chen, and J. A. Burdick. Degradation-mediated cellular traction directs stem cell fate in covalently crosslinked three-dimensional hydrogels. *Nat Mater*, 12(5):458–465, May 2013.

[226] C. Yang, M. W. Tibbitt, L. Basta, and K. S. Anseth. Mechanical memory and dosing influence stem cell fate. *Nat Mater*, 13(6):645–652, Jun 2014.

[227] A. J. "Steward, D. R. Wagner, and D. J. " Kelly. "The pericellular environment regulates cytoskeletal development and the differentiation of mesenchymal stem cells and determines their response to hydrostatic pressure". *"Eur Cell Mater"*, 25:167 − 178, Feb 2013.

[228] O. Jeon, K. H. Bouhadir, J. M. Mansour, and E. Alsberg. Photocrosslinked alginate hydrogels with tunable biodegradation rates and mechanical properties. *Biomaterials*, 30(14):2724–2734, May 2009.

[229] S. C. Tan, C. A. Carr, K. K. Yeoh, C. J. Schofield, K. E. Davies, and K. Clarke. Identification of valid housekeeping genes for quantitative RT-PCR analysis of cardiosphere-derived cells preconditioned under hypoxia or with prolyl-4-hydroxylase inhibitors. *Mol. Biol. Rep.*, 39(4):4857–4867, Apr 2012.

[230] L. Bian, C. Hou, E. Tous, R. Rai, R. L. Mauck, and J. A. Burdick. The influence of hyaluronic acid hydrogel crosslinking density and macromolecular diffusivity on human MSC chondrogenesis and hypertrophy. *Biomaterials*, 34(2):413–421, Jan 2013.

[231] A.J. Steward, D.J. Kelly, and D.R. Wagner. Purinergic signaling regulates the transforming growth factor-β_3-induced chondrogenic response of mesenchymal stem cells to hydrostatic pressure. *Tissue Engineering - Part A*, 22(11-12):831–839, 2016.

[232] E. A. Aisenbrey and S. J. Bryant. Mechanical loading inhibits hypertrophy in chondrogenically differentiating hmscs within a biomimetic hydrogel. *J. Mater. Chem. B*, 4:3562–3574, 2016.

[233] S. J. Bryant, T. T. Chowdhury, D. A. Lee, D. L. Bader, and K. S. Anseth. Crosslinking density influences chondrocyte metabolism in dynamically loaded photocrosslinked poly(ethylene glycol) hydrogels. *Ann Biomed Eng*, 32(3):407–417, Mar 2004.

[234] shaped osteochondral constructs for articular cartilage repair. Anatomically shaped osteochondral constructs for articular cartilage repair. *J Biomech*, 36(12):1853–1864, Dec 2003.

[235] T. Gotterbarm, W. Richter, M. Jung, S. Berardi Vilei, P. Mainil-Varlet, T. Yamashita, and S. J. Breusch. An in vivo study of a growth-factor enhanced, cell free, two-layered collagen-tricalcium phosphate in deep osteochondral defects. *Biomaterials*, 27(18):3387–3395, Jun 2006.

[236] G. I. Im, J. H. Ahn, S. Y. Kim, B. S. Choi, and S. W. Lee. A hyaluronate-atelocollagen/beta-tricalcium phosphate-hydroxyapatite biphasic scaffold for the repair of osteochondral defects: a porcine study. *Tissue Eng Part A*, 16(4):1189–1200, Apr 2010.

[237] P. Duan, Z. Pan, L. Cao, Y. He, H. Wang, Z. Qu, J. Dong, and J. Ding. The effects of pore size in bilayered poly(lactide-co-glycolide) scaffolds on restoring osteochondral defects in rabbits. *J Biomed Mater Res A*, 102(1):180–192, Jan 2014.

[238] N. Mohan, V. Gupta, B. Sridharan, A. Sutherland, and M. S. Detamore. The potential of encapsulating "raw materials" in 3D osteochondral gradient scaffolds. *Biotechnol. Bioeng.*, 111(4):829–841, Apr 2014.

[239] S. Lu, J. Lam, J. E. Trachtenberg, E. J. Lee, H. Seyednejad, J. J. van den Beucken, Y. Tabata, M. E. Wong, J. A. Jansen, A. G. Mikos, and F. K. Kasper. Dual growth factor delivery from bilayered, biodegradable hydrogel composites for spatially-guided osteochondral tissue repair. *Biomaterials*, 35(31):8829–8839, Oct 2014.

[240] C. J. Needham, S. R. Shah, R. L. Dahlin, L. A. Kinard, J. Lam, B. M. Watson, S. Lu, F. K. Kasper, and A. G. Mikos. Osteochondral tissue regeneration through polymeric delivery of DNA encoding for the SOX trio and RUNX2. *Acta Biomater*, 10(10):4103–4112, Oct 2014.

[241] W. S. Toh, C. B. Foldager, J. H. Hui, B. R. Olsen, and M. Spector. Exploiting Stem Cell-Extracellular Matrix Interactions for Cartilage Regeneration: A Focus on Basement Membrane Molecules. *Curr Stem Cell Res Ther*, Jul 2015.

[242] S. V. Murphy and A. Atala. 3D bioprinting of tissues and organs. *Nat. Biotechnol.*, 32(8):773–785, Aug 2014.

[243] A. D. Olubamiji, Z. Izadifar, J. L. Si, D. M. Cooper, B. F. Eames, and D. X. Chen. Modulating mechanical behaviour of 3D-printed cartilage-mimetic PCL scaffolds: influence of molecular weight and pore geometry. *Biofabrication*, 8(2):20–25, Jun 2016.

[244] T. Mesallati, E. J. Sheehy, T. Vinardell, C. T. Buckley, and D. J. Kelly. Tissue engineering scaled-up, anatomically shaped osteochondral constructs for joint resurfacing. *Eur Cell Mater*, 30, 2015.

[245] E. Farrell, S. K. Both, K. I. Odorfer, W. Koevoet, N. Kops, F. J. O'Brien, R. J. Baatenburg de Jong, J. A. Verhaar, V. Cuijpers, J. Jansen, R. G. Erben, and G. J. van Osch. In-vivo generation of bone via endochondral ossification by in-vitro chondrogenic priming of adult human and rat mesenchymal stem cells. *BMC Musculoskelet Disord*, 12, 2011.

[246] S. Khetan, M. Guvendiren, W. R. Legant, D. M. Cohen, C. S. Chen, and J. A. Burdick. Degradation-mediated cellular traction directs stem cell fate in covalently crosslinked three-dimensional hydrogels. *Nat Mater*, 12(5):458–465, May 2013.

Appendix A: Bioreactor Design

A.1   Dynamic Compression Bioreactor

T HIS was a design task that extended on from an undergraduate final year project (fig. A.1).
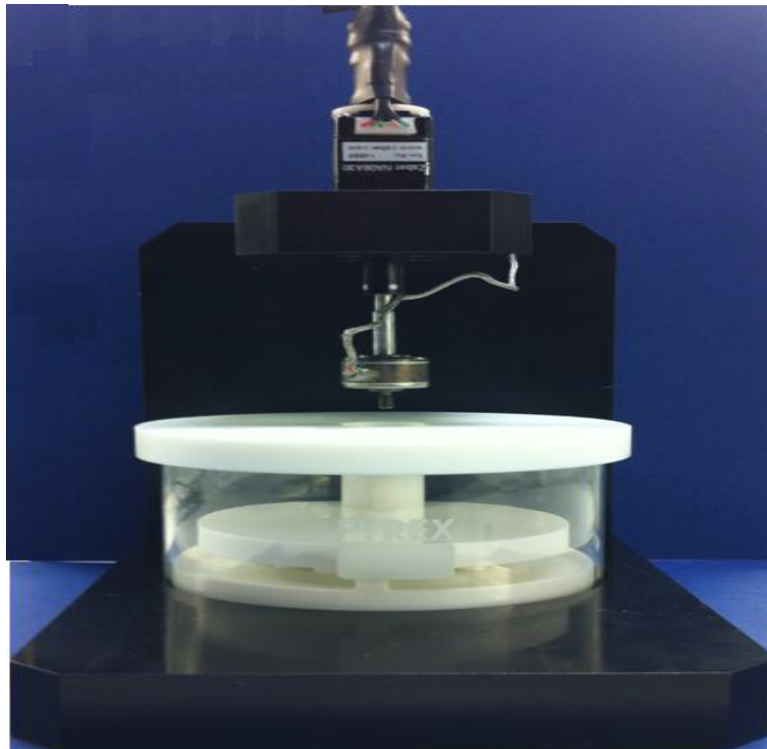

Figure A.1 Original bioreactor system developed in 2012 during an undergraduate final year project.

The actuator system, load cell coupling mechanism and bioreactor culture dish design has since been updated to enhance usability and optimise culturing conditions for repeatable results (fig. A.2).
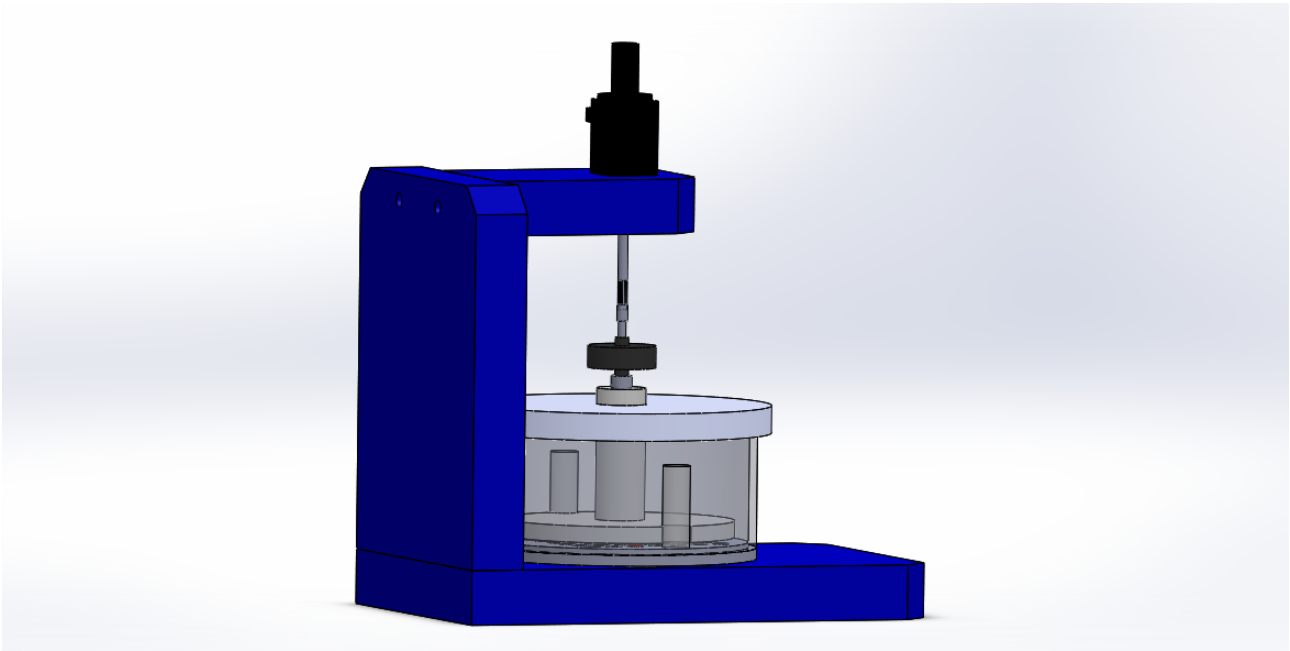
Figure A.2 Solidwork 3-D model of compression bioreactor.

A.2   Design

The following assembly and parts within were designed, technically drawn and machined to specification before being sterilised and used in experiments.

A.2.1   Rig

Function: Base for holding bioreactor dish in alignment with actuator that was held in suspension above the dish.

Material: Black ertalyte machined from cubic block. M4 tapped three times for frame base to back connection. M1 tapped for actuator holder.
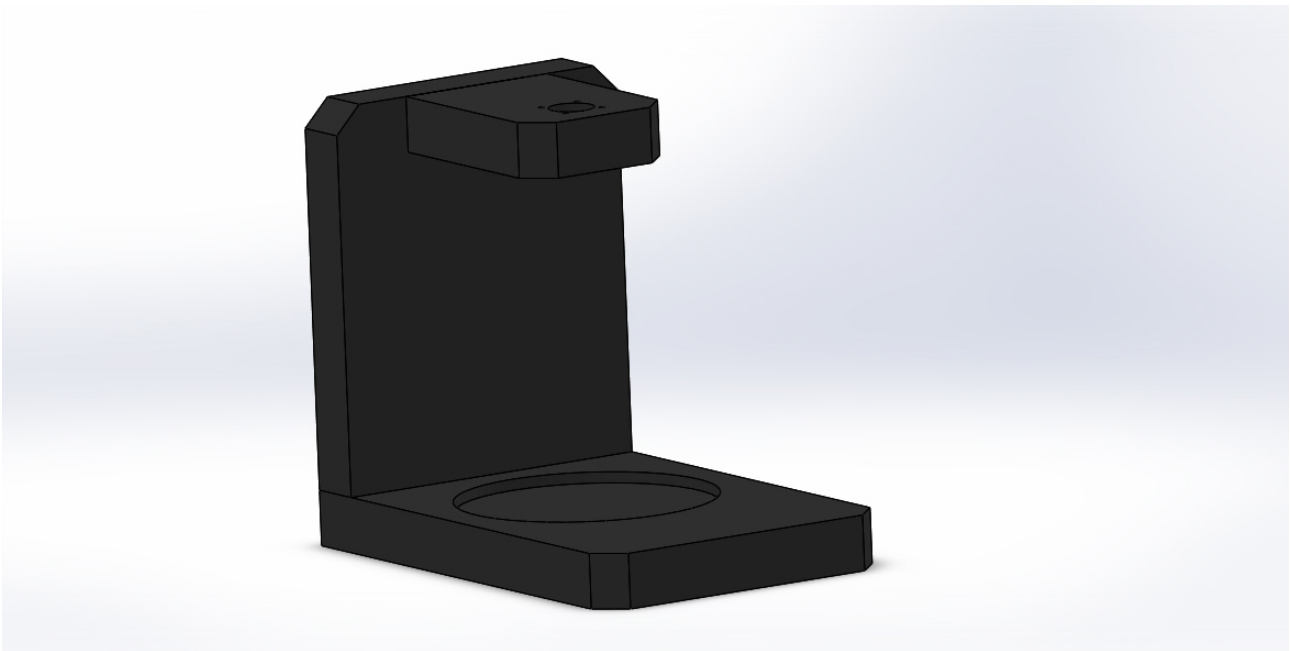
Figure A.3 Solidwork 3-D model of compression bioreactor rig assembly used to place and hold parts.

A.2.1.1 Frame Back
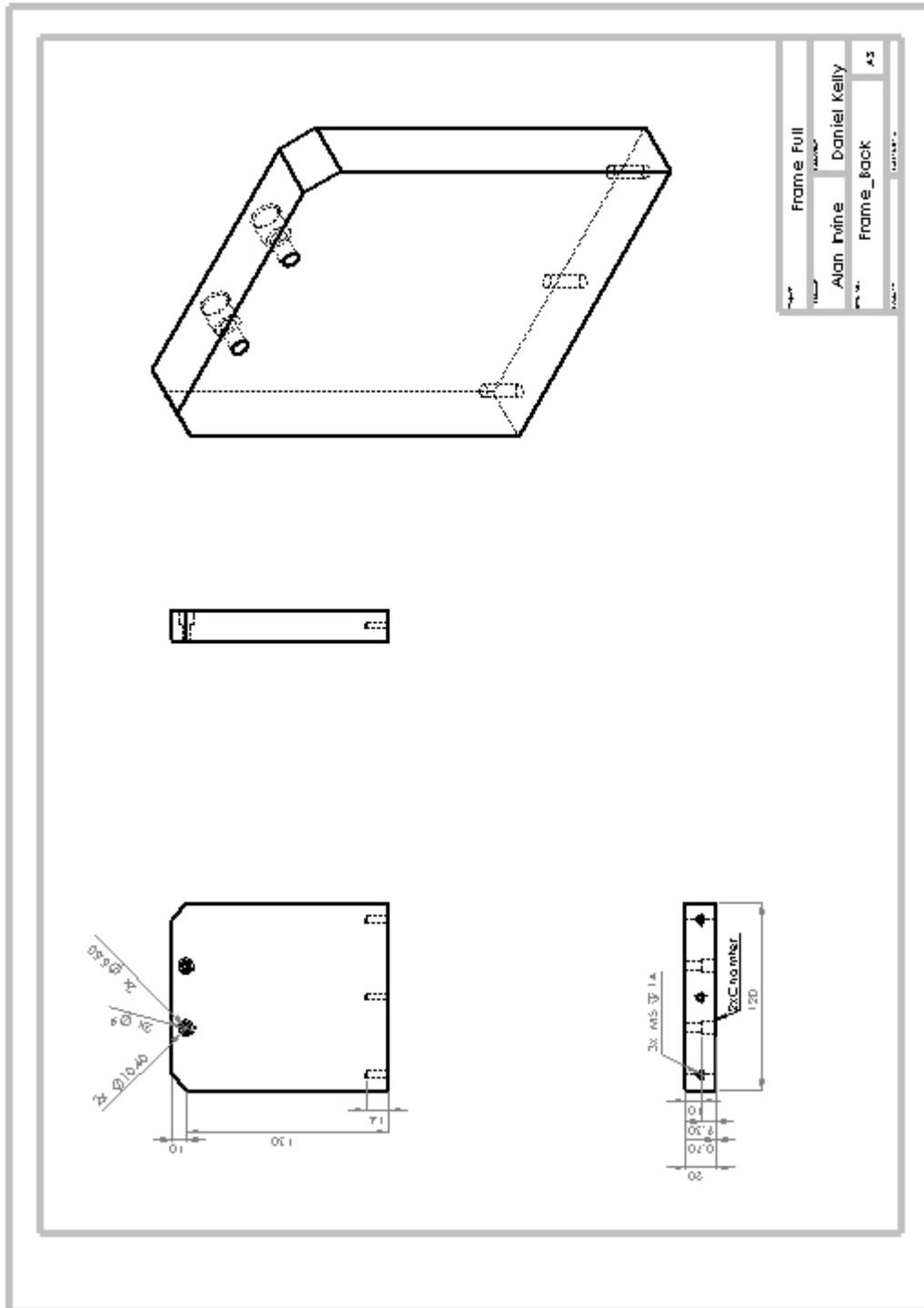
Figure A.4 Technical drawings for the back of the rig frame.

A.2.1.2   Frame Base
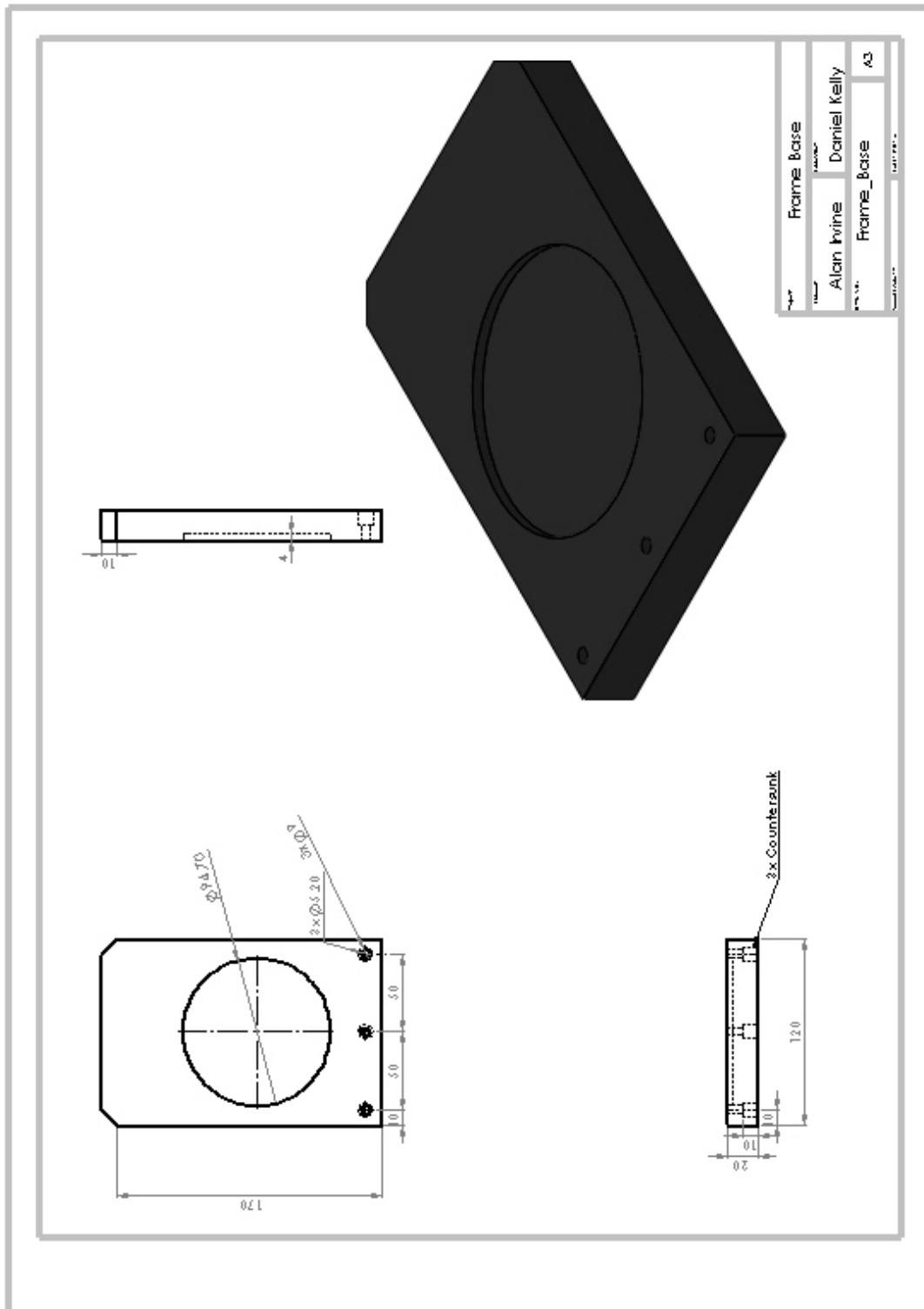
Figure A.5 Technical drawings for the frame base.

A.2.1.3 Actuator Holder
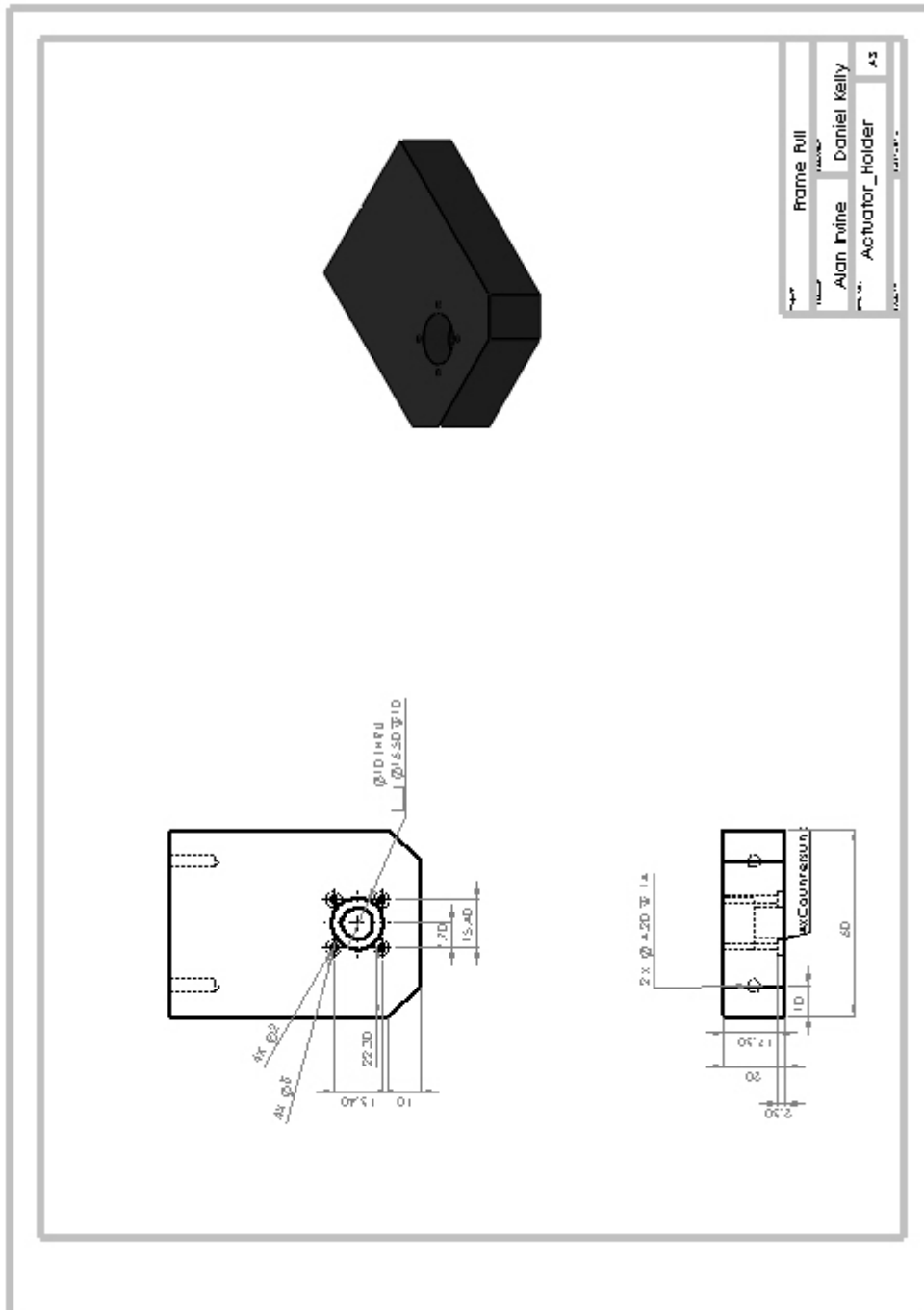
Figure A.6 Technical drawings for the actuator holding section of the rig frame.

A.2.2   Actuator

Function: Linear motor driven actuator bought from Laser2000 and made by Zaber. Model: NA08A30. Driven by controller purchased similarly. Matlab script developed to initiate commands and loading cycles.
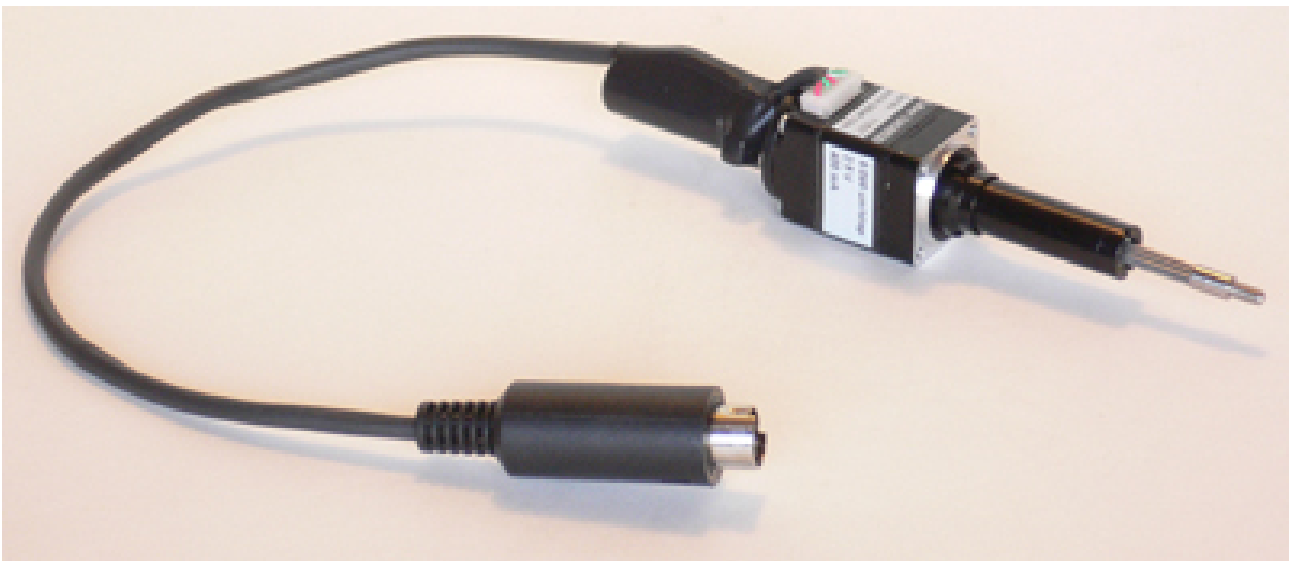
Figure A.7 Zaber NA08A30 linear, motor-driven actuator.

Matlab script developed a graphic usage interface based control system of the actuator system and load cell measurements.
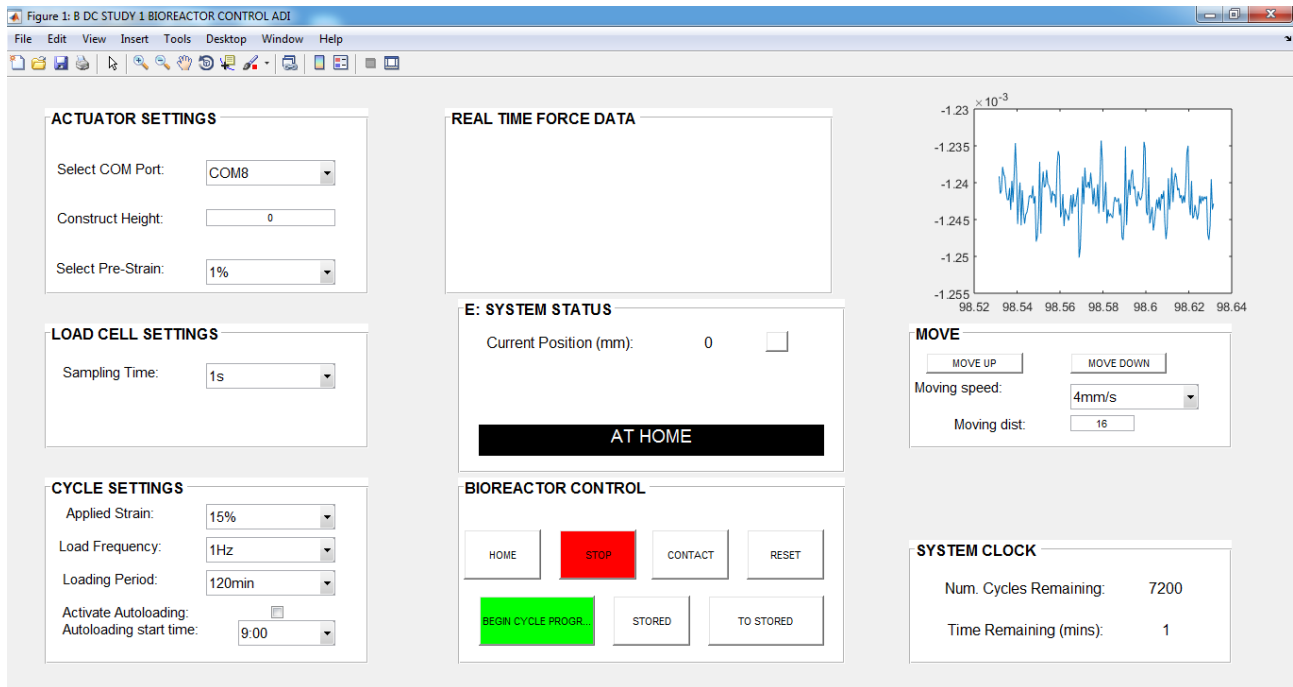
Figure A.8 Matlab controller and script section.

A.2.3   Bioreactor Dish

Function: To aseptically house MSC-laden hydrogel constructs on a stable, flat surface and enable the actuation of the platen to develop dynamic compression unto the constructs.

Materials: White ertalyte base machined from cylindrical block. Similarly white ertalyte for lid and platen machined pieces.

Walls UV cured to base ertylate plate.

Polycarbonate tubing 100mm diameter for dish walls.

Polycarbonate 10mm rod cut for guide posts also UV cured to base insert.
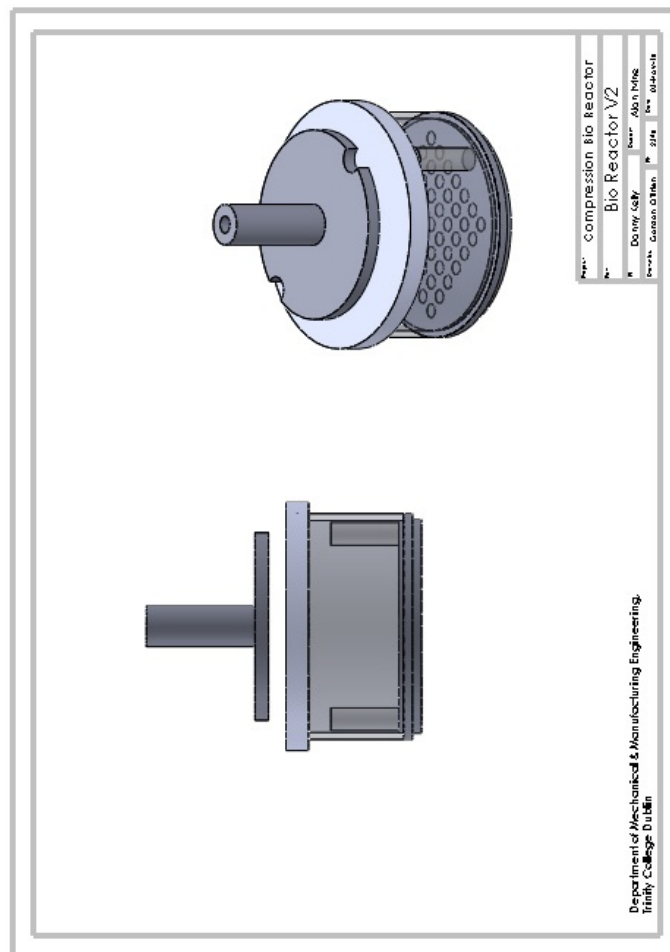
Figure A.9 Solidworks 3-D model of the bioreactor dish.

A.2.3.1 Base
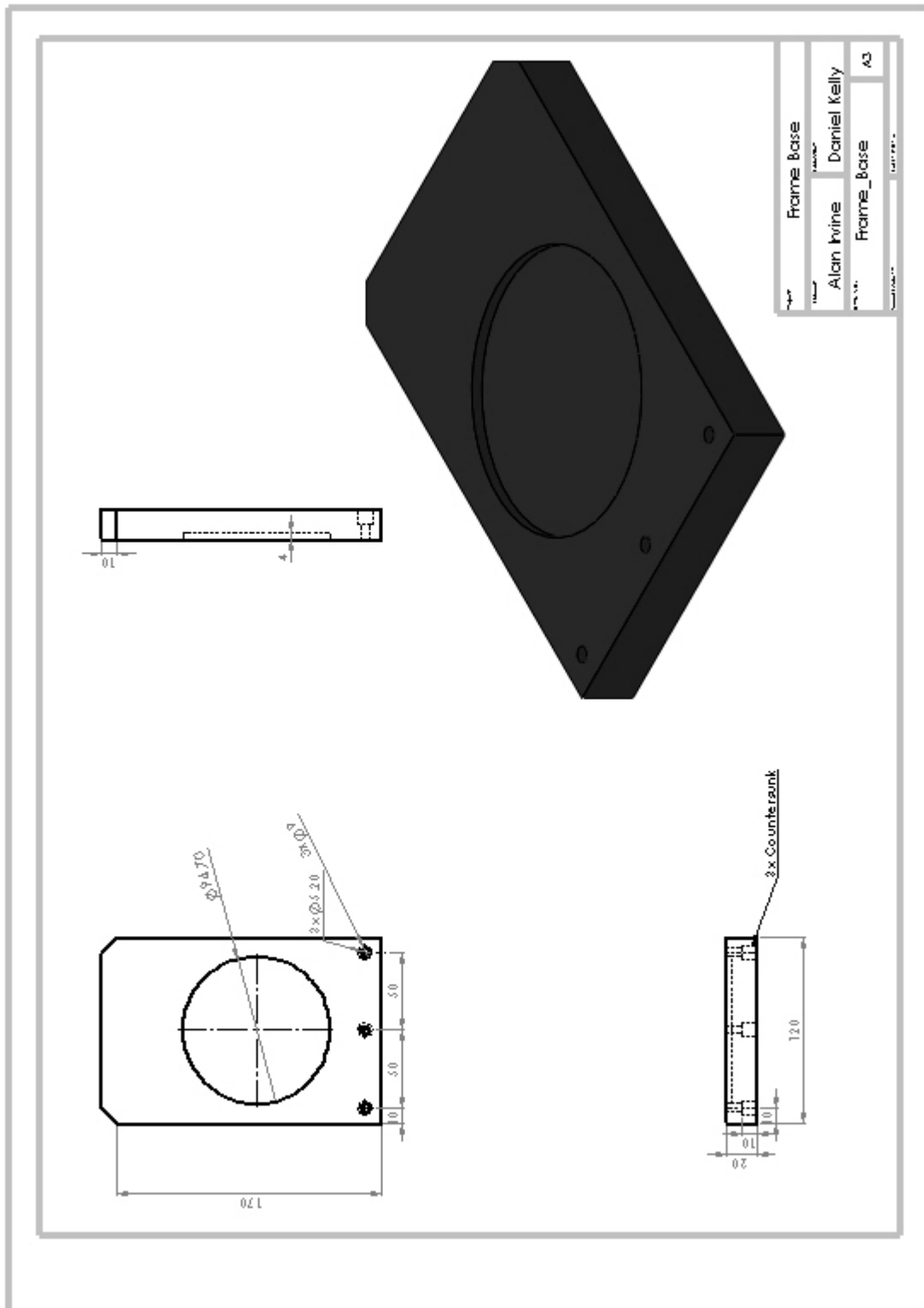
Figure A.10 Technical drawings for the dish base.

A.2.3.2 Walls
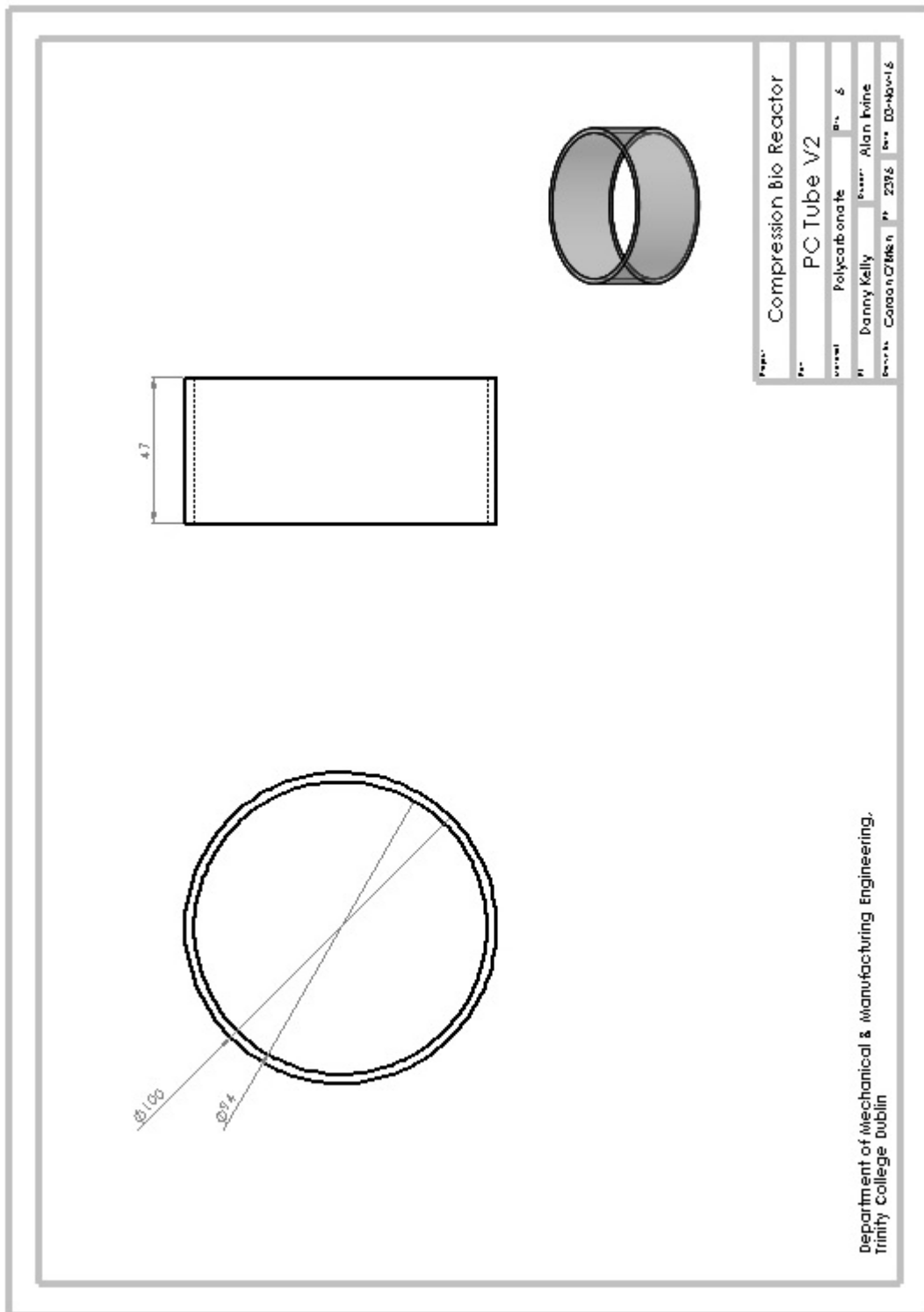
Figure A.11 Technical drawings for the transparent walls of the dish.
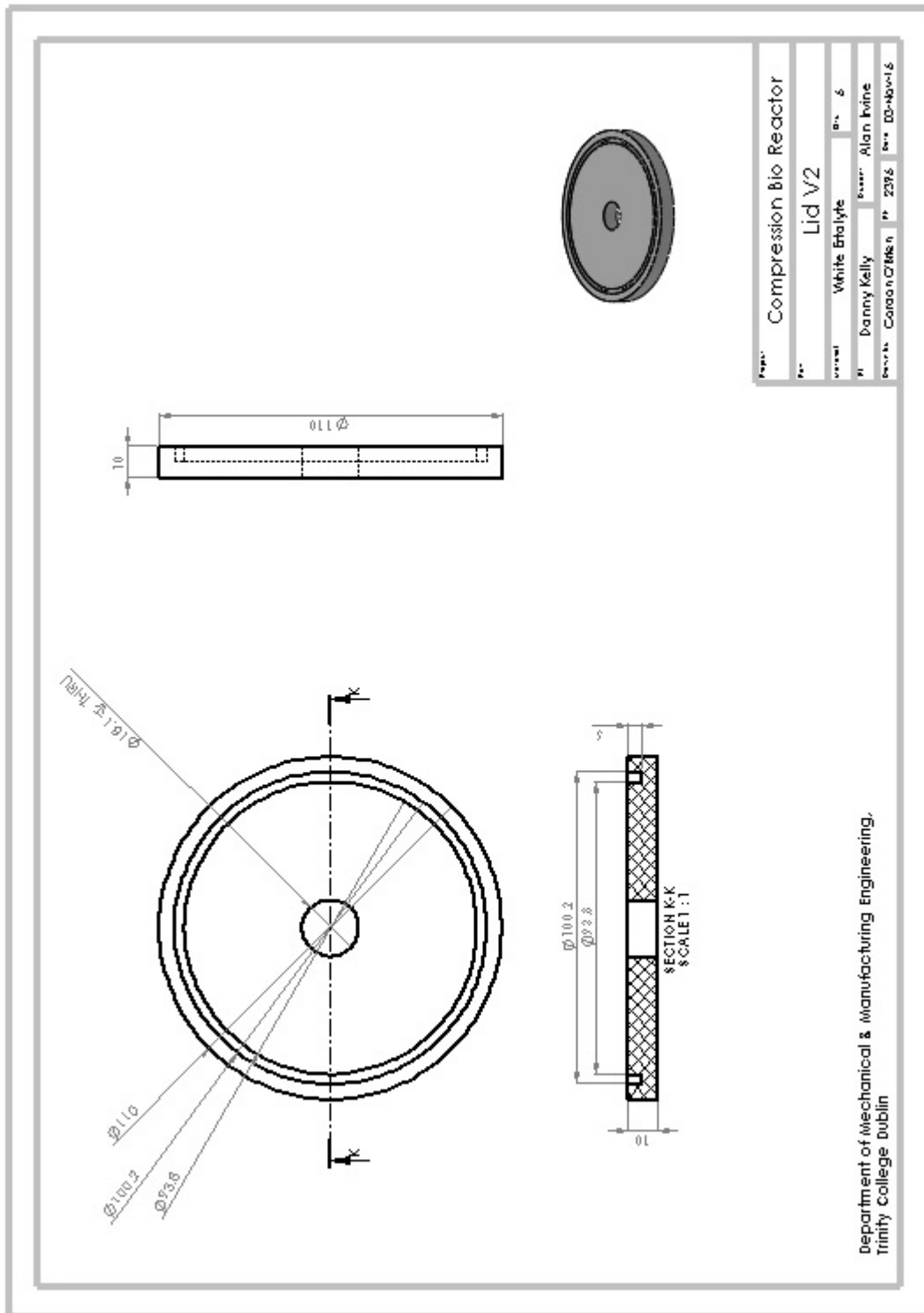
A.2.3.3   Lid

Figure A.12 Technical drawings for the lid of the sterile bioreactor dish.
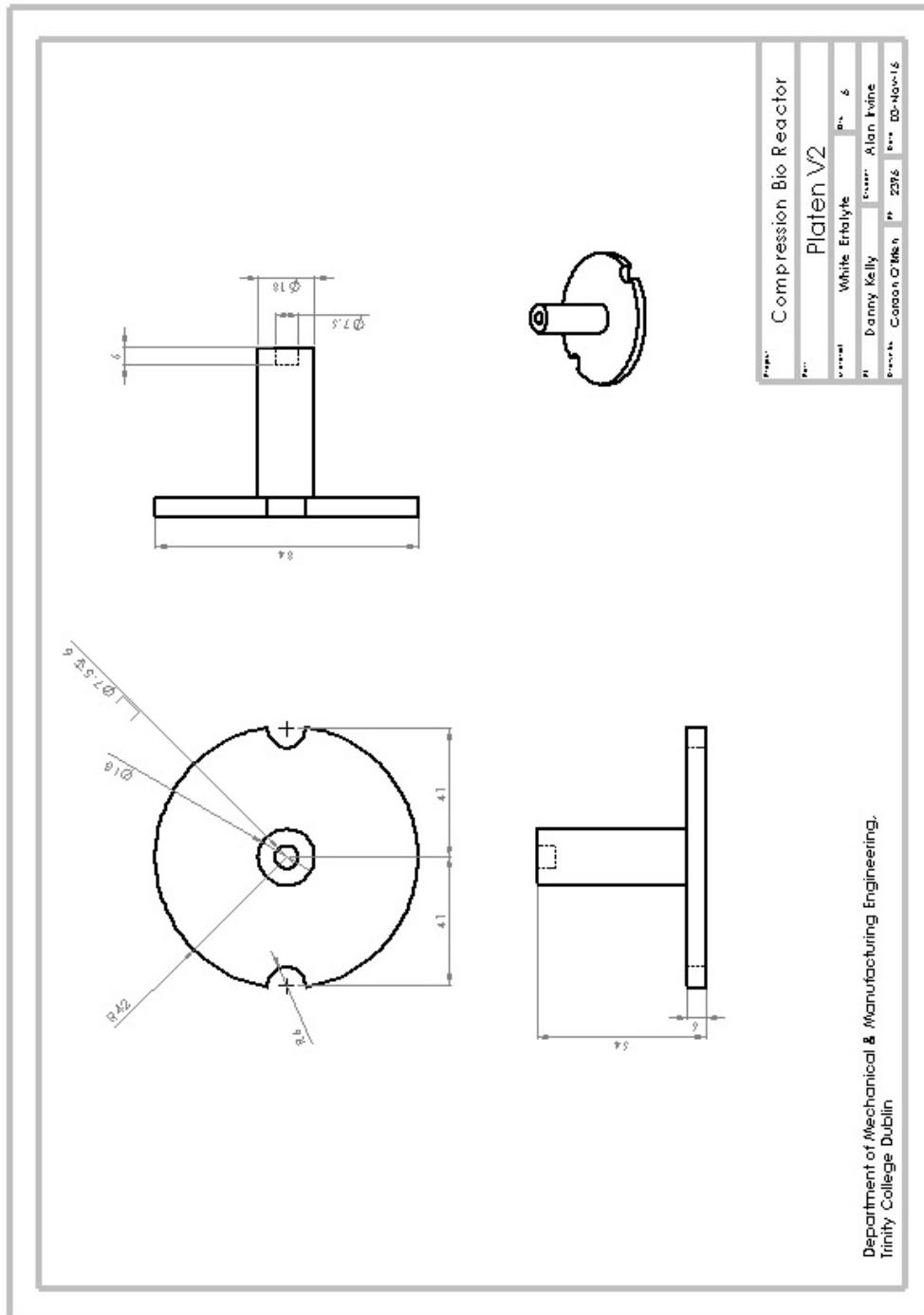
A.2.3.4   Platen

Figure A.13 Technical drawings for the compressing platen that was magnetically coupled to the actuator-load cell assembly.
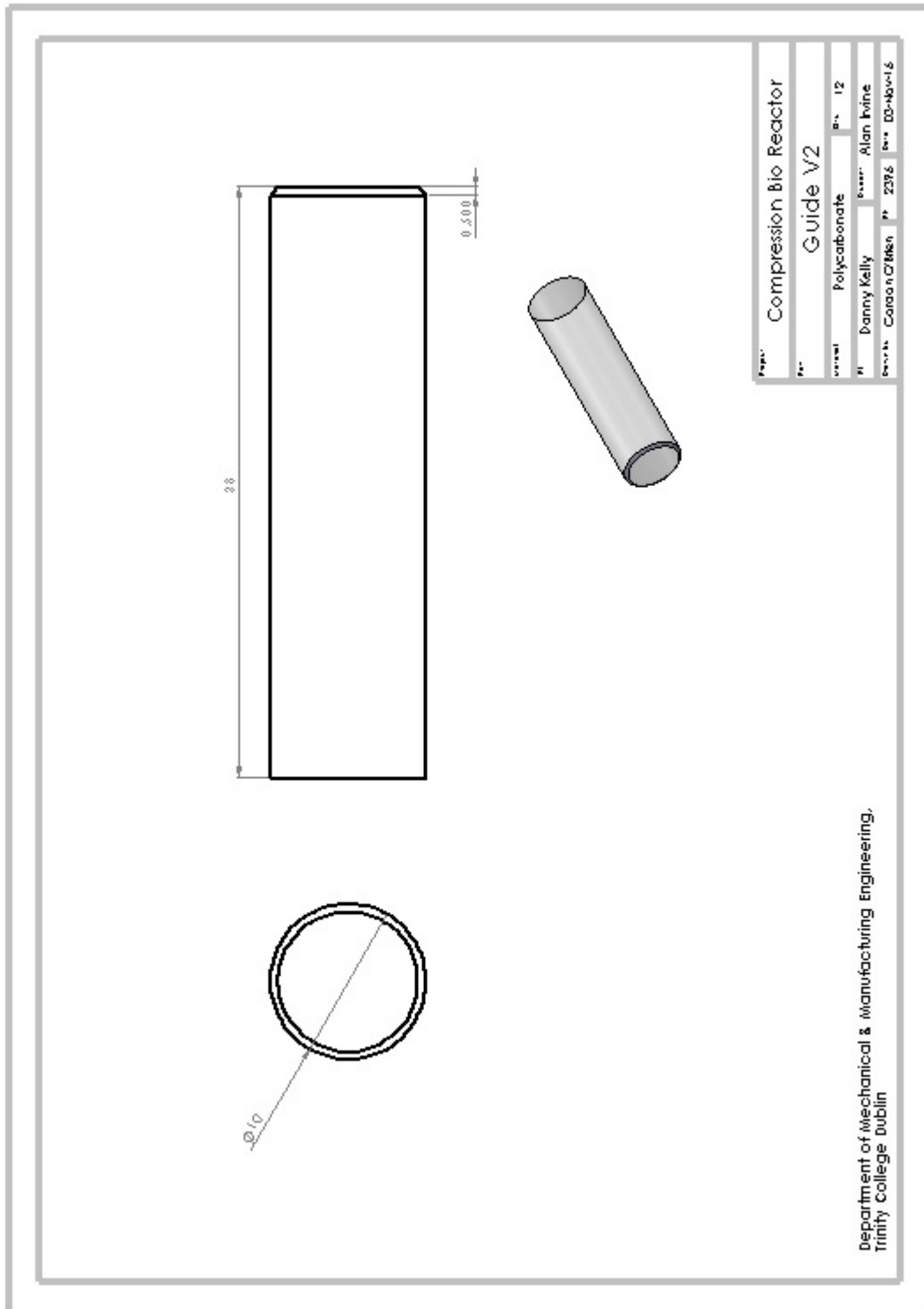
A.2.3.5   Guides

Figure A.14 Technical drawings for the guide posts to direct motion of the platen by preventing possible rotation.

A.3   Sterilisation

All bioreactor pieces ethylene oxide gassed in sterile, sealed packs. Not to be autoclaved. Assembled rig 70 % industrial methylated spirits (IMS) sprayed into hood, UV treated on all surfaces and placed in appropriate incubator. Cables feed through sterile ports and sealed with stopper or clean material such as parafilm.
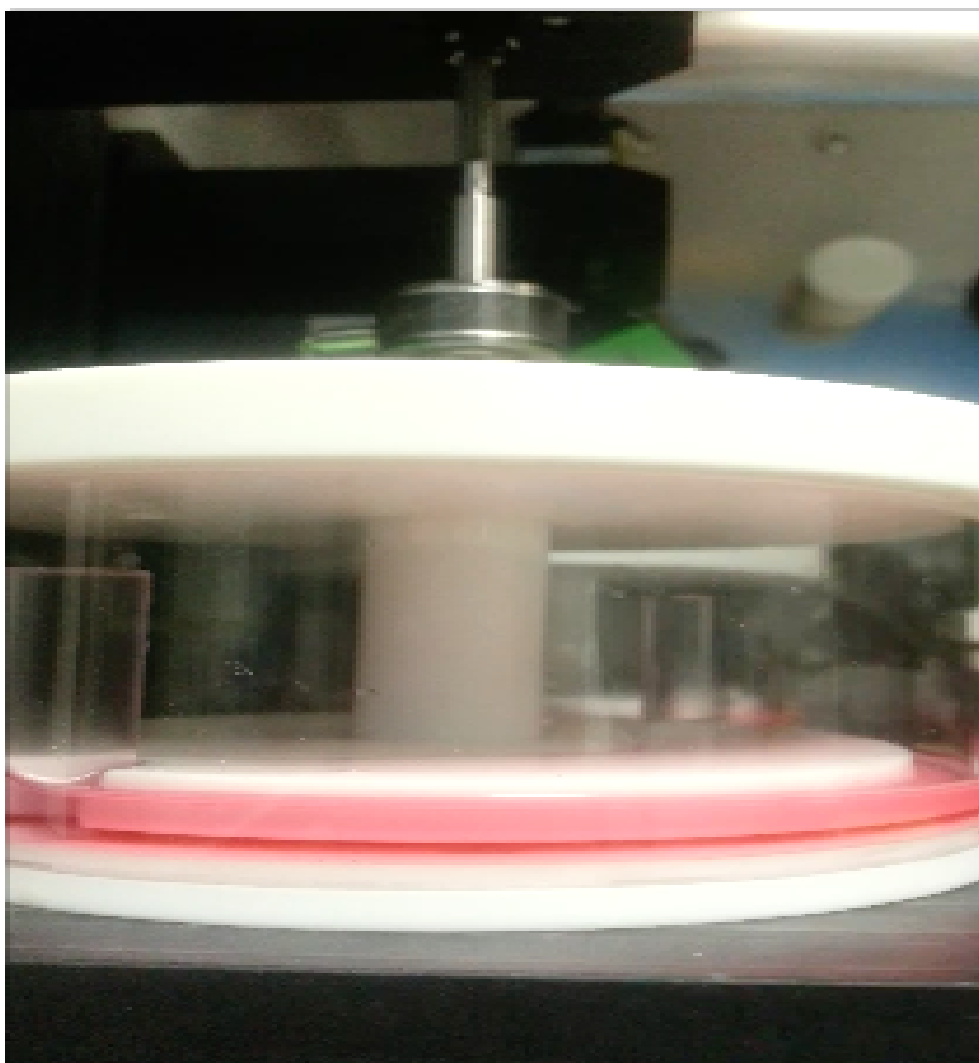

Figure A.15 Bioreactor sterilised and within incubator during *in vitro* culture.

A.4   Viability Study Methods

A.4.1   Cell isolation, expansion and culture

MSCs were isolated from porcine femora. Following isolation, Porcine MSCs were preserved in liquid nitrogen before later being thawed and expanded according to a modified method developed for human MSCs. MSCs were plated at a seeding density of 50,000 cells/cm^2 in high-glucose Dulbecco's modified eagles medium (4.5 mg/mL D-Glucose, 200 mM L-Glutamine; hgDMEM) supplemented with 10 % fetal bovine serum (FBS) and 2 % penicillin (100 µg/ml) - streptomycin (100 µg/ml); and expanded to passage two in a humidified atmosphere at 37 °C and 5 % CO_2.

MSCs were suspended in chondrogenic medium (CM), which consisted of hgDMEM supplemented with penicillin (100 µg /ml) and streptomycin (100 µg/ml), sodium pyruvate (100 µg/ml), L-proline (40 µg/ml), bovine serum albumin (1.5 mg/ml), linoleic acid (4.7 µg/ml), insulin-transferrin-selenium (10 µg/ml), L-ascorbic acid-2-phosphate (50 µg/ml), dexamethasone (100nM) and 10 ng/mL TGF-β_3. The MSC suspension was subsequently mixed with 2.5 % RGD-modified alginate (dissolved in ultra pure water) at a ratio of 1:4 to yield a final gel concentration of 2 % RGD-modified alginate and a cell density of 20 million cells/ml. The alginate-cell suspension was cast in an agarose mould (12 mm diamater by 5 mm deep) containing 100 mM $CaCl_2$ with the incorporation of either a homogenous or gradient mesh within the construct. A similar slab was placed on top each mould that contained 20 sample casts. This housing was then soaked in 100 mM $CaCl_2$ for 30 minutes in an incubated environment. Constructs were maintained separately in 12-well plates with 2 ml of chondrogenic medium in 5 % O_2. Medium was exchanged twice weekly and constructs were cultured in these conditions for 21 days.

A.4.2 Tri-potentiality

The progenitor cells were differentiated toward adipogenic, osteogenic, and chondrogenic lineages to demonstrate their multipotentiality. All of the differentiations were performed in triplicate, and a sample was kept in basal medium during 14 days (adipogenic and osteogenic), and 21 days (chondrogenic) to ensure the non-differentiation of control cells.

For adipogenic differentiation, cells in passage two were plated at 20,000 cells/cm^2 in 24-well plates and cultured under adipogenic conditions for 14 days. The medium was changed every 3 days, the cells were fixed in 4 % formaldehyde solution for 10 minutes, rinsed with PBS and stained with Oil Red-O.

To perform the osteogenic characterisation of MSCs, the progenitor cells at passage 2 were plated at 20,000 cells/cm^2 in 24-well plates and cultured ender osteogenic conditions for 14 days, the medium was changed every 3 days, the cells were fixed in 4 % formaldehyde solution for 10 minutes, rinsed with sterile water and stained with Alizarin Red.

Chondrogenesis was induced in micromass pellet cultures prepared with 1 10^6 cells placed in a 15 ml polypropylene conical tube. The pellet was cultured at 37 °C with 5 % CO_2 in 2 ml of chondrogenic medium, the medium was changed every 3 days. Following a 3-week incubation period, the pellet was fixed in 4 % formaldehyde solution for 24 hours at room temperature, embedded in paraffin and cut into 5?m sections, and was stained with Alcian blue dye to detect sulfated proteoglycans.

A.4.3 Dynamic compression application

Dynamic compressive loading was applied to constructs also supplied with chondrogenic medium following a 21 day culture period. Dynamic compression (DC) was carried out in an incubator housed, custom-built compressive loading bioreactor. Uniaxial, unconfined compression was initiated using an electric linear actuator with 0.05 µm resolution (Zaber Technologies Inc., Vancouver, Canada). A 1000 g load cell (RDP Electronics Ltd, Wolverhampton, UK) attached to the actuator lead screw sensed the load applied. The

system was controlled and data logged using Matlab (fig. 3.1). The dynamic compression protocol consisted of 15 % strain amplitude superimposed on a maximum 1 % preload at a frequency of 1 Hz employed for a period of 3 weeks, 5 days/week and 2 hrs/day. FS controls constructs were housed in the bioreactor dish without any media agitation. Medium was exchanged 2 - 3 times weekly.
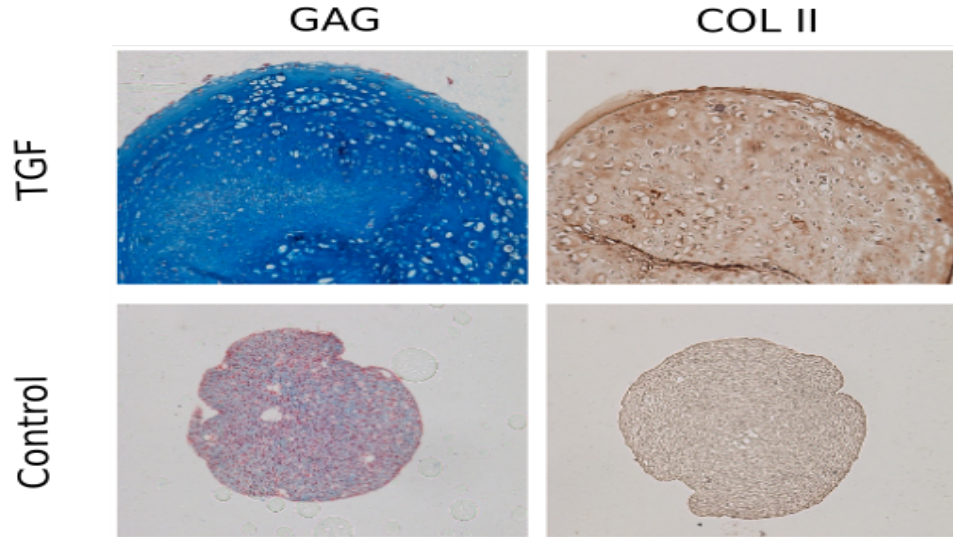
A.4.4   Biochemical content

The biochemical content of constructs (n = 3 or n = 4) was assessed at day 0 and day 21. The wet mass of each construct half was recorded before being frozen at -85 ℃ for later analysis. Samples were digested with papain (125 µg/mL) in 0.1 M sodium acetate, 5 mM L-cysteine HCl, 0.05 M EDTA, pH 6.0 (all Sigma- Aldrich) at 60 ℃ under constant rotation for 18 h. DNA content was quantified using the Hoechst Bisbenzimide 33258 dye assay as previously described [219]. The proteoglycan content was estimated by quantifying the amount of sulfated glycosaminoglycan (sGAG) in constructs using the dimethylmethylene blue dyebinding assay (Blyscan, Biocolor Ltd., Carrickfergus, UK), with a shark chondroitin sulfate standard. Total collagen content was determined through measurement of the hydroxyproline content [220]. A hydroxyproline-to-collagen ratio of 1:7.69 was used.

A.5   Viability Study Results

A.5.1   Tri-potentiality

Pellet culture highlights ability to produce sGAG with TGF-β_3 supplementation. Similarly, with the incorporation of osteo/adipo media in monolayer culture, cells isolate from porcine bone marrow were able to produce calcium as evident by alizarin red and fatty oils stained for using oil red-o. This highlights the tri-potentiality of these cells and highlights their stem ability. Consequently, these cells are thought to be MSCs throughout this thesis.
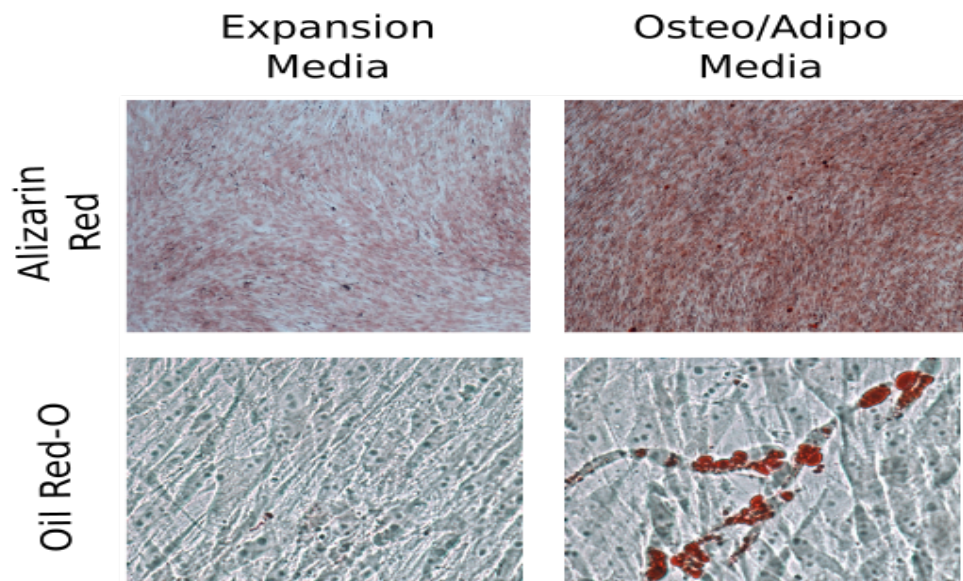
Figure A.16 Histological content of MSC cultured in pellet and monolayer form with or without certain growth factor incorporation to assess stemness. Pellet culture with or without TGF-β_3 and monolayer culture with the presence of expansion media or osteo/adipo mixed media. Staining with alcian blue for sGAG and immunohistochemistry for collagen type II was used to investigatre chondrogenesis for pellet culture. In monolayer, alizarin red staining for calcium and oil red-o staining for fatty acids was used to determine osteogenesis and adipogenesis respectively.

A.5.2 Cells remain viable in RGD-modified alginate hydrogels

Over the course of 42 days in culture, the final 21 days of which were in bioreactor conditions, MSCs remained over 50 % viable in all groups with no difference in DNA content even in comparison to controls outside of bioreactor culturing conditions. MSC chondrogenesis was similar to plate controls in all groups apart from dynamically compressed soft hydrogels. MSC hypertrophy was the same throuhgout soft hydrogel culturing conditions, while the bioreactor culture system promoted hypertrophy in stiff hydrogels that supported little MSC hypertrophy in plate conditions. This highlights the custom built bioreactor system supports viable culturing conditions due to little loss of cell viability in comparison to plate conditions. It also has no detrimental effect on MSC chondrogenesis and hypertrophy.
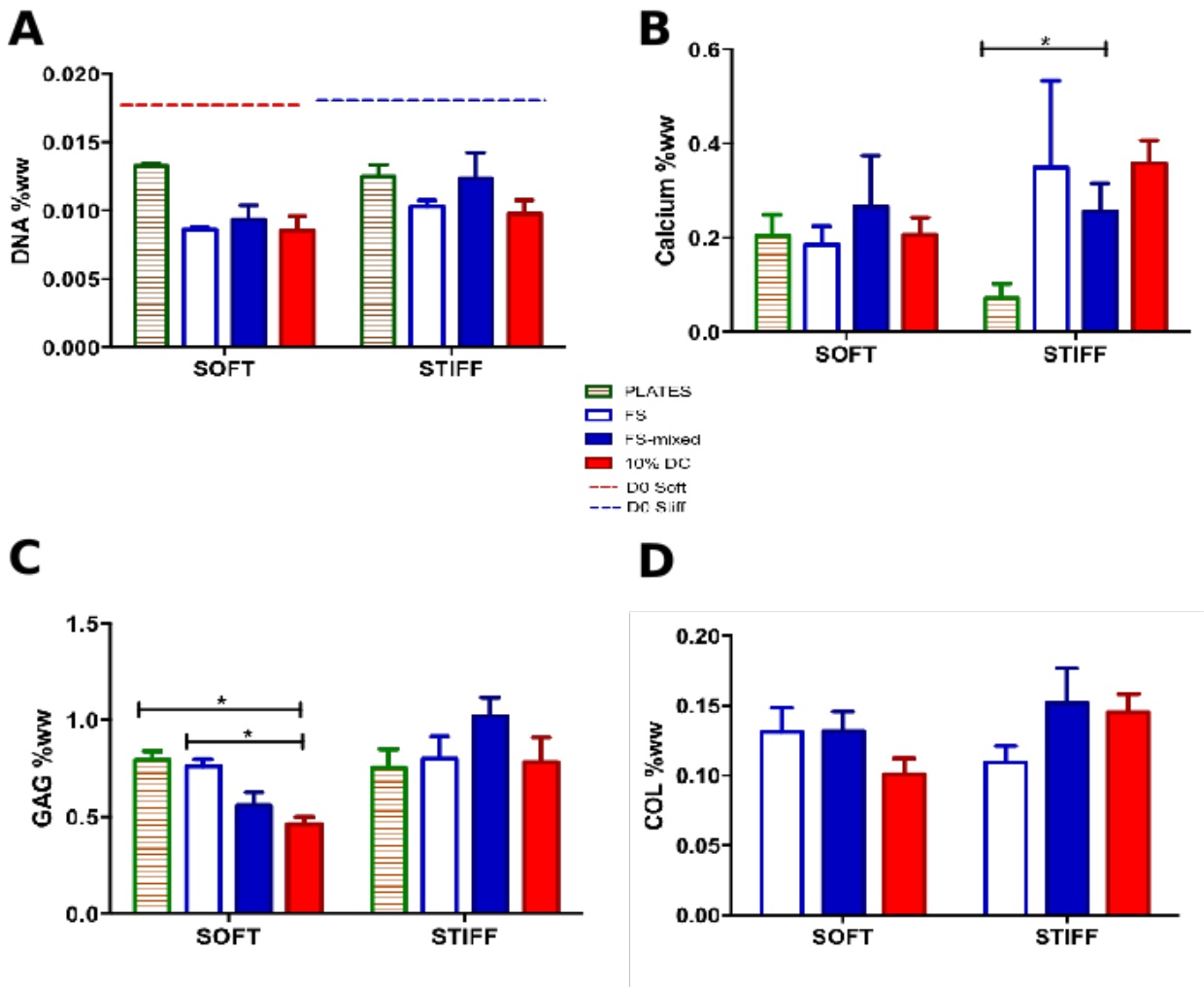
Figure A.17 Biochemical content of alginate hydrogels within the bioreactor culture system. (A) DNA, (B) calcium, (C) GAG (µg) and (D) collagen (ng) contents as a percentage of wet weight (% ww) of soft and stiff RGD-modified alginate hydrogels in both plate and bioreactor culture (FS, 0 % and 10 %). * denotes $p < 0.05$ based on one-way ANOVA post test analysis.